O_2/CO_2-sensitive cyclic AMP-signalling pathway in peripheral chemoreceptors

Ana Rita Silva Martins Nunes

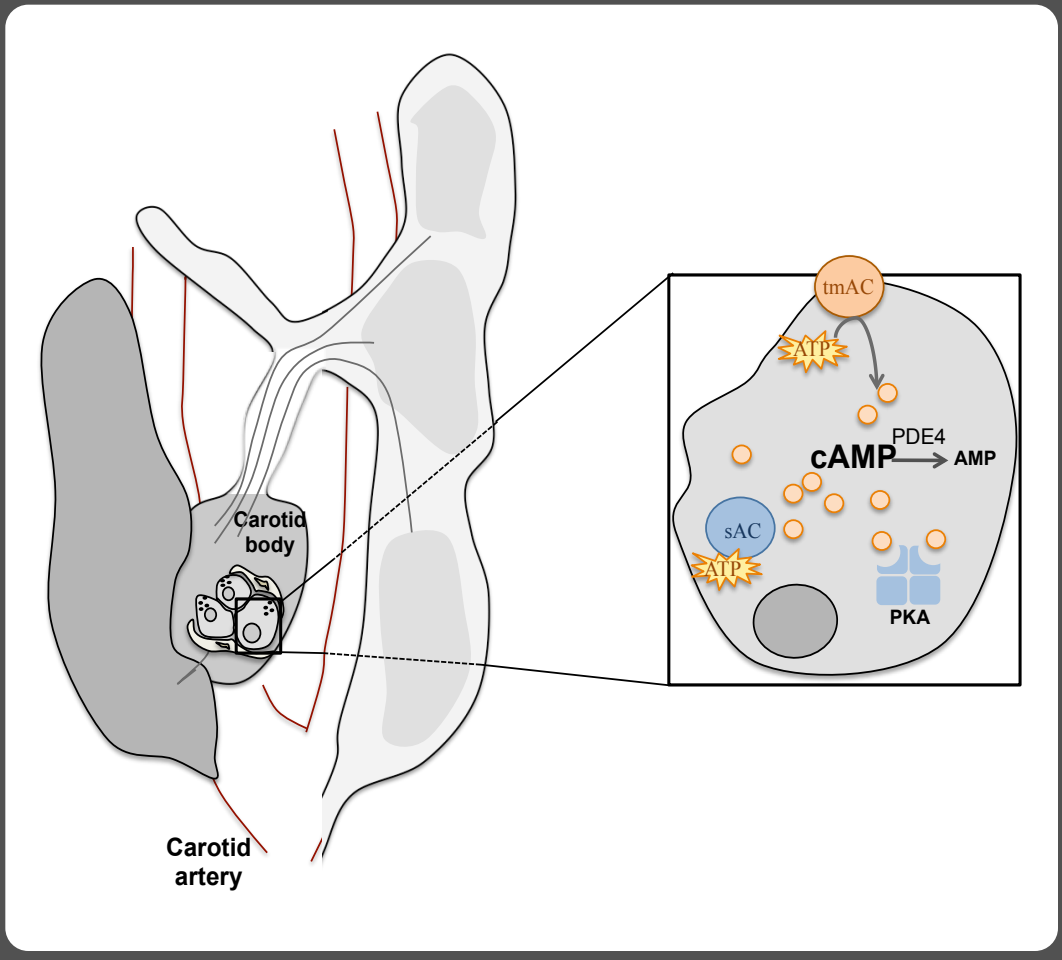

Faculdade de Ciências Médicas | Universidade Nova de Lisboa

Lisboa, 2013

O_2/CO_2-sensitive cAMP-signalling pathway in peripheral chemoreceptors

Ana Rita Silva Martins Nunes

Lisboa, 2013

Dissertation presented to obtain the PhD degree in “Ciências da Vida - Especialidade de Farmacologia” at the Faculdade de Ciências Médicas, Universidade Nova de Lisboa.

Experimental work conducted at the Department of Farmacologia - associated laboratory at Chronic Diseases Research Center (CEDOC), Faculdade de Ciências Médicas da Universidade Nova de Lisboa, under the scientific supervision of Professor Dr. Maria Emilia Monteiro, and in the Department of Pediatrics, Johns Hopkins Medical School, under supervision of Professor Dr. Estelle Gauda.

This work was supported by:

FCT Fundação para a Ciência e a Tecnologia
MINISTÉRIO DA EDUCAÇÃO E CIÊNCIA
Doctoral degree scholarship SFRH/BD/39474/2007

FUNDAÇÃO LUSO-AMERICANA
155/07 one year scholarship (2007)

CEDOC
Chronic Diseases FCM NOVA

ciências médicas NOVA

JOHNS HOPKINS MEDICINE

The author of this thesis performed all the methodology and analyzed all the experimental data included in this thesis, except the carotid nerve recordings (results included in the *Results Chapter 3- "Bicarbonate-sensitive soluble adenylyl cyclase (sAC) and transmembrance adenylyl cyclase in peripheral chemoreceptors"*). Andrew Holmes performed carotid nerve recordings under the supervision of Professor Prem Kumar at College of Medical and Dental Sciences from University of Birmingham, UK.

The scientific content of the present thesis has been included in the publication of the following book chapters and international scientific periodicals with referees:

Book chapters:

Nunes A.R., Batuca J.R. and Monteiro E.C., Functional characterization of phosphodiesterases 4 in the rat carotid body: effect of oxygen concentration. In The arterial chemoreceptors, 129-136, Gonzalez et al (eds.), Springer, Netherlands, 2009.

Nunes A.R., Monteiro E.C., Johnson S.M., Gauda E.B., Bicarbonate-regulated soluble adenylyl cyclase (sAC) expression and activity in peripheral chemoreceptors. In The arterial chemoreceptors, 129-136, Gonzalez et al (eds.), Springer, Netherlands, 2009.

Nunes A.R., Sample V., Xiang Y.K., Monteiro E.C., Gauda E.B. and Zhang J. Effect of oxygen on phosphodiesterases (PDE) 3 and 4 isoforms and PKA activity in the Superior Cervical Ganglia. In Arterial chemoreceptors: From Molecules to systems, 758; 287-294. C.A. Nurse et al (eds.), Springer, Netherlands, 2012.

Papers in International Scientific Periodicals with Referees

Nunes A.R., Batuca J.R. and Monteiro E.C., Different effects of hypoxia on cAMP accumulation induced by PDE4 inhibitors in rat carotid bodies, carotid arteries and superior cervical ganglia. *British Journal of Pharmacology*, 159, 353-361, 2010.

Nunes A.R., Holmes A., Sample V., Kumar P., Monteiro E.C., Zhang J.*, Gauda E. B.*, Bicarbonate-sensitive soluble adenylyl cyclase (sAC) and transmembrane adenylyl cyclase in peripheral chemoreceptors (in submission).

Nunes A.R., Monteiro E.C., Zhang J., Gauda E. B.*, Bicarbonate-sensitive soluble adenylyl cyclase (sAC) and transmembrane adenylyl cyclase in central chemoreceptors (in preparation).

Other manuscripts published during the author's doctoral studies not related with the content of the present thesis:

Papers in International Scientific Periodicals with Referees

Nunes AR, Chavez-Valdez R, Ezell T, Donnelly DF, Glover JC, Gauda EB. Effect of development on [Ca2+]i response kinetics to ATP in petrosal ganglion neurons: a pharmacological approach using optical recording. *Journal Applied Physiol*ogy 112:1393-1402, 2012.

Chavez-Valdez R*, Mason A*, **Nunes AR**, Northington FJ, Tankersley C, Ahlawat R, Johnson S, Gauda EB. Effect of hyperoxic exposure during early development on neurotrophin expression in the carotid body and nucleus tractus solitarii. *Journal Applied Physiol*ogy 112:1762-1772, 2012.

The work presented in this thesis was awarded with the 1st De Castro-Heymans-Neil Award, by *The XVIIIth International Society for Arterial Chemoreception* (ISAC) meeting held in Hamilton, Ontario, Canada, July 10th-15th, 2011.

Table of Contents

List of Tables

List of Figures

Acknowledgments

During the 5 years of my PhD, I met wonderful people from all over the world, since supervisors, collaborators, co-workers and friends, who I have to thank for the encouragement and inspiration, and for all that I've learnt from them.

The first person I would like to thank is Professor Dr. Emilia Monteiro. About 6 years ago she received me in her laboratory and about one year after she gave me the possibility to start my PhD and go abroad. As a strong, successful woman, she has inspired me all of these years. I thank her for her guidance/insight, encouragement and very important, optimism.

I am also very grateful to Professor Dr. Estelle Gauda. She gave me the opportunity to work in a great institution: The Johns Hopkins University. She received me in her lab and in her family! I thank her for her contagious passion for research and travelling! She gave me the opportunity to attend and participate into several scientific meeting, and connect and collaborate with fantastic people.

Throughout these years I had the fantastic opportunity to meet and collaborate with Dr. Cristine Kranz, Dr. Heinz Steiner, Dr. Shree Johnson, Dr. Glover, Dr. Donnelly, Dr. Kim Insook and be mentored by Dr. Jin Zhang. Thanks for the insight, good suggestions and advices. I thank Prof. Constancio Gonzalez for the opportunity to spend 3 months in his laboratory, prior to the start of this PhD. I would like to thank Dr. Prem Kumar and Andrew for all the insight and help in this project.

All the hours in the lab would not be as fun as they were without my lab mates. Ariel, besides her excellent lab skills and her promptly help, she is also a great friend and a great roomy. Tarrah, thank you for your help and your hugs! Thank you Dr. Raul for all your help since I came to Baltimore and thank you for my first American beer! Thank you, Shree and Ruth. Special thanks to Dr. Mclemore for being always available and helping me reviewing the english of this thesis. I thank the Jin Zhang's lab with a special thanks to Vedangi, for the

suggestions over the lab meetings and help with the experiments. I would like to thank the Department of Pharmacology in Portugal, specially, Dr. Silvia, Dr. Sofia, Joana, Lucilia, Inês, Dr. Teresa, Teresa, Daniela. A special thanks to Joana for teaching me how to dissect carotid bodies when I first came to the laboratory, Sílvia for some CB discussions, for teaching me some techniques over the three months I spent in Valladolid with her and the great time we had there, and also Daniela and Lucília for the help, support and friendship over the last months.

A big thanks to all my friends that have helped me pass through all these good and bad, easy and difficult roller coaster times that were part of this PhD. To all my friends in Portugal that encouraged me to go to USA and they received me back and made me feel at home again. Special thanks to mana Catarina, Miguel, Ines, Ivo (o quarteto Guerreiro!), Joao e Sonia Quaresma, Catia, Sergio. My friends that I met in the Charm city (Baltimore), in special, Veronica, Susy and Colin, Eva, Nisha, Mariana, Recep, Mateus, Lia, Maarje, Vinny, and so many more…. I would like to thank Eva and Jenny for letting me stay in their house the last 3 months I was in Baltimore and thank you everybody for the great times we had together!

I would like also to thank the Centre for Metabolism and obesity research (CMOR), Dr. Wolfgang and Susana Rodrigues for letting me use the speed vacuum and the fluorescent microplate reader.

And at last, but so important: my FAMILY: Mãe e Pai, Pedro e Lina e Miguel… não há palavras que cheguem para vos agradecer! Vocês sempre me apoiaram e estão sempre presentes comigo seja onde for! Mãe e pai, obrigada pela vossa paciência, pelas horas intermináveis ao telefone, pelo apoio, por toda a força que me deram e acima de tudo, motivação!

I also would like to thank Fundacao para a Ciência e tecnologia (FCT), CEDOC, Faculdade de Ciências Medicas and Universidade Nova de Lisboa.

Abbreviations

ANOVA	Analysis of variance
AM	Adrenomedullin peptide
ΔER	Change in emission ratio
5-HT	Serotonin (5-Hydroxytryptamine).
AC	Adenylyl cyclases
Ach	Acethylcholine
ADO	Adenosine
AKAR	A-kinase Activity Reporter
ANP	Atrial Natriuretic Peptide
ATP	Adenosine triphosphate
BCECF	2'7'-Bis(2-carboxyethyl)-5(6)-carboxyfluoresceinacetoxy methyl ester
CA	Catecholamines
Ca^{2+}	Calcium ion
CAH	Carbonic Anhydrase
CaM	Calmodulin
cAMP	cyclic adenosine monophosphate
CB	Carotid Body
CCK	Cholescystokinin
CFP	Cyan fluorescent protein
CGRP	Calcitonin gene-related peptide
CNG	Cyclic nucleotide gated channel
CNS	Central nervous system
CO	Carbon Monoxide
CO_2	Carbon dioxide
COPD	Chronic Obstructive Pulmonary Disease
CSF	Cerebrospinal fluid
CSN	Carotid sinus nerve
DA	Dopamine
DRG	Dorsal respiratory group
EIA	Enzyme immunoassay
EPAC	Exchange proteins activated by cAMP
FRET	Flourescence resonance energy transfer
FSK	Forskolin
GPCR	G-protein coupled receptors
GPN	Glossopharyngeal Nerve

H^+	Proton
H_2CO_3	Carbonic acid
H_2O	Water
HCO_3^-	Bicarbonate ion
K^+	Potassium ion
KMM	Krebs modified medium
LC	Locus coeruleus
LHA	Lateral Hypothalamus
Mg^{2+}	Magnesium ion
MIL	Milrinone
mmHg	millimetre of mercury
NA^+	Sodium ion
NADH	Nicotinamide adenine dinucleotide reduced form
NE	Norepinephrine
NO	Nitric Oxide
NG	Nodoso ganglia
NHE	Na^+/H^+ exchanger
NM	Neuromodulator
NP	Neuro peptide
NT	Neurotransmitter
nTS	Nucleus Tractus Solitarius
O_2	Oxygen
OSA	Obstructive Sleep Apneia
P	Posnatal day of life
$PaCO_2$	Partial pressure of carbon dioxide in arterial blood
PaO_2	Partial pressure of oxygen in arterial blood
PBS	Phosphate buffered saline
PDE	Phosphodiesterases
PG	Petrosal ganglia
pH_i	intracellular pH
PI	Propidium iodide
PKA	Protein Kinase A
PNA	Fluoresceinated peanut agglutinin
preBotC	pre-Botzinger complex
PRG	Pontine Respiratory Group
RT-qPCR	Real-time quantitative polymerase chain reaction
RN	Raphe Nucleus
ROL	Rolipram
RTN	Retrotrapezoid nuclei
sAC	soluble adenylyl cyclase

SCG	Superior cervical ganglia
SD	Sprague-Dawley rats
SEM	Standard error of the mean
TASK	TWIK-related acid-sensitive potassium
TH	Tyrosine Hydroxylase
tmAC	transmembrane adenylyl cyclase
VIP	Vasointestinal peptide
VLM	Ventrolateral medulla
VRG	Ventral respiratory group
YFP	Yellow fluorescent protein

Abstract

The carotid body (CB) is a small-paired organ sensitive to changes in blood PaO_2, $PaCO_2$ and pH. Type I (glomus) cells of the CB, the sensor units, detect the stimulus and release neurotransmitters. These neurotransmitters bind either to pos-synaptic receptors in the terminals of the carotid sinus nerve (CSN) to trigger the hyperventilatory reflex, or to pre-synaptic receptors located in cells to modulate their activity. These receptors can be ionotropic or metabotropic; the later are coupled to transmembrane adenylyl cyclases (tmAC). The exact mechanism by which changes in O_2/CO_2 are detected in the CB is not fully understood, but changes in cAMP levels have been associated with the O_2/CO_2 transduction mechanism of this organ. cAMP levels are regulated by their synthesis via two types of adenylyl cyclase: neurotransmitter-sensitive transmembrane (tmAC) and bicarbonate sensitive-soluble adenylate cyclase (sAC), and by their hydrolysis mediated by phosphodiesterases (PDE). The work present in this dissertation was aimed to investigate the role of cAMP in the rat CB chemotransduction mechanisms, how specific is cAMP signaling pathways in the CB mainly in different CO_2 conditions, and to determine whether the enzymes that participate in cAMP signal transduction in the CB are regulated by O_2/CO_2. To achieve this aim we characterized pharmacologically PDE4 in the CB and non-chemoreceptor tissues and studied the effects of acute hypoxia on the cAMP accumulation induced by PDE inhibitors. Concentration-response curves for the effects of a non-specific (IBMX) and specific PDE2 and PDE4 inhibitors (EHNA, Rolipram and Ro 20-1724, respectively) on cAMP levels were performed in normoxic ($20\%O_2/5\%CO_2$) and hypoxic conditions ($5\%O_2/5\%CO_2$). We further explored the characterization of PDEs in the superior cervical ganglia (SCG) using FRET-based sensors in primary dissociated neurons in the presence of non-specific (IBMX) and specific PDE3 and PDE4 inhibitors (milrinone and rolipram, respectively). Additionally, we assayed for changes in PDE3A-B and PDE4A-D

expression using qRT-PCR in whole SCG, under different O_2 tensions. We also characterized the cAMP synthesis pathway in the CB under different concentrations of HCO_3/CO_2. Our work was focused on the characterization of sAC, an enzyme activated by changes in HCO_3/CO_2, in the CB and peripheral non chemoreceptor tissues (SCG and petrosal and nodose ganglia). We also compared the relative contribution of tmAC and sAC to the CO_2-sensing mechanism in the CB. The experiments assayed for changes in sAC and tmAC mRNA expression (qRT-PCR), cAMP levels (ELISA), activation of protein kinase A (PKA, FRET-based sensors in type I cells) and carotid sinus nerve activity (recording) in the presence and absence of activators or inhibitors of sAC, tmAC and PKA. Lastly, we investigated sAC and tmAC expression and activity in central chemoreceptors (locus coeruleus, raphe nuclei and the ventrolateral medulla) and compared the role of these enzymes in these tissues and CB.

The main findings of this work were: 1) PDE4 isoforms are functional in rat CBs, SCG and carotid arteries (CA), while PDE2 is only functional in the SCG; 2) The effects of PDE inhibitors on cAMP accumulation were increased by acute hypoxia in both CB and CA, but reduced in the SCG; 3) a differential pattern of PDE regulation in the SCG was observed that potentially represents subpopulations of ganglion cells with different physiological functions; 4) sAC is ubiquitously expressed and functional in CB and central chemoreceptors, but apparently does not mediate a role in hypercapnia sensing; instead sAC activity seems to be maximal under normocapnic conditions; 5) tmAC and sAC apparently contribute more to cAMP accumulation when situations of low HCO_3/CO_2 occur; 6) Inhibition of tmAC activity decrease the CSN discharge in the same extent between normocapnic and hypercapnic conditions; 7) The sensibility of the CB to CO_2 seems to be mediated by pH.

Taken together, our results suggest that cAMP has a role in the homeostasis of the CB, and it is not a specific mediator of hypoxia/hypercapnia transduction of this organ. The O_2/CO_2 regulation of the enzymes studied in this work is not specific to the carotid body. The present work demonstrated that

increases in cAMP described by others in hypercapnic conditions are not observed when the pH is controlled.

Resumo

O corpo carotídeo (CB) é um pequeno órgão sensível a variações na PaO_2, $PaCO_2$ e pH. As células tipo I (células glómicas) do corpo carotídeo, as unidades sensoriais deste órgão, libertam neurotransmissores em resposta às variações dos gases arteriais. Estes neurotransmissores atuam em recetores pós-sinápticos localizados nas terminações do nervo do seio carotídeo (CSN) desencadeando hiperventilação, ou em recetores pré-sinápticos localizados nas células do CB, modulando assim a atividade deste órgão. Estes recetores podem ser classificados em ionotrópicos ou metabotrópicos, estando estes últimos acoplados a adenilatos ciclases transmembranares (tmAC). O mecanismo exato pelo qual as variações dos gases arteriais são detetadas pelo CB ainda não está completamente elucidado, mas tem sido sugerido que as alterações nos níveis de cAMP estejam associadas ao mecanismo de deteção de variações de O_2 e CO_2. Os níveis de cAMP podem ser regulados pela sua via de síntese, mediada por dois tipos de adenilatos ciclases: tmAC sensível aos neurotransmissores e adenilato ciclase solúvel (sAC) sensível a variações de HCO_3/CO_2; e pela sua via de degradação mediada por fosfodiesterases.

Os principais objetivos do presente trabalho foram, em primeiro lugar, esclarecer o papel da via de sinalização do cAMP no mecanismo de quimiotransdução do CB de rato; foi igualmente nosso propósito investigar qual a especificidade da via de sinalização do cAMP no CB em resposta a diferentes concentrações de CO_2 e, por fim, determinar se os enzimas que participam na via de transdução de sinal do cAMP são reguladas por O_2/CO_2.

Com este intuito, caracterizamos farmacologicamente a PDE4 no CB e em tecidos não quimiorecetores e, observámos o efeito de hipóxia aguda na acumulação dos níveis de cAMP, induzidos pelos inibidores de PDEs. Foram elaboradas curvas de dose-resposta para os efeitos de inibidores, não específicos (IBMX) e específicos para a PDE2 e PDE4 (EHNA, Rolipram e Ro 20-1724), nos níveis de cAMP acumulados, em situações de normóxia

(20%O_2/5%CO_2) e hipóxia (5%O_2/5%CO_2). Foi aprofundada a caracterização das PDE no gânglio cervical superior (SCG) utilizando-se a técnica de FRET em culturas primárias de neurónios na presença de inibidores não específicos (IBMX) e específicos para a PDE3 e

PDE4 (milrinone e rolipram, respetivamente). Foram ainda estudadas as alterações na expressão de PDE3A-B e PDE4A-D em resposta a diferentes percentagens de oxigénio no SCG através de RT-qPCR. Caracterizámos a via de síntese do cAMP no CB em resposta a variações na concentração de HCO_3/CO_2. Esta componente do trabalho baseou-se na caracterização da sAC, um enzima regulado por HCO_3/CO_2, no CB e em tecidos não quimioreceptores periféricos (SCG, gânglio petroso e gânglio nodoso). Foi ainda comparada a contribuição relativa da tmAC e sAC no mecanismo de sensibilidade ao CO_2 no CB. Para o efeito, foram estudadas as alterações nos níveis de expressão de sAC e tmAC (RT-qPCR), nos níveis de cAMP (ELISA), na ativação da proteína cinase A (PKA, FRET baseado em sensores) e na atividade do CSN (registos) na presença e ausência de ativadores e inibidores das AC, tmAC e PKA. Por último, a expressão e actividade da sAC e da tmAC foram estudadas em tecidos quimioreceptores centrais (locus ceruleus, rafe e medula ventro-lateral) e não quimioreceptores (córtex), comparando a sua actividade com a observada no CB.
O nosso trabalho teve os seguintes resultados principais: 1) PDE4 está funcional no corpo carotídeo, SCG e artérias carótidas (CA) de rato, embora a PDE2 só se encontre funcional no SCG; 2) Os efeitos dos inibidores de PDE nos níveis de acumulação de cAMP foram exacerbados em situações de hipóxia aguda no CB e CA, mas foram atenuados no SCG; 3) No SCG, diferentes tipos de células apresentaram uma caracterização específica de PDEs, sugerindo uma subpopulação de células no gânglio com funções fisiológicas distintas; 4) sAC encontra-se expressa e funcional no CB e nos quimiorecetores centrais (locus coeruleus, rafe e medula ventrolateral), mas não desempenha qualquer papel na deteção de situações de hipercapnia; no entanto a sua actividade parece ser máxima em condições de normocapnia; 5) tmAC e sAC parecem ter uma maior

contribuição para o aumento dos níveis de cAMP em condições de baixos níveis de bicarbonato e CO_2; 6) A inibição da atividade da tmAC diminui a frequência de descarga do CSN de forma identica quer em condições de nomocapnia quer de hipercapnia; 7) A sensibilidade do CB às variações de CO_2 é provavelmente mediada por variações de pH.

Em conclusão, os resultados obtidos neste trabalho sugerem que o cAMP tem um papel importante na homeostase do CB, mas que não é um mediador específico da transdução à hipóxia e hipercapnia neste orgão. A regulação por alterações nos níveis de O_2/CO_2 dos enzimas estudados neste trabalho, e que envolvem a via de sinalização do cAMP, não é específica do corpo carotídeo. O presente trabalho demonstrou ainda que os aumentos de cAMP, induzidos por condições de hipercápnia, descritos na literatura, não se observam quando o pH se encontra controlado.

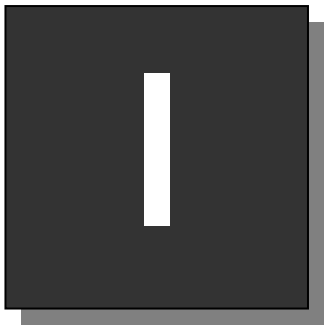

INTRODUCTION

Overview

Organisms closely maintain the partial pressures of oxygen (PaO_2) and carbon dioxide ($PaCO_2$) in arterial blood within a narrow range in order to maintain homeostasis. Small changes in PaO_2 and $PaCO_2$ are rapidly detected by specialized chemoreceptors that mediate reflex responses to adjust the levels of these gases in the blood within the physiological range. Thus, understanding the O_2 and CO_2 transduction and regulation mechanisms of these chemoreceptors is of clinical relevance. Although many advances have been made in the recent decades, the specific molecules and processes modulating chemotransduction are not yet fully understood.

Oxygen (O_2) is fundamental to the survival of mammalian cells. O_2 enters in the lungs and passes into the alveoli, and diffuses into the bloodstream in exchange for CO_2. O_2 is transported in the blood by hemoglobin or dissolved in plasma at a PaO_2 of 100 mmHg in most mammalian species, and diffuses into systemic tissues in exchange for the CO_2 produced in the cell. Once in the cell, O_2 is required directly as the final electron acceptor in the mitochondrial electron transport chain, a series of electron carriers embedded in the eukaryotic mitochondrial membrane. Through a series of redox reactions, high-energy electrons are passed from cofactors nicotinamide adenine dinucleotide (NADH; reduced form) and flavin adenine dinucleotide ($FADH_2$; reduced form) to O_2. In this process, an electrochemical proton (H^+) gradient is generated and used to synthesize adenosine triphosphate (ATP), the energy currency of the cell, and energy-rich organic substrates are broken down into CO_2 and water (H_2O). CO_2 diffuses readily from cells into the bloodstream, where it can combine with H_2O to form carbonic acid (H_2CO_3), which dissociates to liberate a H^+ and a bicarbonate ion (HCO_3^-) through the following reaction catalyzed by carbonic anhydrases (CAH, EC 4.2.1.1):

$$CO_2 + H_2O <-----> H_2CO_3 <-----> HCO_3^- + H^+ \quad (1)$$

Cells actively transport H^+ and HCO_3^- across their cell membranes to maintain constant intracellular pH (pH_i), and to buffer intracellular and extracellular fluids. The physiological level of HCO_3^- in the blood in healthy individuals is 24-27 mmol/L; higher levels reflect metabolic alkalosis, while lower concentrations are indicators of metabolic acidosis. Under normal conditions, CO_2 is dissolved in the blood at a $PaCO_2$ of approximately 35-45mmHg (4.6-5.9% CO_2), the range at which CO_2 diffuses from the blood into the alveoli in exchange for O_2.

Hence, the exchange of the blood gases between the alveoli and the blood continuously supplies O_2 to the cells and reduces CO_2 to maintain homeostasis. This mechanism is regulated by peripheral and central chemoreceptors that send input to the respiratory center in the brainstem to adjust ventilation and to maintain the arterial blood gases within a physiological range.

Control of breathing: A role of peripheral and central chemoreceptors

In mammals, classic O_2-sensitive chemoreceptors are found in the peripheral nervous system: the carotid (CB) and aortic bodies. Both organs trigger hyperventilation in response to hypoxia (decrease in PaO_2), although the major contributor to hypoxia-induced hyperventilation is the CB (for a review (Gonzalez *et al.*, 1994). More recently, evidence for O_2 sensitivity has been reported in the central nervous system (CNS) in the C1 sympathoexcitatory region of the rostral ventrolateral medulla, hypothalamus, pre-Botzinger complex (preBotC) and nucleus tractus solitarius (nTS) (for a review (Neubauer and Sunderram, 2004).

CO_2-sensitive chemoreceptors are present primarily in the CNS (brainstem). However, specialized cells within the CB also depolarize in response to changes in CO_2/H^+, a mechanism that appears to be faster and important in initiating the central CO_2 sensitivity mechanism (Smith *et al.*, 2006).

The contents of this thesis are devoted to the cellular features of the CB, comparing some aspects of the CB with some central chemoreceptor areas.

Peripheral chemoreceptors- Carotid body

The CB is a small (≈ 40 μg wet weigh and 600 μm length in the rat, (McDonald, 1980) and heterogeneous organ composed of type I (glomus or chemosensitive units) and type II (sustentacular) cells, afferent and efferent nerve endings, blood vessels and connective tissue (**Figure 1A**). Type I cells are the primary sensory element within the CB. Type II cells have a glial-like function and it has been shown that these cells may be dormant stem cells, which proliferate in response to hypoxia and differentiate into new type I cells (Pardal *et al.*, 2007). Recently it has been proposed that type II cells may function as ATP amplifiers during chemotransduction via activation of pannexin-1 (a gap junction like protein) and P2Y2 receptors (Zhang *et al.*, 2012).

The CB is strategically located bilaterally in the bifurcation of the common carotid artery (**Figure 1B**), the artery that provides the main oxygenated blood supply to the brain. The arterial blood flows into the CB through a short artery, a branch of the internal or external carotid artery, which ends in a dense capillary network that supplies a large flow of blood into the organ. Thus, the CB quickly detects changes in PaO_2 and responds to hypoxic (low PaO_2) conditions.

When type I cells detect decreases in PaO_2 they activate a transduction mechanism (in more detail in *Chemotransduction mechanisms for O_2 and CO_2 in the carotid body*) that involves calcium (Ca^{2+}) entry and release of multiple neurotransmitters. There are a large variety of neurotransmitters released from these cells (**Table 1**). Once in the synaptic cleft, the neurotransmitters activate receptors located on type I cells (pre-synaptic receptors), on afferents of the carotid sinus nerve (CSN) (post-synaptic receptors), or both. There are different types of metabotropic and ionotropic pre- and post-synaptic receptors characterized in the CB that have excitatory or inhibitory effects (**Table 2**). The activation of excitatory post-synaptic receptors is translated into an increase of CSN action potential frequency with subsequent depolarization of petrosal

ganglion (PG) neurons and resultant depolarization of a group of specific neurons in the NTS in the brainstem.

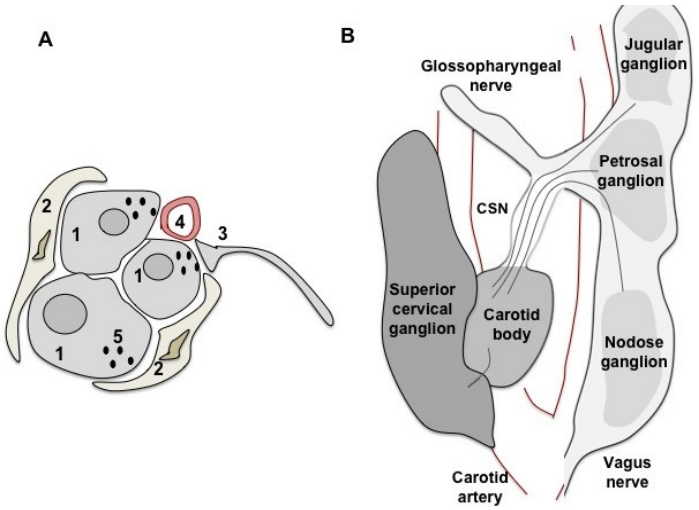

Figure 1 - **Carotid body (CB) peripheral chemoreceptors. A)** Representation of the histological structure of the CB representing the four principal components of this organ: type I cells (1) grouped in clusters and surrounded by type II cells (2), sensory nerve endings (3) originated from the carotid sinus nerve and capillaries (4). Synaptic vesicles (5) are a characteristic of type I cells. The CB also contains a large fraction of connective tissue. **B)** Representation of the carotid artery bifurcation. The CB is at the bifurcation, innervated by sensory fibers originated in the petrosal ganglion via the carotid sinus nerve. The superior cervical ganglion also innervates the CB via ganglioglomerular nerves. (Figure adapted and modified by Gonzalez *et al.*, 1992, Ichikawa, 2002).

The activation of excitatory pre-synaptic receptors (also called autoreceptors) induces an increase in intracellular Ca^{2+}, $[Ca^{2+}]_i$, and subsequent release of other neurotransmitters/ neuromodulators from the CB that can thus bind to excitatory or inhibitory receptors (e.g. the effect of Ach reviewed in (Shirahata *et al.*, 2007)). Although some of the neurotransmitters are shown to be important mediators of hypoxic sensitivity, they may also be responsible for the transduction of other stimuli in the CB (for a review, (Gonzalez *et al.*, 1994)). The CB not only senses changes in PaO_2, but in $PaCO_2$, pH and glucose, cytokines, circulating hormones, extracellular ions (K^+), osmolarity and temperature, thereby acting as a polymodal receptor (Gonzalez *et al.*, 1994, Kumar, 2009). The excitatory/ inhibitory effect on the CSN activity of the neurotransmitters released can vary between species (e.g. dopamine exerts inhibitory effects on the CB in most species, except rabbit, (Iturriaga *et al.*, 2009)).

Table 1 - Neuropeptide /Neurotransmitters/ Neuromodulators present in the carotid body**.**

NP/NT /NM		Localization					Species	Ref
		TIC	CA	PG	CB	G		
Neuropeptides	SP	+	+	+	+		Cat, guinea pig, rat, monkey, feline, rabbit, canine	1
	NA	+	+				Cat	2
	ENK	+	+				Cat, rat, rabbit, piglet, dog, human	3
	NY	+	+				Rat,	4
	ANP	+					Cat, human	5
	GA	+	+	+			Guinea pig, monkey, rat, chicken	6
	CCK	+					Dog, human	7
	VIP	+	+		,		Cat, rat, dog, pig, monkey, human	8
	CGRP		+	+			Mammals, birds and amphibious	9
	AM	+					Rat, human	10
	NTSin	+					Human and experimental animals	11
	ST		+				Chicken, guinea pig, amphibious	12
	BO				+		Human	13
	AT II	+			+		Rat	14
	KISS	+					Rat, human	15
NT/ neuromodulators	DA	+		+	+		All mammalian species	16
	NE	+	+	+			Mouse, rat	17
	ADO				+		Rat	18
	5-HT						Human, rat, mouse, chicken	19
	GABA	+					Mouse, cat, rat	20
	Ach	+			+		Cat, rat, rabbit, cat	21
	ATP	+					Cat	22
	NO					+	Rat, cat	23
	CO	+					Rat, cat	24

NP, neuropeptide; *NT*, neurotransmitter; *NM*, neuromodulator; *TIC*, type I cells; *CA*, carotid artery; *PG*, petrosal ganglia; *CB*, whole carotid body; *G*, glossopharingeal nerve; *SP,* Substance P*; NA,* Neurokinin A; *ENK,* Leu- and Met- enkephalins; *NY,* Neuropeptide Y; *ANP*, Atrial natriuretic peptide; *GA*, Galanin; *CCK,* Cholescystokinin; *VIP,* Vasointerstinal peptide; *CGRP,* Calcitonin Gene-related peptide; *AM,* Adrenomedullin; *NTSin*, neurotensin; *ST,* Somatostatin*; BO,* Bombesin; *ATII,* Angiotesin II; *KISS,* Kisspeptin1; *DA,* Dopamine; *NE,* Norepiniphrine; *ADO,* Adenosine; *5-HT,* Serotonine; *GABA,* gamma-aminotutyric acid; *Ach,* Acetylcholine; *ATP,* adenosine triphosphate; *NO,* nitric oxide; *CO,* carbon monoxide.

References:

1-for a review see Heym and Kummer, 1989; **2**-Prabhakar et al, 1989; **3**- for a review see Porzionato et al, 2008; **4**- Oomori et al, 1991, 2002; **5**-Wang et al, 1991,Benvenuti et al, 1996; **6**- for a review see Porzionato et al, 2008, Heym and Kummer, 1989; **7**- for a review see Porzionato et al, 2008, Heym and Kummer, 1989; **8**- for a review see Heym and Kummer, 1989, Smith et al, 1990; **9**-for a review see Porzionato et al, 2008; **10**- Martinez et al, 2003; Porzionato et al, 2006; **11**- for a review see Porzionato et al, 2008; **12-** for a review see Porzionato et al, 2008; **13**- Smith et al, 1990; **14**- Lam and Leung, 2002; **15**-Porzionato et al, 2011; **16-** For a review see Gonzalez et al, 1994; **17**- Oomori et al. 1994; Christie and Hansen, 1983; **18**- Conde et al, 2004; **19**- Perrin et al, 1986; Oomori et al, 1994; Kameda et al, 1990; **20**-Oomori et al. 1994; Igarashi et al, 2009; Fearon et al, 2003; **21**- Wang et al 1989; Fidone et al, 1976; **22**- Bock P, 1980; **23**- For a review see Campanucci *et al.*, 2012; **24**- Prabhakar *et al*., 1994.

The expression and activity of specific neurotransmitters and their receptors changes with postnatal development (Bairam and Carroll, 2005), and can influence CB function during development.

CO_2 central chemoreceptors

The central chemoreceptors mainly sense changes in CO_2/pH in the brain. The levels of CO_2/pH in the brain are determined by changes in $PaCO_2$ that occur when alveolar ventilation decreases with a constant rate of CO_2 production in the tissues, or vice-versa. The arterial blood reaches the brain through the carotid and vertebral arteries. Since the CB is located at the bifurcation of the carotid artery, this organ detects changes in $PaCO_2$ quicker than the brain and modulates the central chemoreceptors sensitivity. The carotid and vertebral arteries supply blood to the surface of the ventral medulla and send penetrating dorsal branches deep into the tissue, where some central CO_2 chemoreceptors have been identified: surface of the ventrolateral medulla (VLM), the raphe nuclei (RN), the retrotrapezoid nuclei (RTN), the preBötC, the locus coeruleus (LC), and the NTS (reviewed in(Nattie, 1999)) **(Figure 2)**. Since CO_2 is highly diffusible, when $PaCO_2$ rises, it easily crosses the blood brain barrier (which is relatively impermeable to H^+ and HCO_3^- ions) and diffuses (from the cerebral blood vessels) into the cerebrospinal fluid (CSF), changing the pH. In this sense, the central chemoreceptor neurons predominantly sense alterations in pH in response to CO_2, (i.e., CO_2/H^+ sensing, (Lahiri and Forster, 2003, Putnam *et al.*, 2004)). However, evidence supports the existence of direct CO_2 sensors, which have been demonstrated in the LC and the VLM (Filosa and Putnam, 2003). The levels of CO_2 in the brain are also influenced by the rate of CO_2 production in the medullary tissue and blood flow.

Table 2 - Neuropeptide /Neurotransmitters/ Neuromodulators Receptors.

NT/ NM	Receptor Subtype	Receptor Metabotropic	Receptor Ionotropic	Effector/ Response	Effect on CSN activity	Species	Localization	Ref
DA	D_1	G_s	------	AC stimulation, ↑cAMP	-------	Rat, cat, rabbit	Type I cells/PG/SCG	1
	D_2	G_i/G_0	------	AC inhibition, ↓cAMP	(-)[a]	Rat, rabbit, cat, mouse C57BL/6, human	Whole CB, PG and SCG, type I cells of CB, nerve endings	2
NE	α_{2A}	G_i/G_0	------	AC inhibition, ↓cAMP; PLAs2 stimulation	(-)	Rat, rabbit, cat	SCG (rat), type I cells (rabbit and cat)	3
	β_2	G_s	------	AC stimulation, ↑cAMP	(+)	rat	Whole CB	4
Ach b)	M_2/M_4	Gi/Go	------	↓cAMP, ↓PKA and ↑Ca^{2+} from intrastores	------	cat	CB, SCG, PG	5
	M_1/M_5	G_q/G_{11}	------	↑PLC, ↑PIP2, ↑IP3 and DAG	(+)	Cat	CB, SCG, PG	6
	α4 α7 and ß2, α4ß2 hete α3, α4, α7??, ß2, ß4, α3, α4, α5, α7??, α ? α 4 α3, α7, ß2	------	✓	↑Na+, ↑K+, ↑Ca2+ from extracellular	(+)	rat	type I cells, PG, CSN afferents	7
						Cat	Whole CB s, SCG, PG	8
						M ice (C57BL/6)	CB tissue sections	9
						Human	Whole CB	10
ATP	P2X2/3, P2X3, P2X2, $P2Y_1$	----------	✓	↑ Ca^{2+}	(+)	Rat, cat, humans, mouse	Petrosal ganglion afferents, whole CB, SCG	11
		$G_q/G_{11}, G_i/G_0$	------	PLC stimulation with IP_3	(-) ??	rat	type I cells	12
	$P2Y_{12}$	$G_q/G_{11}, G_i/G_0$	------	PLC stimulation	(-) ??	rat	type II cells	13
ADO	A_1	G_i/G_0	------	AC inhibition	(-) ??	rat	PG	14
	A_{2A}	Gs	------	AC stimulation	(+)	rabbit	Type I cells	15
						Rat, human,	Whole CB, post synaptically on CSN	16
	A_{2B}	Gs	------	AC stimulation	(+)	rat	Whole CB	17
5-HT	5-HT_{2A}	$G_q/G_{11}, G_i/G_0$	-----	PLC+, AC -	(-)	rat	type I cells, PG (just a few in P G)	18
	5-HT_3	---	✓	(+)	Na+, K+, Ca2+	rat	PG	19
	5-ht_{5A}	G_i/G_0	---	(-)	AC inhibition	rat	Type I cells and PG	20

a) Mainly inhibitory, occasionally excitatory (rabbit; Iturriaga et al, 2004); **b)** Although in rat there is less characterization of these receptors, in other species, cat and rabbit, the nAchR α3,4,5,7, and ß2,4 are present in type I cell, α7 in the CNS afferents and α3,4,7, and ß2,4 in PG; the mAchR M1 and M2 are in type I cells, M1 in CSN afferents and M1 and M2 in PG neurons (for a revision, Shirahata e tal, 2007);

?, suggested, but no direct evidences; *Gs*, G protein stimulatory; *Gi/Go,* G protein inhibitory; *AC*, adenylyl cyclase; *PLA2*, phosholipase A2, *PLC*, phospholipase C, *PLD*, phospholipase D, *PIP2,* Phosphatidylinositol4-5-biphosphate; *IP3,* Inositol triphosphate; *DAG*, Diacylglycerol, D, (+) excitatory, (-) inhibitory; *DA*, dopamine; *NE*, norepiniphrine, *Ach*, acetylcholine, ATP, adenosine triphosphate, *ADO*, adenosine, 5-HT, serotonine, *PG,* Petrosal ganglia; *SCG,* Superior cervical ganglia; *CB,* carotd body.

Ref: 1 Bairam et al, 1998; Bairam et al, 1997; Czyzyk-KrZeska et al, 1992, Kahlin et al, 2010, Fagerlunde et al, 2010; **2-** Bairam et al, 1997; Czyzyk-KrZeska et al, 1992, Kahlin et al, 2010, Fagerlunde et al, 2010; **3-** Gauda 2002; Almaraz *et al.*1997; Kou *et al.*, 1991.; **4-** Mir e tal, 1983; **5**- Bairam et al, 2006; **6**- Bairam et al, 2006; **7**-Meza RC, 2010, 2012; Niane et al, 2009; Zhong and Nurse, 1997; He et al, 2005; Gauda, 2002; Conde and Monteiro, 2006; **8**- Bairam et al, 2007; **9**- Kahin et al, 2010; **10**- Ferlunger et al, 2010; **11**- Prasal et al 2000, Fagerlun et al, 2010; Bairam et al, 2007; Rong et al, 2003; **12**- Xu et al, 2005; **13**- Xu et al, 2003; **14**- Gauda et al, 2002; **15**- Rocher et al, 1999; **16**- Kobayashi et al, 2000, Fagerlung et al, 2010; **17**- Kobayashi et al, 2000; **18**- Zhang et al 2003; **19**- Wang et al 2002; **20**- Wang et al, 2000;

Table 2 – cont.

NT/ NM	Receptor			Effector/ Response	Effect on CSN activity	Species	Localization	Ref
	Subtype	Metabotropic	Ionotropic					
Histamine	H_1	G_q/G_{11}	------	AC stimulation	(+)	Cat, human	Type I cells , PG	21
	H_2	G_s/G_{11}	------	PLC stimulation	?	cat	Whole CB	22
	H_3	G_i/G_o	------	AC inhibition	(-)	Cat, human	type II cells, PG	23
S P	NK_1	Gs	------	PLC stimulation	(+)	rat	SCG, PG	24
	NK_2, NK_3	Gs , G_q/G_{11}	------	AC stimulation?				
ET	ET_A	G_q/G_{11}	------	PLC, PLA2, PLDstimulation,	?	rat	type I cells	25
EPO	EPORc)	------	------	c)	?	rat	CB clusters	26
Trophins	TRKBd)	------	------	d)	?	?	Cell type I	27
Kiss	KissR	G_q/G_{11}	------	PLC stimulation	?	Rat and human	Type I cells, SCG	28
Cytokine	IL-1B, IL-6Rx, IL-1RI	------	------	e)	(+)	rat	CB, type I cells	29
	TNF-R1, TNF-R2 f)	------	------	f)	(-)	Cat, rat	Glomus cells	30
	TLR4g)	------	------	g)	?	rat		31
	Ob-Ra, ObRb, OB-RC, Ob-Rf	------	------		?	Rat and human	Type I cells	32
Angiotensin II	AT1	Gq/G11	------	PLC stimulation	(+)	rat	Type I cells	33
ENK	δ ??	Gi/Go ??	------	AC inhibition	(-)	Rat	w hole CB ??	34
GABA	$GABA_A$	------	✓	increases Cl^-	(-)	Rat	Sensory nerve (CSN) endings	35
	$GABA_A$ ($\alpha 2, \alpha 3, b3, g2$)	------	✓	increases Cl^-	(-)	cat	Type I cells, and cell bodies and nerves of PG	36
	$GABA_A$ ($\alpha 2, b3, g2$)	------	✓	Increases Cl^-	(-)	human	Whole CB	37
	$GABA_B$	Gi/Go	------	AC inhibition	(-)	Rat, mouse	Type I cells	38

There is some controversial with the role of histamine: while some considered that it is an excitatory NT in type cells, others (Burlon et al, 2009) do not, considering that the excitatory effect may be mediated by terminal afferents; c) EPOR contains a number of of phosphotyrosines that are phosphorylated by JaK2 and serve as docking sites for a variety of intracellular pathway activators and Stats; d) TrKB has the highest affinity to the binding of brain-derived neurotropjic factor (BDNF) and NT4. TrKB receptor is a tyrosine knase family receptor; ??, suggested, but no direct evidences; GABA, gamma-aminobutyric acid, *ENK*, enkephalins, *SP*, substancia P, *ET*, endothelin

Ref: **21**- Lazarov et al, 2009; Del Rio et al, 2008; **22**- Del Rio et al, 2008; **23**- Lazarov et al, 2009; Del Rio et al, 2008; **24**- Gauda et al, 2002; **25**- Chen et al, 2002; **26**- Lam et al, 2009; **27**- Porzionato et al, 2008; **28**- Porzionato et al, 2011; **29**- Lam et al, 2008; Wang et al, 2002, 2007; **30**- Fernandez et al, 2011; **31**- Fernandez et al, 2011; **32**- Porzionato et al, 2011; **33**- Fung et al, 2001; **34**- Gauda 2002; **35**- Zhang et al 2009; **36**- Igarashi et al, 2009; **37**- Fagerlung et al, 2010; **38**- Fearon et al, 2003 ; Oomori et al, 1994.

Some areas of the cerebellum, hypothalamus and midbrain have also been identified as areas with chemoreceptor properties (Nattie, 1999) **(Figure 2)**. It has also been demonstrated that glia cells in the brain also detect changes in CO_2 /H^+(Erlichman and Leiter, 2010).

These central chemoreceptor sites have specific characteristics that are presented in Table 3. The putative contribution of these putative regions to the overall ventilation may depend on the stimulus intensity, neurotransmitter content, arousal state, maturation and gender (Table 3; Nattie, 1999).

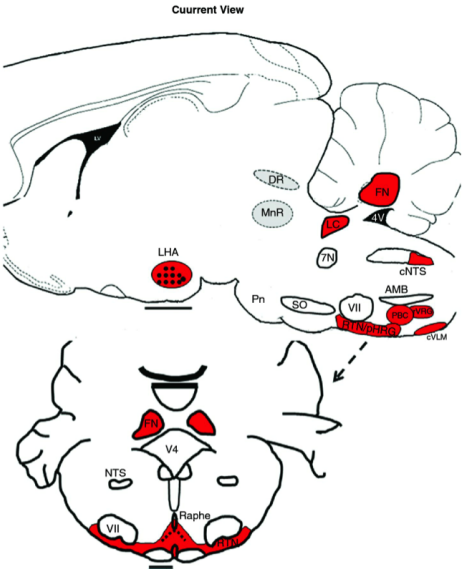

Figure 2 - CO_2 central chemoreceptor localization. LHA, lateral hypothalamus; DR, dorsal raphe; FN, fastigial nucleus; 4v, fourth ventricle; LC, locus coeruleus; 7N, facial nerve; cNTS, caudal nucleus tractus solitarious; AMB, ambiguous; VII, facial nucleus; SO, superior olive; PBC, pre-Botzinge complex; rVRG, rostral ventral respiratory group; cVLM, caudal ventrolateral medulla; RTN/pFRG, retrotrapezoid nucleus/parafacial respiratory group; and Pn, pons. Adapted from Nattie and Li, 2012.

Changes in CO_2 are closely linked to changes in O_2. Although the main O_2 sensors are located in the peripheral chemoreceptors in the CB, as previously mentioned, some central regions also have been identified as O_2-sensitive sites (VLM, NTS, preBötC) (for a review (Neubauer and Sunderram, 2004)).

Table 3- Characteristics of the central CO_2 chemoreceptors

CO_2 site	Location	Neuron type	CO_2 maturation	Stimuli
RTN	Located 130-230 µm from the ventral surface of the medulla and in the marginal glial layer	Glutaminergic	Fully developed at birth and does not change during the 1st two weeks of life	Extracellular pH (pHe)
Raphe nucleus	Medullary raphe located in close proximity to the VLM surface, while the dorsal raphe is found at the surface of the midbrain	Serotonergic	Increase in neurons responsive to hypercapnia during the 1st two weeks. (Wang et al, 1999)	pH
VLM	Located in the braistem	Purinergic	N/A	pH, CO_2
LC	Located at the ponto-medullary border, underneath the 4th ventricle in the pons	Noradrenergic/ catecholami-nergic	No activation in newborn (Wtckstrom et al, 2002); mature electrophysiological responses on Postnatal day (P)1 (Struden et al 2001) and reduction of sensitivity and magnitude of the chemosensory responses around P10 (Nichols et al, 2008).	pH, CO_2
NTS	Located superficially in the dorsal medulla and surrounds the 4th ventricle	Glutaminergic	Fully developed at birth (Conrad et al, 2009)	pH
Pre botzinger	Site of the inspiratory rhythm generation	Glutaminergic	N/A	pH
glia	Astrocytes of the VLM	Purinergic	N/A	CO_2
Lateral hypo-thalamus	Lateral region of the hypothalamus	Orexinergic	N/A	pHe

(Adapted from Hempleman and Pilarski, 2011; Huckstepp and Dale, 2011.)

Integration of peripheral, central chemoreceptors and respiratory neurons

Breathing is tightly regulated by peripheral and central chemoreceptors, which modulate the activity of the respiratory neurons (**Figure 3**). As stated by Smith and co-workers (Smith *et al.*, 2010), "… central and peripheral chemoreceptors are not functionally separate but rather that they are dependent upon one another such that the sensitivity of the medullary chemoreceptors is critically determined by input from the carotid body chemoreceptors and vice versa, that is, they are interdependent".

The excitatory neurotransmitters released by CB type I cells evoke action potential discharge in CSN fibers, which projects to the central pattern generator in the brainstem. The chemo afferents terminals contain glutamate, which binds to NMDA and non-NMDA receptors on second order neurons in the commissural subnucleus of the NTS, a CO_2 central chemoreceptor area, which contains dorsal respiratory group neurons (DRG) (Vardhan *et al.*, 1993) (see **Figure 3C**). The DRG neurons consist mainly in inspiratory neurons that project to cervical and thoracic spinal motor neurons of the phrenic and intercostal nerves to induce the contraction of the diaphragm and external intercostals and subsequently inhalation. It also contains interneurons that project to other CO_2 sensitive areas and/or other respiratory neurons located in the ventral respiratory group (VRG), which contains inspiratory and expiratory (project to the abdominal and internal intercostals) neurons (Smith *et al*., 2009). The rostral VRG contains neurons that project to low motor neurons that innervate the larynx, pharyngeal and upper airways (**Figure 3C** and **D**). The ventral respiratory region contains important respiratory nuclei including the Bötzinger complex and the preBötC (also CO_2 chemosensitive) involved in rhythmogenesis and setting breathing frequency and are regulated by the pontine respiratory group neurons (PRG). The PRG also connects and interacts with the NTS and the hypothalamus (for a review, (Nattie, 1999)).

Inputs from chemoreceptors, via glutamatergic projections from the NTS, converge in the RTN (Takakura *et al.*, 2006). RTN has been recently considered a site of integration between peripheral, central and respiratory neuronal groups since RTN neurons also receive innervations from the medullary raphe (Dias *et al.*, 2008), orexinergic neurons of the lateral hypothalamus (Fortuna *et al.*, 2009) and the caudal VLM, and the RTN neurons project to the central pattern generator in the VRG (Smith *et al.*, 1989; Guyenet *et al*., 2008), activating the inspiratory and expiratory neurons and thus inducing ventilation until PaO_2 and $PaCO_2$ reach

their normal levels. The RTN neurons are subject to negative feedback from the respiratory neurons (Guyenet *et al.*, 2005).

The overall chemosensory activity results in/induces hyperventilation, stimulation of the sympathetic nervous system and modulation of arterial peripheral resistance and cardiac output (Gonzalez *et al.*, 1994). **Figure 3** summarizes the control of breathing from the peripheral to central regions to adjust PaO_2 and $PaCO_2$ to normal levels.

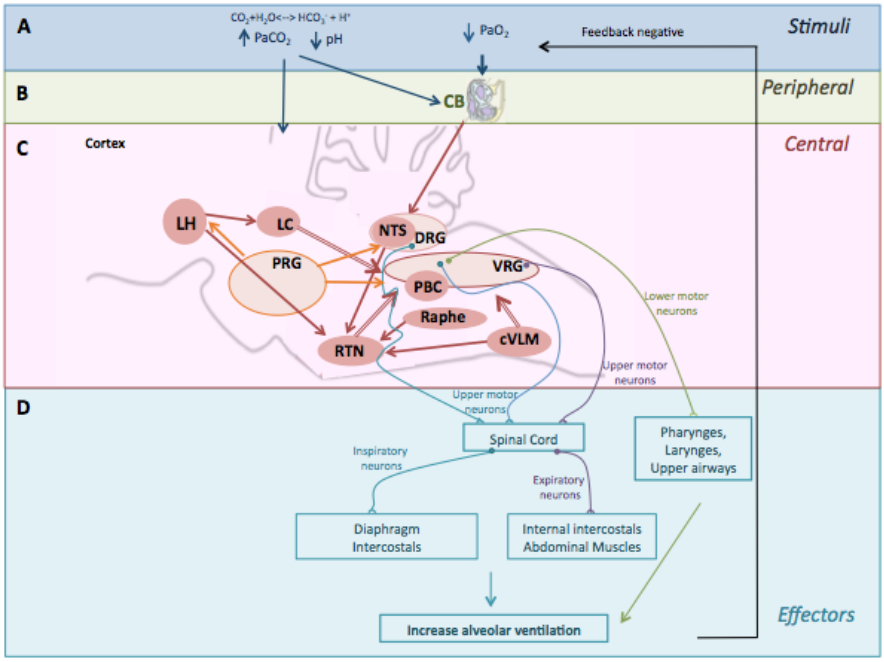

Figure 3 - **Chemoreceptor control of breathing**. PaO_2, $PaCO_2$ and pH are tightly regulated by the organism though specific chemoreceptors located in peripheral and central nervous system. Changes in the arterial pressure of these gases (Panel A) activate peripheral chemoreceptors (carotid body, CB, Panel B) and central chemoreceptors (Panel C). CB senses primarily changes in O_2 but also in CO_2/pH (blue arrows, Panel B). Central chemoreceptors are the main CO_2 sensors through activation by changes in pH or directly by CO_2. Multiple CO_2 chemosensitive areas have been identified in the brainstem and are interconnected (chemoreceptor areas in full pink circles, and connection is red arrows, Panel C). The medulla also contains the respiratory neuronal groups (PRG, DRG and VRG) that control the neurons that activate the respiratory effectors (Panel C and D). PRG modulates DRG and VRG (Panel C). DRG contains primarily inspiratory neurons and VRG contains both inspiratory (rostral) and excitatory (caudal) neurons that depolarize the motor neurons to induce ventilation (Panel D). Light blue lines represent inspiratory neuron; purple lines represent excitatory neurons.
CO_2, carbon dioxide; *O_2*, oxygen; H_2O, water; HCO_3^-, ion bicarbonate; *PaO_2*, partial pressure of O_2 in arterial blood; *$PaCO_2$*, partial pressure of CO_2 in arterial blood; *CB*, carotid body; *LH*, lateral hypothalamus; *LC*, locus coeruleus;, nucleus tractus solitarius; *RTN*, retrotrapezoid nucleus; *PBS*, pre-botzinger complex; *VRG*, ventral respiratory group; *DRG*, dorsal respiratory group; *cVLM*, caudal ventrolateral medulla; *PRG*, pontine respiratory group.

Chemotransduction mechanisms for O_2 and CO_2 in carotid body

Mammalian organisms have evolved exquisite mechanisms to detect and respond to changes in O_2 and CO_2 levels. The first part of this introduction was focused on the integration of O_2 and CO_2 peripheral and central chemoreceptors to ultimately induce ventilation. This second part is mainly focused on the known cellular transduction mechanisms that occur in the CB in response to stimuli.

Type I cells of the CB sense changes in O_2 and CO_2 through sensors that are likely to trigger different cellular events (at the level of the transduction cascade), but all evoke, although in a different extend, discharge of the CSN. Even though differences between species and developmental stage occur, in the adult cat, the discharge of the CSN is initiated when PaO_2 decreases from 100 to 70-75 mmHg (for a review (Gonzalez *et al.*, 1994)). The maximum CSN discharge occurs when the PaO_2 decreases to 10-15 mmHg; below a PaO_2 of 10 mmHg the activity of the CSN is maintained at a constant level or decreases (for a review (Gonzalez *et al.*, 1994)). The threshold for CO_2 excitation of the cat CB is 25 mmHg (Eyzaguirre and Lewin, 1961) and the CSN discharge tends to plateau at a $PaCO_2$ greater than 100 mmHg (Lahiri and Forster, 2003). The CSN responses to CO_2 in rats, as compared to cats, are smaller with no apparent developmental maturation (for a review (Donnelly, 2005)). The O_2-induced responses in the CSN increase throughout development until full maturity is reached after 2 weeks of age in rats (for a review (Donnelly, 2005)). When low O_2 (hypoxia) and high CO_2 (hypercapnia) are applied together, the response (CSN discharge) in the adult rat is greater than the sum of these two stimuli when applied separately (multiplicative interaction) (Pepper *et al.*, 1995).

The following sections are devoted to the cellular mechanisms that occur in type I cells in response to different O_2/CO_2 concentrations, to induce the activation of the CSN chemosensory fibers above described.

O_2 sensing mechanism

Although different chemotransduction hypotheses have been proposed for O_2 sensing in the CB (membrane and mitochondrial hypothesis, for a review see Gonzalez *et al.*, 2010 and Gonzalez *et al.*, 1994), the general consensus for the O_2-sensing mechanism is that hypoxia inhibits O_2 sensitive K^+ channels (a Ca^{2+} and voltage dependent K^+ channel (Br_{Ca}) and a non-voltage dependent "leak channel" (TASK)), which depolarizes the membrane of type I cells (Peers, 1990, Lopez-Barneo *et al.*, 1988, Gonzalez *et al.*, 2009). Type I cell membrane depolarization activates Ca^{2+} channels, with a consequent increase of Ca^{2+}_i (Buckler and Vaughan-Jones, 1994a),and release of neurotransmitters (**Figure 4**).

As mentioned earlier (*Peripheral chemoreceptors- Carotid bodies* section), some of the neurotransmitters released initiate afferent CSN discharge (of note, the release of neurotransmitters is not essential for hypoxic chemotransduction, Donnelly, 1996). It has been proposed that ATP and acetylcholine (co-released) are the main excitatory neurotransmitters that induce CSN discharge in response to hypoxia through their ionotropic receptors present in the afferent terminals (Zhang *et al.*, 2000).

The response mediated by neurotransmitters that bind to ionotropic receptors is fast since it involves Ca^{2+} entry, which rapidly induces cellular responses. However, acetylcholine-ATP co-transmission does not entirely mediate all of the responses of the CB to hypoxia (Reyes *et al.*, 2007, Donnelly, 2009). Adenosine receptors have also been identified on chemoafferents and recent data supports a key role of this neurotransmitter in hypoxic chemotransmission (Conde *et al.*, 2009, Conde *et al.*, 2012, Niane *et al.*, 2012).

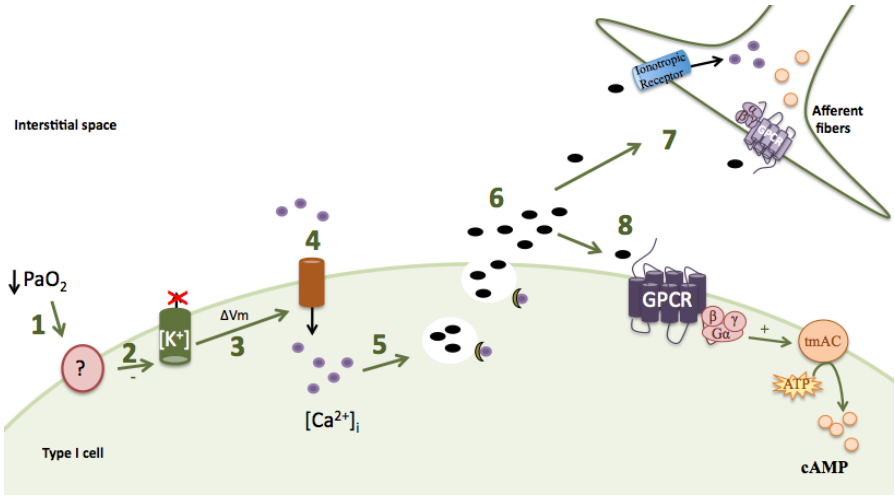

Figure 4- Steps in O_2 chemotransduction mechanim in CB type I cells. A decrease of PaO_2 **(1)** inhibits K^+ channels **(2)**, with consequent depolarization of the cell membrane **(3)**, and opening of calcium channels **(4)**. The levels of intracellular calcium increase (**5)** and bind to the vesicles containing neurotransmitters through synaptotagmin. The neurotransmitters released **(6)** can bind to ionotropic and metabotropic pos-sinaptic receptors in afferent CSN fibers **(7)** and/or pre-synaptic receptors in type I cells **(8)**. The activation of metabotropic receptors modifies transmembrane adenylate cyclase, tmAC, activity and consequent production of cAMP.
O_2, oxygen; *PaO_2*, partial pressure of O_2 in arterial blood; *CB*, carotid body; *K^+*, ion potassium, *Ca^{2+}*, ion calcium; *NTS*, nucleus tractus solitarius; ΔVm, change in voltage, *AC*, adenylate cyclase; *cAMP*, cyclic AMP

Adenosine (and other neurotransmitters) binds to pre- and pos-synaptic metabotrophic receptors, coupled to G-proteins (GPCR, G-protein coupled receptors) that modulate adenylyl cyclase (AC) activity and thus, cyclic AMP (cAMP) levels. The response mediated by neurotransmitters that bind to GPCR is slower than the one mediated by ionotropic receptors, since it modulates the production of the second messenger, cAMP, and consequent activation of cAMP-signaling cascades. Thus, it has been suggested that the cAMP-signaling pathway mediates the hypoxic transduction mechanism in the CB (for a review (Gonzalez *et al.*, 1994)), which will be discussed in more detail in the *Role of cAMP in O_2 and CO_2 detection in the Carotid body* section.

CO_2 sensing mechanism

The CO_2 sensing mechanisms within the CB that mediates a hyperventilatory response are not completely understood. Under physiological

conditions, CO_2 is in constant equilibrium with HCO_3^- and H^+ through the reaction catalyzed by carbonic anhydrases in type I cells (CAH, Ridderstrale and Hanson, 1984). CAH are divided in subgroups according to their cellular localization: cytosolic (CAH-I, CAH-II, CAH-III, CAH-VII, CAH-VIII, CAH-X, CAH-XI and CAH-XIII), mitochondrial (CAH-VA and CAH-VB), secreted (CAH- VI), membrane-bound (CAH-IV and CAH-XV) and transmembrane (CAH-IX, CAH-XII, CAH-XIV) (Supuran, 2008). Althought the precise localization of the CAH in the CB is controversial, there is evidence showing that type I and II cells, and nerve bundles are immunoreactive for CAH-I, II and III isoforms (cytosolic isoforms) (Yamamoto *et al.*, 2003). Inhibition of CAH depresses hypercapnia – induced response discharge in *in vitro* CB (Iturriaga *et al.*, 1991). Thus, increases in $PaCO_2$ causes rapid diffusion of CO_2 into the cytosol of type I cells, which increases H^+ and HCO_3^- levels via CAH (**Figure 5.1-2**). A decrease in intracellular pH (increases in H^+) inhibits K^+ channels, with consequent membrane depolarization and voltage-gated Ca^{2+} channel activation (**Figure 5.3)** (Buckler and Vaughan-Jones, 1994). The K^+ channels (TWIK-related acid-sensitive potassium, TASK, channels) sensitive to acidic stimuli are also sensitive to hypoxia, and thus, it is a site of convergence for hypoxia and hypercapnia chemosensitive signaling in rat type I cells (Buckler *et al.*, 2000). It has also been demonstrated that acidosis can modulate pH regulatory transporters (Na^+/H^+ exchange, NHE), promoting the reversal of Na^+/Ca^{2+} exchange, which results in elevated Ca^{2+}_i concentrations (**Figure 5. 4)** (Rocher *et al.*, 1991). The acidic stimuli increases CSN firing rate, either by inducing release of neurotransmitters, or by activating directly the CSN endings or by making them more sensitive to neurotransmitters released from type I cells (Rigual *et al.*, 1984). The type I cells also contain Na^+ Cl^-/HCO_3^- exchanger and HCO_3^- channels (Rocher *et al.*, 1991).

From the neurotransmitters released, adenosine seems to enhance the response under hypercapnic conditions, a mechanism suggested to be mediated by adenylyl cyclases coupled to GPCRs inducing an increase in intracellular cAMP (Kumar *et al.*, 2000). Both acidic and isoydric hypercapnia induces the

release of ATP and acethylcholine from co-cultures of type I cells and petrosal neurons (Zhang and Nurse, 2004); these neurotransmitters bind to ionotropic receptors increasing $Ca^{2+}{}_i$.

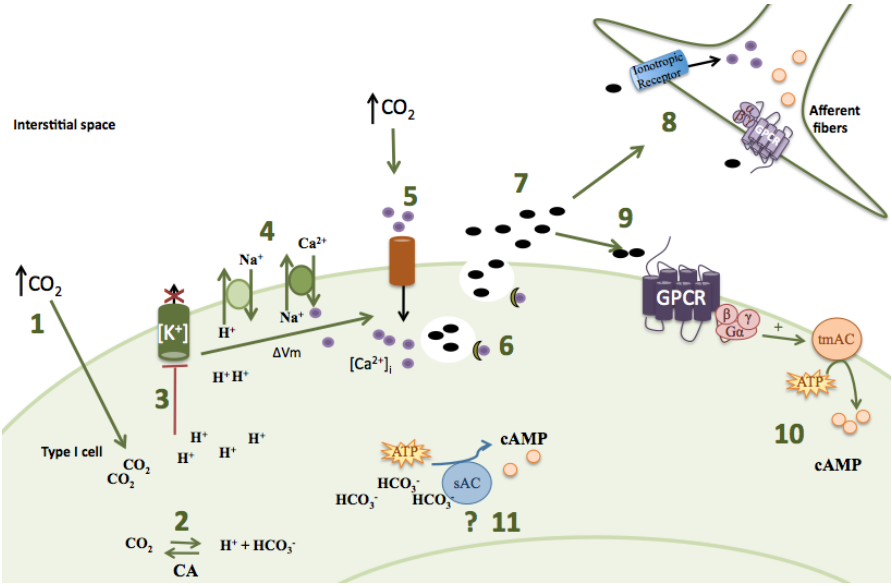

Figure 5 - CO_2 chemotransduction mechanim in CB type I cells. Increases in $PaCO_2$ **(1)** diffuse to the cytosol of type I cell where, by the action of carbonic anhydrase, CA **(2)** is converted in H^+ and HCO_3^-. The protons inhibit potassium, K^+, channels **(3)** with consequent cell depolarization, ΔVm, and opening of calcium channels **(4).** The intracellular calcium, Ca^{2+}, levels increase in the cell **(5)** and induce neurotransmitter release **(6-7).** Some neurotransmitters activate metabotropic receptors **(8-9)** with activation of adenylate cyclase, AC and consequent increase in cAMP levels **(10)**. Some authors propose that acidosis activate pH regulatory transporters (Na^+/H^+ exchange and Na^+/ Ca^{2+} exchange) **(4)**. It has also been suggested that HCO_3^- can activate soluble adenylate cyclase, sAC, increasing cAMP levels in the cell **(11).**
CO_2, carbon dioxide; *$PaCO_2$*, partial pressure of CO_2 in arterial blood, ΔVm, change in voltage, tm*AC*, trasnmembrane adenylate cyclase ; *cAMP*, cyclic AMP.

There is also evidence for an independent CO_2 effect: Summers and collegues (Summers *et al.*, 2002) suggested that CO_2 could activate Ca^{2+} currents directly leading to increased $Ca^{2+}{}_I$, through a cAMP and protein kinase A (PKA)-dependent pathway (**Figure 5.5).** Although it is unknown how molecular CO_2 could increase cAMP levels, this group suggested that this mechanism could be mediated by a particular type of enzymes involved in the synthesis of cAMP that are activated by intracellular HCO_3^- (soluble adenylyl cyclase, sAC) (**Figure 5.11)**.

There are many similarities between cellular signaling mechanisms involved in central CO_2 chemosensitive neurons and type I cells: in both types of cells, acidosis inhibit K^+ currents with consequent membrane depolarization. Some central chemoreceptors are believed to be directly sensitive to CO_2, such as LC and VLM, activating L-type Ca^{2+} channels (Filosa and Putnam, 2003), a similar finding that has been also observed in the type I cells (Summers *et al*., 2002). More recently, it has been demonstrated that central CO_2 chemosensitive regions are coupled to each other and to glial cells by gap junctions and recent work has demonstrated a role of connexin 26 in CO_2-dependent release of ATP in the central chemosensitive cells (Huckstepp *et al*., 2010).

Role of cAMP in O_2 and CO_2 detection in the carotid body

As mentioned above, neurotransmitter release increase in hypoxic and hypercapnic conditions, modulating cAMP levels in the CB mainly through adenosine A2a and A2b receptors (Monteiro *et al.*, 1996, Chen *et al.*, 1997, Conde and Monteiro, 2006a, Conde *et al.*, 2006b), ß-adrenoceptor activity (Mir *et al.*, 1984) and dopamine D2 and D1 receptors (Mir *et al.*, 1984, Almaraz *et al.*, 1991, Batuca *et al.*, 2003). Thus, it has been proposed that cAMP could be mediating the O_2/CO_2 sensing transduction mechanism in the CB. However experiments aimed to answer this question were controversy.

While some investigators have observed increases in cAMP levels with hypoxia/hypercapnia, others have not been able to confirm the role of cAMP in the transduction mechanism (**Table 1** in attachment for more details). The small size of the CB, low levels of cAMP detected (in the order of pmol/CB), inter-experiment variability, species and ages differences, dissection methods, different preparations, the intensity of O_2 and CO_2 stimuli, incubation times and cAMP detection methods, have been credited for the discrepancies found in the literature. These differences are summarized in **Table 4** (also table 1 in attachment for more detail).

Table 4 - Effects of different conditions on cAMP levels

[cAMP]	Conditions											cAMP levels detect	cAMP levels	Ref.
	Spec.	Anes.	Prep.	Basal				Challenge						
				O_2 (%)	CO_2 (%)	Time (min)	Inc. media	O_2 (%)	CO_2 (%)	Time (min)	Inc. media			
=	Cat, 12mo.	Na-pentob. 45mg/Kg i.p.	Whole CB, *In vivo*	R.A.	R.A.	n/a	n/a	5	n/a	3,10,20	n/a	RIA	per CB	Delpiano *et al*., 1984
			Whole CB, *In vitro*	30	3	60-120	Locke's	0	3	Fev-60	Locke's+ [IBMX]=0 or 0.8mM			
-	Cat, 12mo.	Na-pentob. 45mg/Kg i.p.	Whole CB, *In vitro*	35	4	180	Locke's mod.	3	4	2	Locke's modified + [IBMX]=0 or 0.8mM	RIA	per CB	Delpiano and Acker, 1991
-	Rabbit, adult	Na-pentob.	Whole CB, *In vitro*	100	0	30	Tyrodes's	10-Mai	0	10	Tyrodes's	RIA	per mg tissue	Wang *et al*., 1989
-	Rabbit, adult	Na-pentob.	Whole CB, *In vitro*	100	0	30	Tyrodes's	10-Mai	0	10	Tyrodes's with [FSK]=0 - 10 µM	RIA	per mg tissue	Wang *et al*., 1990
-	SD adult rats	Na-pentob 50mg/Kg ip	CB slices, *In vitro*	100	0	30	Locke's with theophylin e 10mM	4	0	10	Locke's with theophyline 10mM	immuno	% + cells	Wang *et al*., 1991
-	Rabbit, adult	Na-pentob., 30-40mg/Kg i.v.	Whole CB, *In vitro*	100/95	0/5	30	Tyrodes's	0, 5, 7, 10	20-Mai	10	Tyrodes's in presence or not of [FSK]=10 µM, [IBMX]=500 µM and Ca^{2+} = 2mM	RIA	per mg tissue	Perez-Garcia *et al*., 1990
-	Rabbit, adult	CO_2	Whole CB, *In vitro*	21	5	20	HCO_3^- medium	21	10	5	HCO_3^- medium	EIA	per µg prot	Summers *et al*., 2002
-	Rabbit, adult	Na-pentob., 30-40mg/Kg i.v	Whole CB, *In vitro*	20	5	30	Tyrodes's modified w ith 24 mM HCO_3^-	7	5	10	Tyrodes's modified w ith 24 mM HCO_3^- w ith IBMX 0.5mM in the presence or absence of Ca^{2+}	RIA	per mg/ tissue per mg/prot	Cachero *et al*., 1996
-	Rabbit, adult	Na-pentob., 35-mg/kg ip	Whole CB, *In vitro*	100	0	30	Modified Tyrodes's	5	0	10	Modified Tyrodes's	RIA	per mg/ tissue	Chen *et al*., 1997
=	SD rat, male, adult	Urethane, 1.25µg/Kg i.p.	Whole CB, *In vivo*	R.A	R.A.	n/a	n/a	5	0	05-Fev	n/a	Prot-binding sat.	per CB	Mir *et al*., 1983
=	Wister rat ages	Na-pentob., dose??	Whole CB, *In vitro*	95	5	15	Tyrodes's mod.	95/20/10/5	5	30	Tyrodes's mod.+ [IBMX]=500 µM	EIA	per mg tissue	Monteiro *et al*., 2012

Spec, species; A*nes*, anesthesia; *Prep, p*reparation; *Inc, i*ncubation; *Ref, r*eference; *R.A.,* room air; *RIA,* radioimmunoassay; *EIA,* enzyme immunoassay

The experimental studies included in this dissertation sought to better understand the role of cAMP-signaling pathway in the chemotransduction mechanism of the rat CB. The specific characteristics of the cAMP signaling pathway will be described bellow.

cAMP/signaling pathway

cAMP was discovered by Earl W. Sutherland and Theodore Rall in 1958 (Sutherland and Rall, 1958). The levels of cAMP within the cells are tightly regulated by adenylyl cyclases (AC) and phosphodiesterases (PDE). Activation of one single AC isoform can originate many cAMP molecules, and amplification of the signal can be achieved rapidly. cAMP diffuses throughout the cell, binding and modulating the activity of three types of effectors: protein kinase A (PKA), cyclic nucleotide gated ion channels and exchange proteins activated by cAMP (EPACs). Although there are only three types of effectors that translate its signal, cAMP is able to elicit highly specific cellular effects in response to external stimuli. One of the reasons for this high specificity seems to be the compartimentation of the cAMP in pools in the cells. These pools are maintained by nearby PDE, which are enzymes that hydrolyze cAMP and, thus, regulate and restore basal cAMP levels, and by scaffolding proteins such as AKAPs that are located in the cytosol of the cells or within specific organelles such as nucleus and mitochondria (for a review, Carnegie *et al.*, 2009). Intracellular cAMP levels can also change due to other distinct cellular mechanisms: diffusion from one cell to another through gap junctions (Bevans *et al.*, 1998) or transport to the extracellular milieu (for a review Bankir *et al.*, 2002).

cAMP Pathway- Adenylyl Cyclases

Adenylyl cyclases (E.C.4.6.1.1) catalyze the synthesis of cAMP through the cyclization of ATP and release of an inorganic phosphate. There are two types

of adenylate cyclases: the classic transmembrane (tmAC) and the more recently described soluble adenylyl cyclase (sAC) (for a review Kamenetsky *et al*., 2006). The former (tmAC) mediates intracellular changes due to extracellular signals (e.g. neurotransmitters, hormones) that bind to GPCR (metabotropic receptors). These receptos comprise seven membrane-spanning α-helices that are linked by extracellular and intracellular loops; the largest intracellular loop interacts with the G-protein. The G-protein contains three subunits α, β and γ. When a GPCR is activated, occours a conformational change in the cytoplasmatic domain of the receptor, which dissociates Gα from the $\beta\gamma$ subunit and from the receptor. Then, Gαs activates tmAC. TmAC is also sensitive to forskolin (Hacker *et al*., 1998), Ca^{2+} signaling pathway (Halls and Copper, 2011) and CO_2 (Townsend et al., 2009; Cook et al., 2012). On the other hand, sAC is regulated by HCO_3^- and Ca^{2+} ions, in a pH independent manner (Jaiswal and Conti, 2003, Chen *et al*., 2000).

The mammalian tmAC has been well characterized and the structural information is very well documented. However, structural information for sAC is lacking. The only existing information available for mammalian sAC is derived from the homolog CyaC, an AC from the cyanobacterium *Spinulina platensis*, which contains 26% of protein sequence identity and includes all conserved key amino-acids implicated in catalysis in mammalian sAC enzymes (Steegborn *et al*., 2005). Both tmAC and sAC are composed of two cytoplasmic regions also termed cyclase homology domain (CHD, or C1a and C2a, **Figure 6** and **Figure 7**). These two CHD domains must heterodimerize with each other to create a hydrophobic pocket allowing the ATP and co-factors to bind and activate the enzyme (the catalytic core, **Figure 6B** and **Figure 7B**). In addition, tmAC contains an N-terminal (N) domain, a short C-terminal (C2b) domain, and two transmembrane regions (TM1-6 and TM7-12), consisting of six hydrophobic transmembrane spanning α-helices each, anchoring the enzyme to the plasma membrane (**Figure 6 A**) (Tesmer *et al*., 1997). The TMs contain extracellular N-glycosylation sites that may be important in the regulation and catalytic activity of

the AC. The two TMs and C1a domains are joined by a linker termed C1b, which, depending on the tmAC isoform type, contains different regulatory sites for G-proteins (which influences the relative orientation of the catalytic domains (Topal et al., 2012), Ca^{2+}/ CaM (calmodulin) and protein kinases (**Figure 6 A**). The small differences in the amino acid sequences of the catalytic core (CHD heterodimer) and C1b domain (Tesmer *et al.*, 1997) among the 9 tmAC isoforms have been counted for the specific regulation of each isoform, tissue distribution, and specific roles in mediating physiological responses **(Fig.8,Table 1.2 in attachment)**.

sAC differs from tmAC by lacking the transmembrane domains; in addition to the 2 CHD, sAC contains a large cytoplasmic domain (ca. 1150 residues) present in the full length isoform (sAC_{fL}) but removed by alternative splicing in the short length form of sAC, sAC_{sL} (**Figure 7**). The absence of the large cytoplasmatic domain may be essential for sAC activation.

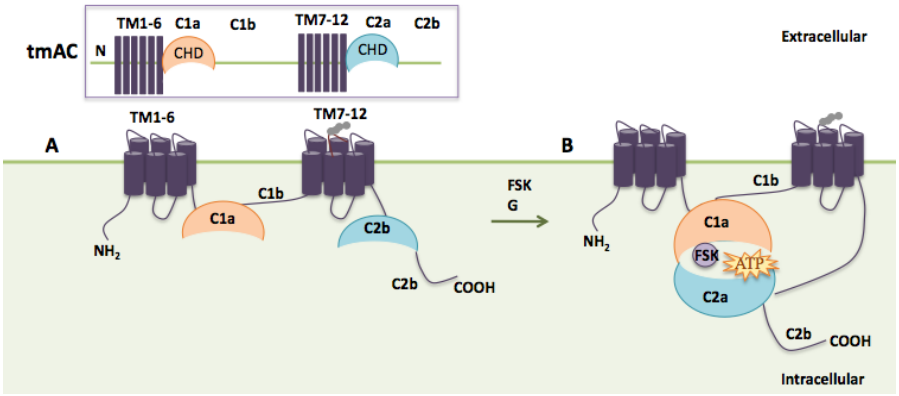

Figure 6- Transmembrane adenylyl cyclase structure. Molecular architecture and mechanism of tmAC activity. (A) tmAC is represented by NH_2 terminus, a first transmembrane cluster (TM), a cytoplasmic region comprising C1a and C1b domains, a second transmembrane cluster (TM) with extracellular N-glycosylation sites and a second cytoplasmatic domain comprising C2a and C2b. B) C1a and C2a dimerize to form the catalytic site, where FSK and ATP bind at opposite sites. FSK anneals the two cytoplasmatic domains by a combination of hydrophobic and hydrogen bonding interactions. tm*AC*, transmembrane adenylate cyclase ;*CHD,* cyclase homogy domain, *FSK,* forskolin.

The characterization of tmAC and sAC is possible using pharmacological tools more specific/sensitive towards each type of enzyme. P-site inhibitors, such as SQ 22536 and 2'3-dd-ADO are nucleotide analogues that bind non-

competitively or uncompetitively to the ATP binding site. Since tmAC has more affinity for ATP than sAC (Km is 30-400 µM vs 1-16 mM), P-site inhibitors are more selective towards tmAC. MDL-12,330A is an irreversible inhibitor, but the mechanism of action is not completely known (Guellaen *et al.*, 1977). Although it is considered to be more selective for tmAC, there is no information regarding its selectivety towards sAC.

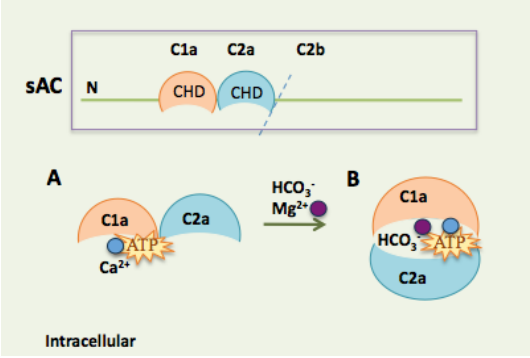

Figure 7- Soluble adenylyl cyclase (sAC) structure. Molecular architecture and representation of sAC structure and mechanism of activity. (A) sAC is composed by two cytoplasm domains C1a and C1b. ATP binds to the open state. (B) Instead of the Asp residue characteristic of the substract binding domais of tmAC, sAC has a Thr, which allows HCO_3^- to bind (Cann *et al.*, 2003). HCO_3^- closes the dimmer and moves the catalytic residues into a favorauble arrangement for cyclization of ATP. Ca^{2+} promotes its activity by increasing the affinity for ATP (Steegborn *et al.*, 2005a). Mg^{2+} ion is also required in the catalytic site of the enzyme to coordinate binding and cycling of ATP. First, ATP with Ca^{2+} bound to its γ-phosphate, coordinates with specific residues in the catalytic center, leaving the CHD dimmer open (open sAC state, **Figure 7A**). Then, HCO_3^- binding recruits a Mg^{2+} ion that binds to the α-phosphate of the ATP, closes the dimmer (closed state) and moves the catalytic residues into an arrangement more favorable for cyclization of ATP (esterification of the α-phosphate with the ribose in adenosine and the concomitant release of the β- and γ-phosphates), **Figure 7B** (Steegborn *et al.*, 2005a).
sAC, soluble adenylyl cyclase, *CHD,* cyclase homology domain, *HCO_3^-,* bicarbonate ion, *Mg^{2} magnesium ion*.

sAC is specifically inhibited by KH7, identified in a small molecule screen with an unknown mechanism of action (Hess *et al.*, 2005), and by catechol derivatives of estrogen, which inhibit sAC by chelating the Mg^{2+} in the active site of the enzyme (Steegborn *et al.*, 2005b). Although adenylyl cyclases are ubiquitously expressed in the organism, the expression and characterization of the isoforms in the CB has never been performed. Evidence supporting the presence of these enzymes in the CB has been demonstrated by activity measurements (Mir *et al.*, 1984) or by the effect of specific neurotransmitter/ neuromodulators

that bind to receptors positively or negatively coupled to this enzyme (Gonzalez *et al.*, 1994). One of the aims of this work was to characterize adenylyl cyclase isoforms in the rat CB and study whether O_2/CO_2 could affect their expression and activity.

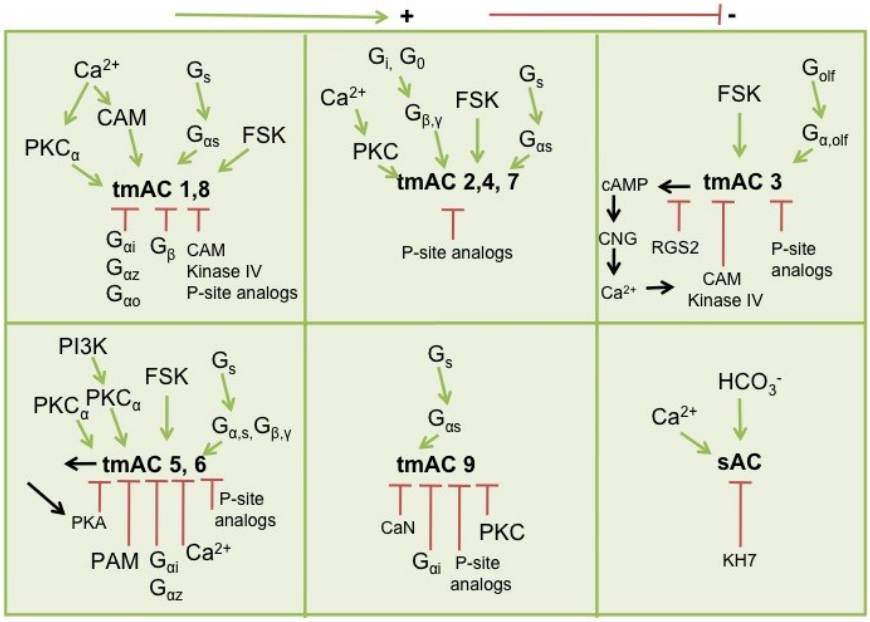

Figure 8- Regulation of adenylate cyclase isoforms.
General patterns of activation (+) and inhibition (-) of the different isoforms. Adapted from (Dessauer, 2009). *CAM*, calmodulin; *FSK*, forskolin; *tmAC*, transmembrane adenylate cyclase; *sAC*, soluble adenylate cyclase; *PKC*, protein kinase C; *CNG*, cyclic nucleotide-gated channel; *RGS2*, regulator of G protein signaling; *PAM*, protein activator od myc; *PI3K*, phosphatidylinositol-3-kinase.

cAMP Pathway- Phosphodiesterases

Phosphodiesterases (PDEs, E.C. 3.1.4.1) catalyze the hydrolysis of the 3'- cyclic phosphate bonds of adenosine 3' 5'-cyclic monophosphate to AMP, terminating the cAMP-signaling cascade. There are 11 PDE families, derived from separate gene families, which differ in their amino acid sequences, endogenous and exogenous regulators and pharmacological properties (**Table 1.3 in attachments**) (Bender and Beavo, 2006). Many of these PDE families have distinct isoforms and splice variants (Bender and Beavo, 2006) (**Table 1.3 attachemnt**). There are over 50 PDE isoforms resulting from the 21 PDE-coding genes identified, most of these are able to generate multiple isoforms. PDEs from

the same family are functionally related to each other through similarities in amino acid sequences, specificity and affinity for cGMP and cAMP, inhibitor specificity, and regulatory mechanisms (**Table 1.3 attachemnt**). PDEs are present ubiquitously in the cell: in the cytosol, plasma membrane, cytoskeleton, and nucleus (Houslay and Adams, 2003) (**Table 1.3, in attachment**). In most cells, PDE3 and 4 are the main players for cAMP hydrolysis.

The general structure of these enzymes consists of two distinct domains: a regulatory domain located at the N-terminus of the protein and a catalytic domain located at the C-terminus (**Figure 9**) (Thompson, 1991). The N-terminal domain contains unique motifs that regulate PDE expression and activity. These motifs are responsible for dimerization, phosphorylation, binding of modulators such as cGMP or Ca^{2+}/calmodulin, interaction with regulatory proteins, and subcellular localization of the PDE isoforms. Thus, the catalytic activities of the PDEs are highly regulated by these motifs, which are inputs from many different pathways. The integration of these signals plays an important role in determining the intensity and duration of the cellular response to external stimulis. This regulatory domain can vary in length and it is a site for alternative splicing, which explains the variety of PDE isoforms that exist (Bender and Beavo, 2006).

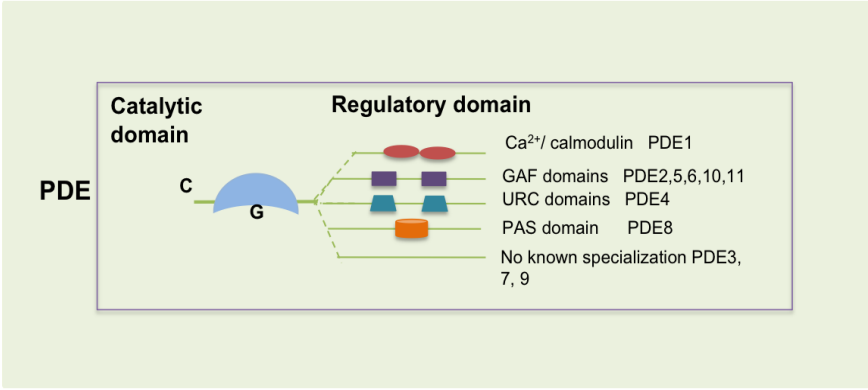

Figure 9- Cyclic nucleotide phosphodiesterase (PDE) structure. PDE have the carboxic domain with the catalytic domain and the regulatory domain. The regulatory domain of the PDE contains unique motifs involved in the regulation of protein expression and enzyme activity. The catalytic domain contains a conserved glutamine (G) that is involved in the nucleotide binding. Adapted from (Menniti *et al.*, 2006). *GAF*, cGMP-specific phosphodiesterases, Adenylyl cyclases and FhlA domain; *URC*, upstream conserved region; *PAS*, Period circadian protein.

The catalytic domain is highly conserved across all isoforms. The molecular mechanisms for specific binding or hydrolysis of the phosphodiester bond are not full understood. The six-member phosphodiester ring of cAMP or cGMP and the purine moiety are critical for the binding with PDEs. The phosphohydrolase reaction involves the nucleophilic substitution of a solvent hydroxyl at the phosphate, disrupting the P-O bond at the 3'oxygen of the ribose (Francis *et al.*, 2001). The catalytic core contains two consensus divalent cation (Zn^{2+} or Mg^{2+})-binding. The cyclic nucleotide binding specificity (either specific to cAMP, cGMP or both) is determined by the orientation of a conserved glutamine in the catalytic pocket (so-called Glutamine switch). In case of a dual-substrate isoform, this glutamine is free to rotate to adapt either orientation (Zhang *et al.*, 2004).

Changes in cAMP levels contribute to many disease states. By degrading cAMP, PDEs are important modulators of cAMP levels, preventing the uncontrolled diffusion of cAMP through the cell and consequently contribute to the formation of localized pools or gradients of cAMP within the cell. Potent and selective PDE inhibitors have been developed as targets for a variety of pathologies, such as pulmonary hypertension, chronic obstructive disease and asthma (Houslay *et al.*, 2005).

In the CB, the activity of cAMP- specific PDE was characterized for the first time by Hanbauer (Hanbauer and Lovenberg, 1977). At that time, two forms of PDEs were identified in the CB: a low KM enzyme ($2.8X10^{-6}$) and a high KM enzyme ($4.0X10^{-5}$). Exposing rats to 5%hypoxia for 30 min with consequent determination of PDE Km after 45 min, only identified the low km enzyme (the high Km enzyme could not be measured under these conditions) (Hanbauer and Lovenberg, 1977). IBMX, a non-specific PDE inhibitor, has been widely used in experiments aimed at measuring cAMP levels at rat. There are PDE that are IBMX-insensitive (or whose sensitivity to IBMX is unknown: PDE8, PDE10 and PDE11 and the cGMP specific PDE5 and PDE6) but these isoforms can be inhibited by dipyridamole (Hayashi *et al.*, 1998, Hetman *et al.*, 2000). The

characterization of the specific PDE isoforms has never been performed in the peripheral chemoreceptors.

cAMP Pathway- Effectors

cAMP produced in the cell by AC and regulated by PDE binds to target proteins to activate the signaling cascade and produce a cellular effect. cAMP binds to protein kinase A (PKA), to the exchange protein activated by cAMP (EPAC) and/or cyclic nucleotide gated ion channels (CNG and HCN channels) (**Figure 10**).

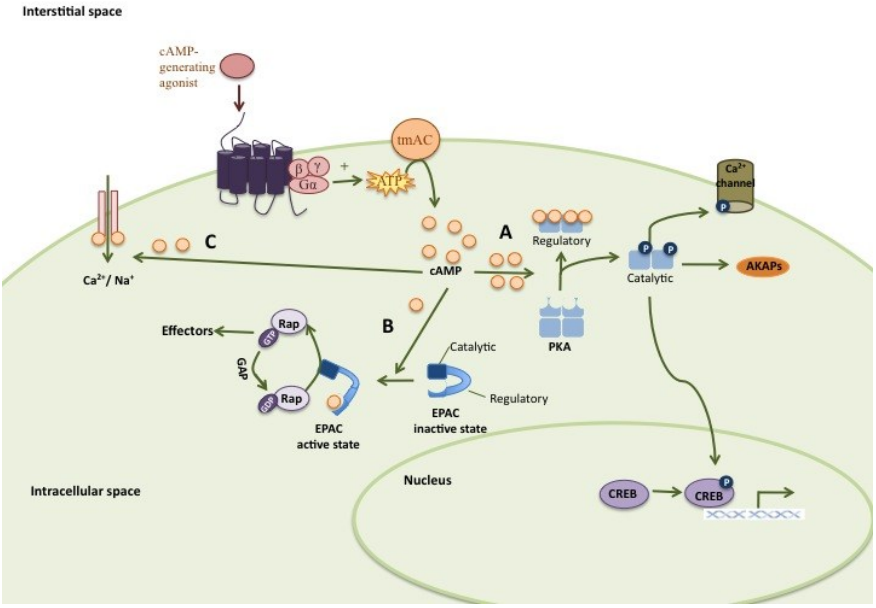

Figure 10- cAMP effectors. cAMP can bind to protein kinse A (PKA, **A**), exchange protein activated by cAMP (EPAC, **B**) and cyclic nucleotide gated ion channels (CNG and HCN channels, **C**). A) The binding of cAMP to the regulatory subunits of PKA releases the active catalytic subunits, resulting in the phosphorilation of ion channels, CREB and A-kinase anchoring proteins (AKAPs). B) cAMP binds to the regulatory subunit of EPAC, unfolding the protein and allowing the of GDP to GTP on Rap 1,2. C) CNG channels are regulated by the binding of cAMP to their cytoplasmic tail, modulating the influx of Ca^{2+} and Na^{+}.
PKA, protein kinase A; *EPAC*, exchange protein activated by cAMP (EPAC), *CNG*, cyclic nucleotide gated ion channels; *CREB*, cAMP response element binding protein; *AKAPs,* A-kinase anchoring proteins; *Rap*, Ras-related proteins.

PKA is a holo-tetrameric serine/threonine kinase composed of two regulatory and two catalytic subunits. Four cAMP molecules bind to the regulatory subunits, each with two cAMP binding sites. The cAMP binding promotes the dissociation of the catalytic subunits that bind ATP to become catalytically active and phosphorylate serine and threonine residues in intracellular targets such as A-kinase anchoring proteins (AKAPs) and ion channels.

AKAPs tether PKA to particular cellular organelles and to the plasma membrane confining the PKA signaling to a small pool within the cell (Beene and Scott, 2007). In the nucleus, PKA can phosphorylate transcription factors, such as cAMP response element binding protein (CREB), and thus regulate gene expression (**Figure 10A**). PKA activity has been demonstrated in the CB through the effects modulated by the PKA antagonist H89 and Rp-cAMPs (Xu *et al.*, 2007, Xu *et al.*, 2006, Wang *et al.*, 1999, Summers *et al.*, 2002). In this tissue, PKA phosphorylates Ca^{2+} channel protein, enhancing L-type Ca^{2+} currents with a consequent increase of intracellular Ca^{2+} (Summers *et al.*, 2002). Epac is a guanine nucleotide exchange factor (GEF) for the Ras GTPase homologues, Rap1 and Rap2. Epac is composed of two regions: an N-terminal regulatory region containing a cAMP-binding site and a C-terminal catalytic region, with GEF activity (de Rooij *et al.*, 1998) (**Figure 10B**). It has been suggested that in the inactive conformation, Epac is folded and the regulatory domain functions as an auto-inhibitory domain. cAMP binding unfolds the protein, allowing Rap to bind (for a review (Gloerich and Bos, 2010)). Rap GTPases cycle between an inactive GDP-bound and an active GTP-bound state, with GEFs mediating the exchange of GDP for GTP. At the end, GTPase-activating proteins convert Rap to the inactive form (Bos, 2003). The activated Rap-GTP activates a variety of different mechanisms in the cell: promotes integrin-mediated cell adhesion, gap junction formation and ERK1/2 MAPK-mediated protein phosphorylation, stimulates phospholipase C-epsilon which hydrolyzes PIP2 to generate diacylglycerol (DAG), and the Ca^{2+} mobilizing second messenger IP3 (for a review (Holz *et al.*, 2006)).

Rocher and co-workers (Rocher *et al.*, 2009) have identified Epac in CB type I cells through the effects of the Epac activator (8-pCPT-2'-*O*-Me-cAMP) and inhibitor (brefeldin) on the release of catecholamines induced by hypoxia. These authors suggest that the effectors of Epac in these cells would be the exocytotic machinery and K^+ channels.

cAMP can also directly bind to cyclic nucleotide-gated (CNG) and hyperpolarization-activated cyclic nucleotide-modulated (HCN) ion channels (**Figure 10C**). These channels belong to a superfamily of voltage-gated cation channels, thus binding of cAMP to these channels are translated into changes in membrane potential and influx of Ca^{2+} and Na^+. The presence of these channels in the rat CB has been suggested by the work of Stea and co-workers (Stea *et al.*, 1995); however, other works have observed that cAMP analogs do not affect Ca^{2+} currents in type I cells (Lopez-Lopez *et al.*, 1993). The direct characterization of these channels has never been characterized in this tissue.

Extracellular and intercellular cAMP signaling

cAMP can be exported out from a variety of cell types and tissues (for a review (Bankir *et al.*, 2002)). The cAMP transport moves against a concentration gradient, it is temperature dependent, is unidirectional and requires energy (Rindler *et al.*, 1978). The efflux of cAMP is believed to be mediated by organic anion transporters (OAT) and multi-drug resistance proteins (MRP) (Sekine *et al.*, 1997, van Aubel *et al.*, 2002). The latter belongs to the superfamily of ATP binding cassette (ABC) proteins, specifically the ABCC subfamily (**Figure 11**). In particular, MRP4, MRP5 and MRP8 have been identified as cyclic nucleotide transporters (Kruh and Belinsky, 2003). AC was also suggested to be involved in cAMP extrusion due to the structural similarities that it shares with the classic ATP-driven transporters (Krupinski *et al.*, 1989).

One of the proposed functions of the extracellular cAMP is to regulate extracellular adenosine (ADO) levels. Extracellular cAMP can be metabolized by

ecto-phosphodiesterases to adenosine monophosphate (5'-AMP), and then by ecto-5'-nucleotidases to ADO (**Figure 11**). The contribution of extracellular cAMP to ADO production has never been investigated in the CB and cAMP released from the CB has never been quantified.

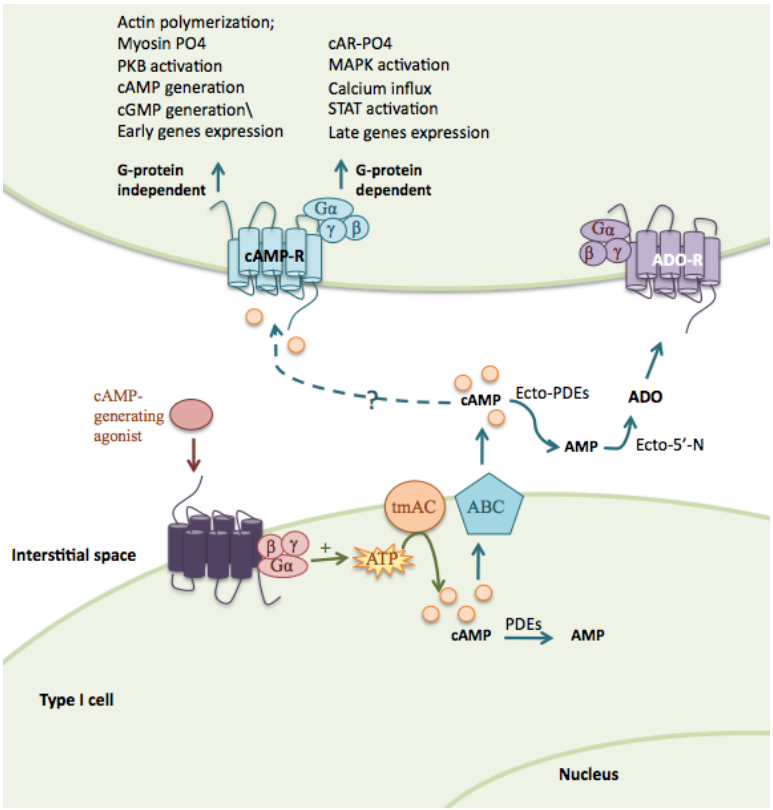

Figure 11- Extracellular cAMP pathway. cAMP synthetized by AC intracellularly can be transported to the extracellular mileu by ABC transporters. Once in the interstitial space, cAMP can be degraded by ecto-phosphodiesterases to AMP and consequently to ADO, by the action of ecto-nucleotidases. cAMP is known to bind to cAMP receptors, cAR, but evidences in mammalian cells are lacking.
tmAC, transmembrane adenylyl cyclase; *ABC*, ATP-binding cassete, *ecto-PDEs*, ecto-phosphodiesterses; *Ecto-5'-N*, ecto-nucleotidases; *ADO-R*, adenosine receptors; c*AMPR*, cAMP receptors

The targets to extracellular cAMP have been well studied in the amoeba dictyostelium discoideum and used as a model for cellular migration and chemotaxis. In this organism, extracellular cAMP binds to cAMP receptors (cAR1, cAR2, cAR3, cAR4) that belong to the superfamily of GPCR (Bankir *et al.*, 2002). The binding of cAMP to cAR activates both G-protein dependent and independent

pathways and a variety of effects that are showed in **Figure 11** (Aubry and Firtel, 1999, Caterina *et al.*, 1995, Milne *et al.*, 1997). Although the effects of extracellular cAMP have been reported in several mammalian cells, no mammalian homologs of the cAR have been identified thus far.

Intracellular cAMP can diffuse intercellularly through gap junctions (Bevans *et al.*, 1998). These gap junctions are located in the membrane of the cells and consist of intercellular channels, each resulting from the association of two hemi-channels or connexons. Each connexon is located in one of the adjacent cells and is composed by six subunits termed connexins (**Figure 12**).

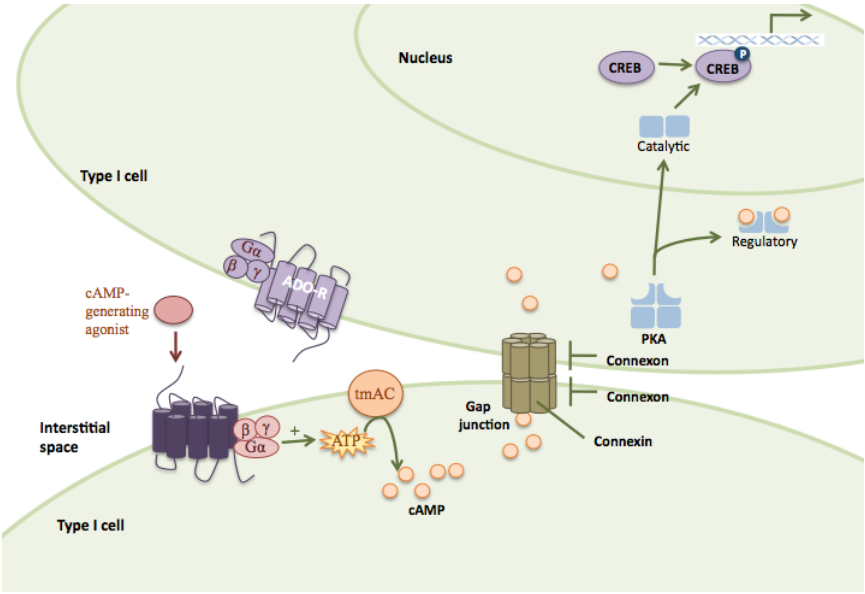

Figure 12- Intercellular cAMP pathway. Gap junctions between two adjacents type I cells in the CB. Each cell membrane contains a connexon, constituted by six connexins. The two connexons connect to each other, forming a channel, allowing the passage of ions and small molecules, such as cAMP, Ca^{2+} Once in adjacent cell, cAMP can mediate a variety of cellular and molecular effects.

These connexins are arranged in a hexagonal shape around an axis perpendicular to the plane of the plasma membrane, forming a channel. These channels allow the passage of not only cAMP, but also ions and other small molecules up to 1.2 kDa (Bennett *et al.*, 1991).

Type I cells and type II cells and carotid nerve terminals in the rat CB are linked through gap junctions, which mediate intercellular communications and transporte of small molecules and ions (Abudara and Eyzaguirre, 1996). Junctional conductance and gap junction formation and connexin expression are regulated by cAMP (Abudara *et al.*, 2000).

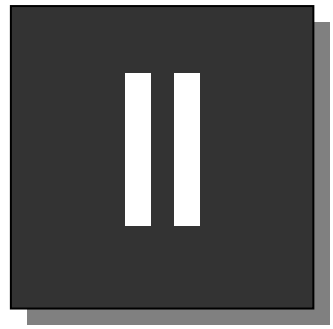

HYPOTHESIS AND AIMS

Pharmacological manipulation of cAMP signaling is currently used as a therapeutic target to treat respiratory pathologies: asthma, pulmonary hypertension, chronic obstructive pulmonary disease, obstructive sleep apnea (OSA) (Houslay *et al.*, 2005). These pathologies have in common the imbalance of O_2/CO_2 and consequent CB activation. **Thus, our overall hypothesis is that the CB activity could be manipulated with drugs that interfere with cAMP-signaling pathway**. **The general aims of the work present in this thesis are 1) to study how specific is cAMP-signaling pathways in the CB mainly in different CO_2 conditions and 2) how O_2 concentrations alter/drives the manipulation of cAMP signaling in the CB.**

The O_2/CO_2 sensing mechanism of the CB is not fully understood, but an involvement of cAMP in this mechanism has been proposed. The experimental studies included in this doctoral thesis sought to investigate the role of cAMP in the rat CB chemotransduction mechanisms and to determine whether the enzymes that participate in cAMP signal transduction in the CB are regulated by O_2/CO_2.

Specific aims:

1) to determine the effects of PDE inhibitors on cAMP signaling pathways in peripheral chemoreceptors;
2) to characterize PDE isoforms in O_2 chemosensitive and non-chemosensitive tissues;
3) to determine potential tissue specific modulation of PDE inhibitors in hypoxia-related disease conditions;
4) to determine whether the effects of PDE inhibitors are translated into apparent changes in PKA activity in primary SCG neurons
5) to characterize sAC and its putative role in the CB and non-chemosensitive related organs.

6) to determine the relative contribution of sAC and tmAC on cAMP signaling in response to hypercapnia in peripheral and central chemoreceptors, mainly the CB, PG and LC.

The relevance of this work is to study and potentially identify new molecular targets (sAC, subtypes of tmAC, PDE isoforms) that could be used to treat diseases and conditions related to control of breathing.

GENERAL METHODS

Surgical procedures

Animals used

The experiments were conducted on two different strains of rodents: Sprague-Dawley (SD) rats at postnatal day (P) 5-9, 16-17 and at 3 months, and Wistar rats at 3 months. All animal care and experimental procedures were carried out according to the European Union directives (Wistar rats) and by the guidelines of Animal Use Committee at the Johns Hopkins University School of Medicine (SD rats). SD rats of both sexes, P5-9 and P16-17, were obtained from Charles River Laboratories (Wilmington, MA). Wistar rats of both sexes, at 3 months of age, were obtained from Faculty Medical Science animal house (Portugal).

Dissection of the biological preparations

Different surgical procedures were performed on SD and Wistar rats, due to the different age and size of the animals.

SD rats were briefly anesthetized with isoflurane (Abbott Laboratories, Inc., Abbott Park, Illinois) and immediately decapitated. Heads were mobilized ventral side up using sterile syringe needles. Dissection involved a cervical midline incision, exposing a mass of glandular, adipose, and lymphoid tissue (**Figure 1A**). This mass of tissue was removed, exposing the omohyoid muscle (**Figure 1B**), which was carefully removed, exposing the carotid artery (**Figure 1C-D**). The carotid bifurcation, including the carotid body (CB), superior cervical ganglia (SCG), and the nodose/petrosal ganglion (NG/PG) complex, was cleaned of surrounding connective tissue and transferred *en bloc* (**Figure 1E**) to a dissecting petri dish coated with agar and containing ice-cold phosphate buffered saline buffer (PBS in mM: NaCl, 137; KCl, 2.7; Na_2HPO_4, 4.3; KH_2PO_4, 1.47; adjusted to pH 7.4). Under a dissecting microscope, the SCG was carefully removed, exposing the CB. Subsequently, the CB, the PG, and NG were quickly dissected from the carotid artery, free of connective tissue and fat, and prepared as mentioned in *Preparations* and *Methodologies*.

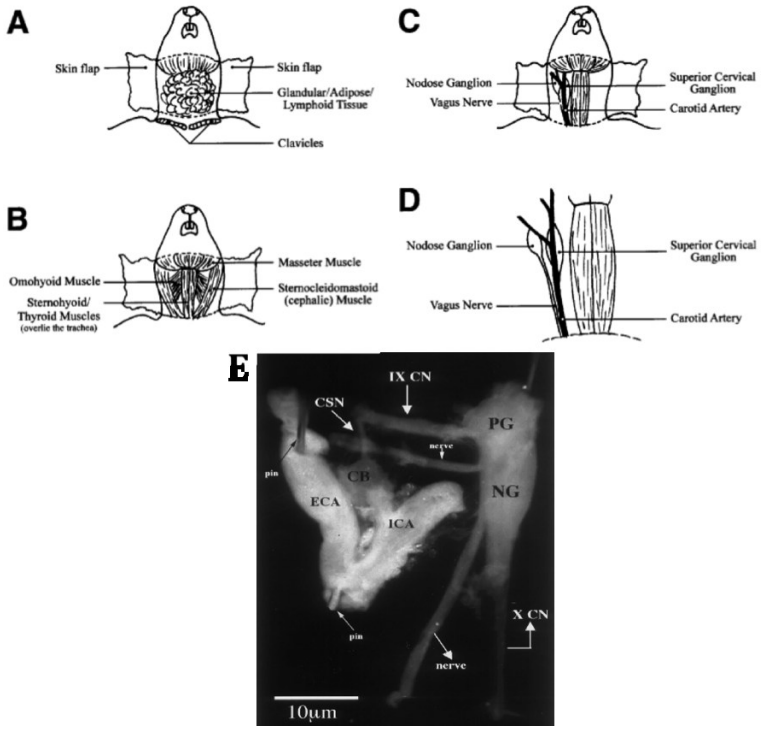

Figure 1- Dissection of peripheral chemo- and non-chemoreceptor tissues from a rat. A) A vertical midline incision in the skin with lateral incisions to the left and right, was made at the level of the clavicles and the mandibles. Skin flaps were retracted laterally, exposing a mass of glandular, adipose, and lymphoid tissue. (B) The tissue was removed, exposing the sternohyoid and thyroid, sternocleidomastoid and omohyoid muscles. (C) The thin omohyoid muscle was carefully removed, exposing the carotid artery. (D) Details of the carotid artery exposure (A-D adapted from Fedoroff and Richardson, 2001). (E) Bifurcation of the carotid artery from SD rat at P10, exposing the carotid body (CB), nodose and petrosal ganglia (NG/PG), internal carotid artery (ICA), external carotid artery (ECA), ninth and tenth cranial nerves, and carotid sinus nerve (CSN) (Gauda and Lawson, 2000) and Fedoroff and Richardson, 2001.

The central chemoreceptor regions were obtained from the brainstems of SD rats. Dissection involved a longitudinal incision from the neck to the snout. The skull was cut longitudinally and anteriorly starting at the cisterna magna, by making 1 medial and 2 lateral cuts, on each side. The cranial nerves were cut and the brain was removed with a spatula and placed in ice-cold PBS to quickly micro-dissect the central chemosensitive tissues of interest: medullary raphé nuclei (RN), ventrolateral medulla (VLM) and the locus coeruleus (LC) (**Figure 2**). Cortex (Cx) was included as a non-chemosensitive region. As previously described by Wang and co-workers (Wang *et al.*, 1998) transverse cuts were made through the pia mater on the ventral surface of the brainstem at the ponto-medullary border,

immediately caudal to the union of the vertebral arteries near the spinomedullary border. Two longitudinal cuts were also made along the middle of both pyramids. A micro-knife was used to remove the pre-cut wedge of tissue with its base at the ventral surface and borders along the previously made cuts, and its apex in the midline approximately half way towards the dorsal surface of the medulla. The micro-dissected region captured the raphé pallidus, raphé magnus, a segment of the raphé obscurus, and tissue immediately adjacent to these nuclei (**Figure 2A**). Similarly, the ventrolateral medulla (VLM) was micro-dissected using a slightly modified approach, as described by Johnson and co-workers (Johnson *et al.*, 2008, Johnson *et al.*, 2001). The brainstem was sliced manually in ~500 μm increments with a micro-knife to capture a transverse slice containing the VLM. Tissue samples were taken from a slice where the inferior olive (IO), midline raphé, pyramids, and semi-compact division of nucleus ambiguus (NA) were visualized and used as identifying landmarks. A longitudinal cut was made immediately lateral to the midline raphé, diagonally above the IO complex, and a transverse cut was made slightly dorsal to the NA (**Figure 2.2B**). Finally, LC samples were obtained from pontine slices at the level of the 4th ventricle and the tract of 7th cranial nerve. The LC and adjacent tissue was bilaterally excised from the slice (**Figure 2.2 C**).

The testicular tissue was removed from SD rats at P16-17 and at 3 months of age. This tissue was used as a positive control organ to study soluble adenylyl cyclase (sAC) expression and activity since this enzyme is highly expressed in this tissue (Braun, 1991). The dissection of testes involved an incision through the scrotal wall and cremasteric fascia, exposing the scrotal sac where the testes were located**.** The testes were removed by cutting the excretory efferent ducts. The testicular capsule was teased off gently and the testes were incubated in "baskets" containing the incubation medium under study conditions.

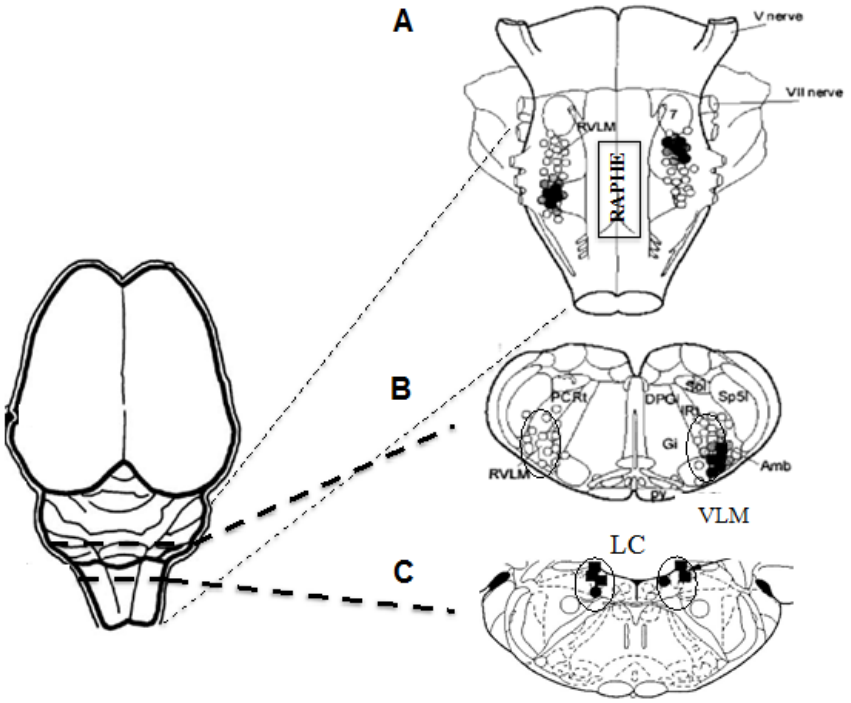

Figure 2- Representation of the CO_2 central chemoreceptor tissues from a rat. A) Dorsal surface of the medulla containing the raphe, B) Slice containing the VLM, and C) Slice containing the LC. *LC*, locous coeruleous, *VLM*, ventro lateral medulla. Figure adapted from (Golanov *et al.*, 2000, Kiyashchenko *et al.*, 2001).

Wistar rats were anesthetized with sodium pentobarbital (60 mg.Kg, i.p.). The dissection involved a longitudinal incision in the middle cervical skin, followed by a tracheostomy to allow spontaneous breathing during the surgical procedure. Retractors were used to expose the carotid arteries and remove the connective tissue. Under a dissection scope (Nikon SMZ-2B) with a cold light (Wetzlar LFQ150), the CBs, SCG and carotid arteries were gently dissected and immediately placed in ice-cold incubation medium in preparation for *in vitro* incubation experiments. The animals were killed by an intracardiac injection of a lethal dose of pentobarbital.

Preparations

In this work, whole organs, slice tissue and single cells preparations were used to study the effect of O_2 and CO_2 on cAMP signaling pathway-mediated chemoreception.

Whole organ

Whole organs were dissected from the rodents as described previously in *Surgical Procedures*, and either processed directly according to the technique to be used or incubated *in vitro* to study the effect of experimental conditions/parameters (O_2, CO_2, bicarbonate ion (HCO_3^-), phosphodiesterase (PDE) inhibitors, adenyly cyclase (AC) activators and inhibitors) on gene expression (quantified by qRT-PCR) or on total cAMP levels (quantified by ELISA). The advantages of the use of whole organs, as oppose to cells, is that this model preserves cell-cell interactions. The isolated CBs are no longer influenced by blood flow changes or efferent nerve discharge; although it still responds to decreases in PO_2 in a similar way to the *in vivo* CBs (Delpiano and Acker, 1980), and along with the small size of this organ, is a well-established model to elucidate O_2-chemoreception (Delpiano and Acker, 1991, Iturriaga *et al.*, 1992, Batuca *et al.*, 2003, Monteiro *et al.*, 2011).

A limitation on using a whole organ approach is the contribution of all the organ components (different cell types, blood vessels, nerve terminals) in the overall response to the stimulus in study. However, a comparison between whole CB and non-chemosensitive related tissues allow us to identify specific properties of the CB chemosensitivity cells.

Dissociated primary cell cultures

Dissociated primary cells from the CB and SCG were used to study the regulation of PKA activity using FRET-based imaging. Dissociated primary cells are a good model to study cellular and molecular mechanisms of specific cell

types, and have been widely used to understand chemotransduction mechanisms in the CB type I cells.

Primary cultures of carotid body cells

Carotid bodies from SD rats at P6-9 were isolated and dissociated enzymatic and mechanically according to the protocol described by Carroll and co-workers (Carroll *et al.*, 2005). Briefly, CBs were removed from rats as described in *Surgical Procedures* section, placed in ice-cold low-Ca^{2+}, low Mg^{2+} PBS and transferred to an enzyme mixture consisting of trysin and collagenase (0.5 mg/ml) in low Ca^{2+}/Mg^{2+} PBS. After 25 min, CBs were mechanically dissociated using a fire polished Pasteur pipette. The enzymatic reaction was stopped by addition of growth medium Ham's F-12 Medium (Gibco, Invitrogen), supplemented with 10% fetal bovine serum (Gibco, Invitrogen), glucose (23 mM, Sigma), L-glutamine (2 mM, Cellgro, Mediatc), penicillin–streptomycin (10 kunits, Cellgro, Mediatc) and insulin (3 $\mu g\ ml^{-1}$, Sigma). The dissociated CBs were then centrifuged for 4 min at ~6000 rpm (~2000 g,). The supernatant was removed and warm supplemented Ham's F12 Medium was added to the cells to gently resuspend the pellet. This step was repeated to remove all traces of the enzymes. Hemocytometer-based trypan blue dye exclusion assay was used to determine a cellular viability of 75.5 $\pm$ 3.3%. Dead cells took up the dye and appeared blue under the miscroscope, while living/viable cells excluded the dye and appeared white. The final cell suspension was handled differently according to the objectives of the experiment. For FRET experiments 10 µl aliquots were plated on small glass-bottomed cell culture dishes (Mat-Tek Corporation) coated with poly-L-lysine (PDL, 100µg/ml, Sigma). Cells were incubated at 37°C/5%CO_2 and after 50 min were fed with warm growth medium culture.

For studies on morphology/ characterization/ immunostaining of cells, drops of cell suspension were plated in the center of regular glass slides coated

with PDL (Millicell® EZ slide, Millipore), which were then placed in a10 cm Petri dish. After one hour of incubation, enough CB growth medium was added to cover the slides.

Figure 3 shows the identification of type I cells from a CB cell culture. Type I cells were identified with tyrosine hydroxylase (TH) and fluoresceinated peanut agglutinin staining.

CB primary cells were plated on slides pre-coated with PDL, fixed with 4% paraformaldehyde and treated with 0.4% Triton X-100 (Fisher) in PBS. Cells were then blocked with 5% BSA (Sigma) in PBS, for an hour, to prevent specific or non-specific background staining. Cells were labelled with anti-TH polyclonal rabbit antibody (1:50, sc-14007, Santa Cruz) in 1% BSA in PBS, overnight, at 4°C, followed by washes with PBS (3x5min) to remove unattached primary antibodies. Type I cells are enriched with TH, the rate-limiting enzyme in catecholamine biosynthesis. TH positive cells were detected using rhodamine donkey anti-rabbit secondary antibody (1:100, sc-2095, Santa Cruz) in 1% BSA in PBS for 2 hours at RT, in the dark. After 3x5 min washes with PBS, coverslips were mounted in DAPI-containing Vectashield mounting medium (Vector lab, Burlingame, CA) and the slices were observed under fluorescent microscope. As shown in **Figure 3A1**, type I cells labeled with TH appeared in clusters, but TH did not labeled all CB cells, as shown in **Figure 3A2** with DAPI staining.

Fluoresceinated peanut agglutinin (PNA) binds to the outer membrane of cells originating from the neural crest and can be used as a good marker to identify live type I cells in primary cultures of CB (Kim *et al.*, 2009). To confirm that PNA-bound CB cells were exclusively TH positive type I cells, CB cells were previously treated with Rhodamine-PNA (Rhod-PNA, 30μg/ml, Vector, CA) in supplemented Ham's F-12 grow Medium for 1 hour, at 37°C. Then, the cells were fixed, permeabilized, blocked as described above and incubated with anti-TH mouse monoclonal primary antibody (1:50, sc-25269, Santa Cruz) in 1% BSA in PBS, overnight. Type 1 cells were detected by FITC goat anti-mouse secondary antibody

(1:100, sc-2010, Santa Cruz) in 1% BSA in PBS (Figure 2.3B1). As observed in Figure 2.3B1 and Figure 2.3B2, TH positive type I cells were PNA labeled.

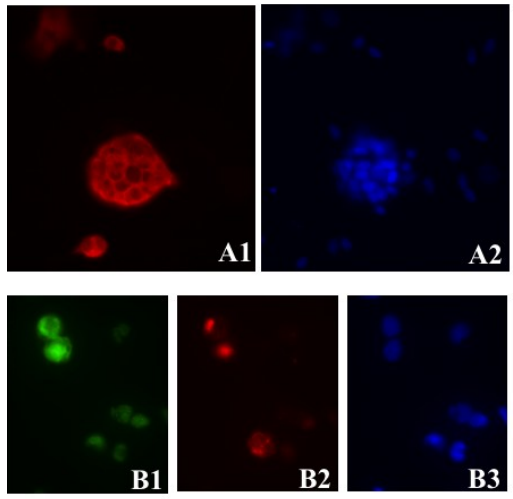

Figure 3- Primary culture of cells dissociated from CB from SD rats at P10.
A1) Identification of type I cells by tyrosine hydroxylase (TH) immunostaining. Type I cells were stained with anti-TH polyclonal rabbit antibody (1:50) and detected using rhodamine donkey anti-rabbit secondary antibody (1:100). **A2)** Nuclei of CB cells were stained with DAPI. 400 fold magnification **B1-B3)** Identification of CB type I cells byfluoresceinated peanut agglutin (PNA) and TH co-staining **B1)** TH staining (1:50, mouse monoclonal TH antibody visualized using FITC goat anti-mouse antibody, 1:100), **B2)** PNA staining (30μg/ml in cell culture media for 1hrvisualized by TRITC filter after incubation with of RHO-PNA in cell culture media during 1 hr, 37°C. **B3)** DAPI staining showing more than type I cell in the CB cell culture. 1000 fold magnification. Cells grown in culture for 24 hours.

Primary cultures of superior cervical ganglia neurons

Superior cervical ganglia isolated from SD rats at PND 6-10 were transferred to sterile Leibovitz's L-15 medium (Gibco, Invitrogen) and dissociated enzymatic and mechanically to obtain primary neuron cultures. The ganglia were teased apart and incubated in a mixture of trypsine and collagenase in Leibovitz's L-15 medium at 37°C for 1 hour. At the end of the enzyme treatment, the ganglia were rinsed in fresh Leibovitz's L-15 medium for 30 min at 37°C, followed by 3 washes in L-15 and once in Neurobasal-A medium (Gibco) with supplements: nerve growth factor (NGF, 100μg/ml, Sigma), L-glutamine (0.6 mM), penicillin/streptomycin (10 kunits) and B27 (Gibco Invitrogen). The ganglia was gently triturated with a pasteur pipette and washed 4 times through a 30-70 μm

pore cell strainer (Falcon). Cells were centrifuged for 6 min at 2000g and ressuspended in Neurobasal-A. Cellular viability was measured (82.3±4.5%). Cells were plated in petri dish pre-coated with PDL and laminin (25μg/ml, Invitrogen) and after 30 min, 2 ml of Neurobasal-A with supplements was added to the cell culture. In the following day, the antimitotic cytosine arabaninoside (Ara-C, 10μM, Sigma) was added to prevent the growth of dividing non-neuronal cells. Neurofilaments (NF) and TH are neuronal markers for sympathetic ganglia (Ahonen, 1991). NF are proteins found specifically in neurons and constitute the main structural elements of neuronal axons and dendrites. **Figure 4** shows the identification of the neuronal ganglia in the SCG cell culture. SCG primary neurons were plated in slides pre-coated with PDL and laminin, fixed with 4% paraformaldehyde and permeabilized with 0.4% Triton X-100 in PBS. After blocking (5% BSA in PBS) for one hour, cells were labeled with two primary antibodies: anti-TH polyclonal rabbit antibody (1:50, sc_14007, Santa Cruz, Figure 2.4A) and anti NF-68kDa mouse monoclonal antibody (1:100, ab78159, abcam, Figure 2.4B), both in 1% BSA/PBS, overnight, 4ºC and visualized with rhodamine donkey anti-rabbit secondary antibody (1:100, sc_2095, Santa Cruz, **Figure 4A**) and FITC- conjugated goat, anti-mouse IgG secondary antibody (1:100, sc_2010, Santa Cruz, Figure 2.4B) in 1%BSA/PBS for 2 hours at RT. After the washing step (3x5min in PBS), the coverslips were mounted with DAPI-containing Vectashield mounting medium and slices were observed under fluorescent microscope (**Figure 4A-D**).

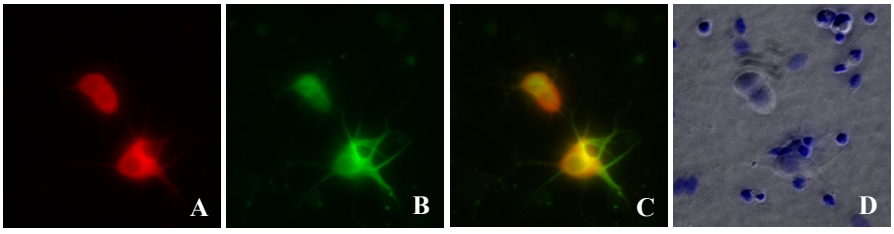

Figure 4- Primary cultures from superior cervical ganglia from SD rats at P10.
A) SCG neurons labeled with anti-Tyrosine hydroxylase (TH) polyclonal rabbit antibody (1:50 in 1%BSA/PBS, overnight at 4ºC) and detected using rhodamine donkey anti-rabbit antibody (1:100). **B)** SCG neurons labeled with neurofilament 68kDa (NF-68) mouse monoclonal antibody (1:100) and visualized by FITC goat anti-mouse antibody (1:100), **C)** Merged imaged showing co-staining of TH and NF-68 in SCG neurons. **D)** DAPI staining showing more than SCG neurons in the culture. 400 fold magnification.

Organotypic slice cultures

Organotypic slice cultures of CB/SCG were used to investigate the effect of PDE inhibitors on PKA activity by FRET. Organotypic slice culture is an advantageous *in vitro* model, allowing the maintenance of fiber projections between cells and avoiding enzymatic and mechanical dissociation of the tissue (as in dissociated cell cultures), which results in better preservation of the cellular physiology and morphology and minimal disruption of type I cell-type II cell contacts.

CB attached to the SCG were isolated from SD rats at P6-8, cleaned of connective tissue and transferred to sterile ice-cold Leibovitz L-15 medium (**Figure 5A**). The tissue complex was then embedded in 3% low melting point agar (Sigma Chemical Co, St Louis, MO). The embedded tissues were mounted on the specimen disc of the vibratome (Vibratome, Ted Pella, Inc, Redding, CA). The disc was then mounted on to the vibratome in a tray filled with ice-cold Leibovitz L-15 and 40μm thick SCG-CB slices were sectioned. 2-3 slices were placed on a Millicell-CM cell culture inserts (Millipore, Bedford, MA) in a six-well plate containing 1 mL of Neurobasal-A medium with supplements (0.3% L-glutamine, 2% B-27 and 1% Pen-Strept). The inserts are porous membrane filter that allow the slices to remain well oxygenated without drying out and with adequate nutrition. The slices were maintained in a CO_2 incubator, at 37°C, and the culture Neurobasal-A medium was changed every 2 days. **Figure 5B** shows an organotypic slice of SCG/CB after 24 hours in culture. As it can be observed by the close up image (**Figure 5C**), sections showed intact morphology with round cell bodies and without gross signs of tissue necroses.

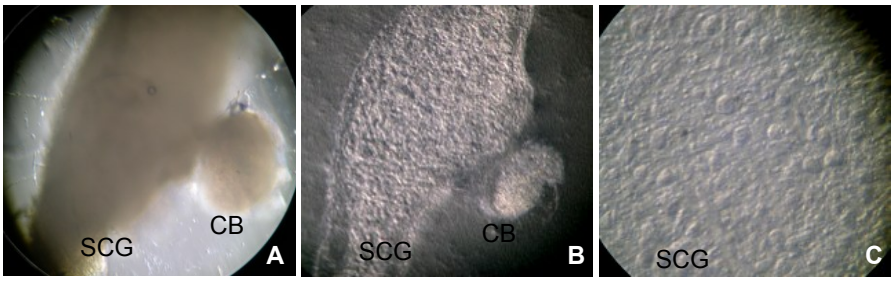

Figure 5- Culture of organotypic SCG/CB slices
A) SCG/CB tissue complex after dissection from SD rat at P6. **B)** 40 μm SCG/CB organotypic slice after 24 hours in culture, 100 fold of magnification **C)** Amplification of the area of the SCG in the SCG/CB organotypic slice, 400 fold of magnification. *SCG*, superior cervical ganglia, *CB*, carotid body.

The viability of the slices was evaluated using propidium iodide (PI), a fluorescent membrane impermeant dye that intercalates between the bases of the DNA of nonviable cells (Jones and Senft, 1985) and the nuclei which appear bright orange-red nuclei when observed with a fluorescent microscope (rhodamine filters, **Figure 6**). Slices cultured for 24 hours were transferred to microscope slides. A positive control was prepared with incubation in 0.3% Triton X-100 in PBS for 10 min, 37ºC, before addition of PI (500nM, **Figure 6A**). PI (500nM) was added to the slices at RT for 5 min (**Figure 6B**). Coverslips were mounted with a drop of glycerol/Tris media and observed under the microscope using rhodamine filters (**Figure 6**).

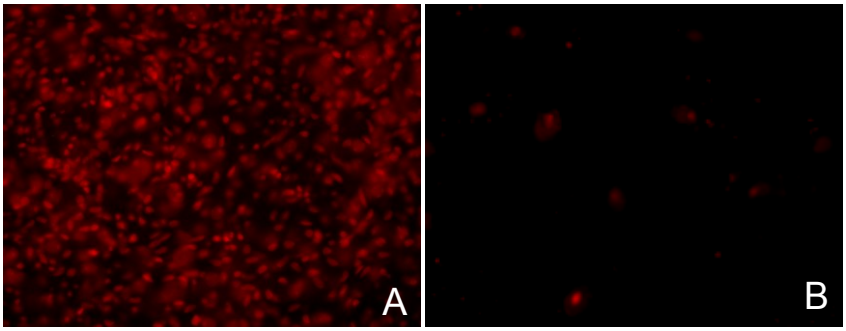

Figure 6- Evaluation of cell death in slice culture
A) Slices incubated with 0.3% Triton X-100 in the presence of PI (500 nM), showing a majority of death cells and**B)** minimal cell death observed in the slices cultured for 24 hours. Fluorescent intensity is depicted in each image as brightly highlighted cell bodies. 400 fold magnification.

Identification of the neuronal SCG in the organotypic slices and the integrity of the slice were done by imunostaining with TH and neurofilament antibodies, using the same protocol described above for SCG cells (**Figure 7**).

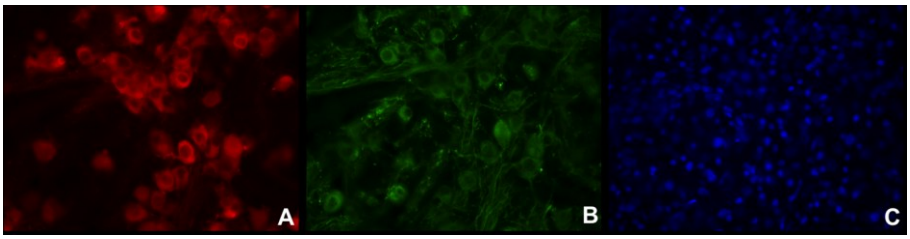

Figure 7- Identification of SCG neurons in organotopyc slices from rat at P6.
A) SCG neurons labeled with anti-Tyrosine hydroxylase (TH) polyclonal rabbit antibody (1:100 in 1%BSA/PBS, overnight at 4ºC) and detected using rhodamine donkey anti-rabbit antibody (1:100). B) SCG neurons labeled with neurofilament 68kDa (NF-68) mouse monoclonal antibody (1:100) and visualized by FITC goat anti-mouse antibody (1:100). D) DAPI staining showing more than SCG neurons in the slice culture. 400 fold magnification.

Methodologies

General in vitro whole tissue (organ) experimental conditions

Tissues were placed into an incubator chamber (1.5 ml eppendorf) containing 1 ml of Krebs modified medium (KMM) containing (in mM): NaCl 135; KCl 5; $CaCl_2$ 2; $MgCl_2$ 1.1, HEPES 10, glucose 5.5, in the presence or absence of HCO_3^- 24, at pH 7.4 and 37ºC (Perez-Garcia *et al.*, 1990) and continuously bubbled with the percentages of O_2 and CO_2 of interest. According to the aim of the experiment, incubation was done in the presence or absence of PDE and/or AC inhibitors. After 15-30 min of pre-incubation, tissues were replaced in fresh KMM in the presence or absence of PDEs and ACs inhibitors and activators (also see **table 1.4** in attachments for reagents information) and equilibrated with different percentages of O_2 and CO_2 for 30-60 min (**Figure 8**). Changes in CO_2 were followed by changes in HCO_3^- to maintain a constant pH, according to the Henderson-Hasselbalch equation: $pH= (6.1+\log [HCO_3^-])/0.03xPCO_2$, and osmolarity was adjusted with NaCl. At the end of the intended period, tissue was collected and processed as described in the following sections.

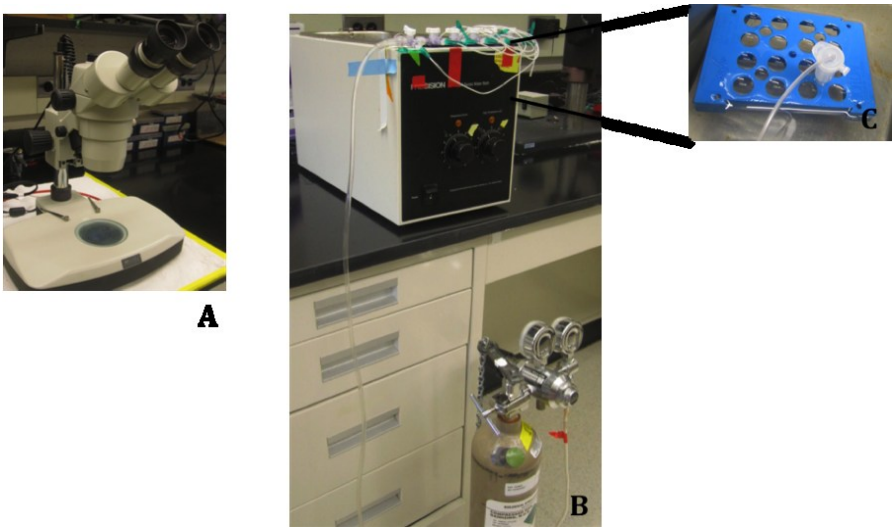

Figure 8- Set up for *in vitro* experiments
A) Dissection microscope. B) Water bath and gas incubation. C) Detail of the incubator chamber bubbled with gas (O_2/CO_2), at 37C in a water bath.

Table 1 summarizes the *in vitro* experimental conditions used throughout this work.

Table 1- *In vitro* whole tissue experimental conditions (see **Table 1.4 in attachment** for reagent information).

Tissue	Aim	Pre- incubation			Incubation			Technique of detection
		Solution	O_2/CO_2 (%)	Time (min)	Solution	O_2/CO_2 %	Time (min)	
CBs, SCG, CA	Effect of [O_2] during recovery pre-incubation period on cAMP content	KMM + 24mM HCO_3^-	95/5	15	KMM+ 24mM HCO_3^- + IBMX500µM	5/5 20/5	30	Quantification of cAMP by ELISA
		KMM + 24mM HCO_3^-	20/5	15	KMM+ 24mM HCO_3^- + IBMX500µM	5/5 20/5	30	
	Effect of PDE inhibitors on cAMP content in CB, SCG and CA	KMM +24mM HCO_3^-	20/5	15	KMM+ 24mM HCO_3^- + IBMX (0.3-500µM)	5/5 20/5	30	
					KMM+ 24mM HCO_3^- + Ro-201724 (0.1-100µM)	5/5 20/5		
					KMM+ 24mM HCO_3^- + Rolipram (0.1-100µM)	5/5 20/5		
					KMM+ 24mM HCO_3^- + EHNA (0.1-100µM)	5/5 20/5		
CB, SCG RN, LC, VLM Cx, Testis	sAC up-regulated gene expression by bicarbonate	KMM	60/0	30	KMM	60/0	60	qRT-PCR
					KMM+ 24mM HCO_3^-	60/5		
					KMM+ 44mM HCO_3^-	60/10		
CB, LC, Cx	sAC up-regulated gene expression by FSK	KMM+ 24mM HCO_3^-	60/5	30	KMM+ 24mM HCO_3^- KMM+ 24mM HCO_3^- + FSK 100µM	60/5	60	qRT-PCR
CB, RN, LC, VLM, PG, SCG, NG, Cx, Testis	HCO_3^- —sAC induced cAMP levels	KMM+ MDL 12,330A (500µM)	60/0	30	KMM+ MDL 12,330A (500µM) + (0,12,24,44 mM HCO_3^- + IBMX(500µM) (+ dipyridamole 500µM for testis)	60/0 60/5 60/10	30	Quantification of cAMP by ELISA
CB, LC and PG	Contribution of sAC and tmAC to cAMP levels in normocapnia and hypercapnia	KMM+ (0, 12,24or 44mM HCO_3^-) +/or MDL 12,330A (500µM)[1]+/or KH7 (10-50µM)[2]+/or ddADO (30-300µM) [3]+/or SQ22365 (80-200µM)	60/0 60/2.5 60/5 60/10	30	KMM+ (0,12,24,44) mM HCO_3^- +IBMX (500µM)+/or MDL 12,330A (500µM) +/or KH7 (10-50µM)[2]+/or ddADO (30-300µM) [3]+/or SQ22365 (80-200µM)	60/0 60/2.5 60/5 60/10	0, 5, 15,30	
SCG, CB	PDE 3 and PDE4 up-regulation by O_2	KMM+ 24mM HCO_3^-	20/5	30	KMM+ 24mM HCO_3^-	5/5 20/5 60/5	60	qRT-PCR

KMM, Krebs modified medium; *CB*, carotid body; *SCG*, Superior Cervical Ganglia; *CA*, carotid arteries; *RN*, raphe nucleus; *LC*, Locus Coeruleus; *VLM*, ventrolateral medulla; *Cx*, cortex; *PG*, petrosal ganglia; *NG*, nodose ganglia; HCO_3^-, bicarbonate ion; *PDE*, phosphodiesterase; *sAC*, soluble adenylyl cyclase; *cAMP*, cyclic AMP; FSK, forskolin; *tmAC*, transmembrane adenylyl cyclase;

Cyclic nucleotide extraction and quantification by EIA

At the end of the *in vitro* incubation experiments, tissues were collected and immersed in cold 6% (w/v) trichloroacetic acid (600 µL, Sigma) for 10 min. Tissues dissected from adult animals (Wistar, 3 months) were weighed in an electrobalance (mc 215 Sartorius, Madrid, Spain) to express the amount of cAMP per weigh of tissue. The tissues from younger animals (SD, P16-17) were not weighed but processed for protein quantification to express the amount of cAMP per µg of protein, as described bellow. Tissues were homogenized using a potter glass homogenizer at 2-8ºC and centrifuged at 12 000 g for 10 min at 4ºC. The pellet was stored for protein assay. The supernatants were washed 4 times with 3 ml of water saturated with diethyl ether solution (50:50), collected for lyophilization (Christ Alpha 1-2 B. Brawn, Biotech International, Melsungen, Germany) and stored at -20ºC until cAMP quantification by commercial enzyme immunoassay (EIA) kit according to the manufacturer's instructions (RPN 2255 GE Healthcare Bio-Sciences AB, Uppsala, Sweden). The EIA assay is based on the competition between unlabelled cAMP (present in the sample) and peroxidase- labelled cAMP for a number of cAMP-specific antibody binding sites. The standard and the unknown samples (both with unlabeled cAMP) are mixed with specific antiserum rabbit antibody and incubated in a 96 well microplate coated with capture antibody. The antiserum binds to the antibody of the plate and the cAMP from the samples and standards binds to the antiserum. Then cAMP-peroxidase conjugate is added to the wells and binds to the anti-cAMP antiserum that is not occupied by unlabeled cAMP. Therefore, the amount of cAMP conjugated that binds to the antibody, is inversely proportional to the concentration of cAMP in the sample. The wells are washed with detergent and the substrate of the cAMP-peroxidase conjugate (TMB) is added. If there is little cAMP pesent in the sample, more substrate will bind to the antiserum-peroxidase conjugate. Protein pellets were stored at -80°C until protein quantification. Samples from all tissues, except from the CB, were quantified by standard Bradford Protein Assay (Bio-RAD). CB

protein was quantified by a fluorescence detection kit, Molecular Probes' NanoOrange Protein (Invitrogen, Eugene, OR), which offers an accurate detection of proteins with a higher level of sensitivity and lower protein-to-protein variability than the Bradford assay. cAMP levels were expressed in femtomoles per microgram of protein (fmol/µg protein).

Western Blot

The presence of sAC protein was determined by Western blot using 20 µL of protein from crude homogenates of CB, SCG (SD rats at P16-17) and testis (SD rat at 3 months old). The tissues were homogenized in buffer containing 20 mM Tris-HCL (Sigma), 5mM ethylene glycol tetraacetic acid (EGTA, Sigma), 10mM Benzamidine (Sigma), 0.1 mM phenylmethylsulfonyl fluoride (Sigma, PMSF) and 1mM ethylenediaminetetraacetic acid (EDTA, Sigma), 10% sucrose (Sigma) and complete protease inhibitor (Roche Molecular Diagnostics Pleasanton, CA, 1 tablet/50mL buffer). The samples were diluted 2:1 (v/v) in loading buffer containing 0.125 M Tris –HCl pH 6.8 (Sigma), 4% sodium dodecyl sulfate (Sigma), Dl-dithiothreitol (Sigma), 20% (w/v) glycerol (Sigma), 0.004% bromophenol blue (Sigma) and 10% 2-mercaptotehanol (Sigma), boiled for 5 min and loaded on 10% sodium dodecyl sulfate polyacrylamine gel electrophoresis (SDS-PAGE). Protein was transferred to nitrocellulose membrane using standard electroblotting procedures and confirmed by Ponceau S. Nitrocellulose membrane was blocked with 5% nonfat dry milk in 0.1% Tween-Tris Buffered Saline (TTBS, Quality Biological Inc). Blots were incubated with monoclonal anti-sAC R21 antibody (1:500, provided as a generous gift from Dr. Buck and Dr. Levin) or with the protein loading control goat anti-mouse monoclonal β-actin (1:10000, Sigma Chemical), overnight, at 4^{o}C. The R21 monoclonal antibody was raised against amino acids 203-216 of human sAC encompassing the catalytic regions (C1 and C2) (Zippin *et al.*, 2003). After exposure to the primary antibody, the membrane was washed several times with TTBS at RT and incubated with anti-mouse HRP-

conjugated secondary antibody (1:10,000, Bio-Rad) for 1 hour at RT. Immunoreactivity was detected with enhanced chemiluminescence using SuperSignal kit (Thermo Scientific, Wilmington, DE) and densitometric analysis (optical density OD) was done with IP Lab Gel H softaware (Signal Analytics) adjusted for background. Protein levels were expressed as adjusted OD levels corrected for loading.

Quantitative Real-time Polymerase Chain Reaction (RT-PCR)

The comparison of the levels of gene expression of adenylate cyclases and phosphodiesterase and their regulation was done by quantitative real Time-PCR (qRT-PCR) experiments. These experiments were divided into three steps: tissue collection, homogenization and total RNA isolation; cDNA synthesis; and real Time-PCR.

Tissues were collected in RNAse free eppendorf tubes and quick-frozen on dried ice and stored at -80^{o}C. On the day of the experiment, the tissues were thawed on ice and processed to obtain total RNA according to the manufacturer's instructions (Micro-to-Midi Total RNA Purification, Invitrogen). DNase treatment (PureLink DNase, Invitrogen) was performed during RNA purification, to avoid contamination with genomic DNA. RNA yield was measured by spectrophotometry at 260 and 280 nm: conventional UV spectrophotometer (Beckman Du 530) was used to measure OD_{260}/OD_{280} of the RNA samples from all the tissues, except from the CB, where a NanoDrop spectrophotometer (Thermo Scientific) was used. Only RNA samples with an optical density ratio (OD_{260}/OD_{280}) between 1.8 and 2.0 were used.

Total RNA (about 1 μg) was used for first-strand cDNA synthesis using an iSCRIPt cDNA synthesis kit (Bio-Rad Laboratories, Hercules, CA).
The respective primer sequences used are shown in **Table 2**.

Table 2 Sequences of primers

Gene	Sequence (5'-3')	size
sAC[1]	Sense: CATGAGTAAGGAATGGTGGTACTCA; Antisense: AGGGTTACGTTGCCTGATACAATT	111
AC1[2]	Sense: ACCAGCCAAGAGGATGAAGTT; Antisense:ATACCAGCAGCAGCAGGACAG	446
AC2[2]	Sense: GGGAAGATTAGTACCACGGAT; Antisense:AGGAGAAGCCAAGGATGGACG	334
AC3[2]	Sense: ATGAGCACGAACTGAACCAGCT; Antisense: GTCCCATGTAGTACTGGAGACAGCTC	456
AC4[2]	Sense: AGCCAGCCTACCCAGGTT; Antisense: GCTTGGGTCTGAGGTCA	283
AC5[2]	Sense: CAGAGAACCAACTCCATTGGACACAATCCG; Antisense: CACACAGGCGTAGATCACAGATATTTTCAC	456
AC6[2]	Sense: TGCTGCTGGTCACCGTGCTCAT; Antisense: GGACGCTAAGCAGTAGATCATAGTTGTCAA	495
AC7[2]	Sense: GCTCCTACTGAAGCCCAAGTTC; Antisense: AATCACTCCAGCAATCACAGGC	256
AC8[2]	Sense: CAGTCTGGGCCTGAGGAAATT; Antisense:AAGTCAGGTTCTTCAAGGGTA	478
AC9[2]	Sense: ACCTACCTTTACCCAAAGTGCACGGACAAT; AntisenseCTCGGCGCTGCCTCACACACTCTTTGAGAC	360#
PDE3a	Sense: GTGGCCGTATTCTGAGCCAGGTG; Antisense: GCTGTGTTGTGAGATACCACACGGC	——
PDE3b	Sense: CGACCAATTCCTGGCTTACAGCAGC; Antisense: GCAGGAATGTTTGAAGACAGGCAGCC	——
PDE4a	Sense: CCTGCACGCAGCGGATGTGC; Antisense: GGAACTGGTTGGAG-ACGCCAGG	——
PDE4b	Sense: CCTGGCTGCCATTTTTGCAGCTGC; Antisense: GAGCTTGAATCCCACAGCGAGGTG	——
PDE4c	Sense: CCAGGAGGAGCAGCTGGCTAAG; Antisense: CACGTTGGAGTGGTAGTGCCCTTC	——
PDE4d	Sense: GCG-GAGCTGTCTGGCAACCG; Antisense: GACTGGACGACATCTG-CAGCATGG	——
G6PDH	Sense: GAAGCCTGGCGTATCTTCAC; Antisense: GTGAGGGTTCACCCACTTGT	162
GAPDH[3]	Sense:CACGGCAAGTTCAACGGCACAGTCA; Antisense: GTGAAGACGCCAGTAGACTCCACGAC	152
β-actin	Sense: GGCCAACCGTGAAAAGATGAC; Antisense: GCCACGCTCGGTCAGGATCTT	253

1- (Pastor-Soler *et al.*, 2003); 2- (Chang *et al.*, 2003); 3-(Wang and Xu, 2010)

Suitability of primers for RT-PCR amplification was tested by amplifying the product from cDNA in a conventional PCR reaction using Phusion DNA polymerase (New England Biolabs). The absence of non-specific PCR products was confirmed by a single band product by electrophorese separation of the products in 2% ethidium bromide staining agarose gel. A master mix was prepared containing 0.5µM anti-sense primer, 0.5µM sense primer, 10% template CB cDNA, 1X of 5X Phusion Buffer, 200µM of each dNTP and 0.02U/µl Phusion DNA polymerase and the cycling conditions were denaturing 2 min at 98°C, followed by 30 cycles at 98°C for 20 sec, 62°C for 20 sec, 72°C for 5 sec and a terminal extension period at 72°C for 5 min. The products were run in a 2% agarose gel (**Figure 9**).

Real Time-qPCR was performed with a MyiQ iCycler RT-qPCR system (Bio-Rad) with the SYBR Green detection system. The intensity of the dye SYBR Green is proportional to the amount of PCR product. Each qPCR reaction consisted of 1 µl of cDNA and 3.5 µl of 300 nM primers diluted in DEPC-H_2O and 10µl of SYBR Green Supermix (Bio-Rad) for a final volume of 20 µl. We performed triplicates for each sample. qPCR conditions for sAC gene expression and regulation were: denaturing 8 min at 95°C, followed by 40 cycles at 95°C for 1 min, 60°C for 30 sec, 72°C for 45 sec, and a terminal extension period (72°C, 10 min). RT-qPCR conditions for AC (tmAC and sAC) expression and regulation were: denaturing 5 min at 95°C, followed by 40 cycles at 95°C for 20 sec, 62°C for 20 sec, 72°C for 20 sec, and a terminal extension period (72°C, 10 min). We analyzed the specificity of the RT-qPCR product by performing melting curves with 0.5°C increments in temperature. Product formation during the exponential phase of the reaction was analyzed for semi-quantification of relative expression in the specific tissues using the Pfaffl method (Pfaffl, 2001) or relative quantification to reference gene based on the threshold cycle (CT) for amplification as $2^{(\Delta CT)}$, where $\Delta C_T = C_{T,reference} - C_{T,target}$.

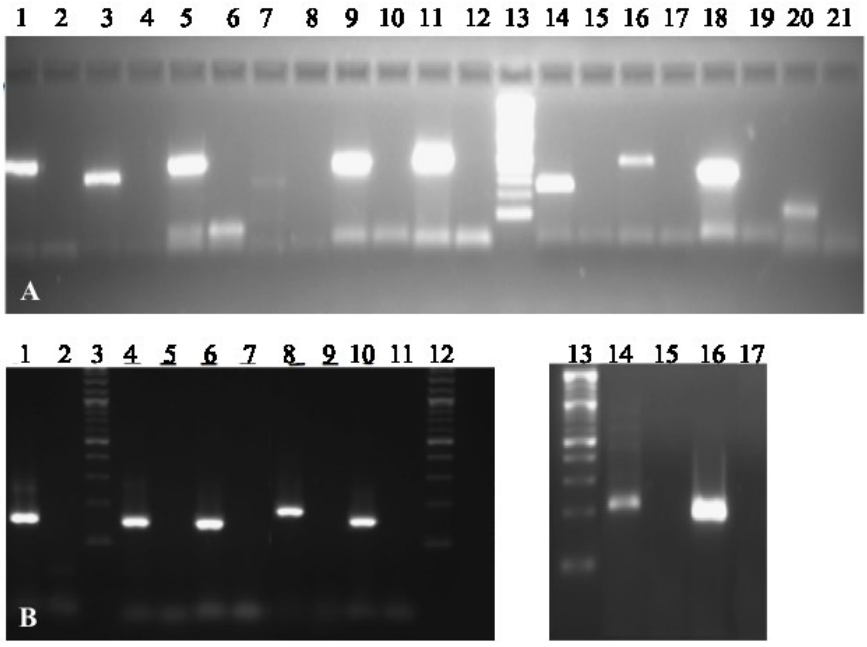

Figure 9- Specificity of the primers. Visualization of thePCR amplification products in 2% agarose gel using different primer setsas indicated. No template cDNA was added to the negative control lanes (-). A) Adenylate cyclase primers: 1) AC1, 2) - AC1, 3) AC2, 4) -AC2, 5) AC3, 6) -AC3, 7) AC4, 8) -AC4, 9) AC5, 10) -AC5, 11) AC6, 12) -AC6, 13) Marker, 14) AC7, 15) -AC7, 16) AC8, 17) -AC8, 18) AC9, 19) -AC9, 20) sAC and 21) -sAC. B) Phosphodiesterases 3 and 4 (PDE3a-b and PDE4a-d) primers: 1) PDE3b, 2) -PDE3b, 3) Marker, 4) PDE4a, 5) - PDE4a, 6) PDE4b, 7) P- PDE4b, 8) PDE4d, 9) - PDE4d, 10) G6PDH, 11) - G6PDH, 12) Marker, 13) Marker, 14) PDE4c, 15) - PDE4C, 16) PDE3a, 17) - PDE3a.

The reference gene used was the glucose-6-phosphate dehydrogenase (G6PDH). We also validate our results using two other different reference genes: glyceraldehyde 3-phosphate dehydrogenase (GAPDH) and beta-actin (β-actin). We evaluated the expression of the three reference genes in all the studied tissues and conditions using a website that combined 4 different algorithms used to determine the stability of the reference genes: geNorm, Normfinder, Bestkeeper and comparative ΔCt method (http://www.leonxie.com/referencegene.php?type=reference). We found that GAPDH is the most stable gene across our experiments, but the gene expression levels normalized with this reference gene showed the same trend of results as shown when normalized with G6PDH.

Fluorescence resonance energy transfer (FRET)

The FRET-based imaging technique was performed in the laboratory of Pharmacology, Department of Pharmacology at Johns Hopkins University, under the supervision of Dr. Jin Zhang. The aim of this collaboration was to investigate the effect of PDE inhibitors and AC activators and inhibitors on cAMP downstream effectors such as PKA, using FRET-based imaging in primary cell cultures and organotypic slices of CB and SCG.

Primary cells (CB and SCG) and organotypic slices were infected with adenovirus to express the third generation of protein kinase A (PKA) activity reporter, AKAR3. AKAR3 is composed by a substrate peptide for PKA, a phosphorylation recognition domain, a cyan florescent protein (CFP) and a yellow florescent protein (YFP) (Zhang *et al.*, 2001). PKA, when activated, is able to phosphorylate the substrate peptide sequence, whereupon the phosphorylation recognition domain forms an intracellular complex with the phosphorylated peptide. This conformational change alters the distance and or relative orientation between the two fluorescent proteins, generating a FRET change. A dephosphorylation of the peptide by phosphatases reverses the FRET signal (Zhang *et al.*, 2001).

Cells/slices were infected with AKAR3 virus in cell culture medium, 37°C, 5%CO_2, for 24 hours and viral infection was confirmed. **Figure 10** confirms AKAR3 expression in PNA-labeled type I cells of the CB.

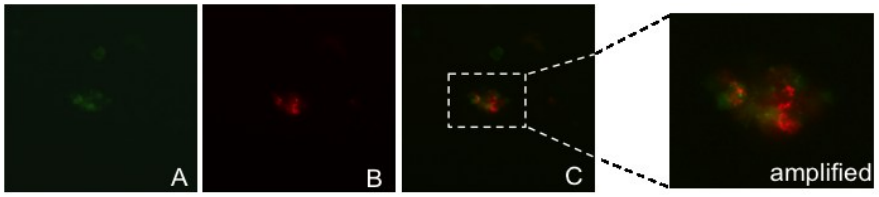

Figure 10- PNA-labeled type I cells expressing A-Kinase Activity Reporter (AKAR3). A) AKAR3 expression, visualized with the FITC channel. B) Type I cells labeled with Rho-PNA (30ug/mL) visualized with TRITC channel. C) Co-localization of AKAR3 and Rho-PNA, confirming the infection of type I cells with AKAR3. 400 fold magnification.

Figure 11 confirms, by immunostainig, the expression of AKAR3 on TH-positive SCG neurons, a specific marker for these cells, as mentioned above in SCG primary cultures.

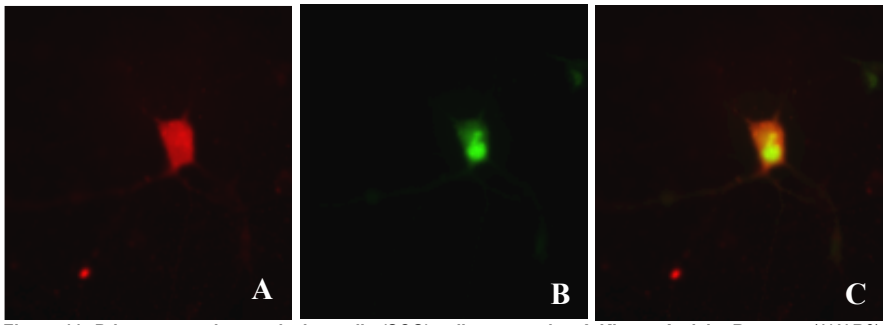

Figure 11- Primary superior cervical ganglia (SCG) cells expressing A-Kinase Activity Reporter (AKAR3) can be identified by expression of tyrosine hydroxylase (TH, a specific marker of these cells). A) Immunostaining of SCG cells labeled with anti-TH (1:50) and visualized with Rhodamine secondary antibody (1:100). B) Expression of AKAR3 in SCG cells, as visualized by FITC channel. C) Co-localization of AKAR3 and TH (1:50) in SCG cells. 400 fold magnification.

Figure 12 confirms the expression of AKAR3 in organotypic SCG slices.

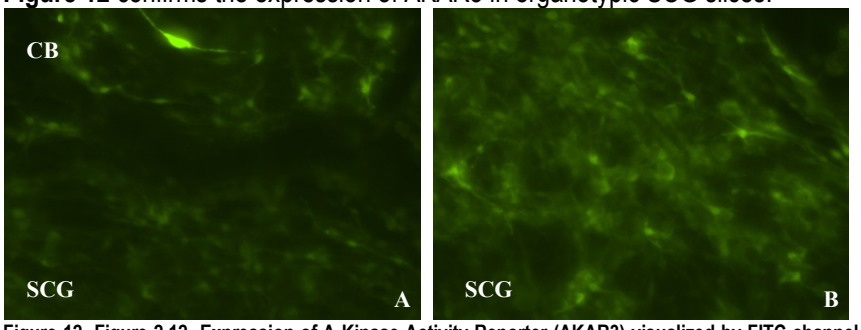

Figure 12- Figure 2.12- Expression of A-Kinase Activity Reporter (AKAR3) visualized by FITC channel in organotypic slices from rat at P7, infected with AKAR3 for 48 hours after 2 days in culture. **A)** AKAR3 expression in slices containing CB and SCG cells. **B)** AKAR3 expression in SCG organotypic slices. 200 fold magnification.

Figure 13 shows the set up for FRET imaging. The cells were imaged on a Zeiss Axiovert 200M microscope (Carl Zeiss) with a 40X oil immersion objective and a cooled charge-coupled device camera (Roper Scientific) controlled by Metafluor 6.2 software (Molecular Devices). Dual emission ratio imaging used a 420DF20 excitation filter, a 450DRLP dichroic mirror and two emission filters (475DF40 for cyan fluorescent protein, CFP, and 535DF25 for yellow fluorescent protein, YFP).

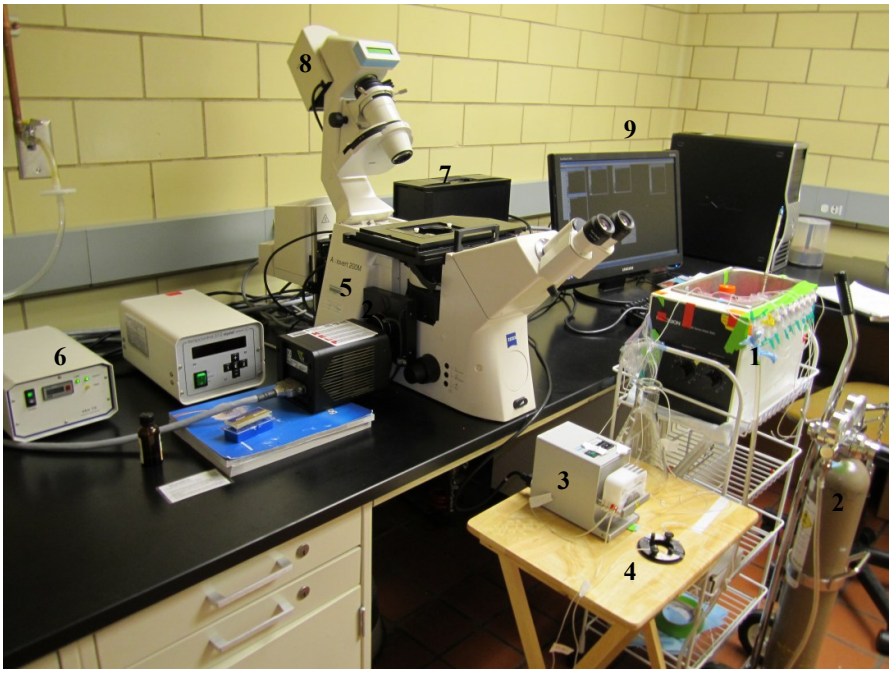

Figure 13- Perfusion system for FRET imaging. Solutions containing PDE inhibitors and AC activators and inhibitors were warmed up in the water bath (1), equilibrated with different % of O_2/CO_2 (2). The solution passed through a pump (3; 2 ml/min) connected to a perfusion chamber (4) containing a petri-dish tightly closed with parafilm and containing the cells/slice. The perfusion chamber was placed next to the lens of an inverted fluorescent microscope Zeiss Axiovert (5) for image acquision. The microscope setup uses an external light source (6) and a filter control (7) to excite the cyan fluorescent protein (CFP) and yellow fluorescent protein (YFP) of the FRET sensors. Fluorescent intensities were recorded by a digital CCD camera (8), controlled by Metaflour 6.2 software (9).

Exposure time was 50-500ms and images were acquired every 20 sec. Background correction of the fluorescence images was performed by subtracting autofluorescent intensities of regions of the imaging dish with no cells. Graph

curves were normalized by setting the emission ratio at baseline (before the addition of any drugs) as equal to one.

In one set of experiments SCG neurons were placed on the heating stage of a Zeiss Axiovert 20M microscope with a 40X oil immersion objective lens, and sequentially were treated with rolipram (ROL, specific PDE4 inhibitor, 1μM), milrinone (MIL, specific PDE3 inhibitor, 10μM), IBMX (non-specific inhibitor, 100μM), Forskolin (FSK, transmembrane adenylyl cyclase activator, 50μM) and H89 (PKA inhibitor, 10μM).

In another set of experiments, the imaging dishes containing SCG or CB or slice cultures were placed into a perfusion chamber (Warner Instruments) to allow perfusion of the cells with a constant flow rate of 2 ml/min (Ismatec pump, Cole Parmer Instruments) with Krebs modified solution in the presence or absence of different PDE and AC activators and inhibitors, equilibrated with different % of CO_2/O_2. **Figure 14** shows the effect of the PDE inhibitors on PKA activity on SCG organotypic slices expressing AKAR3. These slices showed high basal activation of PKA, which did not allow us to observe changes between the different inhibitors.

To test the contribution of tmAC and sAC in PKA activity in the CB type I cells, we performed two sets of experiments: CB cells were incubated in the presence of 1) tmAC and sAC activators, forskolin (50 μM) and HCO_3^-/CO_2 (0/0-44/10 mM/%), respectively, and 2) in the presence of tmAC and sAC inhibitors, MDL 12,330A (500 μM) and KH7 (50 μM), respectively. In both set of experiments, PDEs were inhibited by IBMX (10-100 μM).

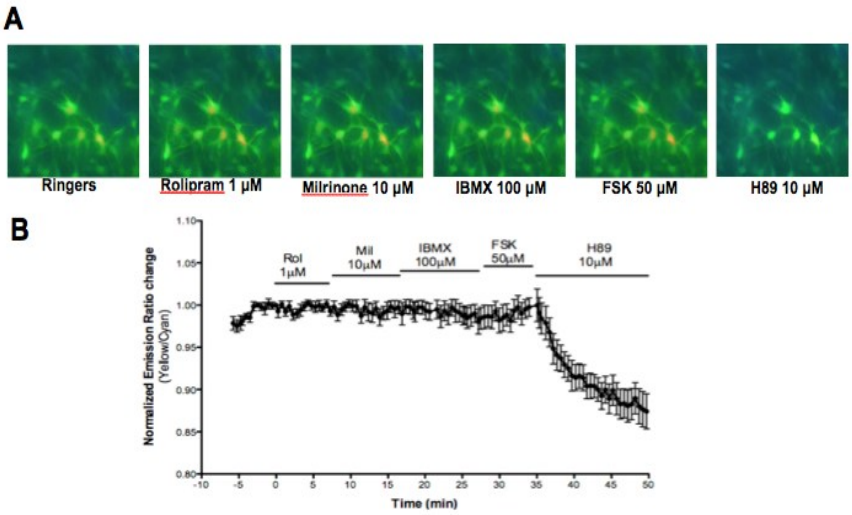

Figure 14- SCG organotypic slices expressing AKAR3 contain high basal PKA activity. A) Pseudocolor images of SCG slices expressing AKAR3. B) Average time-course response of AKAR3 showing no change in emission ratio in response to rolipram (Rol), milrinone (Mil), IBMX and forskolin (FSK). Addition of H89 10 uM decreased emission ratio by 15%.

Intracellular pH measurements

Two different approaches were considered to evaluate changes in intracellular pH in CB cells: iridium oxide pH sensor microelectrodes and fluorescent pH sensitive fluorescent dye.

Iridium oxide pH sensor microelectrodes

Iridium oxide microelectrodes were developed and tested as a pH sensor in the Analytical and Bioanalytical Chemistry Institute, University of Ulm, Germany, under the supervision of Dr. Cristine Kranz. The aim of this collaboration was to develop a pH sensitive microelectrode to investigate changes in intracellular pH when the CB was exposed to Krebs modified solution (KMS) containing different concentrations of HCO_3^-/CO_2.

Iridium oxide pH sensor microelectrodes were used instead of the typical glass pH sensor microelectrodes, since they have higher stability over a wide pH

range, are more rigid thus less breakable, compared to other electrodes. Microelectrodes were prepared as described in Marzouk and co-workers (Marzouk *et al.*, 1998). Briefly, a platinum wire was placed inside of a borosilicate glass capillary tube, and the tip of the glass broken to expose the wire. Insulated copper wire was connected with the platinum wire. The pH sensor was prepared by electrochemical $IrCl_4$ deposition producing an iridium oxide film. A microscope (Nikon) was used to estimating the diameter of the tip of the iridium microelectrode and the formation of the oxide film. The diameters of the microelectrodes tested ranged from 11-35 μm. Cyclic voltammetry and pH measurements were measured using a potentiostat consisting of an electrochemical workstation, a faraday cage and a CHI program (CH Instruments Inc, Austin, Tx) (**Figure 15A**). The electrochemical cell was a three-electrode setting with an Ag/AgCl reference electrode, a platinum wire as a counter electrode and the working microelectrode (**Figure 15B**).

Titration curves were done to characterize the pH responses. The microelectrodes were calibrated measuring their potential response (mV) with respect to the reference electrode and comparing with the potential (mV) and pH value measured by a glass commercial pH meter, in a series of phosphates' buffer solutions in the pH range from 2 to 10. The buffers were prepared by dropwise addition of 1M of HCl and NaOH to the solutions. As observed in **Figure 16A**, a linear relation between the potential (mV) and pH was observed, following the Nernst equation: $E = E^0 + (2.303RT/ nF) \times pH$ (E= total potential (in mV) developed between the sensing and reference electrodes, Eo= a constant characteristic of the particular working/reference electrode pair, (2.303RT/ nF)= a slope of the straight line plot of mV *vs* pH). This linear relation was parallel with the response obtained with glass commercial electrode. The sensitivity of the microelectrode was assessed under relevant conditions to the work presented in this thesis. The effects of pH measurement in Krebs modified solution (KMS) were evaluated by comparison with commercial pH glass electrode and no differences were observed between them over time (**Figure 16B**).

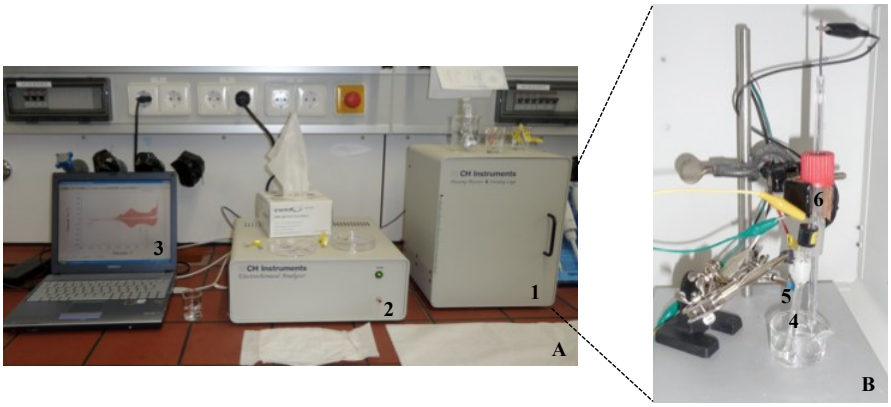

Figure 15- Potentiostat system

A) Potentiostat system consists of a 1) Picoamp boster and faraday cage, used to lower the noise, make relatively fast measurements of small currents and eliminate electrical interference, a 2) electrochemical workstation and the 3) CH program version 8.10. All the equipment is from CH Instruments Inc, Austn, Tx. B) Electrochemical cell inside the faraday cage: 4) Ag/AgCl reference electrode, microelectrode the potential of which remains constant throughout the experiment, 5) working electrode (behind the reference electrode), microelectrode the potential of which varies with the experiment and 6) platinum counter electrode which simply serves to conduct electricity from the signal source though the solution.

However, when KMS in the presence of 24mM HCO_3^- was equilibrated with 60%O_2/5%CO_2, no linear relation between potential and pH was obtained using the iridium oxide microelectrode (**Figure 16C**). Measurements of potential (mV) by iridium oxide microelectrodes were very unstable in the presence HCO_3^-/CO_2/O_2, which are critical/essential parameters/conditions for the experiments of this thesis. Thus, other approach was performed to measure intracellular pH.

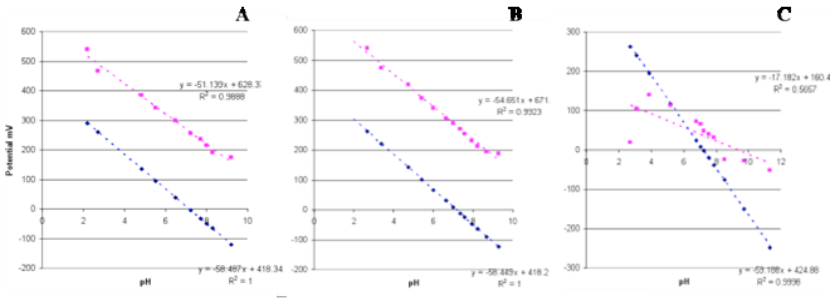

Figure 16 - Calibration curves of the iridium oxide microelectrode and commercial glass electrode. Potentiometric responses of the same iridium oxide microelectrode (pink) and commercial glass pH electrode (blue) to pH changes in different medium solutions: A) phosphate buffer, B) Krebs modified solution and C) Krebs modified solution in the presence of 24mMHCO_3^-/5%CO_2/60%O_2. Except for graph C), iridium oxide microelectrode showed Nernstian mV/pH responses.

Fluorescent intracellular pH measurement

Intracellular pH (pH_i) was measured using the pH-sensitive fluorescence dye, 2',7'-bis(2-carboxyethyl)-5(6)-carboxyfluoresceinacetoxy methyl ester (BCECF-AM (Molecular Probes, Eugene, OR) using a protocol previously described by Iturriaga and co-workers (Iturriaga *et al.*, 1992). The carotid bifurcation with the CB was dissected from the rats, incubated with trypsin (0.02%, Sigma) and collagenase (0.01%, Sigma) for 30 minutes, and rinsed in PBS. Then, the CB was cleaned of connective tissue and fat, remaining attached to the carotid artery. The complex was then incubated with BCECF-AM (5 µM) at 37°C for 1 hour and washed to remove excess of dye. The complex was placed in a perfusion chamber and the detection of labeled cell clusters allowed identification of CB type I cells in the whole CB. These regions were selected as regions of interest (ROI) to analyze changes in BCECF-AM fluorescence intensity while the whole organ was superfused with different concentrations of oxygen solutions. All solutions were titrated to pH 7.4 as described above. Fluorescent images were examined with a fluorescent microscope (Nikon Eclipse E-400, Nikon Instruments, Melville, NY) captured at 400x with an attached charge-coupled device (CCD) camera (Hamamatsu, Photonic ItSystems, Bridgewater, NJ). The BCECF dye was excited at 495 nm, and emission was recorded at 519 nm. The images were captured over a period of 200 frames corresponding to 2.38 minutes and analyzed by Ivison (BioVision Technologies, PA). To avoid photobleaching, the intensity of light was controlled by Exfo X-cite 1200PC (0.12 intensity, Exfo Photonic Solutions, Ontario, Canada). Cells were superfused with the nigericin (10 µM)/high K^+calibration solutions of pH 6.5-8.0 (KCl 140mM, $MgCl_2$ 1.1 mM, $CaCl_2$ 2.2mM, nigericine 10µM and Hepes 5 mM, titrated to the desired pH). Nigericin acts as both potassium and proton ionophore. By raising external potassium to 140 mM the membrane potential should be reduced to around 0 mV and pH_i should become equal to extracellular pH (pH_o). The pH_i is then controlled by changing pH_o (Thomas *et al.*, 1979). Cells were exposed to NH_4Cl (50mM) to

ensure that dye intensity corresponded to changes in intracellular pH (Buckler *et al.*, 1991). NH_4Cl initially increased the fluorescence (alkaline), which was followed by a reduction of the sign (acid). The initial increase in pH was due to the increase concentration of NH_3 in the cell. After NH_4Cl withdrawal, acidification was produced by the exit of NH_3, leaving H^+ in the cells. Changes in BCECF-AM fluorescence intensity were measured while the whole organ was superfused with oxygenated KMS containing increasing concentrations of HCO_3^-/CO_2 and pHi values were extrapolated from the calibration curves.

Statistical analysis

Statistical analysis were obtained using Graph Pad prism. Data are presented as means ± standard error of the mean and $p<0.05$ was considered significant. Specific analyses for each group of experiments are described in the results chapter.

Methods- Diagram

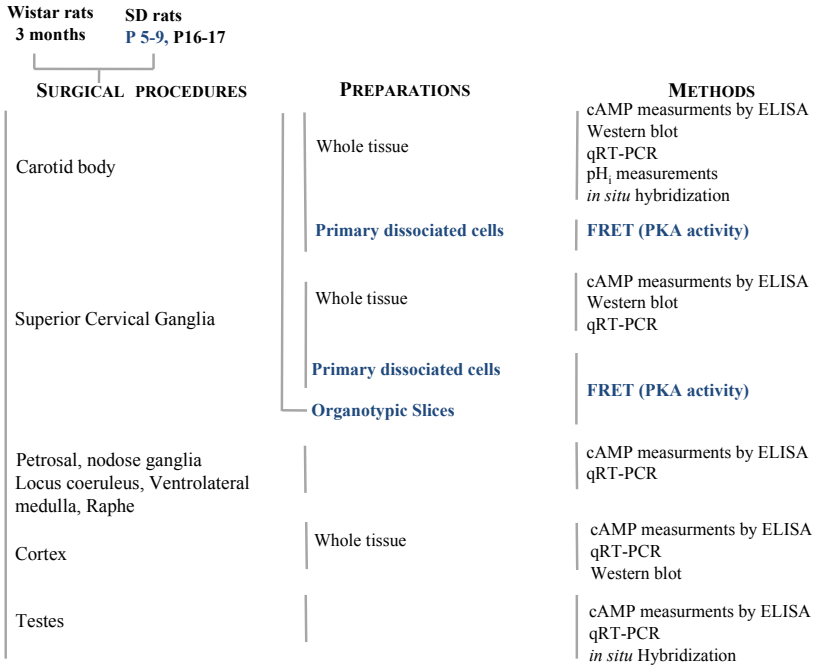

Figure 17- Diagram of the methods used in the work presented in this thesis

IV

RESULTS

CHAPTER 1

Chapter 1 is devoted to the experiments performed in CB and related non-chemosensitive strutures to characterize PDE4 and the effects of O_2 in its activity. The results obtained in this part of the work originated 1) one book chapter and 2) one publication in the British Journal of Pharmacology. The main findings are listed bellow:

1) Functional characterization of phosphodiesterases 4 in the rat carotid body: effect of oxygen concentrations.

***Nunes AR**, Batuca JR, Monteiro EC. Adv Exp Med Biol. 2009; 648:113-9.*

a) PDE 4 inhibitors induced an increase in cAMP levels in both normoxic and hypoxic conditions in CB, consistent with the presence of PDE4 activity in this tissue. Fig.1, page 78.
b) In normoxia, only high levels of inhibitors caused clear effects on cAMP levels while hypoxia increased the effects of the inhibitors at a lower range. Fig.1, page 78.
c) Acute hypoxia increased efficacy and potency of the inhibitors. Emax obtained for all inhibitors (PDE4 inhibitors and non-selective PDE inhibitor, IBMX) were similar in hypoxia and higher than in normoxia, suggesting a higher contribution of PDE4 in the hydrolise of cAMP in this tissue. – Figure 1 and table 1, page 78 and 79;

2) Acute hypoxia modifies cAMP level induced by inhibitors of phosphodiesterase-4 in rat carotid bodies, carotid arteries and superior cervical ganglia

***Nunes AR**, Batuca JR, Monteiro EC. British Journal of Pharmacology*, 2010, 159:353-336

a) cAMP levels did not change significantly between pre-incubations of either 95%O_2 (hypercapnic conditions) or 20%O_2 (normocapnic conditions) in CB, SCG and carotid arteries in the presence of IBMX- Fig 1 page 86;

b) Hypoxic conditions (5%O_2) did not modify cAMP concentrations in the rat CB, SCG and carotid arteries comparatively with basal (20%O_2) – Fig 2,page 86;

c) IBMX (0.3-500uM), rolipram (0.1- 100 uM) and ro 20-1724 (0.1-100 uM) increased cAMP content in CBs in a concentration-response manner in normoxia, and hypoxia shifted the concentration-response curves to the left. This shift was statistically significant for IBMX (>50 uM) and rolipram (<100 uM). Fig 3 and table 1, page 87 e 88;

d) IBMX (0.3-500uM), rolipram (0.1- 100 uM) and ro 20-1724 (0.1-100 uM) increased cAMP content in carotid arteries in hypoxic conditions, specially at low concentrations of Ro 20-1724 and IBMX and high concentrations of rolipram. Fig 4, page 88.

e) In the SCG, both PDE4 inhibitors, IBMX and PDE2 inhibitor, EHNA, increased cAMP levels in normoxic conditions. Hypoxia induced a significant decrease in cAMP levels in the presence of these inhibitors. Fig 5, page 89.

Functional characterization of phosphodiesterases 4 in the rat carotid body: effect of oxygen concentrations

A.R. NUNES, J.R. BATUCA AND E.C. MONTEIRO

Department of Pharmacology, Faculty of Medical Sciences, New University of Lisbon, Campo Mártires da Pátria, 130, Lisbon 1169-056, Portugal. emilia.monteiro@fcm.unl.pt

ABSTRACT

The non-specific cAMP phosphodiesterase (PDE) inhibitor isobutylmethylxanthine (IBMX) has been used to manipulate cAMP levels in carotid body (CB) preparations but the characterization of different PDE isoforms in CB has never been performed. PDE4 is one of the PDE families that uses cAMP as a specific substrate and changes its activity and affinity for drug inhibitors according to the degree of its phosphorylation. We investigated the effects of hypoxia on cAMP accumulation induced by different PDE4 inhibitors in the CB based on the hypothesis that acute changes in O_2 could interfere with their affinity.

Concentration-response curves for the effects of the PDE4 selective inhibitors, rolipram and Ro 20-1724 and IBMX on cAMP were obtained in CBs, removed from rats and incubated in normoxia (20%O_2) or hypoxia (5%O_2).

No differences were found between cAMP concentrations in normoxic and hypoxic conditions in the absence of PDE inhibitors. In both conditions, the E_{max} calculated for IBMX was similar to that of the specific PDE4 inhibitors. Hypoxia shifted the concentration response curves to the left with the following rank order of potency IBMX> RO 20-1724=rolipram and increased E_{max} by about 25%.

This pharmacological approach supports the hypothesis that there is PDE4 activity in CBs that is enhanced by acute hypoxia although the low potency of the PDE4 inhibitors to increase cAMP do not support an important role for PDE4 activation in the O_2-sensing machinery at the CB.

Key words: Carotid body; Hypoxia; phosphodiesterases; cAMP; IBMX; rolipram; Ro 20-1724

1. INTRODUCTION

Gonzalez et al. (eds.), The Arterial Chemoreceptors, 129-136

cAMP is an ubiquitous intracellular second messenger common to metabotropic receptors coupled to transmembrane adenylate cyclase and hydrolysed by cyclic nucleotide phosphodiesterases (PDE). cAMP concentrations in the CB are regulated by the stimulatory effects of adenosine mediated by A_{2A} and A_{2B} receptors (Chen et al. 1997;Conde et al. 2006;Monteiro et al. 1996), by beta-adrenoceptor activity (Mir et al. 1984) and by dopamine D_2 and D_1 receptors (Almaraz et al. 1991;Batuca et al. 2003;Mir et al. 1984). Some evidence also suggests a modulatory role for cAMP in the O_2-sensing machinery in the CB (Gonzalez et al. 1994) but it has also been shown that cyclic nucleotides alone do not modify K^+ current inhibition by hypoxia in isolated type I carotid body cells (Hatton et al. 1996).

The non-specific cAMP phosphodiesterase (PDE) inhibitor isobutylmethylxanthine (IBMX) has been used to manipulate cAMP levels in CB preparations but the characterization of different PDE isoforms in CB, has never been performed. Eleven kinetically distinct PDE isoform families that differ in their affinity for subtracts (cAMP and/or cGMP), pharmacological inhibitors and their response to modulators have so far been identified (Bender et al. 2006).

PDE4 is one of the PDE families that uses cAMP as a specific substrate, its activity is not regulated by Ca^{2+} but changes its activity and affinity for drug inhibitors according to the degree of its phosphorylation (Bender et al. 2006). Chronic hypoxia (several days) regulates PDE4 activity in pulmonary arteries (Millen et al. 2006) as well as the activity of cAMP-PDE in rat blood (Spoto et al. 1998) but little is known about the effect of acute hypoxia. Increases in the activity of a Ca^{2+}-dependent PDE in CBs of rats submitted *in vivo* to 40 min of hypoxia have been reported (Hanbauer et al. 1977).

We investigated the effects of hypoxia on cAMP accumulation induced by different PDE4 inhibitors at the CB based on the hypothesis that acute changes on O_2 could interfere with their affinity.

2. METHODS

2.1. Surgical procedures

The experiments were performed on CBs, isolated from adult (3 months old) male and female Wistar rats. Rats were obtained from the Faculty of Medical Sciences animal house, kept at a constant temperature (21ºC) with a regular light (08-20h) and dark (20-08h) cycle, with food and water *ad libitum*. Experiments were carried out in accordance with the Portuguese regulations for the protection of the animals. Surgical procedures for isolation of the tissues have been described previously (Batuca et al.

2003;Conde et al. 2004). In brief, rats were anaesthetised with sodium pentobarbital (60mg.Kg^{-1} i.p.), then tracheostomised to allow spontaneous breathing during the surgical procedure. After the CBs had been removed the animals were killed by an intracardiac injection of a lethal dose of pentobarbital, in accordance with the EU directives for the use of experimental animals (Portuguese laws no. 1005/92 and 1131/97). The tissues removed were further prepared as follows.

The CBs removed were pre-incubated to allow recovery from the surgical manipulation in a 37ºC shaker bath for 15 minutes in a medium containing: NaCl 116 mM, $NaHCO_3$ 24 mM, KCl 5 mM, $CaCl_2$ 2 mM, $MgCl_2$ 1.1 mM, Hepes 10 mM, Glucose 5.5 mM and adjusted to pH 7.40 (Perez-Garcia et al. 1990) and equilibrated with 20%O_2 ($PO_2 \approx 142$ mmHg). After the pre-incubation period, all the CBs were incubated in a fresh incubation medium, equilibrated in normoxia or hypoxia (5%O_2, $PO_2 = 33$ mmHg) for 30 minutes in the absence or the presence of PDE inhibitors. Only one PDE inhibitor at one concentration was tested in each experiment.

2.2. Cyclic nucleotide extraction and quantification

After incubation, CBs were immersed in cold 6% (w/V) trichloroacetic acid (TCA, 600 µL) for 10 min, weighed on an electrobalance (mc 215 Sartorius), homogenized using a Potter glass homogeniser at 2-8ºC and centrifuged at 12000 g for 10 min at 4ºC. The supernatants were washed four times in 3 ml of water saturated with diethyl ether solution (50:50), collected for lyophilisation (Christ Alpha 1-2 B. Brawn, Biotech International) and stored at -20ºC until cAMP quantification by enzyme immunoassay, using an EIA commercial kit (RPN 2255 GE Healthcare Bio-Sciences AB).

2.3. Data analysis and statistical procedures

cAMP content was expressed in picomoles per milligram tissue (pmol/mg tissue). Data were evaluated using Graph Pad Prism (GraphPad Software Inc., version 4, San Diego, CA, USA) and expressed as means ± s.e.m. Statistical differences between normoxic and hypoxic basal cAMP levels, were assessed by the Mann-Whitney nonparametric test. Comparison between the effects of hypoxia on different PDE inhibitors in CBs was performed by two-way analysis of variance with Bonferroni´s post test. Concentration-response curves for the effects of inhibitors were analysed using sigmoidal curve-fitting analysis, extrapolating the E_{max} (mean maximal effect (%) observed in cAMP levels) and the EC_{50} value (concentration of inhibitor required to elicit 50% of maximum effect observed) for each inhibitor.

3. RESULTS

In the absence of PDE inhibitors, the basal cAMP content observed in CBs incubated with 20%O_2 was 0.75±0.08 pmol/mg (n=15) and hypoxia did not significantly modify cAMP concentrations (0.63±0.05 pmol/mg, n=15).

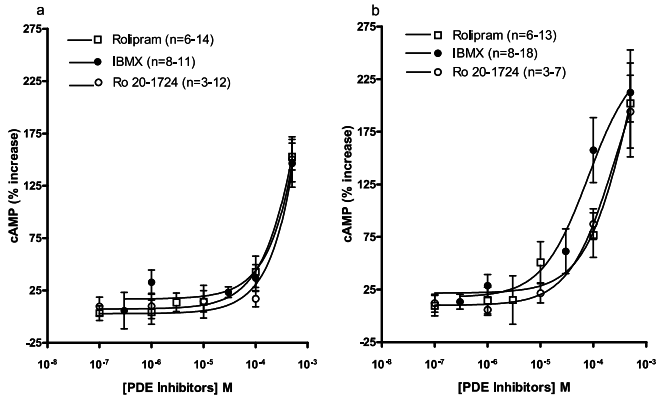

Figure 1 Effects of rolipram, Ro 20-1724 and IBMX on cAMP levels in rat carotid bodies in (a) normoxia (20%O2) (0% effect- 0.75±0.08 pmol cAMP/mg) and (b) hypoxia (5%O2) (0% effect- 0.63±0.05 pmol cAMP/mg). Data values represent means ± s.e.m.

Table 1 Comparison between the efficacies and potencies of PDE inhibitors in normoxia and hypoxia.

IBMX (0.3-500 μM)				Rolipram (0.1-500 μM)				Ro 20-1724 (0.1-500 μM)			
20%O2		5%O2		20%O2		5%O2		20%O2		5%O2	
EC50 (μM)	Emax (%)	EC50 (μM)	Emax (%)	EC50 (μM)	Emax (%)	EC50 (μM)	Emax (%)	EC50 (μM)	Emax (%)	EC50 (μM)	Emax (%)
211.8	146.5 ±22.8	50.4	212.4 ± 27.9	203.7	152.9 ± 12.8	145.2	202.0 ± 50.8	260.6	147.0 ± 41.6	117.8	194.1 ± 34.5

Emax= Mean maximal effect (%) observed in cAMP levels. EC50= Drug concentration that produces 50% of the maximal effect

Figure 1 shows the comparison between the effects of PDE inhibitors in CBs incubated in normoxic (Figure 1a) and hypoxic (Figure 1b) conditions. In normoxia only high concentrations of inhibitors (500 μM) caused clear effects on cAMP levels (Figure 1a) but hypoxia increased the effects of the PDE4 inhibitors (rolipram and Ro 20-1724) as well as the non-specific inhibitor IBMX (Figure 1b). The EC_{50} and E_{max} values obtained from these concentration-response curves are represented in Table 1. The E_{max}

values found in hypoxia were similar for the three inhibitors and higher than those obtained in normoxia (Table 1 and Figure 2). Similar potencies, quantified as EC_{50}, for IBMX, Ro 20-1724 and rolipram were found in normoxia (Table 1). Hypoxia increased the potency of these drugs with a more pronounced effect on IBMX (Table 1). Although higher levels of cAMP were found in the CBs incubated in hypoxia with IBMX, Ro 20-1724 and

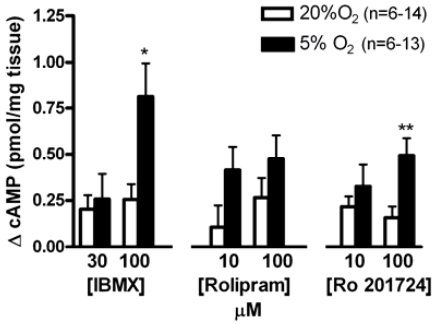

Figure 2 Effects of hypoxia in the presence of selective (rolipram and Ro 20-1724) and non-selective (IBMX) PDE inhibitors on cAMP levels in rat carotid bodies. * P<0.05 and ** P<0.01 two way ANOVA with Bonferroni´s post test. Values represent means ± s.e.m.

rolipram than those obtained in normoxia, only the differences in experiments with 100 μM of IBMX and Ro 20-1724 achieved statistical significance (Figure 2).

4. DISCUSSION

This pharmacological approach provided evidence that PDE4 is active at the CB and that acute hypoxia modifies the effects of PDE4 inhibitor.

An initial work showing an increase in the activity of a Ca^{2+}-dependent PDE in CBs of rats submitted *in vivo* to 40 min of hypoxia appeared in 1977 (Hanbauer et al. 1977) but no further studies are known and the characterisation of PDE isoforms has never been performed at the CB. From the eleven PDE isoform families (PDE1-PDE11) identified and cloned within the superfamily of PDE only three types are known to hydrolyse cAMP selectively (PDE4, PDE7 and PDE8) and five hydrolyse both cAMP and cGMP (PDE1, PDE2, PDE3, PDE10 and PDE11). This work was focused on PDE that use cAMP as a specific substract and that are not modulated by cGMP.

PDE4 isoezymes are characterised by high affinity and specificity for cAMP, low K_M (1.2-10 μM), insensitivity to Ca^{2+} and cGMP, selective inhibition by the archetypal rolipram and Ro 20-1724 (IC_{50} of 1 μM and 2 μM, respectively) (Bender et al. 2006). No specific inhibitors are available for PDE8 but it is known that both PDE7 and 8 are insensitive to rolipram (Lugnier 2006). IBMX is a commonly used tool for causing non-specific

inhibition of PDE1 to PDE5 but is devoid of effects on PDE7, PDE8 and PDE9 (Lugnier 2006).

In this study we observed concentration-dependent effects of Ro 20-1724, rolipram and IBMX in CBs, and concluded that PDE4 is present in the CB. The efficacy of the non-selective inhibitor, IBMX, to increase cAMP was similar to that of the PDE4 selective inhibitors Ro 20-1724 and rolipram in CBs suggesting that probably no other PDE is relevant in terms of hydrolysing specifically cAMP in this tissue.

cAMP concentrations were used to investigate the effects of PDE inhibitors and to characterise PDE in different tissues. Since cAMP accumulation depends basically on the equilibrium between adenylate cyclase activation and degradation by PDE, this is not a direct, specific method to characterise the enzyme isoforms in comparison, for instance, with enzymatic activity and/or protein expression methodologies. However, from the point of view of drug effects, quantifying cAMP provided functional and integrated results useful for choosing the most appropriate tool and its concentrations to manipulate cAMP.

Since whole CBs were used in this study the effects on cAMP accumulation can be attributed to PDE4 inhibition in chemosensitive elements (type I and II cells and CSN afferent endings) as well as vessels and autonomic nerve endings.

In normoxic conditions the EC_{50} calculated for all the PDE4 inhibitors studied were in general higher than the IC_{50} values described in the literature (rolipram= 1μM; Ro 20-1724= 2 μM and IBMX= 1-50 μM (Bender et al. 2006)) but were similar to the concentrations of IBMX and Ro 20-1724 ($> 3x10^{-5}M$) needed to increase cAMP in isolated cardiomyocytes (Katano et al. 1990). Since both IBMX and the specific inhibitors, rolipram and Ro 20-1724, showed similar EC_{50} values (respectively 208, 203.7 and 262.4 μM) the low potencies should be attributed to low PDE4 activity in the CBs instead of any particular drug effect.

The effect of chronic hypoxia (several days) on PDE activity has been addressed in other preparations (Millen et al. 2006;Spoto et al. 1998) but this work showed for the first time that acute hypoxia increases the effect of PDE inhibitors on cAMP accumulation. With the methodological approach used in the present work we cannot exclude that the effects of hypoxia include changes in adenylate cyclase activity. In the absence of PDE inhibitors hypoxia did not increase basal cAMP values. In the assumption that hypoxia activates transmembrane adenylate cyclase, this means that hypoxia should also increase cAMP degradation. The hypothesis that hypoxia preferentially regulates degradation than cAMP production is in keeping with the general pharmacological principle that regulation of any ligand or second messenger degradation can often make a more rapid and larger percentage change in concentration than comparable regulation of the rates of synthesis. This is particularly true in the case of cAMP/cGMP where PDE activity is at

least one order of magnitude higher than adenylate and guanylate cyclases in all tissues (see e.g. (Bender et al. 2006)).

Acute hypoxia increased the efficacy as well as the potency of the inhibitors suggesting that probably an increase in both PDE activity and drug affinities are involved. Complex cAMP driven mechanisms through protein kinase A and extracellular signal regulated kinase mediated phosphorylation can modify PDE4 specific isoforms activity and subsequently alter sensitivity to selective inhibitors (Bender et al. 2006). The hypothesis that acute hypoxia may cause PDE4 activation by PKA- or ERK mediated phosphorylation could be advanced.

In conclusion, this pharmacological approach supports the hypothesis that there is PDE4 activity in CBs that is enhanced by acute hypoxia although the low potency of the PDE4 inhibitors to increase cAMP do not support an important role for PDE4 activation in the O_2-sensing machinery at the CB.

ACKNOWLEDGMENTS

This work was financially supported by CEPR/FCT. The authors are grateful to the Department of Microbiology, Faculty of Medical Sciences for the valuable help in sample lyophilisation.

REFERENCES

Almaraz, L., Perez-Garcia, M. T., & Gonzalez, C. 1991, Presence of D1 receptors in the rabbit carotid body, *Neurosci.Lett.*, 132: 259-262.

Batuca, J. R., Monteiro, T. C., & Monteiro, E. C. 2003, Contribution of dopamine D2 receptors for the cAMP levels at the carotid body, *Adv.Exp.Med.Biol.*, 536: 367-373.

Bender, A. T. & Beavo, J. A. 2006, Cyclic nucleotide phosphodiesterases: molecular regulation to clinical use, *Pharmacol.Rev.*, 58: 488-520.

Chen, J., Dinger, B., & Fidone, S. J. 1997, cAMP production in rabbit carotid body: role of adenosine, *J.Appl.Physiol*, 82: 1771-1775.

Conde, S. V. & Monteiro, E. C. 2004, Hypoxia induces adenosine release from the rat carotid body, *J.Neurochem.*, 89: 1148-1156.

Conde, S. V., Obeso, A., Vicario, I., Rigual, R., Rocher, A., & Gonzalez, C. 2006, Caffeine inhibition of rat carotid body chemoreceptors is mediated by A2A and A2B adenosine receptors, *J.Neurochem.*, 98: 616-628.

Gonzalez, C., Almaraz, L., Obeso, A., & Rigual, R. 1994, Carotid body chemoreceptors: from natural stimuli to sensory discharges, *Physiol Rev.*, 74: 829-898.

Hanbauer, I. & Lovenberg, W. 1977, Presence of a calcium2+-dependent activator of cyclic-nucleotide phosphodiesterase in rat carotid body: effects of hypoxia, *Neuroscience*, 2: 603-607.

Hatton, C. J. & Peers, C. 1996, Hypoxic inhibition of K+ currents in isolated rat type I carotid body cells: evidence against the involvement of cyclic nucleotides, *Pflugers Arch.*, 433: 129-135.

Katano, Y. & Endoh, M. 1990, Differential effects of Ro 20-1724 and isobutylmethylxanthine on the basal force of contraction and beta-adrenoceptor-mediated response in the rat ventricular myocardium, *Biochem.Biophys.Res.Commun.*, 167: 123-129.

Lugnier, C. 2006, Cyclic nucleotide phosphodiesterase (PDE) superfamily: a new target for the development of specific therapeutic agents, *Pharmacol.Ther.*, 109: 366-398.

Millen, J., MacLean, M. R., & Houslay, M. D. 2006, Hypoxia-induced remodelling of PDE4 isoform expression and cAMP handling in human pulmonary artery smooth muscle cells, *Eur.J.Cell Biol.*, 85: 679-691.

Mir, A. K., McQueen, D. S., Pallot, D. J., & Nahorski, S. R. 1984, Direct biochemical and neuropharmacological identification of dopamine D2-receptors in the rabbit carotid body, *Brain Res.*, 291: 273-283.

Monteiro, E. C., Vera-Cruz, P., Monteiro, T. C., & Silva e Sousa MA 1996, Adenosine increases the cAMP content of the rat carotid body in vitro, *Adv.Exp.Med.Biol.*, 410: 299-303.

Perez-Garcia, M. T., Almaraz, L., & Gonzalez, C. 1990, Effects of different types of stimulation on cyclic AMP content in the rabbit carotid body: functional significance, *J.Neurochem.*, 55: 1287-1293.

Spoto, G., Di Giulio, C., Contento, A., & Di Stilio, M. 1998, Hypoxic and hyperoxic effect on blood phosphodiesterase activity in young and old rats, *Life Sci.*, 63: L349-L353.

BJP BRITISH JOURNAL OF PHARMACOLOGY
BPS BRITISH PHARMACOLOGICAL SOCIETY

British Journal of Pharmacology (2010), 159, 353–361

0007-1188/10
www.brjpharmacol.org

RESEARCH PAPER

Acute hypoxia modifies cAMP levels induced by inhibitors of phosphodiesterase-4 in rat carotid bodies, carotid arteries and superior cervical ganglia

Ana R. Nunes, Joana R. Batuca and Emília C. Monteiro

Department of Pharmacology and CEDOC, Faculty of Medical Sciences, New University of Lisbon, Campo Mártires da Pátria, 130, Lisbon, Portugal

Background and purpose: Phosphodiesterase (PDE) inhibitors are useful to treat hypoxia-related diseases and are used in experiments studying the effects of oxygen on 3′-5′-cyclic adenosine monophosphate (cAMP) production. We studied the effects of acute hypoxia on cAMP accumulation induced by PDE inhibitors in oxygen-specific chemosensors, the carotid bodies (CBs) and in non-chemosensitive CB-related structures: carotid arteries (CAs) and superior cervical ganglia (SCG).
Experimental approach: Concentration–response curves for the effects of a non-specific PDE inhibitor [isobutylmethylxanthine (IBMX)], PDE4 selective inhibitors (rolipram, Ro 20-1724) and a PDE2 selective inhibitor (erythro-9-(2-hydroxy-3-nonyl)adenine) on cAMP levels were obtained in normoxic (20% O_2/5% CO_2) or hypoxic (5% O_2/5% CO_2) conditions.
Key results: Responses to the PDE inhibitors were compatible with the presence of PDE4 in rat CBs, CAs and SCG but in the absence of PDE2 in CAs and CBs. Acute hypoxia enhanced the effects of IBMX and PDE4 inhibitors on cAMP accumulation in CAs and CBs. In SCG, acute hypoxia reduced cAMP accumulation induced by all the four PDE inhibitors tested. Differences between the effects of Ro 20-1724 and rolipram on cAMP were found in CAs and CBs during hypoxia.
Conclusions and implications: The effects of PDE4 inhibitors could be potentiated or inhibited by acute hypoxia depending on the PDE isoforms of the tissue. The similarities between the characterization of PDE4 inhibitors at the CBs and CAs, under normoxia and hypoxia, did not support a specific role for cAMP in the oxygen-sensing machinery at the CB and suggested that no direct CB-mediated, hyperventilatory, adverse effects would be expected with administration of PDE4 inhibitors.
British Journal of Pharmacology (2010) **159**, 353–361; doi:10.1111/j.1476-5381.2009.00534.x; published online 15 January 2010

Keywords: cAMP; carotid body; carotid artery; hypoxia; PDE inhibitors; superior cervical ganglia; rolipram; IBMX; Ro 20-1724; EHNA

Abbreviations: AC, adenylate cyclase; cAMP, 3′-5′-cyclic adenosine monophosphate; CA, carotid artery; CB, carotid body; EHNA, erythro-9-(2-hydroxy-3-nonyl)adenine; IBMX, isobutylmethylxanthine; PDE, phosphodiesterase; SCG, superior cervical ganglia

Introduction

The carotid body (CB) is a small paired organ located in the bifurcation of the common carotid artery (CA) and is sensitive to changes in blood P_{O2}, P_{CO2} and pH. Morphologically, CB includes specific chemoreceptor cells (type I or glomus cells), sustentacular cell (type II) vessels that originate from the common CA bifurcation, sensory nerve endings of the carotid sinus nerve and efferent nerve endings from the superior cervical ganglia (SCG) and glossopharyngeal nerve (McDonald and Mitchell, 1975). Arteries and efferent nerve endings at the CB can be considered non-chemosensitive structures in comparison with type I and II cells and the sensory endings of the carotid sinus nerve.

Hypoxia is the primary stimulus that activates CB chemosensors triggering respiratory reflexes in order to adjust ventilation to the metabolic needs. Although the chemosensory mechanism of the CB is poorly understood, several studies suggested that 3′-5′-cyclic adenosine monophosphate (cAMP) plays a modulatory role in the oxygen-sensing machinery in this organ (Delpiano and Acker, 1991; Gonzalez *et al.*, 1994; Chen *et al.*, 1997). cAMP is the second messenger common to metabotropic receptors coupled to adenylyl cyclase (AC, E.C. 4.6.1.1). In the CB, levels of cAMP are regulated by the stimulatory effects of adenosine mediated by A_{2A} and A_{2B} receptors (Monteiro *et al.*, 1996; Chen *et al.*, 1997;

Correspondence: Emília C. Monteiro, Department of Pharmacology, Faculty of Medical Sciences, New University of Lisbon, Campo Mártires da Pátria, 130 Lisbon 1169-056, Portugal. E-mail: emilia.monteiro@fcm.unl.pt
Received 23 May 2009; revised 24 July 2009, 15 August 2009; accepted 30 August 2009

Conde *et al.*, 2006), by β-adrenoceptor activity (Mir *et al.*, 1984) and by dopamine D_2 and D_1 receptors (Mir *et al.*, 1984; Almaraz *et al.*, 1991; Batuca *et al.*, 2003; receptor nomenclature follows Alexander *et al.*, 2008).

Hydrolysis of cAMP is mediated by cyclic nucleotide phosphodiesterases (PDE, E.C. 3.1.4.17). So far, 11 kinetically distinct PDE isoforms have been identified. These isoforms differ in their affinity for substrates [cAMP and/or 3′-5′-cyclic guanosine monophosphate (cGMP)], their response to modulators and their pharmacological inhibitors (Bender and Beavo, 2006).

PDE inhibitors are useful in the treatment of several pathological conditions related to hypoxia such as pulmonary hypertension, chronic obstructive pulmonary disease and asthma (see Jeon *et al.*, 2005) and are also common tools used to indirectly study AC activity in response to different oxygen concentrations.

Frequently, studies measuring cAMP in the CB under acute hypoxic and normoxic conditions have used the non-isoform-selective PDE inhibitor, isobutylmethylxanthine (IBMX, 500 μM) (Mir *et al.*, 1984; Pérez-Garcia *et al.*, 1990; 1991; Delpiano and Acker, 1991; Batuca *et al.*, 2003). However, PDE activities of the CB have never been characterized and the interpretation of the effects of IBMX could also be confused by changes in PDE activity caused by hypoxia itself. For instance, acute hypoxia (20 min) increased the activity of a Ca^{2+}-dependent PDE in CB (Hanbauer and Lovenberg, 1977), and chronic hypoxia (7 or 12 days) regulates PDE4 activity in pulmonary arteries (Millen *et al.*, 2006) as well as the activity of cAMP-PDE in rat blood (Spoto *et al.*, 1998).

In this study, a pharmacological characterization of the PDE activity present in whole CB, CA and SCG was performed in normoxic and acute hypoxic conditions. CAs and SCG were used as non-chemosensitive structures related to the CBs. This methodological approach has been used previously (Conde and Monteiro, 2004), due to the small size of rat CBs. PDE in these tissues has never been characterized and the effects of oxygen concentrations on their PDE activity are unknown. If cAMP accumulation is relevant to the specificity of oxygen-sensing machinery in chemosensitive tissues, an effect of hypoxia on cAMP catalytic enzymes could be expected.

Manipulation of cyclic nucleotides with PDE inhibitors has been used to induce vasodilation in clinical studies, but the functional effects of cAMP-PDE inhibitors during different oxygen exposures are not known. The long forms of the PDE4 sub-types can be phosphorylated by protein kinase A, causing a conformational change and a 60% to 250% increase in activity of the catalytic domain that leads to an increased affinity for rolipram (Bender and Beavo, 2006). We hypothesized that acute (30 min) changes in oxygen concentrations could affect the degree of PDE phosphorylation and, consequently, the potency and efficacy of PDE inhibitors.

The results of this work will contribute towards interpreting data obtained when PDE inhibitors are used as tools to manipulate cAMP in these tissues, to characterize PDE in oxygen-chemosensitive and non-chemosensitive tissues and to study the potential tissue-specific modulation of PDE inhibitors in hypoxia-related disease conditions. A preliminary report of some of these findings has been published in the proceedings of a conference (Nunes *et al.*, 2009).

British Journal of Pharmacology (2010) **159** 353–361

Methods

Surgical procedures

All animal care and experimental procedures were carried out in accordance with the European Union directives for the use of experimental animals (Portuguese laws no. 1005/92 and 1131/97). We used CBs, SCG and CAs, isolated from adult (approximately 3 months old) male and female Wistar rats (n = 188). Rats were obtained from the Faculty of Medical Sciences animal facilities, kept at a constant temperature (21°C) with a regular light (08–20 h) and dark (20–08 h) cycle, with food and water *ad libitum*. Surgical procedures for isolation of the tissues *in situ* have been described previously (Batuca *et al.*, 2003; Conde and Monteiro, 2004; 2006). In brief, rats were anaesthetized with sodium pentobarbital (60 mg·kg^{-1} i.p.), then tracheostomized to allow spontaneous breathing during the surgical procedure (approximately 30 min). After the CBs, SCG and CAs had been removed, the animals were killed by an intracardiac injection of a lethal dose of pentobarbital. The tissues removed with intact endothelium were weighed (the mean weight of the rat CBs, CAs and SCG were 148 μg, 1.579 mg and 1.360 mg respectively) and further prepared as follows.

Effects on cAMP content of oxygen concentrations during the recovery pre-incubation period

The rat CBs, SCG and CAs were removed *in vivo* and pre-incubated to allow recovery from the surgical procedures in a 37°C shaker bath for 15 min in a medium containing (in mM): NaCl 116, $NaHCO_3$ 24, KCl 5, $CaCl_2$ 2, $MgCl_2$ 1.1, HEPES 10, glucose 5.5 and adjusted to pH 7.40 (Pérez-Garcia *et al.*, 1990). This medium composition was used in all experiments throughout the work. Two groups of experiments were performed in order to study the effect of oxygen concentrations: hyperoxia (95% O_2/5% CO_2, P_{O2} ≈ 677 mmHg) and normoxia (20%O_2/5%CO_2, P_{O2} ≈ 142 mmHg) during the pre-incubation period. After the pre-incubation period, all the CBs, SCG and CAs were incubated in a fresh incubation medium containing 500 μM of IBMX, a non-selective PDE inhibitor, equilibrated in normoxia or hypoxia (5% O_2/5% CO_2, P_{O2} = 33 mmHg) for 30 min. This incubation period was chosen because we have previously shown that cAMP concentrations obtained during incubations of 30 min were significantly higher than those obtained during 10 min (Batuca *et al.*, 2003) and maintained normal values of cellular viability (Conde and Monteiro, 2004).

Effects of hypoxia on cAMP content in CBs, SCG and CAs in the absence of PDE inhibitors

CBs, SCG and CAs with intact endothelium were removed *in vivo* and pre-incubated in a 37°C shaker bath in incubation medium (previously described) adjusted to pH 7.40 and equilibrated with 20% O_2/5% CO_2. After 15 min, the tissues were incubated for 30 min in a fresh medium at 37°C, pH 7.40, in the absence of any inhibitor. The tissues were divided into two experimental groups: one equilibrated in normoxia and the other equilibrated in hypoxia.

Effect of PDE inhibitors on cAMP content in CBs, SCG and CAs
Tissues (CBs, SCG and CAs) previously pre-incubated with 20% O_2/5% CO_2 for 15 min were incubated in a fresh medium in the presence of PDE inhibitors. The PDE inhibitors used were IBMX (non-selective PDE inhibitor, 0.3–500 μM), Ro 20-1724 (PDE4 selective inhibitor, 0.1–100 μM), rolipram (PDE4 selective inhibitor, 0.1–100 μM) and erythro-9-(2-hydroxy-3-nonyl)adenine (EHNA) (PDE2 selective inhibitor, 0.1–100 μM). Only one PDE inhibitor at one concentration was tested in each experiment. The incubation medium containing each PDE inhibitor was equilibrated with 20% O_2/5% CO_2 or 5% O_2/5% CO_2 in a shaker bath at 37°C for 30 min, which corresponds to the period necessary to detect changes in the kinetic properties of PDEs (Hanbauer and Lovenberg, 1977).

Cyclic nucleotide extraction and quantification
After incubation, CBs, SCG and CAs were immersed in cold 6% (w/V) trichloroacetic acid (600 μL) for 10 min, weighed on an electrobalance (mc 215 Sartorius, Madrid, Spain), homogenized using a Potter glass homogenizer at 2–8°C and centrifuged at 12 000 g for 10 min at 4°C. The supernatants were washed four times with 3 mL of water saturated with diethyl ether solution (50:50), collected for lyophilization (Christ Alpha 1-2 B. Brawn, Biotech International, Melsungen, Germany) and stored at –20°C until cAMP quantification by enzyme immunoassay, using an EIA commercial kit (RPN 2255 GE Healthcare Bio-Sciences AB, Uppsala, Sweden).

Data analysis and statistical procedures
cAMP content present in CBs, SCG and CAs was expressed in picomoles per milligram of tissue (pmol/mg tissue) instead of mg protein due to the small size of the CB (ca 150 μg, see above). Data were evaluated using Graph Pad Prism (GraphPad Software Inc., version 4, San Diego, CA, USA) and expressed as means ± SEM. Statistical differences between two pre-incubation conditions in the CBs, between normoxic and hypoxic basal cAMP levels in the three different tissues, between cAMP levels from normoxic and hypoxic CAs incubated with 1 μM and 30 μM of IBMX and between normoxic and hypoxic cAMP levels in SCG incubated with 100 μM of EHNA were assessed by the Mann–Whitney non-parametric test. Comparison between the hypoxic effects on different PDE inhibitors in CBs was performed by two-way analysis of variance with Bonferroni's post-test. Concentration–response curves for the effects of inhibitors were analysed using sigmoidal curve-fitting analysis, extrapolating the E_{max} [mean maximal effect (%) observed in cAMP levels] and the EC_{50} value (concentration of inhibitor required to elicit 50% of maximum effect observed) for each inhibitor. The comparison between concentration–response curves for the effects of the PDE inhibitors was assessed using Graph Prism to compare the curve-fitted points (log EC_{50} and Hill slope). The null hypothesis (one curve for all data sets) was rejected on the basis of the *F*-test. In all cases, *P*-values of 0.05 or less were considered as significant differences. Also, *n* corresponds to the number of different experiments performed in each group.

Materials
Sodium pentobarbital, IBMX, 4-[3-(cyclopentyloxy)-4-methoxy-phenyl]-2-pyrrolidinone (rolipram), 4-[(3-butoxy-4-methoxyphenyl)-methyl]-2-imidazolidinone (Ro 20-1724) and EHNA were obtained from Sigma (St. Louis, MO, USA). Rolipram and Ro 20-1724 were dissolved in dimethyl sulphoxide in 1 and 5 mM stock solutions and all subsequent dilutions were made in incubation medium.

Results

Effects of oxygen concentrations during the recovery pre-incubation period on cAMP content
In previous studies where cAMP was quantified, the CBs were allowed to recover from the ischaemia, to which the preparations were submitted during dissection, with a pre-incubation period of 15 min in a medium equilibrated with 100% O_2/5% CO_2 or 95% O_2/5% CO_2 (Pérez-Garcia *et al.*, 1990; Almaraz *et al.*, 1991; Monteiro *et al.*, 1996; Chen *et al.*, 1997; Batuca *et al.*, 2003). As hyperoxia is not a physiological condition and prolonged exposure to normobaric hyperoxia attenuates CB chemosensory response to hypoxia (Mokashi and Lahiri, 1991; Torbati *et al.*, 1993; Mokashi *et al.*, 1994), an initial group of experiments was carried out to define the oxygen concentrations to be used during the recovery from ischaemia, in this study. This rationale was applied to the three preparations used in the present work and the results are shown in Figure 1. In these experiments, the non-specific PDE inhibitor IBMX in a high concentration (500 μM) was added to the incubation medium, keeping all the other experimental conditions (recovery and incubation time as well as medium composition) constant throughout the different group of experiments (see Methods section). In light of the absence of statistically significant differences ($P > 0.05$, Mann–Whitney test) between the two pre-incubation conditions for CBs, CAs and SCG, we decided to perform all the experiments pre-incubating these tissues with 20% O_2/5% CO_2, which is comparable to an atmospheric oxygen concentration.

Effects of hypoxia on cAMP content in CBs, SCG and CAs in the absence of PDE inhibitors
In the absence of PDE inhibitors, the basal cAMP content observed in CBs, SCG and CAs incubated with 20% O_2/5% CO_2 is shown in Figure 2. It is apparent here that, in normoxia, cAMP accumulation was higher in CBs than in other tissues (CBs > SCG > CAs) and that hypoxia did not significantly modify cAMP concentrations in either CBs or SCG, but decreased cAMP levels in CAs ($P < 0.001$). As expected, in these group of experiments, cAMP content in both normoxic and hypoxic conditions was clearly lower, about half that obtained in the presence of 500 μM of IBMX (Figure 1).

Effect of PDE inhibitors on cAMP content in CBs
The effects of PDE inhibitors on CBs were assayed indirectly quantifying cAMP content. The concentrations used for each inhibitor were selected according to the published IC_{50} values: rolipram = 1 μM; Ro 20-1724 = 2 μM; IBMX = 2–50 μM

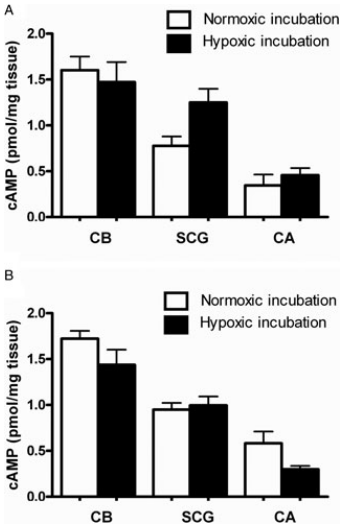

Figure 1 Effect of different pre-incubation conditions on cAMP levels of carotid body (CB, $n = 6–9$), superior cervical ganglia (SCG, $n = 2–5$) and carotid artery (CA, $n = 4–5$) in response to hypoxia (5% O_2/5% CO_2) and in the presence of isobutylmethylxanthine (500 μM). Tissues were pre-incubated in (A) hyperoxia (95% O_2/5% CO_2) or (B) normoxia (20% O_2/5% CO_2). $P > 0.05$.

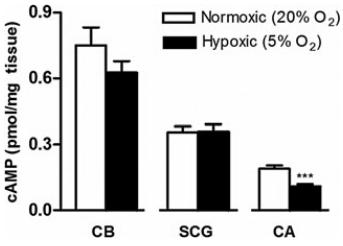

Figure 2 Effects of hypoxia on cAMP levels (expressed as pmol/mg tissue) in rat carotid bodies (CBs, $n = 15$), superior cervical ganglia (SCG, $n = 11$) and carotid arteries (CAs, $n = 11–12$) in the absence of PDE inhibitors. Data represent means ± SEM ***$P < 0.001$ Mann–Whitney non-parametric test, corresponding to the differences between normoxia and hypoxia.

(Bender and Beavo, 2006) and EHNA = 2 μM (Podzuweit *et al.*, 1995). EHNA (0.1–100 μM) did not modify cAMP concentrations in CBs incubated in either normoxia or hypoxia. However, IBMX (0.3–500 μM), rolipram (0.1–100 μM) and Ro 20-1724 (0.1–100 μM) increased cAMP content in CBs in a concentration-dependent manner in normoxia (Figure 3) and hypoxia shifted their concentration–response curves to the left. This shift was statistically significant ($P < 0.001$) for IBMX and rolipram but not for Ro-20-1724 (Figure 3). This effect of hypoxia was apparent only for concentrations <100 μM for the specific PDE4 inhibitors and higher than 50 μM for the non-selective PDE inhibitor IBMX. The EC_{50} and E_{max} values calculated for concentrations between 0.1 and 100 μM for Ro 20-1724 and rolipram and between 0.1 and 500 μM for IBMX are presented in Table 1. The E_{max} values found in normoxia for concentrations between 0.1 and 100 μM were similar for rolipram, Ro 20-1724 and IBMX (56 ± 11%, 35 ± 8% and 37 ± 13%, respectively, Figure 3). The effect of hypoxia on cAMP accumulation caused by PDE inhibition was more pronounced in the case of rolipram (Figure 3), although no apparent changes in drug potency (EC_{50}) were observed (Table 1). The EC_{50} values obtained for Ro 20-1724 and rolipram in the CBs were <10 μM (Table 1).

Effects of PDE inhibitors on cAMP content in CAs

The effects of PDE inhibitors were also tested in rat CAs, both in normoxic and hypoxic conditions. As observed with the CBs, EHNA (0.1–100 μM) did not affect the cAMP levels in CAs either in normoxia or hypoxia. The effects of Ro 20-1724 (0.1–100 μM) and rolipram (0.1–100 μM) on cAMP in the CAs incubated with 20% O_2/5% CO_2 were similar and caused increases <40% (Figure 4A,B). Hypoxia clearly heightened the effects of both PDE4 selective inhibitors on cAMP content, specifically with higher concentrations of rolipram (>10 μM) and low concentrations of Ro 20-1724 (1 μM) (Figure 4A,B). The difference between cAMP accumulation in CAs during normoxia and hypoxia was particularly evident with rolipram ($P < 0.0001$, Figure 4A). Increases in cAMP accumulation caused by IBMX in CAs in both normoxic and hypoxic conditions were clearly more accentuated than those observed with Ro 20-1724 and rolipram (Figure 4C). These increases in cAMP in CAs induced by the non-specific PDE inhibitor, IBMX, apparently involve two mechanisms, one observed at low concentrations (<30 μM) which was heightened by hypoxia, and another observed with very high concentrations (0.1–1 mM) which was not modified by changes in oxygen (Figure 4C). The comparisons between the potency of the PDE4 inhibitors and the magnitude of their effects on cAMP are shown in Table 1 and expressed as EC_{50} and E_{max}. In this table, the effects on cAMP content in CAs induced by low (1–100 μM) concentrations of IBMX are shown separately in order to emphasize the effect of hypoxia observed in these experimental conditions.

Effect of PDE inhibitors on cAMP content in SCG

In rat SCG, the effects of rolipram, Ro 20-1724, IBMX and EHNA on cAMP levels were also compared in normoxic and hypoxic conditions (Figure 5). Concentration-dependent increases in cAMP levels in normoxia were particularly evident for the PDE4 inhibitors: IBMX, Ro 20-1724 and rolipram (Figure 5A–C). In normoxia, the efficacy of the three inhibitors was similar (Figure 5A–C and Table 1). In contrast with the results obtained with CBs and CAs, in SCGs, hypoxia caused a statistically significant reduction in the effects of the PDE4 inhibitors on cAMP accumulation (Figure 5A–C).

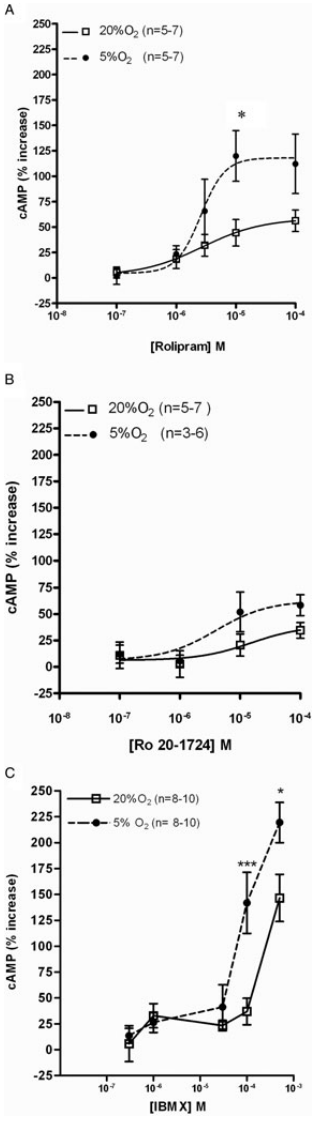

Figure 3 Effects of PDE4 inhibitors on cAMP levels in rat carotid bodies (CBs). Concentration–response curves of (A) rolipram, (B) Ro 20-1724 and (C) isobutylmethylxanthine (IBMX) for effects on cAMP levels induced during normoxia (20%O_2) [0% effect – 0.75 ± 0.08 pmol cAMP/mg (n = 15)] and hypoxia (5%O_2) (0% effect – 0.63 ± 0.05 pmol cAMP/mg (n = 15). *P < 0.05 and ***P < 0.001 two-way analysis of variance with Bonferroni's *post hoc* test. Data values represent means ± SEM.

The effects of EHNA on cAMP accumulation in SCG were concentration-dependent (0.1–100 μM) and more pronounced (≈50%) than those obtained in CAs (<6%) and CBs (<10%). However, this effect was clearly less than those of the PDE4 inhibitors and apparently was not modified by hypoxia, except with concentrations higher than 10 μM (P < 0.05 comparing the effects of 100 μM in normoxia and hypoxia) (Figure 5D).

Discussion

A comparison between the effects of different PDE inhibitors in a functional study using tissues structurally related to peripheral oxygen chemosensors suggested that the *in vivo* effects of PDE inhibitors could be affected by acute hypoxia and demonstrated the presence of PDE4 isoforms in rat CBs, CAs and SCG. PDE2 appears to be absent in CBs and CAs and slightly active in SCG. The effects of PDE inhibitors on cAMP accumulation were increased by acute hypoxia in CBs and CAs but reduced in SCG. The differences in the sensitivity to hypoxia between cAMP accumulation induced by the two PDE4 selective inhibitors, rolipram and Ro 20-1724 indicate that they probably operate through different PDE4 isoforms.

This work was focused on PDE that use cAMP as a specific substract (PDE4, PDE7 and PDE8) and that are not modulated by cGMP, because cGMP levels are negligible and difficult to assess in a functional study of the CBs (Fidone *et al.*, 1990). PDE4 isoenzymes are characterized by high affinity and specificity for cAMP, low K_M (1.2–10 μM), insensitivity to Ca^{2+} and cGMP, selective inhibition by the archetypal rolipram and Ro 20-1724 (IC_{50} of 1 μM and 2 μM, respectively) (Bender and Beavo, 2006). No specific inhibitors are available for PDE8, but it is known that both PDE7 and PDE8 are insensitive to rolipram (Lugnier, 2006). IBMX is a commonly used tool to produce non-specific inhibition of PDEs1–5, but is devoid of effects on PDE7, PDE8 and PDE9 (Dousa, 1999; Lugnier, 2006). In addition to rolipram, Ro 20-1724 and IBMX, which allow the identification of PDE4, we have also investigated the effects of EHNA on cAMP accumulation in CBs, CAs and SCG. EHNA is a selective PDE2 (IC_{50} = 2 μM, Podzuweit *et al.*, 1995) inhibitor and PDE2 hydrolyses both cAMP and cGMP and is activated by cGMP (Lugnier, 2006). The rationale for including the effects of EHNA was that it also inhibits adenosine deaminase (K_i = 10^{-9} M) (Agarwal *et al.*, 1977) and has been used as a tool to prevent adenosine degradation in experiments aimed to investigate the effects of adenosine receptors on cAMP in CBs (Monteiro *et al.*, 1996).

Molecular characterizations of PDE have been extensively performed in systemic arteries and demonstrate that PDE3

Table 1 Comparison between the efficacies and potencies of phosphodiesterase inhibitors (IBMX, rolipram and Ro 20-1724) in normoxia (20% O_2) and hypoxia (5% O_2)

	Rolipram (0.1–100 μM)				*Ro 20-1724 (0.1–100 μM)*				*IBMX (0.3–500 μM)*			
	20% O_2		*5% O_2*		*20% O_2*		*5% O_2*		*20% O_2*		*5% O_2*	
	EC_{50} (μM)	E_{max} (%)	EC_{50} (μM)	E_{max} (%)	EC_{50} (μM)	E_{max} (%)	EC_{50} (μM)	E_{max} (%)	EC_{50} (μM)	E_{max} (%)	EC_{50} (μM)	E_{max} (%)
CB	2.2	56 ± 11	2.4	112 ± 29	7.9	35 ± 8	2.7	58 ± 10	>100	147 ± 23	>100	219 ± 20
SCG	5.6	160 ± 14	4.6	82 ± 8	7.8	206 ± 19	1.9	89 ± 19	16.6	202 ± 37	70	96 ± 16
CA	–	18 ± 13	5.5	163 ± 31	1.9	31 ± 14	0.17	54 ± 20	*54.5	*180 ± 20	*28.9	*222 ± 38

*EC_{50} and E_{max} calculated for IBMX 1–100 Mm.
CA, carotid artery; CB, carotid body; EC_{50}, drug concentration that produces 50% of the maximal effect; E_{max}, mean maximal effect (%) observed in cAMP levels; IBMX, isobutylmethylxanthine; SCG, superior cervical ganglia.

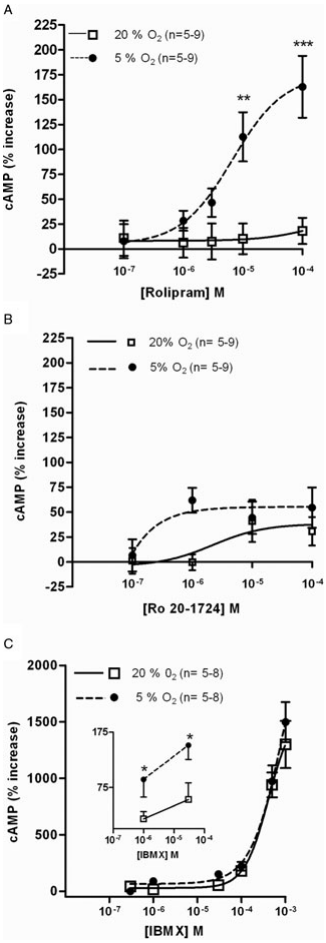

Figure 4 Effects of PDE4 inhibitors on cAMP levels in rat carotid arteries (CAs) incubated in normoxia [20%O_2; 0% of effect corresponds to 0.19 ± 0.02 pmol·mg^{-1} (n = 12)] and hypoxia [5%O_2; 0% of effect corresponds to 0.11 ± 0.01 pmol·mg^{-1} (n = 11)]. Concentration–response curve of (A) rolipram, (B) Ro 20-1724 and (C) isobutylmethylxanthine (IBMX) for effects on cAMP levels. **P < 0.01 and ***P < 0.001 two-way analysis of variance with Bonferroni's *post hoc* test. Values represent means ± SEM.

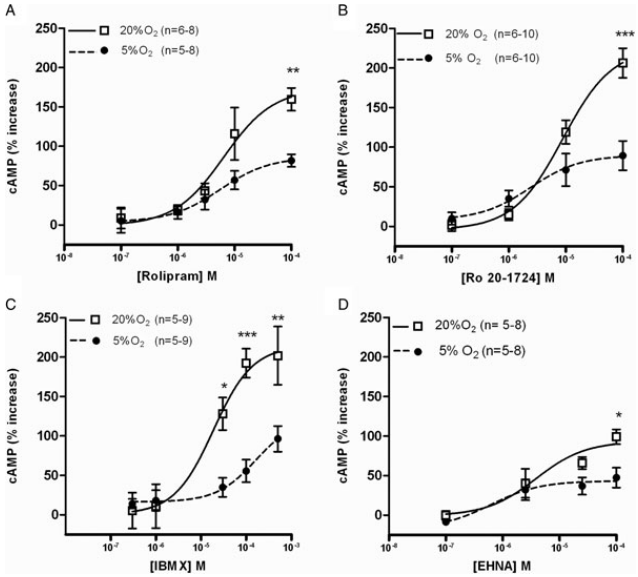

Figure 5 Concentration–response curves for the effects of (A) rolipram, (B) Ro 20-1724, (C) isobutylmethylxanthine (IBMX) and (D) erythro-9-(2-hydroxy-3-nonyl)adenine (EHNA) on cAMP levels in rat superior cervical ganglia in normoxia (20%O_2) [0% effect – pmol 0.36 ± 0.03 pmol cAMP/mg tissue ($n = 11$)] and in hypoxia (5%O_2) [0% effect – 0.35 ± 0.04 pmol·cAMP·mg^{-1} tissue ($n = 11$)]. *$P < 0.05$, **$P < 0.01$ and ***$P < 0.001$. Data values represent means ± SEM.

and PDE4 families are the more active isoforms in aorta, coronary and renal arteries (Phillips *et al.*, 2005). The characterization of PDE4 in CA was here performed for the first time because, so far, there was only one report, in bovine tissue, where three types of PDE were postulated: a PDE with high affinity for cAMP, two types of PDE with mixed affinity for cAMP and cGMP and a third type with high affinity for cGMP (Murtaugh and Bhalla, 1979). PDE2 is probably present in CAs, but, as found in pulmonary (Pauvert *et al.*, 2002) and aortic arteries (Palmer *et al.*, 1998) its activity is so much lower than, for instance, that of PDE4 (Phillips *et al.*, 2005) that the consequences of its inhibition did not seem to be relevant in a pharmacological approach such as this. IBMX, apart from its ability to inhibit PDE non-selectively (K_i = 1–10 μM, Dousa, 1999) and IC_{50} = 2–50 μM, (Bender and Beavo, 2006), is a xanthine able to antagonize adenosine receptors at the same order of concentration (K_i = 7–28 μM, Daly, 1991). In arteries, the adenosine receptors are mainly of the A_2-receptor sub-type positively coupled to AC (http://www.iuphar-db.org/GPCR/index.jsp) and, as a consequence, the increase in cAMP accumulation after IBMX observed in CAs cannot be attributed to its antagonism of adenosine receptors.

An initial work regarding PDE isoforms in the CB appeared in 1977 (Hanbauer and Lovenberg, 1977), but no further studies are known and the characterization of PDE isoforms has never been performed in the CB. These authors provided evidence for a Ca^{++}-dependent PDE in the CB and we have here characterized a PDE4, known as a Ca^{++}-independent enzyme. In the CBs, the presence of active PDEs, other than PDE4 and sensitive to IBMX, was not conclusively shown because non-selective doses of the PDE4 inhibitors caused increases in cAMP of the same order of magnitude as those after IBMX and the contribution of the vascular component of the CB cannot be discarded. In addition, the selective PDE2 inhibitor EHNA (2.5–100 μM) did not modify cAMP concentrations in CBs. This is an interesting finding that validates the use of EHNA as a tool for manipulating endogenous concentrations of adenosine at the CB without apparent interference with PDE activities.

In the absence of PDE inhibitors, no changes in cAMP levels were observed in the CBs in response to hypoxia, although other studies have shown such changes previously (Pérez-Garcia *et al.*, 1990). Species differences (rabbit, in the experiments by Pérez-Garcia *et al.*, 1990) in the overall balance of AC/PDE could contribute to this difference in cAMP values obtained in response to changes in oxygen concentrations. In addition to species, other differences in the experimental procedures were found between the work of Pérez-Garcia *et al.* (1990) and the present one. In the earlier study, CBs were removed from CB bifurcations *in vitro*, allowed to recover in

hyperoxic conditions and the effect of hypoxia was calculated from the comparison between cAMP concentrations obtained during incubations in 100% and 5% O2. We postulated that this latter issue could also contribute to the differences in cAMP accumulation because we have provided evidence that differences in the pre-incubation medium used to allow recovery of the preparations from surgical procedures did not cause significant changes in responses to further incubation.

The profile of responses to PDE inhibitors found in SCG, with the selective PDE inhibitors, rolipram and Ro 20-1724 more potent than IBMX, was compatible with a PDE 4 family predominantly active in cAMP hydrolysis. A similar potency for Ro 20-1724 was also found in a biochemical study that characterized a PDE4 in SCG in normoxic conditions (Giorgi *et al.*, 1994). In this study, cGMP did not stimulate or inhibit PDE activity in SCG, suggesting that PDE 2 and PDE3 are absent or inactive (Giorgi *et al.*, 1994). The results obtained here with the selective PDE2 inhibitor EHNA in SCG were not as clear as those obtained with CBs or CAs and did not allow the exclusion of PDE2 because a small concentration-dependent increase, attenuated by hypoxia, was observed with EHNA.

Hypoxia heightened the effects of PDE4 inhibitors on cAMP accumulation in CBs and CAs but, surprisingly, caused the opposite effect in SCG. In measuring cAMP, we cannot exclude the possibility that the effects of hypoxia include changes in AC. However, several data strongly support the hypothesis that oxygen concentrations selectively modify PDE activity. In the absence of PDE inhibitors, hypoxia did not increase basal cAMP values: they remained constant (SCG) or decreased (CAs and CBs). In addition, if the observed changes induced by hypoxia in cAMP concentrations were due to changes in AC activity, the differences found between the effects of hypoxia on different PDE inhibitors in the same preparation would be difficult to explain and changes in cAMP concentrations would be more pronounced with high concentrations of the PDE inhibitors when the catalytic pathway is completely blocked.

Increases in PDE activity induced by chronic hypoxia have been reported in a few studies (Maclean *et al.*, 1997; Spoto *et al.*, 1998; Hashimoto *et al.*, 2004; Millen *et al.*, 2006), but the effects of acute hypoxia are confined to the report of the increased activity of a Ca^{2+}-dependent activator of cyclic nucleotide PDE in rat CB (Hanbauer and Lovenberg, 1977).

Currently, the PDE4 family represents the largest PDE family constituted by four genes A, B, C and D, but inhibitors targeting specific PDE splice variants are not available. Although rolipram and Ro 20-1724 do not apparently display isoform selectivity and present similar IC_{50} in purified enzyme preparations, some differences have been reported previously. Rolipram caused a much greater increase in isoprenaline-induced cAMP accumulation in rat pulmonary microvascular endothelial cells than Ro 20-1724 (Thompson *et al.*, 2002). The rank order of potency for recombinant human PDE4C inhibition was rolipram > denbufyllin > Ro 20-1724 > IBMX (Engels *et al.*, 1995). In general, rolipram is more potent than Ro 20-1724 in all (A, B, C and D) human PDE4 isoforms (Wang *et al.*, 1997). In the experimental conditions of the present work, rolipram was devoid of effect in CAs in normoxia, and Ro 20-1724 was more potent than rolipram in the SCG and CA in hypoxia. The exact meaning of these findings is not clear but could suggest that specific PDE4 isoforms in the tissues are regulated in opposite directions by oxygen concentrations. In chronic experimental conditions, hypoxia increased the expression of PDE4 A, B and D in human pulmonary artery smooth muscle cells, but no overall increase in PDE4 activity was observed (Millen *et al.*, 2006).

In conclusion, this pharmacological approach indicates that acute hypoxia could simultaneously potentiate cAMP production in systemic arteries induced by PDE4 inhibitors and reduce cAMP accumulation in sympathetic ganglia (SCG). The similarities between the characterization of PDE4 inhibitors at the CBs and CAs, under normoxia and hypoxia, did not support a specific role for cAMP in the oxygen-sensing machinery at the CB and suggests that probably no direct CB-mediated hyperventilatory adverse effects would be expected with administration of PDE4 inhibitors. Systemic vasodilator and, in general, smooth muscle-relaxing properties of specific PDE4 inhibitors, like rolipram, could be preferentially apparent in acute hypoxic conditions.

Acknowledgements

This work was supported by pluri-annual Centro de Estudos de Doenças Crónicas/Fundação para a Ciência e Tecnologia funding. The authors are grateful to the Department of Microbiology, Faculty of Medical Sciences for the valuable help in sample lyophilization.

References

Agarwal RP, Spector T, Parks RE (1977). Tight-binding inhibitors-IV. Inhibition of adenosine deaminases by various inhibitors. *Biochem Pharmacol* **26**: 359–367.

Alexander SPH, Mathie A, Peters JA (2008). Guide to Receptors and Channels (GRAC), 3rd edition (2008 revision). *Br J Pharmacol* **153** (Suppl. 2): S1–S209.

Almaraz L, Perez-Garcia MT, Gonzalez C (1991). Presence of D1 receptors in the rabbit carotid body. *Neurosci Lett* **132** (2): 259–262.

Batuca JR, Monteiro TC, Monteiro EC (2003). Contribution of dopamine D2 receptors for the cAMP levels at the carotid body. *Adv Exp Med Biol* **536**: 367–373.

Bender AT, Beavo JA (2006). Cyclic nucleotide phosphodiesterases: molecular regulation to clinical use. *Pharmacol Rev* **58**: 488–520.

Chen J, Dinger B, Fidone SJ (1997). cAMP production in rabbit carotid body: role of adenosine. *J Appl Physiol* **82** (6): 1771–1775.

Conde SV, Monteiro EC (2004). Hypoxia induces adenosine release from rat carotid body. *J Neurochem* **89**: 1148–1156.

Conde SV, Monteiro EC (2006). Activation of nicotinic Ach receptors with α4 subunits induces adenosine release at the rat carotid body. *Br J Pharmacol* **147**: 783–789.

Conde SV, Obeso A, Vicario I, Rigual R, Rocher A, Gonzalez C (2006). Caffeine inhibition of rat carotid body chemoreceptors is mediated by A2A and A2B adenosine receptors. *J Neurochem* **98** (2): 616–628.

Daly JW (1991). Caffeine analogs: structure–activity relationships at adenosine receptors. *Pharmacology* **42** (6): 309–321.

Delpiano MA, Acker H (1991). Hypoxia increases the cyclic AMP content of the cat carotid body in vitro. *J Neurochem* **57** (1): 291–297.

Dousa TP (1999). Cyclic-3′,5′- nucleotide phosphodiesterase isozymes

in cell biology and pathophysiology of the kidney. *Kidney Int* **55**: 29–62.

Engels P, Sullivan M, Muller T, Lubbert H (1995). Molecular cloning and functional expression in yeast of a human cAMP-specific phosphodiesterase subtype (PDE IV-C). *FEBS Lett* **358**: 305–310.

Fidone S, Gonzalez C, Dinger B, Stensaas L (1990). Transmitter dynamics in the carotid body. In: Acker H, Trzebski A, O'Reagan RG (eds). *Chemoreceptors and Chemoreceptor Reflex*. Plenum Press: New York, pp. 3–13.

Gonzalez C, Almaraz L, Obeso A, Rigual R (1994). Carotid body chemoreceptors: from natural stimuli to sensory discharges. *Physiol Rev* **74**: 829–898.

Giorgi M, Squitti R, Bonse P, Paggi P, Toschi G (1994). Activities of 3′5′cyclic nucleotide phosphodiesterases in the superior cervical ganglion of rat: characterization, compartmentalization and observations in young and old animals. *Neurochem Int* **25**: 493–500.

Hanbauer I, Lovenberg W (1977). Presence of a calcium 2+-dependent activator of cyclic nucleotide phosphodiesterase in rat carotid body: effects of hypoxia. *Neuroscience* **2**: 603–607.

Hashimoto T, Sugiyama A, Taguchi S (2004). Myosin heavy chain isoforms expression and cyclic AMP concentrations in hypoxia-induced hypertrophied right ventricle in rats. *Comp Biochem Physiol B Biochem Mol Biol* **138** (4): 365–370.

Jeon YH, Heo YS, Kim YL, Lee TG, Cho JM (2005). Phosphodiesterases: overview of protein structures, potential therapeutic applications and recent progress in drug development. *Cell Mol Life Sci* **62**: 1198–1220.

Lugnier C (2006). Cyclic nucleotide phosphodiesterase (PDE) superfamily: a new target for the development of specific therapeutics agents. *Pharmacol Ther* **109**: 366–398.

McDonald DM, Mitchell RA (1975). The innervation of glomus cells, ganglion cells and blood vessels in the rat carotid body: a quantitative ultrastructural analysis. *J Neurocytol* **4**: 177–230.

Maclean MR, Johnston ED, Mcculloch KM, Pooley L, Houslay MD, Sweeney G (1997). Phosphodiesterases isoforms in the pulmonary arterial circulation of the rat: changes in pulmonary hypertension. *J Pharmacol Exp Ther* **283** (2): 619–624.

Millen J, Maclean MR, Houslay MD (2006). Hypoxia-induced remodelling of PDE4 isoform expression and cAMP handling in human pulmonary artery smooth muscle cells. *Eur J Cell Biol* **85** (7): 679–691.

Mir AK, McQueen DS, Pallot DJ, Nahorski SR (1984). Direct biochemical and neuropharmacological identification of dopamine D2-receptors in the rabbit carotid body. *Brain Res* **291** (2): 273–283.

Mokashi A, Lahiri S (1991). Aortic and carotid body chemoreception in prolonged hyperoxia in the cat. *Respir Physiol* **86**: 233–243.

Mokashi A, Di Giulio C, Morelli L, Lahiri S (1994). Chronic hyperoxic effects on cat carotid body catecholamines and structure. *Respir Physiol* **97**: 25–32.

Monteiro EC, Vera-Cruz P, Monteiro TC, Silva e Sousa MA (1996). Adenosine increases the cAMP content of the rat carotid body in vitro. *Adv Exp Med Biol* **410**: 299–303.

Murtaugh TJ, Bhalla RC (1979). Multiple forms of cyclic nucleotide phosphodiesterase from bovine carotid artery smooth muscle. *Arch Biochem Biophys* **2**: 465–474.

Nunes AR, Batuca JR, Monteiro EC (2009). Functional characterization of phosphodiesterases 4 in the rat carotid body: effect of oxygen concentrations. In: González C, Nurse C, Peers C (eds). *The Arterial Chemoreceptors*. Springer: New York, pp. 129–136.

Palmer D, Tsoi K, Maurice DH (1998). Synergetic inhibition of vascular muscle smooth cell migration by phosphodiesterase 3 and phosphodiesterase 4 inhibitors. *Circ Res* **82**: 852–861.

Pauvert O, Salvail D, Rousseau E, Lugnier C, Marthan R, Savineau JP (2002). Characterization of cyclic nucleotide phosphodiesterase isoforms in the media layer of the main pulmonary artery. *Biochem Pharmacol* **63**: 1763–1772.

Pérez-Garcia MT, Almaraz L, Gonzalez C (1990). Effects of different types of stimulation on cyclic AMP content of the rabbit carotid body: functional significance. *J Neurochem* **57**: 1287–1293.

Pérez-Garcia MT, Almaraz L, Gonzaléz C (1991). Cyclic AMP modulates differentially the release of dopamine induced by hypoxia and other stimuli and increased dopamine synthesis in the rabbit carotid body. *J Neurochem* **57**: 1992–2000.

Phillips PG, Long L, Wilkins MR, Morrell NW (2005). cAMP phosphodiesterase inhibitors potentiate effects of prostacyclin analogs in hypoxic pulmonary vascular remodeling. *Am J Physiol* **288**: L103–L115

Podzuweit T, Nennstiel P, Muller A (1995). Isozyme selective inhibition of cGMP-stimulated cyclic nucleotide phosphodiesterases by erythro-9-(2-hydroxy-3-nonyl) adenine. *Cell Signal* **7**: 733–738.

Spoto G, Di Giulio C, Contento A, Di Stilio M (1998). Hypoxia effect on blood phosphodiesterase activity in young and old rats. *Pharm Lett Life Sci* **63**: 349–353.

Thompson WJ, Ashikaga T, Kelly JJ, Liu L, Zhu B, Vemavarapau L *et al*. (2002). Regulation of cyclic AMP in rat pulmonary microvascular endothelial cells by rolipram-sensitive cyclic AMP phosphodiesterase (PDE4). *Biochem Pharmacol* **63**: 797–807.

Torbati D, Sherpa AK, Lahiri S, Mokashi A, Albertine KH, Di Giulio C (1993). Hyperbaric oxygenation alters carotid body ultrastructure and function. *Respir Physiol* **92**: 183–196.

Wang P, Myers JG, Wu P, Cheewatrakoolpong B, Egan RW, Billah M (1997). Expression, purification and characterization of human cAMP-specific phosphodiesterase PDE4 Subtypes A,B,C and D. *Biochem Biophys Res Commun* **234**: 320–324.

CHAPTER 2

Chapter 2 is devoted to the effect of O_2 on PDE3 and PDE4 and PKA activity in the superior cervical ganglia. The results obtained in this part of the work originated one book chapter. The main findings are listed bellow:

Effect of oxygen on phosphodiesterases (PDE) 3 and 4 isoforms and PKA activity in the Superior Cervical Ganglia.

***Nunes A.R.**, Sample V., Xiang Y.K., Monteiro E.C., Gauda E.B. and Zhang J. In Arterial chemoreceptors: From Molecules to systems, 758; 287-294. C.A. Nurse et al (eds.), Springer, Netherlands, 2012.*

a) Using FRET-based imaging, PDE inhibitors were able to increase PKA activity in SCG neurons. Fig 39.1, page 98.

b) Different patterns of PDE activities were observed: some SCG neurons presented high PDE4 activity, others high PDE3 activity and others both PDE3 and PDE4 activity. Fig 39.2, page 99.

c) No differences were observed in the emission ratio (no differences in PKA activity) between normoxic and hypoxic conditions in SCG neurons, in the presence of IBMX 500μM.

d) PDE3a-b and PDE4a-d are expressed in the rat SCG, being PDE3a, PDE4b and PDE4d the most expressed isoforms in this organ. Figure 39.3a, page 100.

e) Hypoxic (5%O2), normoxic (20%O2) and hypercapnic (60%O2) conditions did not change isoform expression in the rat SCG. Figure 39.3b, page 100.

Chapter 39
Effect of Oxygen on Phosphodiesterases (PDE) 3 and 4 Isoforms and PKA Activity in the Superior Cervical Ganglia

Ana Rita Nunes, Vedangi Sample, Yang K. Xiang, Emília C. Monteiro, Estelle Gauda, and Jin Zhang

Abstract The cAMP-protein kinase A (PKA) signaling pathway is involved in regulating the release of transmitters from neurons and other cells. Multiple phosphodiesterase (PDE) isoforms regulate this pathway, however, the pattern of isoform expression and stimulus response across tissues has not been fully characterized.

Using fluorescent resonance energy transfer (FRET)-based imaging in primary superior cervical ganglia (SCG) neurons and real-time qPCR, we explored the role of PDE3 and PDE4 isoforms and oxygen tension in the activation of PKA and changes in gene expression. These primary neurons were infected with an adenovirus containing A-Kinase activity reporter (AKAR3) and assayed for responses to PDE inhibitors: rolipram (ROL, 1 μM), milrinone (MIL, 10 μM) and IBMX (100 μM), and adenylyl

A.R. Nunes
Department of Pediatrics, Johns Hopkins University, School of Medicine,
CMSC 6-104, 600 N. Wolfe Street, Baltimore, MD 21287-3200, USA
e-mail: aritanunes@gmail.com

CEDOC, Departamento de Farmacologia, Faculdade de Ciências Médicas, Universidade NOVA de Lisboa, Lisbon, Portugal

V. Sample
Department of Pharmacology and Molecular Sciences, Johns Hopkins University, School of Medicine,
725 N. Wolfe Street, Hunterian 307, Baltimore, MD 21205, USA

Y.K. Xiang
Department of Molecular and Integrative Physiology, University of Illinois at Urbana, Urbana, IL, USA

E.C. Monteiro
CEDOC, Departamento de Farmacologia, Faculdade de Ciências Médicas,
Universidade NOVA de Lisboa, Campo Mártires da Pátria 130, 1169-056, Lisbon, Portugal

E. Gauda (✉)
Department of Pediatrics, Johns Hopkins University, School of Medicine, CMSC 6-104, 600 N. Wolfe Street,
Baltimore, MD 21287-3200, USA
e-mail: egauda@mail.jhmi.edu

J. Zhang (✉)
Department of Pharmacology and Molecular Sciences, Johns Hopkins University, School of Medicine,
725 N. Wolfe Street, Hunterian 307, Baltimore, MD 21205, USA

Department of Neuroscience and Oncology, Johns Hopkins University, School of Medicine,
Baltimore, MD, USA
e-mail: jzhang32@jhmi.edu

C.A. Nurse et al. (eds.), *Arterial Chemoreception: From Molecules to Systems*,
Advances in Experimental Medicine and Biology 758, DOI 10.1007/978-94-007-4584-1_39,

cyclase activator forskolin (FSK, 50 μM). Different PDE activity patterns were observed in different cells: high PDE4 activity (n = 3), high PDE3 activity (n = 3) and presence of activity of other PDEs (n = 3). Addition of PKA inhibitor H89 (10 μM) completely reversed the response. We further studied the effect of oxygen in the PKA activity induced by PDE inhibition. Both normoxia (20%O_2/5%CO_2) and hypoxia (0%O_2/5%CO_2) induced a similar increase in the FRET emission ratio (14.5 ± 0.8 and 14.7 ± 0.8, respectively).

PDE3a, PDE4b and PDE4d isoforms mRNAs were highly expressed in the whole SCG with no modulation by hypoxia.

CONCLUSION: Using a FRET-based PKA activity sensor, we show that primary SCG neurons can be used as a model system to dissect the contribution of different PDE isoforms in regulating cAMP/PKA signaling. The differential patterns of PDE regulation potentially represent subpopulations of ganglion cells with different physiological functions.

Keywords Superior cervical ganglia (SCG) • Phosphodiesterases (PDE) • Cyclic AMP (cAMP) • Hypoxia • Protein kinase A (PKA)

39.1 Introduction

Cyclic AMP is a ubiquitous second messenger involved in synaptic transmission and signal transduction. The levels of cAMP are regulated by the synthetic activity of adenylate cyclases (AC) and by the hydrolytic activity of phosphodiesterases (PDE); the latter determines the intracellular concentration of cAMP (Bender and Beavo 2006). Thus, PDEs have become important targets of study in the past years and have been pursued as therapeutic targets (Bender and Beavo 2006). There are 11 PDE isoforms that differ in their affinity for cAMP and/or cGMP and inhibitors, and in their responses to modulators (Bender and Beavo 2006).

Superior cervical ganglion (SCG) has a key role in the sympathetic nervous system and sends neuronal projections to the carotid body (CB) controlling the vascular tone. We have recently observed that acute hypoxia decreased cAMP levels induced by PDE inhibitors in these ganglia, an opposite effect to that observed in the CB (Nunes et al. 2010).

The aim of this work is to characterize the role of PDE3 and PDE4 regulation on cAMP/PKA activity in the SCG under different oxygen concentrations. We also wanted to explore whether the effect of hypoxia observed in cAMP production induced by IBMX is translated into apparent changes in PKA activity in primary SCG neurons.

To answer these questions we investigated the effect of PDE inhibitors on the activation of PKA in dissociated SCG neurons using fluorescence resonance energy transfer (FRET)-based imaging and studied the expression of PDE3 and PDE4 and their regulation by oxygen in the whole SCG by quantitative RT-PCR.

39.2 Methods

39.2.1 Surgical Procedures

The experiments were performed using SCGs isolated from Sprague–Dawley rats (Charles River Laboratories, Wilmington, MA) of both sexes at postnatal days 5–9. The Animal Care and Use Committee at the Johns Hopkins University School of Medicine approved all experimental protocols.

The animals were anesthetized briefly with isoflurane and immediately decapitated. The carotid bifurcation was isolated and the SCG dissected and cleaned of surrounding connective tissue under a dissecting microscope. The tissues removed were further prepared as follows.

39.2.2 Measurement of Protein Kinase A (PKA) Activity in Primary Superior Cervical Ganglia Neurons by FRET

SCGs were mechanically and enzymatically dissociated with an enzyme mixture consisting of trypsin and collagenase (~0.5 mg/ml). SCG cells were plated on poly-D-Lysine and laminin coated imaging dishes and cultured for 2–4 days in neurobasal-A supplemented with NGF and Ara-C (10 μM). To monitor PKA activity, we infected the SCG neurons with an adenovirus containing a 3rd-generation of a genetically encoded A-Kinase activity reporter (AKAR3) for 24 h.

In one set of experiments we imaged the SCG neurons at 37 °C and sequentially treated them with rolipram (ROL, specific PDE4 inhibitor, 1 μM), milrinone (MIL, specific PDE3 inhibitor, 10 μM), IBMX (non-specific inhibitor, 100 μM), Forskolin (FSK, transmembrane adenylyl cyclase activator, 50 μM) and H89 (PKA inhibitor, 10 μM).

In another set of experiments, we placed the imaging dish into a chamber (Warner Instruments) to allow superfusion of the cells with a constant flow rate of 2 ml/min (Ismatec, Cole Parmer instrument) with Kreb's modified solution containing (in mM): NaCl 116, $NaHCO_3$ 24, KCl 5, $CaCl_2$ 2, $MgCl_2$ 1.1, Hepes 10, Glucose 5.5 and adjusted to pH 7.40 (Perez-Garcia et al. 1990), equilibrated either with normoxia (20%O_2/5%CO_2) or hypoxia (0–5%O_2/5%CO_2) in the presence or absence of IBMX (100 μM).

The cells were imaged on a Zeiss Axiovert 200 M microscope (Carl Zeiss) with a 40X oil immersion objective and a cooled charge-coupled device camera (Roper Scientific) controlled by Metafluor 6.2 software (Molecular Devices). Dual emission ratio imaging used a 420DF20 excitation filter, a 450DRLP dichroic mirror and two emission filters (475DF40 for cyan fluorescent protein (CFP) and 535DF25 for yellow fluorescent protein (YFP)). Exposure time was 50–500 ms and images were acquired every 20 s. Background correction of the fluorescence images was performed by subtracting autofluorescent intensities of regions of the imaging dish with no cells. Graph curves were normalized by setting the emission ratio at baseline (before the addition of any drugs) as equal to one.

39.2.3 PDE mRNA Gene Expression and Regulation

In one set of experiments we compared PDE3 and PDE4 gene expression levels in the whole SCG. The tissues were isolated (3 rats per condition; n = 3 independent experiments), quick-frozen on dry ice and stored at −80 °C.

In another set of experiments, we studied the effect of changes in oxygen tension on the expression of PDE3 and PDE4 in the whole SCG. Tissues were pre-incubated in a 37 °C shaker bath for 30 min in Kreb's modified medium equilibrated with 20%O_2/5%CO_2 (normoxia). After the pre-incubation period, tissues were incubated in a fresh incubation medium, equilibrated in normoxia, hypoxia (5%O_2/5%CO_2) or hyperoxia (60%O_2/5%CO_2) for 60 min. Tissues were quick-frozen on dry ice and stored at −80 °C.

Frozen tissues were processed to obtain total RNA (about 1 μg, micro-to-Midi Total RNA Purification, Invitrogen) that was used for first-strand cDNA synthesis using an iSCRIPt cDNA synthesis kit (Bio-Rad Laboratories). The primer sequences used were: forward 5′-GTGGCCGTATTCTGAGCCAGGTG-3′ and reverse 5′-GCTGTGTTGTGAGATACCACACGGC-3′

for PDE3a, forward 5′-CGACCAATTCCTGGCTTACAGCAGC-3′ and reverse 5′- GCAGGAATG-TTTGAAGACAGGCAGCC-3′for PDE3b, forward 5′-CCTGCACGCAGCGGATGTGC-3′ and reverse 5′-GGAACTGGTTGGAG-ACGCCAGG-3′ for PDE4a, forward 5′-CCTGGCTGCCAT-TTTTGCAGC-TGC-3′ and reverse 5′-GAGCTTGAATCCCACAGCGAGGTG-3′ for PDE4b, forward 5′-CCAGGAGGAGCAGCTGGCTAAG-3′ and reverse 5′- CACGTTGGAGTGGTAGTGCCCTTC-3′ for PDE4c, forward 5′-GCG-GAGCTGTCTGGCAACCG-3′ and reverse 5′-GACTGGACGACATCTG-CAGCATGG-3′ for PDE4d, and forward 5′- GATGGCCTTCTACCCG-AAGACACC-3′ and reverse 5′- GCCAGCTACATAGGAGTTACGGGC-3′ for G6PDH.

qRT-PCR was performed with a MyiQ iCycler qRT-PCR system (Bio-Rad Laboratories) with Syber Green detection. qRT-PCR conditions were: 5 min at 95 °C, followed by 40 cycles at 95 °C for 20 s, 60 °C for 20 s, 72 °C for 20 s, a terminal extension period (72 °C, 10 min) and a melting curve with 0.5 °C increments in temperature. Product formation during the exponential phase of the reaction was analyzed for relative quantification to the reference gene based on the threshold cycle (C_T) for amplification as $2^{(\Delta CT)}$, where $\Delta C_T = C_{T,reference} - C_{T,target}$.

39.3 Results

We investigated the role of PDE3 and PDE4 on the activation of PKA in primary SCG neurons using FRET-based imaging. Figure 39.1 shows a representative response in a SCG neuron induced by sequential addition of specific and non-specific PDE inhibitors. While ROL did not induce a change in emission ratio (ΔER), Mil induced an increase in ΔER with no further changes with IBMX and FSK. Addition of H89 (10 μM) completely reversed the response. This pharmacological profile suggests that there is high PDE3 activity in this neuron. However, this pattern was not consistent in all SCG neurons. PDE inhibitors differentially modulated PKA activity, suggesting that there are subpopulations of SCG neurons with different PDE activity patterns.

Figure 39.2 shows the profiles of PDE3 and PDE4 activity in regulating PKA in different SCG neurons: 1) high PDE4 activity with 20.0 ± 0.4% ΔER in response to ROL with no further increase with MIL, IBMX and FSK (n = 3, Fig. 39.2a), 2) high PDE3 activity with 1.9 ± 0.6% ΔER in response to ROL and 19.0 ± 7.2% ΔER to MIL with no further increase with IBMX and FSK (n = 3, Fig. 39.2b), and 3) activity of other PDEs than PDE3/PDE4, with 1.6 ± 0.8% ΔER in response to ROL, 5.7 ± 1.1% in response to MIL and 18.7 ± 2.7% in response to IBMX and no further increase in the presence of FSK (n = 3, Fig. 39.2c). Addition of H89 reversed the response in all neurons (Fig. 39.2).

To determine whether oxygen tension modifies PKA activity by affecting PDE activity, we perfused SCG neurons with Kreb's modified solution in the presence and absence of IBMX (100 μM) equilibrated either with normoxia or hypoxia.

ΔER increased as a consequence of perfusion with IBMX in normoxia and this effect was completely reversible after washout. No differences were observed in the ΔER between normoxia and hypoxia in the presence of IBMX (14.5 ± 0.8 ΔER and 14.7 ± 0.8 ΔER, respectively, n = 10).

We further characterized the gene expression of the PDE3a-b and PDE4a-d isoforms in the whole SCG. Even though all isoforms were expressed in the SCG: PDE3a, PDE4b and PDE4d were the most abundant (Fig. 39.3). This pattern of expression was similar in SCG incubated with control oxygen concentrations (hypoxia, normoxia and hyperoxia) (Fig. 39.3b) and those that were quick frozen without incubations (Fig. 39.3a). Exposing SCGs with different percentages of oxygen did not significantly modulate PDE expression (Fig. 39.3b).

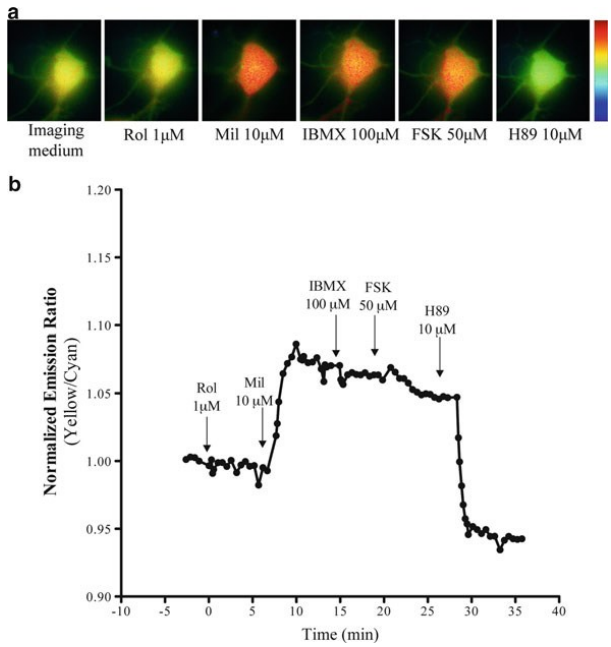

Fig. 39.1 (**a**) Pseudocolor images (400X) and (**b**) representative response curve of AKAR3 to rolipram (Rol, 1 μM), milrinone (Mil, 10 μM), IBMX (100 μM), FSK (50 μM) and H89 (10 μM) in a SCG neuron

39.4 Discussion

In this work, we characterized the PDE3 and PDE4 expression in the SCG and investigated the role of these PDE isoforms in the activation of PKA in ganglion neurons. We demonstrated that FRET-based imaging could be used to study the contribution of PDE isoforms in the regulation of cAMP/PKA signaling in primary SCG neurons as a model system. We observed differential patterns of PDE regulation in subpopulations of SCG neurons, which can potentially represent those subpopulations with different physiological functions. The level of oxygen tension did not modulate PDE expression and did not change the effect of PDE inhibition in the PKA activity.

SCG contains subpopulations of sympathetic neurons (secreto-, pilo-, vasomotor neurons), which receive input from the cervical sympathetic pre-ganglionic nerve fibers and provides innervations of the neck and head structures (Asamoto 2005). Each subpopulation of neurons projects exclusively to specific targets (Li and Horn 2006), which could explain the differences in PDE regulating PKA activity between SCG neurons described in our work.

We identified for the first time PDE3 and PDE4 mRNA expression patterns in the SCG. This finding adds to the literature by identifying PDE3 isoforms in this ganglion and is consistent with previous reports that characterize PDE4 by the effects of their specific inhibitors (Giorgi et al. 1994; Lakics et al. 2010; Li and Horn 2006; Nunes et al. 2010). We found that PDE3a, PDE4b and PDE4d

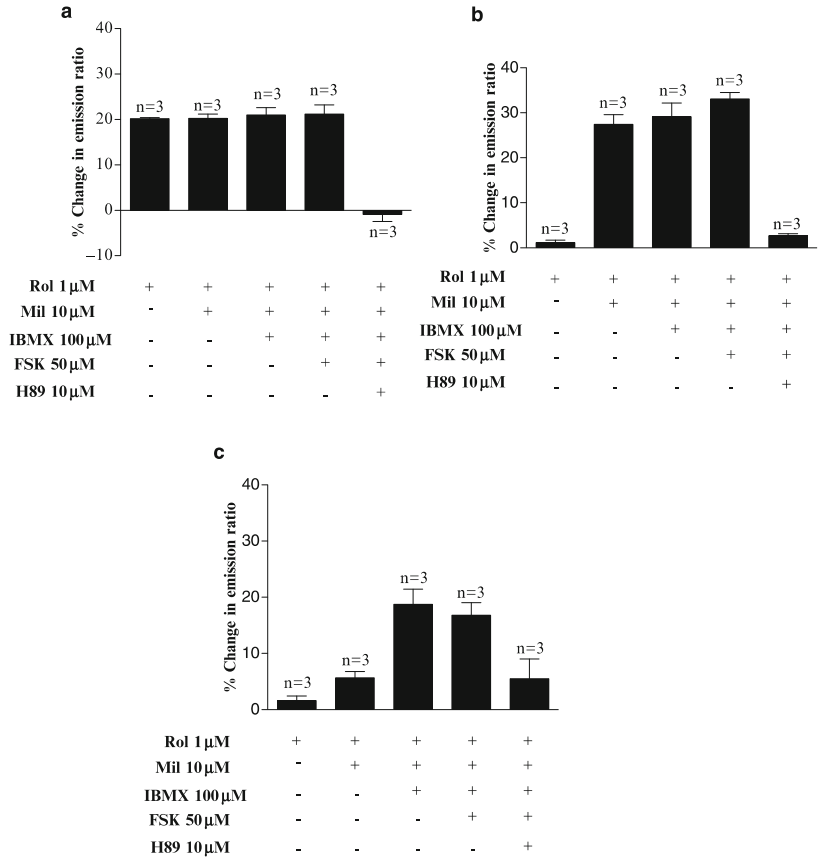

Fig. 39.2 Heterogenous responses in PKA activity induced by PDE inhibitors in SCG neurons. Composite data showing different response patterns of AKAR3 induced by PDE inhibitors, within a population of SCG neurons. SCG neurons containing (**a**) high PDE4 activity, (**b**) high PDE3 activity, and **c**) activity from other PDEs than PDE3 and PDE4. Values represent means ± SEM

were the most abundant isoforms in the SCG. It has been shown that these isoforms are highly expressed in specific tissues: PDE3a in the heart, PDE4b in the CNS and PDE4d in the muscle (Lakics et al. 2010).

We had previously observed that acute hypoxia induced a decrease in cAMP levels in the presence of the non-specific PDE inhibitor, IBMX and specific PDE2 and PDE4 inhibitors, in whole SCG of adult Wistar rats (Nunes et al. 2010). In the present work, hypoxia did not modulate either the levels of gene expression or PDE inhibition induced PKA activity. Taken together, these findings suggest that changes in IBMX-induced cAMP accumulation caused by changing oxygen concentrations are

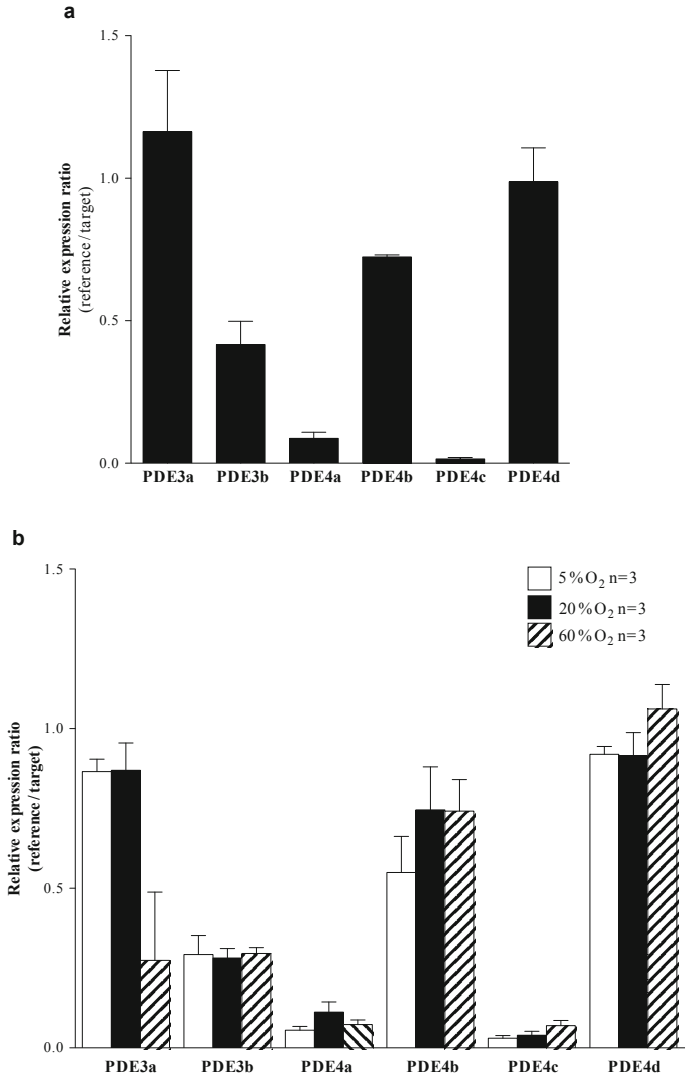

Fig. 39.3 Effect of different oxygen concentrations on PDE3 and PDE4 isoform gene expression in the whole superior cervical ganglia (SCG). (**a**) PDE3a-b and PDE4a-d isoform expression levels and their (**b**) regulation by hypoxia ($5\%O_2$), normoxia ($20\%O_2$) and hyperoxia ($60\%O_2$)

not translated into changes in PKA activity. No effect of oxygen tension on changes in PKA activity could be due to saturation of PKA activity under high levels of cAMP caused by the PDE inhibition. Further experiments will test whether changes in oxygen concentrations directly modify PDE activity.

The results suggest selective distribution of PDE3a, PDE4b and PDE4d isoforms in subpopulations of ganglion cells that potentially represent subpopulations with dif ferent physiological functions.

Acknowledgment A.R. Nunes was supported by the Portuguese Fundacao de Ciencia e Tecnologia (FCT, SFRH/BD/39473/2007). This w ork is also supported by NIH R01 DK073368 (to JZ) and HL082846 (to YKX).

References

Asamoto K (2005) Network of the sympathetic nervous system: focus on the input and output of the cervical sympathetic ganglion. Anat Sci Int 80:132–140

Bender AT, Beavo JA (2006) Cyclic nucleotide phosphodiesterases: molecular regulation to clinical use. Pharmacol Rev 58:488–520

Giorgi M, Squitti R, Bonsi P, Paggi P, Toschi G (1994) Activities of 3'5' cyclic nucleotide phophodiesterases in the superior cervical ganglion of rat: characterization, compartmentalization and observation in young and old animals. Neurochem Int 25(5):493–500

Lakics V, Karran EH, Boess FG (2010) Quantitative comparison of phosphodiesterase mRNA distribution in human brain an peripheral tissues. Neuropharmacol 59:367–374

Li C, Horn JP (2006) Physiological classification of sympathetic neurons in the rat SCG. J Neurophysiol 95:187–195

Nunes AR, Batuca JR, Monteiro EC (2010) Acute hypoxia modifies cAMP levels induced by inhibitors of phosphodiesterase-4 in rat carotid bodies, carotid arteries and superior cervical ganglia. Br J Pharmacol 159:353–361

Perez-Garcia MT, Almaraz L, Gonzalez C (1990) Effects of different types of stimulation on cyclic AMP content in the rabbit carotid body: functional signi fication. J Neurochem 55:1287–1293

Chapter 3

Chapter 3 is devoted to the characterization of sAC and tmAC isoforms in peripheral and central chemoreceptors and the effect of changes in HCO_3^-/CO_2 in the activity of these enzymes. The results obtained in this part of the work originated 1) one book chapter and 2) and 3) manuscripts that are in submission and preparation for publication, respectively. The main findings are listed bellow:

1) Bicarbonate-regulated soluble adenylyl cyclase (sAC) mRNA expression and activity in peripheral chemoreceptors

Nunes AR, Monteiro EC, Johnson SM, Gauda EB. Adv Exp Med BIol 2009; 648:235-41

a) sAC is higly expressed in the CB comparatively to the SCG, PG and NG, except for the testis, the tissue control. Table 1, page 108.
b) Increasing concentrations of HCO_3/CO_2 during 1 hr up-regulated sAC gene expression only in CB. Table 2, page 108.
c) sAC protein is expressed in the CB, SCG and testis. Fig. 1, page 109.
d) Changes from 0 to 24 m$MHCO_3^-$/5%CO_2, in the presence of IBMX, PDE inhibitor, and MDL 12 330A, tmAC inhibitor, induced an increase in cAMP levels in the only in the CB. Table 3, page 109.

2) Bicarbonate-sensitive soluble adenylyl cyclase (sAC) and transmembrane adenylyl cyclase in peripheral chemoreceptors.

Nunes AR, Holmes APS, Sample V, Kumar P, Cann MJ, Monteiro EC, Zhang J and Gauda EB. J Physiol (Submitted).
e) The amount of cAMP in the CB was dependent on the HCO_3^-/CO_2 (0/0, 12/2.5, 24/5, 44/10). cAMP levels were highest in 24 mM HCO_3/CO_2 (normocapnic conditions). Peripheral non-chemosensitive tissues did not change cAMP levels in the presence of different concentrations of HCO_3^-/CO_2. Fig 1, page 123.

f) Changes of HCO_3^-/CO_2 did not alter pHi in CB type I cells. Fig 3, page 125.

g) Different HCO_3^-/CO_2 concentrations did not change PKA activity in type I cells.

h)The profile of expression of adenylyl cyclase isoforms was different between CB and PG. In the CB, the expression of tmAC 1, 3, 4, 6 and 9 were higher than sAC. Fig 5, page 129.

i) There is a higher contribution of tmAC and sAC for cAMP accumulation in response to 12 mM HCO3/2.5CO2 than to normocapnic and hypercapnic conditions. Fig 7, page 131.

j) The inhibitory effect of KH7 (sAC inhibitor, 10uM) and ddADO 100uM (tmAC inhibitor) was the same after 5 or 30 min of incubation in all the concentrations of HCO_3^-/CO_2 tested. Fig 8, page 133.

k) CSN discharge was increased by acidic but not isohydric hypercapnia. Inhbiton of tmAC but not sAC, decreased the basal discharge of the CSN and its response to acidic hypercapnia. Fig 9, page 133.

3) Bicarbonate-sensitive soluble adenylyl cyclase (sAC) and transmembrane adenylyl cyclase in central CO_2 chemoreceptors- a comparative study with the carotid body (in preparation)

m) sAC mRNA wass expressed in the central chemoreceptors regions; expression levels in central chemoreceptors were lower than in the CB. sAC expression is upregulated by concentrations of HCO_3/CO_2 in the LC, but not in the other central regions. Fig 1, page 148.

n) tmAC inhibitors blocked only 50% of the cAMP production in the LC. Fig 2, page 148.

o) The amount of cAMP in the LC, VLM and RN, but not cortex, was dependent on concentrations of HCO_3^-/CO_2. Fig 3, page 150.

p) tmAC isoforms 1, 2, 3, 4, 6, 8 and 9 were more expressed than sAC in the LC. Fig 4, page 151.

q) tmAC and sAC were partially active in the LC normocapnia, but in hypercapnia tmAC may not be functional. Fig 5, page 151.

Bicarbonate-Regulated Soluble Adenylyl Cyclase (sAC) mRNA Expression and Activity in Peripheral Chemoreceptors

A. R. NUNES[1, 2], E. C. MONTEIRO[2], S. M. JOHNSON[3], E. B. GAUDA[1]

[1]Pediatrics, Johns Hopkins Medical Institutions, Baltimore, MD; [2]Pharmacology, Faculty of Medical Sciences, New University of Lisbon, Portugal; [3]Physiology and Biophysics, Howard University College of Medicine, Washington, DC. egauda@mail.jhmi.edu

ABSTRACT

Peripheral arterial chemoreceptors in the carotid body (CB) are modulated by pH/CO_2. Soluble adenylyl cyclase (sAC) is directly stimulated by bicarbonate ions (HCO_3^-). Because CO_2/HCO_3^- mediates depolarization in chemoreceptors, we hypothesized that sAC mRNA would be expressed in the CB, and its expression and function would be regulated by CO_2/HCO_3^-.
Sprague-Dawley rats at postnatal days 16-17 were used to compare sAC mRNA gene expression between CB and non-chemosensitive tissues: superior cervical (SCG), petrosal (PG) and nodose ganglia (NG) by quantitative real time-PCR. Rat sAC gene expression was standardized to the expression of GAPDH (housekeeping gene) and the data were analyzed with the Pfaffl method. Gene and protein expression, and sAC regulation in the testis was used as a positive control. To determine the regulation of sAC mRNA expression and activity, all tissues were exposed to increasing concentrations of bicarbonate (0, 24, 44 mM, titrated with CO_2 and maintained a constant pH of 7.40). RESULTS: sAC mRNA expression was between 2-11% of CB expression in the SCG, PG and NG. Furthermore, only in the CB did HCO_3^- upregulate sAC gene expression and increase cAMP levels. CONCLUSION: sAC mRNA and protein expression is present in peripheral arterial chemoreceptors and non-chemoreceptors. In the CB, CO_2/HCO_3^- not only activated sAC but also regulated its expression, suggesting that sAC may be involved in the regulation of cAMP levels in response to hyper/hypocapnia.

Keywords: cAMP, carotid body (CB), soluble adenylyl cyclase (sAC), peripheral arterial chemoreceptors, CO_2/HCO_3^-, qRT-PCR

1. INTRODUCTION

Gonzalez et al. (eds.), The Arterial Chemoreceptors, 251-257

Breathing is modulated by peripheral arterial chemoreceptors distributed in Type I cells in the carotid body (CB), which are sensitive to changes in pCO_2/pH (for a review see (Gonzalez et al. 1994)). cAMP is an important mediator of O_2-chemotransduction (for a review see (Gonzalez et al. 1994)) through activation of transmembrane adenylyl cyclase (tmAC), and hypercapnia increases cAMP levels in the CB (Perez-Garcia et al. 1990); however, the specific cellular mechanisms responsible for CO_2 sensitivity in this organ are not well understood. Recently, a soluble adenylyl cyclase (sAC) that is activated and regulated by changes in HCO_3^-/CO_2 has been characterized in testis and somatic tissues (Buck et al. 1999;Schmid et al. 2007;Sinclair et al. 2000;Sun et al. 2003;Wang et al. 2005). Unlike tmAC, sAC is insensitive to G proteins or to foskolin, and is unique in its activation by HCO_3^- (reviewed in (Kamenetsky et al. 2006)). In this study, we examined the role of sAC in chemotransduction and hypothesized that sAC mRNA will be expressed in the CB and that changes in CO_2/HCO_3^- levels will regulate sAC mRNA expression and activity as evidenced by changes in cAMP levels.

2. METHODS

Sprague-Dawley rats at postnatal days 16-17 were used. Animals were anesthetized with isoflurane and decapitated. Carotid body (CB), superior cervical (SCG), petrosal (PG), nodose (NG) ganglia and testis were removed, and prepared for quantitative real-time polymerase chain reaction (qRT-PCR), immunoblotting or cAMP measurements. Experiments were approved by the Animal Care and Use Committee at the Johns Hopkins University School of Medicine.

2.1. sAC mRNA Gene Expression and Regulation

We characterized sAC mRNA gene expression in the CB and non-chemoreceptor tissues pooled from six rats from the same litter. The experiment was done in triplicate using a total of 18 animals from 3 different litters.

In order to study the effect of HCO_3^- on sAC mRNA levels in the CB, SCG and testis, the tissues were pre-incubated in Krebs modified solution containing (in mM) NaCl 116; KCl 5; $CaCl_2$ 2; $MgCl_2$ 1.1; HEPES 10; glucose 5.5, pH 7.40 (Perez-Garcia et al. 1990) with 0 mM HCO_3^-/ 0%CO_2/60%O_2, for 30 minutes. The tissues were then incubated in Krebs modified solution containing one of the following conditions: 1) 0 mM HCO_3^-/0% CO_2/60% O_2, 2) 24 mM HCO_3^-/5% CO_2/60% O_2, and 3) 44 mM HCO_3^-/10% CO_2/60% O_2 at 37ºC, pH 7.4 (4 rats per condition, n=3

independent experiments). After 1 hour, the tissues were stored at -80ºC and then processed for qRT-PCR.

The primer sequences used for the target gene and house keeping gene were : sAC, sense 5´-catgagtaaggaatggtggtactca-3´ (complementary to 4961- 4986 base pairs of rat sAC gene (AF081941)) and anti-sense 5´-agggttacgttgcctgatacaatt-3 (complementary to the 5049-5072 base pairs) and G6PDH, sense 5'-gaagcctggcgtatcttcac-3' and anti-sense 5'-gtgagggttcacccacttgt-3' (Pastor-Soler et al. 2003). Relative expression of sAC between the tissues was analysed by the excel Pfaff method (Pfaffl 2001). qRT-PCR was performed with a MyiQ iCycler qRT-PCR system (Bio-Rad Laboratories Inc., Hercules, CA) with Syber Green detection.

Immunoblotting was performed using 20 µL of protein from crude homogenates of pooled CBs, SCGs and testes, and sAC protein was detected with monoclonal anti-sAC R21 (1:500, (Zippin et al. 2004), provided as a generous gift from Drs. Jochen Buck and Lonny R. Levin). Protein expression levels were normalized with β-actin detected with a goat anti-mouse monoclonal β-actin antibody (1:10000; Sigma Chemicals Company, St. Louis, MO).

2.2. Bicarbonate-Regulated cAMP Levels

sAC activity was detected indirectly by measuring changes in cAMP levels in response to increasing concentrations of HCO_3^-. Tissues (CB, SCG, PG and testes) were removed and pooled from 2 pups per litter, from a total of 3-8 litters. Tissues were incubated in Krebs modified solution without HCO_3^-/CO_2 and in the presence of MDL-12,330A (500 µM; a specific tmAC inhibitor, Sigma) for 30 minutes. Then the tissues were transferred to Krebs modified solution in the presence of MDL-12,330A (500 µM), IBMX (500 µM; a non-specific phosphodiesterase inhibitor; Sigma), plus $HCO_3^-/CO2$ in one of three concentrations: 0 mM HCO_3^-/0 % CO_2, 24 mM HCO_3^-/5% CO_2, or 44 mM HCO_3^-/10 % CO_2, pH 7.4, and incubated for 30 minutes at 37°C.

Cyclic nucleotides were extracted from tissues as described by Batuca and co-workers (Batuca et al. 2003) with cAMP quantification by enzyme immunoassay, using an EIA commercial kit (RPN 2255, GE Healthcare Bio-Sciences AB, Piscataway, NJ). Protein levels were measured via standard Bradford Protein assay (Bio-Rad) and fluorescent detection using a NanoOrange Protein Quantification Kit (Invitrogen, Eugene, OR). cAMP levels were expressed in fentomoles per microgram of protein (fmol/µg protein).

2.3. Data Analysis and Statistical Procedures

The data are represented as mean ± SEM, and differences ($P<0.05$) between the experimental groups were calculated by non-parametric

Spearman's Rank-Order Correlation and by Kruskal-Wallis one-way ANOVA with the Dunnett's post hoc test using GraphPad Prism (GraphPad Software, Inc., version 4, San Diego, CA) or SPSS (SPSS Inc., version 12, Chicago, IL).

3. RESULTS

3.1. sAC mRNA Gene Expression and Regulation

sAC mRNA expression was lower in SCG, PG and NG than in CB and testis removed from rats at postnatal days 16-17 (Table 1).

Table 1 - sAC mRNA expression in peripheral chemoreceptors and non-chemoreceptors relative to CB

Tissues	Chemo-sensitive	Non- chemosensitive			
	CB	SCG	NG	PG	testis
% of CB. sAC expression (m±SEM)	100	11.3±1.33	3.05±0.22	3.78±0.54	254±47.9

Increasing concentrations of HCO_3^- upregulated sAC gene expression only in the CB ($p < 0.01$; Spearman's correlation), but did not affect sAC mRNA gene expression in other tissues, including testis (Table 2).

Table 2- Effect of HCO_3^-/CO_2 on sAC mRNA relative gene expression (relative expression to 0mM HCO_3^- for each tissue)

	HCO_3^- (mM) / CO_2 (%)		
Tissues	**0 mM / 0 %**	**24 mM / 5 %**	**44 mM / 10 %**
CB	1.00 ± 0.00	1.58 ± 0.15	2.12 ± 0.30
SCG	1.00 ± 0.00	1.00 ± 0.14	0.90 ± 0.04
testis	1.00 ± 0.00	0.67 ± 0.47	0.97 ± 0.23

Western immunoblot was used to determine the presence of sAC protein detected with the monoclonal anti-sAC antibody, identified as R21 (Figure 1). We detected an intense band at 50 kDa in the CB, SCG and testis corresponding to the sACt isoform. In the testis we also detected bands at 130 kDa and 31 kDa.

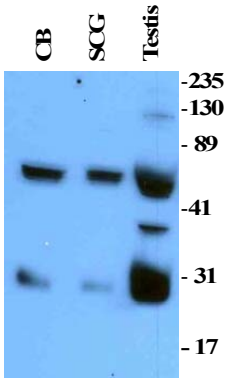

Figure 1- Immunoblot showing sAC protein expression in CB, SCG and testis. *CB*, carotid body, *SCG*, superior cervical ganglia.

3.2. Bicarbonate-Regulated cAMP Levels

The effect produced by increasing the concentrations of HCO_3^- on cAMP levels in CB and non-chemoreceptor tissues (SCG, PG, testis) in the presence of IBMX (500 µM) and MDL-12,330A (500 µM) is shown in Table 3. Previous experiments have demonstrated that MDL-12,330A (500 µM) was effective in blocking tmAC. In the CB, increasing HCO_3^- concentrations from 0 to 24 mM significantly increased cAMP levels from 15.27 ± 3.22 to 35.27 ± 6.04 fmol/µg protein ($p<0.01$). Exposing the CB to higher concentrations of HCO_3^-/CO_2 (44 mM HCO_3^- with 10%CO_2) did not produce any additional increase in cAMP levels in this tissue. Increasing HCO_3^- concentrations did not increase cAMP levels in non-chemoreceptor tissues (SCG, PG and testis). These results suggest that sAC could be involved in chemoreception of HCO_3^-/CO_2 in peripheral arterial chemoreceptors.

Table 3- Effects of changes in HCO_3^-/CO_2 on cAMP levels (fentomoles /µg of tissue)

Tissues	HCO_3^- (mM) / CO_2 (%)		
	0 mM / 0 %	24 mM / 5 %	44 mM / 10 %
CB	15.3± 3.22 (n=16)	35.3 ± 6.04 (n=14) **	26.3 ± 2.83 (n=14)*
SCG	31.6 ± 5.41 (n=9)	43.5 ± 14.8 (n=7)	36.06 ± 6.96 (n=8)
PG	16.8 ± 6.125 (n=6)	15.9 ± 6.69 (n=6)	17.9± 8.09 (n=5)
testis	9.21 ± 1.75 (n=10)	8.99 ± 1.49 (n=10)	9.32 ± 1.44 (n=10)

* $p<0.05$ by one-way Kruskal-Wallis test with the Dunnett's post-test corresponding to differences between cAMP levels in response to increasing concentration of concentrations of HCO_3^-.

4. DISCUSSION

We describe the novel finding of increased sAC gene expression and regulation in the carotid body, which is sensitive to changes in pH/CO_2. These results demonstrate that sAC gene expression occurs in both the CB and in non-chemoreceptor tissues: SCG, PG, NG. Unlike non-chemoreceptor tissues, sAC gene expression is greatest in the CB, where it is modulated by HCO_3^- in a concentration-dependent manner.

We identified several protein isoforms of sAC using homogenates of testicular tissue, CB, and the SCG that were consistent with the previously described truncated sAC isoform (sAC_t: 48 kDA) (Buck et al. 1999) reported for testicular tissue. Our data also show that other novel isoforms of sAC are expressed in the homogenates of the testis but the functions of these isoforms have not been characterized.

We tested the role of HCO_3^-/CO_2 on sAC gene expression and activity in CB and SCG, PG and testis, and showed that increasing concentrations of CO_2/HCO_3^- increased sAC mRNA gene expression in a concentration-dependent manner and induced an increased in cAMP levels but *only* in the CB. We excluded the effect of external pH variations by maintaining the extracellular pH at 7.4, but the intracellular pH was not measured. However, it has been shown that when the extracellular pH maintains constant and pCO_2 increases, there is little change in intracellular pH in Type I cells (Buckler et al. 1991) of the carotid body. Additionally, sAC activity is also independent of changes in intracellular pH (Chen et al. 2000). Taken together, sAC gene expression in the CB is most likely regulated by changes in HCO_3^- concentration. Yet, we can not be certain whether these findings are specific to Type I cells, since homogenates of the CB were used. Similar to other reports, we detected sAC gene expression in testicular tissue. However, in response to CO_2/HCO_3^-, we did not observe an increase in cAMP levels in this tissue, which could be explained by the fact that we used whole testis homogenates from younger animals than has been previously reported (Jaiswal et al. 2001).

In this study, we describe for the first time that sAC gene expression and its activity differs between CB chemosensitive tissues and non-chemosensitive tissues (PG, NG, and SCG). The regulation of sAC gene expression and activity suggests different cellular roles for sAC in these tissues. Our results also suggest that in peripheral arterial chemoreceptors, sAC may mediate cAMP-dependent pathways, responding to changes in CO_2, while in response to hypoxia these pathways are activated by tmAC.

ACKNOWLEDGMENTS

We would like to thank Dr. Jochen Buck and Dr. Lonny R. Levin from Cornell University Medical College for the generous gift of the sAC antibody

(R21), Mr. Devin Mack for assistance with Western blotting, Dr. Raul Chavez for helpful suggestions and Dr Gabrielle Mclemore for the review of the paper. This work was supported by grant R01 EBG, HL 072748; AR Nunes was supported by FLAD, 155/2007.

REFERENCES

Batuca, J. R., Monteiro, T. C., & Monteiro, E. C. 2003, Contribution of dopamine D2 receptors for the cAMP levels at the carotid body, *Adv.Exp.Med.Biol.*, 536: 367-373.

Buck, J., Sinclair, M. L., Schapal, L., Cann, M. J., & Levin, L. R. 1999, Cytosolic adenylyl cyclase defines a unique signaling molecule in mammals, *Proc.Natl.Acad.Sci.U.S.A*, 96: 79-84.

Buckler, K. J., Vaughan-Jones, R. D., Peers, C., Lagadic-Gossmann, D., & Nye, P. C. 1991, Effects of extracellular pH, PCO2 and, *J.Physiol*, 444: 703-721.

Chen, Y., Cann, M. J., Litvin, T. N., Iourgenko, V., Sinclair, M. L., Levin, L. R., & Buck, J. 2000, Soluble adenylyl cyclase as an evolutionarily conserved bicarbonate sensor, *Science*, 289: 625-628.

Gonzalez, C., Almaraz, L., Obeso, A., & Rigual, R. 1994, Carotid body chemoreceptors: from natural stimuli to sensory discharges, *Physiol Rev.*, 74: 829-898.

Jaiswal, B. S. & Conti, M. 2001, Identification and functional analysis of splice variants of the germ cell soluble adenylyl cyclase, *J.Biol.Chem.*, 276: 31698-31708.

Kamenetsky, M., Middelhaufe, S., Bank, E. M., Levin, L. R., Buck, J., & Steegborn, C. 2006, Molecular details of cAMP generation in mammalian cells: a tale of two systems, *J.Mol.Biol.*, 362: 623-639.

Pastor-Soler, N., Beaulieu, V., Litvin, T. N., Da Silva, N., Chen, Y., Brown, D., Buck, J., Levin, L. R., & Breton, S. 2003, Bicarbonate-regulated adenylyl cyclase (sAC) is a sensor that regulates pH-dependent V-ATPase recycling, *J.Biol.Chem.*, 278: 49523-49529.

Perez-Garcia, M. T., Almaraz, L., & Gonzalez, C. 1990, Effects of different types of stimulation on cyclic AMP content in the rabbit carotid body: functional significance, *J.Neurochem.*, 55: 1287-1293.

Pfaffl, M. W. 2001, A new mathematical model for relative quantification in real-time RT-PCR, *Nucleic Acids Res.*, 29: e45.

Schmid, A., Sutto, Z., Nlend, M. C., Horvath, G., Schmid, N., Buck, J., Levin, L. R., Conner, G. E., Fregien, N., & Salathe, M. 2007, Soluble adenylyl cyclase is localized to cilia and contributes to ciliary beat frequency regulation via production of cAMP, *J.Gen.Physiol*, 130: 99-109.

Sinclair, M. L., Wang, X. Y., Mattia, M., Conti, M., Buck, J., Wolgemuth, D. J., & Levin, L. R. 2000, Specific expression of soluble adenylyl cyclase in male germ cells, *Mol.Reprod.Dev.*, 56: 6-11.

Sun, X. C., Zhai, C. B., Cui, M., Chen, Y., Levin, L. R., Buck, J., & Bonanno, J. A. 2003, HCO(3)(-)-dependent soluble adenylyl cyclase activates cystic fibrosis transmembrane conductance regulator in corneal endothelium, *Am.J.Physiol Cell Physiol*, 284: C1114-C1122.

Wang, Y., Lam, C. S., Wu, F., Wang, W., Duan, Y., & Huang, P. 2005, Regulation of CFTR channels by HCO(3)--sensitive soluble adenylyl cyclase in human airway epithelial cells, *Am.J.Physiol Cell Physiol*, 289: C1145-C1151.

Zippin, J. H., Farrell, J., Huron, D., Kamenetsky, M., Hess, K. C., Fischman, D. A., Levin, L. R., & Buck, J. 2004, Bicarbonate-responsive "soluble" adenylyl cyclase defines a nuclear cAMP microdomain, *J.Cell Biol.*, 164: 527-534.

RESEARCH PAPER

BICARBONATE- SENSITIVE SOLUBLE AND TRANSMEMBRANE ADENYLYL CYCLASES IN PERIPHERAL CHEMORECEPTORS

A R Nunes[1,2], A Holmes[3], V Sample[4], P Kumar[3], M J Cann[5], E C Monteiro[2], J Zhang[3] and E B Gauda[1*]

[1]Pediatrics, [4]Pharmacology and Molecular Sciences, Johns Hopkins Medical Institutions, Baltimore, MD; [2]CEDOC, Pharmacology, Faculdade de Ciências Médicas, Universidade Nova de Lisboa, Portugal; [3]School of Clinical and Experimental Medicine, College of Medical and Dental Sciences, University of Birmingham, Birmingham, [5]School of Biological and Biomedical Sciences, Durham University, U.K.

Background and purpose: The CO_2-sensing mechanisms in mammalian carotid body (CB) are not fully understood. As cAMP levels are associated with the chemotransduction mechanism, this study investigates if changes in HCO3-/CO2 modify chemodischarge through a HCO3/CO2 responsive – soluble adenylyl cyclase (sAC) and/or a neurotransmitter/ hormone responsive-transmembrane adenylate cyclase (tmAC) dependent mechanism. **Experimental approach**: We examined changes in sAC and tmAC mRNA expression (quantitative Real Time-PCR), cAMP levels (ELISA), activation of protein kinase A (PKA, FRET-based sensors) and carotid sinus nerve activity (in vitro nerve recordings) in the presence and absence of activators or inhibitors of sAC, tmAC, and PKA.

Key Results: Increases in HCO_3^-/CO_2 from 0/0% to normocapnia, in the presence of IBMX, a phosphodiesterase inhibitor, and MDL-12 330, a tmAC inhibitor, increased cAMP levels in the rat CB, but no further increases were observed in response to hypercapnia (44/10%). Forskolin, but not isohydric hypercapnia, increased PKA activity in type I cells of the CB. In the CB, the level of expression for tmAC1,4,6 and 9 isoforms was more highly expressed than sAC. Both sAC and tmAC inhibitors (KH7 10-50 μM, sAC inhibitor, and 2'3'-ddADO 100 μM) decreased cAMP levels in CB in both normo- and isohydric hypercapnia, with a higher contribution of tmAC. However, sAC and tmAC inhibitors induzed a higher inhibitory effect on the cAMP levels under 12 mM $HCO_3/2.5\%CO_2$ than normocapnia or isohydric hypercapnia. cAMP levels did not change significantly during different incubation times (5-30 min) in the presence of different concentrations of HCO_3^-

/CO_2, in the presence or absence of adenylyl cyclase inhibitors. CSN discharge was increased by acidic but not isohydric hypercapnia. Inhibition of tmAC, but not sAC, decreased the basal discharge of the CSN and its response to acid hypercapnia.

Conclusions and Implications: sAC and tmAC are functional in peripheral chemoreceptors, and tmAC but not sAC, is envolved in setting the basal chemoafferent discharge and the response to acidic hypercapnia. Isohydric hypercapnia causes no change in cAMP, PKA and discharge frequency. Evidence supports a particular contribution of these enzymes in situations when low HCO_3^- concentrations occur. Collectively, these data support that transduction of CO2 requires an absolute change in pHi, which is dependent on cAMP deived from tmAC.

Keywords: cAMP, cyclic adenosine monophosphate; CB, carotid body; sAC, soluble adenylyl cyclase; tmAC, transmembrane adenylate cyclase; peripheral arterial chemoreceptors; HCO_3^-/CO_2, bicarbonate/ CO_2.

***Correspondence author:** Estelle B. Gauda, M.D., Department of Pediatrics, Division of Neonatology, Johns Hopkins Medical University, 600 N. Wolfe Street, CMSC 6-104, Baltimore, MD 21287-3200 USA**,** egauda@mail.jhmi.edu

Running title: sAC and tmAC in carotid body.

Introduction

Peripheral arterial chemo-receptors located in the carotid body (CB) and central chemoreceptors located in the brainstem contain specialized cells that either depolarise in response to changes in PaO_2 or in response to changes in CO_2/H^+. Type I (glomus) cells of the CB, the peripheral chemoreceptor units, are innervated by carotid sinus nerve (CSN) afferents, a branch of the glossopharyngeal nerve, which have somas in the petrosal ganglion (PG), and relay on to neurons in the nucleus tractus solitarius in the brainstem (Gonzalez *et al.*, 1994).Although peripheral chemoreceptors were believed to be the major O_2 sensors while central chemoreceptors contributed predominantly to the CO_2/pH ventilatory response, recent evidence suggest that the central and peripheral chemoreceptors interact with each other, and the latter can modulate the central sensitivity to CO_2/pH (for a review see (Forster and Smith, 2010)). The specific cellular CO_2 sensing mechanisms that trigger hyperventilation in order to maintain metabolic demands are not fully understood although recent work has demonstrated a role for connexin 26 in CO2-dependent release of ATP in central

chemosensitive cells (Huckstepp *et al*., 2010).

cAMP is an essential secondary messenger that activates a multitude of downstream effectors through protein kinase A (PKA), exchange proteins activated by cAMP (EPACs) and cyclic nucleotide gated ion channels (CNGs). Two types of adenylyl cyclase mediate the production of cAMP in mammalian cells: the family of transmembrane adenylyl cyclase (tmAC) isoforms and the soluble adenylyl cyclase (sAC). In peripheral chemoreceptors, cellular cAMP levels are modulated by neurotransmitters/ neuromodulators that bind to G-protein coupled receptors (GPCRs) and alter tmAC activity (Gonzalez *et al*., 1994, Lahiri *et al*., 2006). At least nine specific tmAC isoforms have been identified in mammalian genomes, but they have not been characterized in this tissue. tmAC isoforms are sensitive to G proteins, forskolin, Ca^{2+}- signaling pathway (Halls and Cooper, 2011), and CO_2 (Townsend *et al*., 2009; Cook *et al.* 2012). sAC is activated by HCO_3^- and Ca^{2+} (reviewed by Kamenetsky *et al*., 2006). We have previously identified sAC mRNA and protein in the CB and related peripheral non-chemosensitive structures suggesting a functional role for sAC in this tissue (Nunes *et al*., 2009).

In this work, we explored whether isohydric hypercapnia increases chemodischarge through a HCO_3^-/CO_2 responsive-soluble adenylyl cyclase (sAC) and neurotransmitter responsive-transmembrane (tmAC) dependent mechanism.

Materials and Methods

Surgical procedures

The Animal Care and Use Committee at the Johns Hopkins University School of Medicine approved all experimental protocols. CSN recording experiments were performed at the University of Birmingham and were approved by the Biomedical Services Unit.

Peripheral arterial chemoreceptors, as well as non-chemoreceptor tissues, were isolated from Sprague-Dawley rats (SD, Charles River Laboratories, Wilmington, MA) of both sexes at postnatal days (P) 16 and 17. At this age CB hypoxic chemosensitivity is mature (Kholwadwala and Donnelly, 1992). The non-chemoreceptor tissues included the superior cervical (SCG), petrosal (PG) and nodose (NG) ganglia. Since sAC is highly expressed and has been well characterized in testicular tissue from rats at 3 months of age (Sinclair *et al*., 2000)

we included this tissue from this age animal as a positive control.

In one set of experiments, prior to tissue removal or dissection, the animals were anesthetized briefly with isoflurane and immediately decapitated. The carotid bifurcation, including the CB, SCG, and the NG/PG complex, was removed *en bloc.* Subsequently, tissues were isolated and cleaned of surrounding connective tissue under a dissecting microscope. In another set of experiments, we dissected CB for dissociation of type I cells from SD rats at P5-9. At this age dissociated cells were easier to obtain and no statistical differences in cAMP accumulation were observed between the whole CB from rats DOL 7 (23.5± 3.1 fmol/µg protein, n=6) and P17 (33.9± 4.6 fmol/µg protein, n=4) in normocapnic conditions. Lastly, CSN recording experiments were performed with tissues obtained from adult male SD rats (50-100g, Charles River UK Ltd, Margate, UK). CBs were harvested as described previously (Pepper et al, 1995). Briefly, anaesthesia was induced in an airtight induction chamber using 4% isoflurane in medical O_2 administered at a flow rate of 1.5 – 3 ml/min. Surgical anaesthesia was continuously maintained through a nose cone with 1.5 – 2.0% isoflurane in O_2, at a flow rate of 1.5 – 3 ml/min. The carotid bifurcation along with the superior cervical ganglion, vagus nerve, glossopharyngeal nerve, carotid sinus nerve and the carotid body were all excised. The tissue was immediately placed in ice-cold bicarbonate buffered extracellular Krebs solution containing, in mM: 125 NaCl, 3 KCl, 1.25 NaH_2PO_4, 5 Na_2SO_4, 1.3 $MgSO_4$, 24 $NaHCO_3$, 2.4 $CaCl_2$, 11 D-glucose, equilibrated with 95% O_2 and 5% CO_2.

Effects of HCO_3^-/CO_2 on cAMP levels

A control experiment was performed to confirm the efficacy of MDL-12,330A (Sigma) in blocking tmAC under our experimental conditions. PGs were pre-incubated in Krebs modified solution in the presence of 24 mM HCO_3^- for 30 minutes followed by incubation in fresh Krebs modified medium, for 30 minutes, in the presence of 24 mM HCO_3^- plus forskolin (1-100 µM; Sigma) and 3-isobutyl-1-methylxanthine (IBMX, 500 µM; Sigma), a phosphodiesterase (PDE) inhibitor. Based on the concentration-response curves for forskolin on cAMP levels, we divided CBs, PGs and testes into two experimental groups - one treated with forskolin (10 µM) in the absence of MDL-12,330A (500 µM) and the other treated with forskolin (10 µM) in the presence of MDL-12,330A.

To study the effect of changes in HCO_3^-/CO_2 in cAMP levels, as an indirect

measurement of sAC activity, we pre-incubated the CB and non-chemosensitive tissues (SCG, PG, testis and nodose ganglia) tissues in Krebs modified solution without HCO_3^-/CO_2 and in the presence of MDL-12,330A (500 µM), a tmAC inhibitor (Delpiano and Acker, 1991). After 30 minutes, we incubated the tissues in fresh Krebs modified solution in the presence of MDL-12,330A (500 µM), and either 0 mM HCO_3^-/0 % CO_2; 12 mM HCO_3^-/2.5% CO_2; 24 mM HCO_3^-/5% CO_2; or 44 mM HCO_3^-/10 % CO_2 for 30 minutes, pH 7.4, 37°C. We modified the incubation buffer by changing CO_2 and HCO_3^- concentrations, adjusting the osmolarity with NaCl. This approach allows the assessment of CO_2 effect, preventing major changes in pH.

All the experiments were conducted in the presence of a non-specific inhibitor for phosphodiesterase (PDE) IBMX (500 µM). To treat the testicular tissues, we also added dypiridamole (500 µM) to the incubation medium due to the elevated expression of PDE8 in this tissue, which is not inhibited by IBMX (Lugnier, 2006). Tissues were pooled from 2 animals from the same litter and the experiments were repeated using animals from different litters. Tissues were processed for cAMP extraction and the quantification was done as outlined below in *cyclic nucleotide extraction and quantification*. All the experiments were done in the presence of 60%O_2 since hypoxia has been known to increase the chemosensitivity response to CO2 (Fitzgerald and Parks, 1971).

Contribution of sAC and tmAC to cAMP levels under different concentrations of HCO_3^-/CO_2.

We tested the effect of the tmAC selective inhibitor, 2'5'-ddADO (100 µM, Sigma), or sAC inhibitor (KH7, 10-100 µM), or both on the cAMP accumulation in the CB during 30 min and over time (0, 5, 15, 30 min of incubation) under different concentrations of HCO_3^-/CO_2. Control experiments were also performed to compare the effect of the tmAC inhibitors: MDL-12,330A (500 µM), ddADO (30-300 µM) or SQ 22536 (200 µM). All experiments were conducted in the presence of IBMX (500 µM).

Cyclic nucleotide extraction and quantification

cAMP was measured as previously reported (Batuca *et al.*, 2003) and briefly described here. We immersed tissues in cold 6% (w/v) trichloroacetic acid (TCA; 600 µl) for 10 minutes, and then all the tissues were homogenized at 2 - 8ºC and centrifuged them at 12,000 g for 10 minutes at 4ºC. The supernatants were

washed four times in 3 ml of water saturated with diethyl ether solution (50:50) and then lyophilized. The sample was then stored at -20ºC until cAMP quantification by enzyme immunoassay (EIA, RPN 2255, GE Healthcare Bio-Sciences AB, Piscataway, NJ). Protein pellets were stored at -20°C until measured with the standard Bradford Protein Assay (Bio-RAD) or by using a fluorescence detection kit, NanoOrange Protein (Invitrogen, Eugene, OR). cAMP levels were expressed in femtomoles per microgram of protein (fmol/µg protein), which is more accurate than normalizing to grams of tissue, especially for small tissue samples, such as the CB.

Intracellular pH measurement in carotid body

Intracellular pH (pH_i) was measured using the pH-sensitive fluorescence dye, BCECF-AM (Molecular Probes, Eugene, OR) using a protocol previously described by Iturriaga and co-workers (Iturriaga *et al*., 1992). The isolated CB was incubated with trypsin (0.02%, Sigma) and collagenase (0.01%, Sigma) for 30 minutes, and rinsed in phosphate buffered saline (PBS). Then, the CB was incubated with BCECF-AM (5 µM) at 37ºC for 1 hour and washed to remove excess dye. Since type I cells, the sensors of the CB, appear usually in clusters, we selected these regions as the regions of interest (ROI) and analyzed the change in BCECF-AM fluorescence intensity while the whole organ was superfused with oxygenated solutions containing increasing concentrations of HCO_3^-/CO_2. All solutions were titrated to pH 7.4 as described above. Fluorescent images were examined with a fluorescent microscope (Nikon Eclipse E-400, Nikon Instruments, Melville, NY) captured at 400x with an attached charge-coupled device (CCD) camera (Hamamatsu, Photonic ItSystems, Bridgewater, NJ). The BCECF dye was excited at 495 nm, and emission was recorded at 519 nm. The images were captured over a period of 200 frames corresponding to 2.38 minutes and analyzed by Ivison (BioVision Technologies, PA). To avoid photobleaching, the intensity of light was controlled by Exfo X-cite 1200PC (0.12 intensity, Exfo Photonic Solutions, Ontario, Canada). A calibration curve for each CB was performed at the end of each experiment using the nigericin (10 µM)/high K^+ method (Thomas *et al*., 1976) to determine changes in fluorescence intensity *versus* pH (6.5-8.0). Exposure to ammonium chloride (NH_4Cl, 50mM) was used to ensure that dye intensity

corresponded to changes in intracellular pH (Buckler *et al.*, 1991).

Changes in protein kinase A (PKA) activity in dissociated type I cells of the CB using FRET-based sensors

CBs isolated from SD rats P5-9 were mechanically and enzymatically dissociated with an enzyme mixture consisting of trypsin and collagenase (~0.5mg/ml, Sigma) according to the protocol described by Carroll and co-workers (2005). CB cells were plated on poly-D-Lysine coated imaging dishes and cultured for 3 hours. To monitor PKA activity we used a 3rd generation of a genetically encoded A-Kinase activity reporter dependent on FRET (AKAR3). AKAR3 consist of a fusion of a CFP, a phosphothreonine-binding domain, a PKA substrate, and the YFP variant venus (Allen and Zhang, 2006). When PKA is activated, the catalytic subunit of PKA phosphorylates the target in AKAR3, causing a conformational reorganization that increases FRET between CFP and YFP (Allen and Zhang, 2006). We obtained the adenoviruses expressing the AKAR3 reporter by Yang K. Xiang's laboratory and infected the CB type I cells for 24 hours. One hour before FRET imaging, CB type I cells were labeled with rhodamine PNA (Rho-PNA, 30 μg/ml) in complete CB medium at 37°C as previously described by Kim and co-workers (2009). After an hour, we placed the imaging dish containing the cells infected with AKAR3 and labeled with Rho-PNA into a chamber (Warner Instruments, Hamden, CT) to allow superfusion of the cells with a constant flow rate of 2 ml/min (Ismatec, Cole Parmer instrument CO, Vernon Hills). The cells were imaged on a Zeiss Axiovert 200M microscope (Carl Zeiss, Thornwood, NY) with a 40X oil immersion objective and a cooled charge-coupled device camera (Roper Scientific, Trenton, NJ) controlled by Metafluor 6.2 software (Molecular Deices, Downingtown, PA). Dual emission ratio imaging used a 420DF20 excitation filter, a 450DRLP dichroic mirror and two emission filters (475DF40 for CFP and 535DF25 for YFP). Exposure time was 50-500 ms and images were acquired every 20 sec. Background correction of the fluorescence images was performed by subtracting intensities from regions of the imaging dish with no cells. To test the contribution of tmAC and sAC in PKA activity we performed two sets of experiments: CB cells were incubated in the presence of 1) tmAC and sAC activators, forskolin (50 μM) and HCO_3^- /CO_2 (0/0-44/10 mM/%), respectively, and 2) in the presence of tmAC and sAC

inhibitors, MDL 12,330A (500 µM) and KH7 (50 µM), respectively. In both set of experiments, PDEs were inhibited by IBMX (10-100 µM). Graph curves were normalized by setting the emission ratio before drug addition equal to one.

tmAC and sAC mRNA gene expression

The mRNA expression levels for sAC and the nine isoforms of tmAC in the CB and PG were compared. The tissues were isolated as mentioned in surgical procedure (4 rats per condition; n=3 independent experiments), cleaned from surrounded tissue and quick-frozen on dry ice and stored at -80ºC.

In independente experiments FSK, a tmAC activator, was used to investigate its effects on the regulation of sAC gene expression. The CB were pre-incubated in Krebs modified solution containing (in mM): NaCl 135; KCl 5; $CaCl_2$ 2; $MgCl_2$ 1.1; HEPES 10; glucose 5.5, pH 7.40 (Perez-Garcia *et al.*, 1990) with 24 mM $NaHCO_3$ and equilibrated with 5%CO_2/60%O_2. After 30 minutes, we replaced the pre-incubation buffer with incubation buffer containing 24 mM $NaHCO_3$ and FSK (100 µM), equilibrated with 5%CO_2/60%O_2, for 1 hour at 37ºC, pH 7.4. Tissues were pooled from 4 animals from the same litter and the experiments were repeated 4 times using animals from different litters. At the end, tissues were quick-frozen on dry ice and stored at -80ºC until further processing for RT-qPCR, as outlined below.

Real time – quantitative PCR

Tissues used to study sAC and tmAC mRNA gene expression and regulation levels were processed to obtain total RNA (Micro-to-Midi Total RNA Purification, Invitrogen, Carlsbad, CA) according to the manufacturer's instructions. DNase treatment (PureLink DNase, Invitrogen) was performed to avoid genomic DNA contamination. RNA yield and quality was measured at 260 and 280 nm by conventional UV spectrophotometer (Beckman Du 530) or NanoDrop spectrophotometer (for RNA from CB samples, Thermo Scientific, Wilmington, DE). Total RNA (about 1 µg) was used for first-strand cDNA synthesis using an iSCRIPt cDNA synthesis kit (Bio-Rad Laboratories, Hercules, CA).

The respective primer sequences for each adenylyl cyclase isoform used are shown in Table 2, *General Methods, quantitative RT-PCR section* (Pastor-Soler *et al.*, 2003b, Chang *et al.*, 2003). Relative expression of AC genes between the tissues and conditions was standardized with levels of glucose-6-phosphate dehydrogenase (G6PDH) expression, the reference gene. We also validate our

results using two more different reference genes: glyceraldehyde 3-phosphate dehydrogenase (GAPDH) and Beta-actin (β-actin) (Table 2, *General Methods, quantitative RT-PCR section* , Wang and Xu, 2010). We evaluated the expression of the three reference genes in all the studied tissues and conditions using a web site that combined 4 different algorithms used to determine the stability of the reference genes: geNorm, Normfinder, Bestkeeper and comparative ΔCt method (http://www.leonxie.com/referencegene.php?type=reference). We found that GAPDH is the most stable gene across our experiments, but AC gene expression levels normalized with this reference gene showed the same trend of results as shown when normalized with G6PDH.

RT-qPCR was performed with a MyiQ iCycler RT-qPCR system (Bio-Rad) with the SYBR Green detection system. Each qPCR reaction consisted of 1 µl of cDNA and 3.5 µl of 300 nM primers diluted in DEPC-H_2O and 10 µl of SYBR Green Supermix (Bio-Rad) for a final volume of 20 µl. We performed triplicates for each sample. qPCR conditions for sAC gene expression and regulation were: denaturing 8 min at 95°C, followed by 40 cycles at 95°C for 1 min, 60°C for 30 sec, 72°C for 45 sec, and a terminal extension period (72°C, 10 min). qPCR conditions for AC (tmAC and sAC) expression and regulation were: denaturing 5 min at 95°C, followed by 40 cycles at 95°C for 20 sec, 62°C for 20 sec, 72°C for 20 sec, and a terminal extension period (72°C, 10 min). We analyzed the specificity of the RT-qPCR product by performing a melting curve with 0.5ºC increments in temperature. Product formation during the exponential phase of the reaction was analyzed for semi-quantification of relative expression in the specific tissues using the Pfaffl method (Pfaffl, 2001) or relative quantification to reference gene based on the threshold cycle (CT) for amplification as $2^{(\Delta CT)}$, where $\Delta C_T = C_{T,reference} - C_{T,target}$.

Extracellular CSN recordings

The carotid bifurcation, along with the superior cervical ganglion, vagus nerve, glossopharyngeal nerve, carotid sinus nerve and the carotid body was pinned out in a small volume (*ca* 0.2 ml) dissecting chamber with a Sylgard 184 base (Dow Corning). The tissue was continuously superfused with a bicarbonate buffered extracellular Krebs solution containing, in mM: 125 NaCl, 3 KCl, 1.25 NaH_2PO_4, 5 Na_2SO_4, 1.3 $MgSO_4$, 24 $NaHCO_3$, 2.4 $CaCl_2$, 11 D-glucose, equilibrated with 95% O_2 and 5% CO_2. Connective tissue was removed and the superior cervical

ganglion, branches of the vagus nerve and the occipital artery were all individually excised. The carotid sinus nerve was cut away from the glossopharyngeal nerve exposing the nerve endings. The whole tissue was partially digested by incubation in a bicarbonate buffered, equilibrated 95% O_2 and 5% CO_2 enzyme solution (0.075 mg/ml collagenase type II, 0.0025 mg/ml dispase type I; Sigma) at a temperature of 37°C, for 20 – 30 min, in a water bath at 37°C (Grant W14, Grant Instruments Cambridge Ltd).

Extracellular recordings were made from the cut end of the CSN using glass suction electrodes pulled from GC150-10 capillary glass (Harvard Apparatus). Voltage was amplified using an AC pre-amplifier (NeuroLog NL104; Digitimer), then filtered between 50 Hz and 3 kHz (NeuroLog NL125; Digitimer) and amplified further with an AC amplifier (NeuroLog 105; Digitimer). Total amplification was x4000. Derived voltage was recorded using a CED micro1401 (Cambridge Electronic Design) and visualised on a PC with Spike2 (version 7.1) software (Cambridge Electronic Design). Offline analysis using Spike2 allowed for discrimination of single unit activity.

Flow meters with high precision valves (Cole Palmer Instruments) were used in order to gas the superfusate with a desired gas mixture. The superfusate PO_2 was continuously measured using an O_2 meter (OXELP, World Precision Instruments) and was maintained throughout at 300 mmHg. The superfusate PCO_2 was increased from 40 mmHg to 80 mmHg to monitor carotid body responses to acidic hypercapnia. In isohydric hypercapnia experiments, a PCO_2 of 80 mmHg and a $NaHCO_3$ concentration of 44 mM were used to maintain pH. Here, osmolality was balanced by reducing the NaCl concentration.

Data analysis and statistical procedures

The data are represented as mean ± SEM and differences between the experimental groups were determined using statistical software from GraphPad Prism (GraphPad Software Inc., version 4, San Diego, CA) or SPSS (SPSS Inc, version 12, Chicago, IL). Statistical significance was set at $P<0.05$.

Results

Bicarbonate-regulated cAMP levels

We had previously reported that, when tmAC is inhibited, increases in HCO_3/CO_2 from 0/0 to 24/5 (mM/%) augmented cAMP levels in the CB but not in peripheral non-chemosensitive tissues (Nunes *et al.*, 2009). In this work we explored the effects of more concentrations of HCO_3^-/CO_2

(mM/%: 0/0, 12/2.5, 24/5, and 44/10) on cAMP production in peripheral chemo- and non-chemosensitive tissues as well as in testis from 3 month-old rats (control tissue). To differentiate between the activity of tmAC and sAC, we incubated the tissues with MDL-12,330A (500µM), an effective tmAC inhibitor in our preparations (**Fig.1**). In response to 10 µM of FSK (an effective concentration to induce increases in cAMP levels, **Fig.1A**), MDL-12,330A (500µM) blocked 95%, 81% and 91% of cAMP production in the CB (**Fig.1B**), PG (**Fig.1C**) and testes (**Fig.1D**). Experiments were performed in the presence of IBMX (500 µM), a non-specific PDE inhibitor.

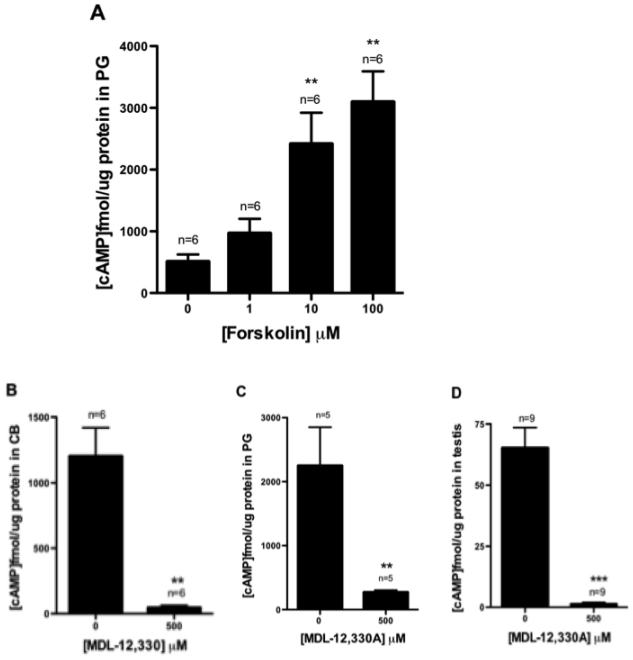

Figure 1 – Effect of a) Forskolin (1-100 µM) and MDL-12,330A (500 µM) on cAMP levels in b) carotid body (CB), c) petrosal ganglia (PG) and d) testicular tissue. ** p<0.01, *** p<0.001 Paired t- test corresponding to differences between cAMP levels in the presence and absence of MDL-12,330A.

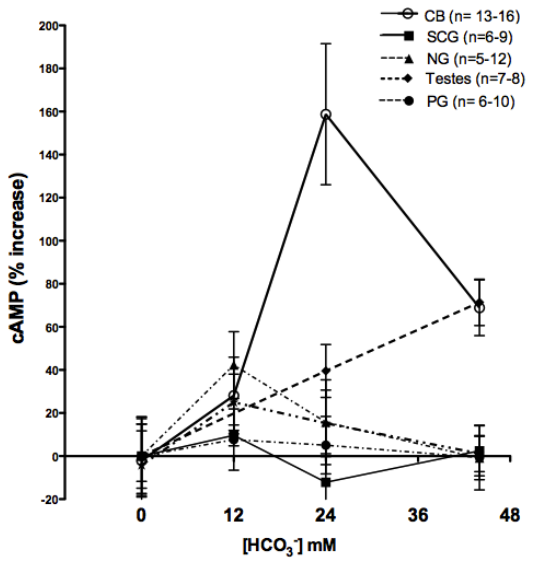

Figure 2 - Concentration- response curves of HCO_3^-/%CO_2 for effects on cAMP levels in the CB and non-chemosensitive tissues. 0% increase was obtained with 0 mM HCO_3/0%CO_2: 17.8 ±2.9 fmol/µg protein (CB, n=21); 31.6±5.4 fmol/µg protein (SCG, n=9); 23.9 ±6.9 fmol/µg protein (PG, n=6); 8.7 ±2.9 fmol/µg protein (NG, n=3); 2.79 ±0.33 fmol/µg protein (testis, n=7).

In non-chemosensitive tissues, concentrations of HCO_3^-/CO_2 did not induce changes in cAMP levels, except in testicular tissues (**Fig.2**). Although sAC mRNA is highly expressed in testes, we had not been previously able to show sAC activity in testes from young animals (Nunes *et al.*, 2009). In the present work, the results obtained using testes from adult rats support that sAC function increase with development in this tissue (Sinclair *et al.*, 2000, Braun and Dods, 1975).

The amount of cAMP in the chemo-sensitive tissue, CB, was dependent on the concentration of HCO_3^-/CO_2 (0/0,12/2.5,24/5 mM HCO_3^-/%CO_2, **Fig.2**). cAMP levels in the CB were highest in normocapnia (24 mM HCO_3^-/5%CO_2); higher concentrations of HCO_3^-/CO_2 (44 mM HCO_3^- /10%CO_2) had no additional effect on cAMP levels in this organ (**Fig.2**). These results suggested to us that when tmAC is blocked, sAC reached a maximal level of activity under physiological (normocapnic) conditions, 24 mM HCO_3^- /5%CO_2.

To determine whether the changes in cAMP levels in response to different concentrations of HCO_3^-/CO_2 were mediated by a direct effect of bicarbonate or due to changes in intracellular pH (pH_i) in the CB, we measured pH_i using a pH-

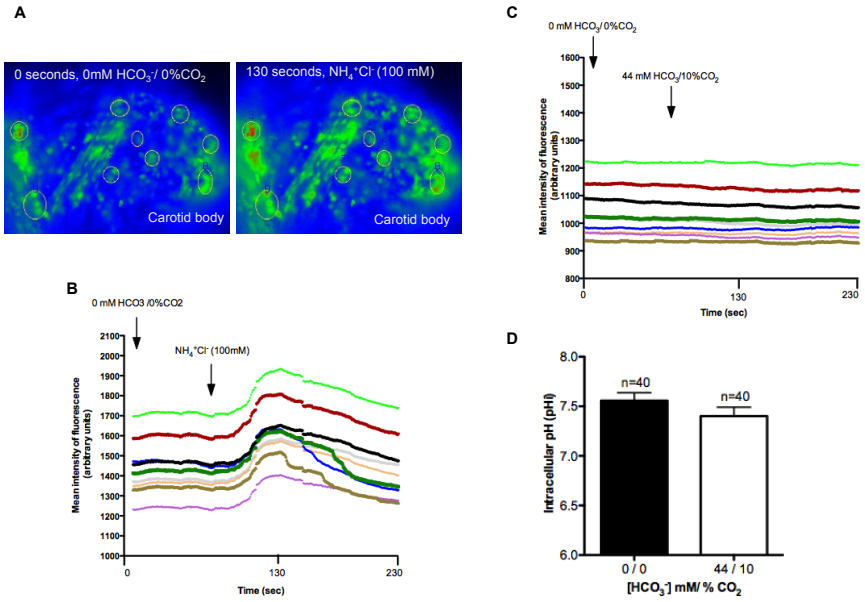

Figure 3- BCECF dye fluorescent intensity representing changes in intracellular pH (pH_i) in the superfused CB. A) Representative photomicrographs of the CB showing changes in fluorescent intensity (pseudocolor) in the ROI captured prior to (left panel) or in response to exposure to $NH_4^+Cl^-$ (100 mM, right panel). Increased green pseudocolour and red areas in the ROI in the right photomicrograph represents increasing areas of fluorescent intensity corresponding to increased pH_i. Tracing below photomicrographs was obtained prior to, during and after exposure to $NH_4^+Cl^-$ (100 mM). C) Representative tracing from one experiment showing no change in mean fluorescence intensity (pH_i) for the ROIs in the CB when the superfusate was changed from 0mM HCO_3^-/0%CO_2 to 44mM HCO_3^-/10%CO_2. D) Composite data obtained from four different preparations, with a total of different 40 ROIs showing no change in mean fluorescence intensity. Values represent means ± SEM.

sensitive fluorescence dye BCECF-AM. A control experiment with NH_4Cl showed that there was a distinct change in fluorescent intensity in the cells of the CB (**Fig.3A,B**). Furthermore, we observed incremental changes in fluorescent intensity associated with changes in extracellular pH (6.5-8.0), using the nigericin (10 µM)/high K^+) method to construct calibration curves. We observed no variation in pH_i associated with changes from 0mM HCO_3^- /0%CO_2 to 44mM HCO_3^- /10%CO_2 within each selected region of the whole CB (**Fig. 3C,D**). These results suggest that increases in HCO_3^-/CO_2 with constant extracellular pH did not change pH_i in our preparation.

Changes in protein kinase A (PKA) activity in dissociated type I cells of the CB

As the CB O_2/CO_2 sensors are located in type I cells, we explored whether the lack of effect of isohydric hypercapnia on cAMP accumulation observed in the whole CB was consistent with modulation of downstream targets of cAMP in isolated type I cells. Thus, we determined the effect of different concentrations of HCO_3^-/CO_2 on PKA activity in type I cells of the CB using a genetically encoded AKAR3 reporter dependent on FRET. Preliminary experiments confirmed the co-localization of Rho-PNA with tyrosine hydroxylase (see *General Method- FRET* section), and co-localization of Rho-PNA with AKAR3 virus expression in type I cells of the CB (see method section).

Cells were perfused with medium containing 0 mM $HCO_3^-/0\%CO_2$, followed by application of a sub-maximal concentration of IBMX (10 μM) to avoid saturation of the reporter, which increased FRET emission ratio by 6 ± 4.8% (n=21 cells). IBMX (10 μM) was maintained through the experiment, and the perfusate medium was changed from 0 mM $HCO_3^-/0\%CO_2$ to 24 mM $HCO_3^-/5\%CO_2$ or to 44 mM $HCO_3^-/10\%CO_2$ with no observed change in FRET emission ratio. Addition of FSK (50 μM, tmAC activator) markedly increased the emission ratio to 7.4 ±1.1%. H89 (10 μM, IC_{50}= 50 nM, Rocher et al, 2009), a PKA inhibitor, decreased the emission ratio by 14.6 ±1.4%(n=21, **Fig.4**). These results are consisitent with the measurments of cAMP in whole CB and suggest that isohydric hypercapnia does not increase PKA activity in type I cells. We can not exclude that changes in HCO_3^-/CO_2 concentrations could induce small changes in PKA activity that, together with the high PDE degradation rate (PDEs were not completely blocked by IBMX), were not measurable.

We further studied the effect of sAC and tmAC inhibitors on PKA activity, perfusing type I cells either with MDL-12,330A (100-500 μM, IC_{50}= 250 μM, Guellaen et al, 1977) or KH7 (50 μM, IC_{50}= 2-5μM, Ramos et al 2008) in the presence of IBMX (100 μM) in normocapnic and hypercapnic conditions. KH7 is a specific sAC inhibitor and it is known to be inert towards tmACs in vitro at concentrations up to 300 μM (Hess et al, 2005). However, for concentrations up to 50 μM this inhibitor tends to precipitate, and, as observed by others, the precipitation is exacerbated by the continuous gas bubbling necessary during these experiments (Tresguerres et al, 2010). For

both conditions (normocapnia and hypercapnia) FRET emission ratio increased upon perfusion of type I cells in the presence of IBMX (100 μM). The effect of the AC inhibitors was normalized to the effect on the emission ratio by IBMX. Perfusion with 100 μM of MDL-12,330A together with 24 mM HCO_3^-/5%CO_2 did not change FRET emission ratio. Perfusion with 500 μM of MDL-12,330A together with 24 mM HCO_3^-/5%CO_2 decreased the emission ratio by 108.9±5.3% (n=25). Perfusion with KH7 (50 μM) together with 24 mM HCO_3^-/5%CO_2 decreased emission ratio by 141.7± 31.1% (n=23). Perfusion of type I cells with MDL-12,330A (500 μM) together with 44 mM HCO_3^-/10%CO_2 (hypercapnia) decreased the emission ratio by 198.2±27.7% (n=20), a higher inhibitory effect than the one observed in normocapnia ($p<0.01$, t-test). Perfusion with KH7 (50 μM) decreased the FRET emission ratio in the same extent between normocapnia and hypercapnia conditions. In summary, the results showed that in type I cells, PKA activity depends in both sAC and tmAC activity. The highest inhibition on cAMP-dependent PKA activity mediated by MDL-12,330A in hypercapnia suggests that either tmAC has a role in CO_2 sensitivity or raises a concern about the specificity of the inhibitor. To address these questions we studied the expression of tmAC and its involvement in CO_2 sensing in the CB, using different selective tmAC inhibitors.

sAC and tmAC (I-IX isoforms) gene expression

mRNA levels for sAC and the 9 tmAC isoforms were quantified in the CB and PG. As previously observed (Nunes et *al*, 2009), we confirmed that sAC expression was higher in the CB than in the PG ($p<0.05$, Paired t-test, **Fig. 5**). However, in the CB, gene expression for the isoforms: tmAC1 (Ca^{2+} and calmodulin stimulated), tmAC4 (G- protein Gβγ stimulated), tmAC6 (PKA, PKC and Ca^{2+} inhibited) and tmAC9 (Ca^{2+} inhibited) were significantly greater than sAC ($p<0.001$, two-way repeated measures ANOVA with Bonferroni's comparison test, **Fig.5**). We observed that the CB and PG expression profile for the 9 tmAC isoforms differed (**Fig.5**); tmAC1 (Ca^{2+} and calmodulin stimulated),tmAC4(Gβγstimulated), and tmAC6 (PKA, PKC and Ca^{2+} inhibited) were higher in the CB than in the PG ($p<0.001$, **Fig.5**), while the levels of tmAC2 (Gβγ and PKC stimulated) were lower ($p<0.001$, **Fig.5**). tmAC3 and tmAC8 (calmodulin- Ca^{2+} stimulated), tmAC5 and tmAC7 (PKC-stimulated), and tmAC9

(Ca^{2+}-inhibited) gene expression did not differ between tissues. These results demonstrated that even though sAC mRNA is higly expressed in the CB, it is much lower than of the level of expression for tmAC.

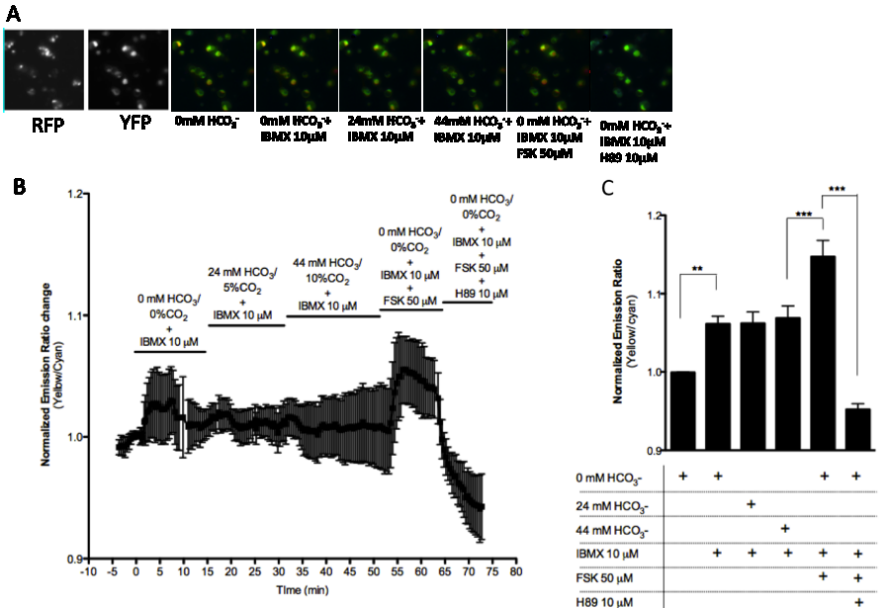

Figure 4- Effect of activators of sAC and tmAC on PKA activity in type I cells using FRET-based reporters. A) RFP image showing PNA labeling in type I cells, YFP image showing the expression of the 3rd generation of A-Kinase activity reporter (AKAR3) and pseudocolor images showing the response of AKAR3 to different concentrations of HCO_3^-/CO_2 (0/0-44/10), forskolin (FSK, 50 µM, tmAC activator) and H89 (10 µM, PKA inhibitor) in the presence of IBMX (10 µM, non-selective PDE inhibitor), 40X. B) Time course of representative response to HCO_3^-/CO_2 (0/0-44/10 mM/%), FSK (50 µM) and H89 (10 µM) in the presence of IBMX (10 µM, n=14 cells). C) Composite data showing that emission ratio increased by 1.6± 4.8% with addition of IBMX, did not significantly change with the addition of 24 or 44 mM HCO_3^-, markedly increased to 7.4 ± 1.1% with addition of FSK and decreased 14.6 ± 1.4% with H89 (n=21 cells). Paired t-test ** p<0.01 and ***<0.001.

Relative contribution of sAC and tmAC to cAMP accumulation in the carotid body

To investigate if these enzmes have a role in HCO_3^-/CO_2 sensing in the CB, we first studied the effect of the tmAC inhibitors MDL-12,330A (500 µM, IC_{50}=250 µM, Guellaen et al, 1977), 2'5'-ddADO (30-300 µM, IC_{50}=3-16 µM, Ramos et al, 2008) and SQ 22536 (200 µM, IC_{50}=20 µM, Rocher et al, 2009), and sAC inhibitor KH7 (10-100 µM, IC_{50}= 2-5µM, Ramos et al 2008) on cAMP production during isohydric hypercapnia. All the experiments were performed in the presence of IBMX (500 µM). MDL-12,330A (500 µM) inhibited all tmAC activity, blocking cAMP production by 96.1±0.4% (n=22, **Fig.6**).

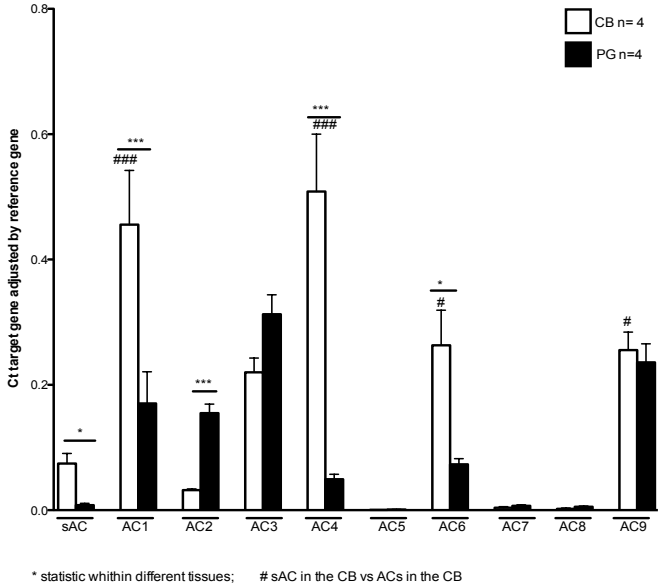

Figure 5- sAC and tmAC mRNA expression in the carotid body (CB) and petrosal ganglia (PG) using qRT-PCR. Two way repeated measurements ANOVA with Bonferroni's comparison test: * p<0.05 and *** p<0.001 for comparison of the same AC isoform between different tissues and # p<0.05 and ###p<0.001 for comparison between sAC and different tmAC

This result was not reproduced by other tmAC specific inhibitors, 2'5'-ddADO (100 μM, 60.0±10.5% of inhibition, n=6, **Fig.6)** and SQ 22536 (200 μM, 63.0±3.5% of inhibition, n=3, **Fig.6**), suggesting that MDL-12,330A is not a specific tmAC inhibitor at the concentrations used in this work. KH7 blocked cAMP production in a concentration-dependent manner (10 μM of KH7 blocked cAMP levels by 6.9±13.0%, n=9; 50 μM by 60.7±13.0%,n=9; 100 μM by 69.4±6.7%,n=8 **Fig.6**).

To investigate if these enzymes have a role in HCO_3^-/CO_2 sensing in the CB, we incubated this tissue in the absence and presence of 2'5'-ddADO (100 μM) and KH7 (10-50 μM) or both, during 30 min, under different concentrations of HCO_3^-/CO_2 (mM/%, 12/2.5; 24/5 and 44/10). We observed that at 12 mM HCO_3^-/ 2.5%CO_2 sAC was partially blocked by KH7 10μM (36.7±9.9% of inhibition, n= 6, **Fig.7**). Higher concentrations of KH7 (50μM) blocked 68.6±7.3% of cAMP production (n=4, **Fig.7**), a similar effect produced by 2'5'-ddADO (100 μM, 73.1±3.1%, n=9, **Fig.7**) and by the presence of both inhibitors (2'5'-ddADO 100 μM + KH7

10μM, 73.1±2.6%, n=4 and 2'5'-ddADO 100 μM + KH7 50μM, 67.9±1.8%, n=3, **Fig.7**). The inhibitory effect of 2'5'-ddADO under 12 mM HCO_3/2.5%CO_2 (73.2±3.1%) was more pronounced than in normocapnic (55.1±5.5%, n=8) and isohydric hypercapnic (55.3±6.7%, n=10) conditions ($p<0.05$, one way ANOVA, **Fig.7**). KH7 (10μM) blocked sAC activity by 21.1±9.6% (n=6, **Fig.7**) and by 6.9±12.9% (n=9, **Fig.7**) under normocapnic and isohydric hypercapnic conditions, respectively.

In summary, there is a higher contribution of tmAC and sAC for cAMP accumulation in response to 12 mM HCO_3/2.5%CO_2 than to normocapnia and isohydric hypercapnia conditions. Although both enzymes are functional within the CB, tmAC contributes more to cAMP accumulation than sAC in normocapnia. The levels of depression in cAMP accumulation induced by sAC or tmAC inhibition does not change significantly between normocapnia and isohydric hypercapnia, suggesting that sAC or tmAC activity is not up regulated in response to isohydric hypercapnia, consistent with no global increase in cAMP levels in this condition.

Since sAC is directly activated by HCO_3^- while neurotransmitters released by the cells under these conditions bind to GPCR coupled to tmAC, we postulated that sAC could be activated earlier than tmAC. We explored this hypothesis by determing the time courses of cAMP production during different concentrations of HCO_3^-/CO_2. In the absence of sAC and tmAC inhibitor, cAMP levels did not change significantly during different incubation times and in the presence of different concentrations of HCO_3^-/CO_2 (**Fig.8**). These results confirmed that sAC is not apparently involved in the production of cAMP under different concentrations of HCO_3^-/CO_2, either after 5 or 30 min of incubation. The inhibitory effect induced by KH7 (10μM) and 2'5'-ddADO (100μM) was the same after 5 or 30 min of incubation in all the concentrations of HCO_3^-/CO_2 tested.

The impact of sAC and tmAC inhibition on the functional chemoafferent response to hypercapnia

Initial experiments examined the functional impact of acidic and isohydric hypercapnia on the CSN chemoafferent discharge frequency. The single fiber frequency measured in normocapnia was significantly elevated in acidic but not isohydric hypercapnia (n=6, **Fig. 9A-C**), supporting the hypothesis that the CSN frequency response to raised PCO_2 is tightly coupled to a decrease in pH.

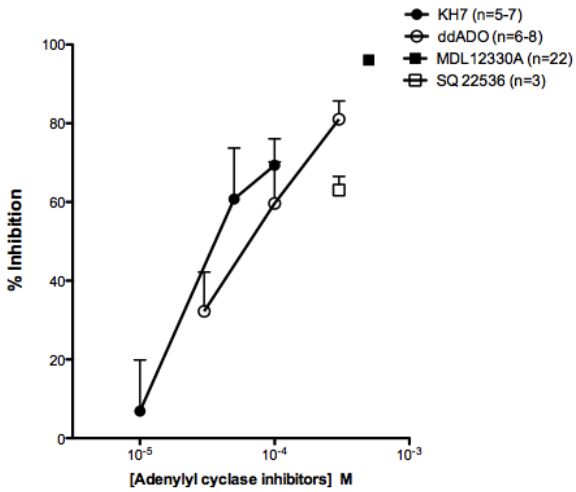

Figure 6- Effect of tmAC inhibitors: MDL-12,330A (500 µM), SQ22356 (200 µM), 2'5'-ddADO (30-300 µM) and sAC inhibitor KH7 (10-100 µM) on cAMP production after 30 min of incubation in hypercapnia conditions (44mM HCO_3^-/10%CO_2) in the carotid body.

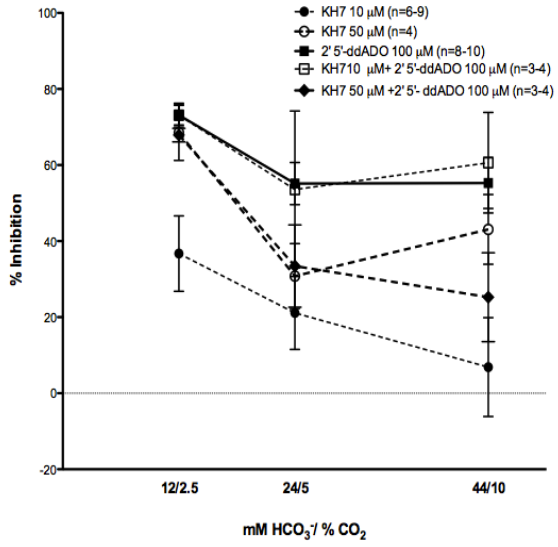

Figure 7- Effect of tmAC 2'5'-ddADO (100 µM), KH7 (10-50 µM) or both on cAMP production in response to different concentrations of HCO_3/CO_2 (mM/%: 12/2.5, 24/5 and 44/10) in the carotid body, after 30 min of incubation.

Addition of 10 μM KH7 did not change single fiber chemoafferent frequency recorded in normocapnic or in acidic hypercapnic conditions, even after 30 minutes of exposure (n=5, **Fig. 10A-B**). Accordingly, this absence of an effect was associated with no change in the calculated CO_2 sensitivity (n=5, **Fig,10C**).Therefore, despite sAC inhibition attenuating cAMP generation in normocapnia, this did not translate in functional inhibition of CB chemoafferent discharge frequency. These data also point toward sAC dependent cAMP production not being central to the acidic hypercapnic stimulus excitation coupling in the CB.

Inhibition of tmAC was targeret using SQ 22536 (200 μM). Previous experiments had showed that SQ 22536 inhibits tmAC to the same extent as did 2'5'-ddADO (100 μM; 59.6± 10.5% inhibitory effect induced by SQ 22536, n=6,versus 63.0± 3.5% inhibitory effect of 2'5'-ddADO, n=3, in the CB). Addition of SQ 22536 elicited an acute and marked reduction in single fiber discharge frequency under basal normocapnic conditions and depleted the absolute response to acidic hypercapnia (n=7, **Fig. 10D-E**). The calculated CO2 sensitivity was also determined as being significantly attenuated in the presence of SQ 22536 (n=6, **Fig.10F**). Is it suggested therefore that cAMP generation through tmAC activity has an important role in mediating basal CB activity in normocapnia and in regulating the functional response of the CB to acidic hypercapnia.

Effect of tmAC on the regulation of sAC gene expression

Since sAC inhibition did not block cAMP levels during isohydric hypercapnia, we investigated whether cAMP produced by tmAC contributes to the regulation of sAC gene expression. We observed that, in normocapnic conditions, FSK (100 μM) increased sAC gene expression in CB (n=4) by 144%, supporting that sAC expression is dependent on tmAC activity.

Discussion

The present results show that both sAC and tmAC contribute to the accumulation of cAMP in hypocapnia and normocapnia, with cAMP levels derived from tmAC being greater than those generated by sAC. Isohydric hypercapnia did not change sAC and tmAC activity, consistent with no change in observed cAMP levels, PKA activity or discharge frequency. Furthermore, our results demonstrate that for the CB discharge frequency to increase with CO_2, it needs to be associated with a concurrent fall in pHi.

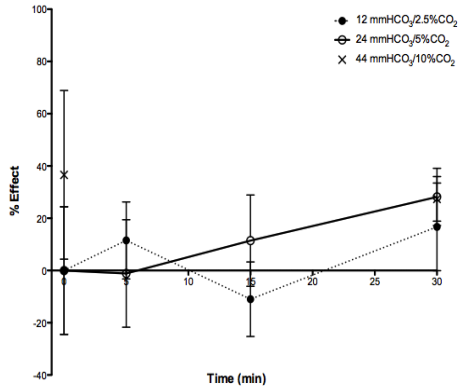

Figure 8- Effect of different concentrations of HCO_3/CO_2 (mM/%: 12/2.5, 24/5 and 44/10) on the levels of cAMP in the carotid body during 5-30 minutes of incubation, in the absence of AC inhibitors. The cAMP levels formed under 0 mM HCO3/0%CO2 during the different incubation times (0-30 min) were subtracted from the cAMP accumulated under 12/2.5, 24/5 and 44/10 mM/%.

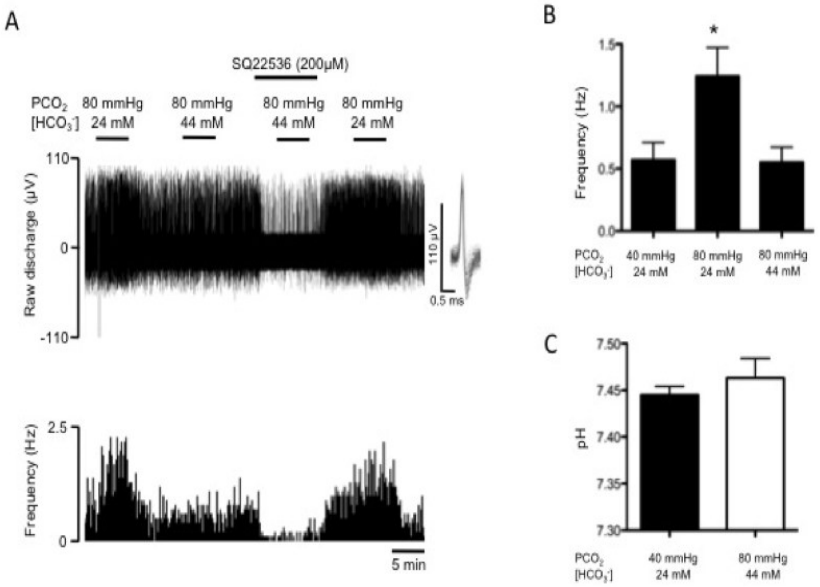

Figure 9- Acidic hypercapnia but not isohydric hypercapnia induces chemoafferent stimulation. **A)** An example extracellular recording showing raw carotid sinus nerve discharge (upper trace) and frequency interval histograms (lower trace) in 10s groups, recorded in control normocapnia, isohydric hypercapnia and acidic hypercapnia. The absence of a response in isohydric hypercapnic conditions was also apparent in the presence of the tmAC inhibitor SQ 22536. Overdraw action potentials are shown inset to demonstate the single fiber discrimination used to obtain the frequency histograms. B) Mean frequencies measured in normocapnia, acidic hypercapnia and isohydric hypercapnia. C) Concurrent increases in PCO2 (40-80 mmHg) and [HCO3] (24-44 mM) did not significantly alter the superfusate pH. Data presented is from 6 fibers from 3 animals for electrophysiology and pH measurments were analysed from superfusates from 3 independent experiments. Error bars indicate mean ± SEM. * denotes P< o.o5 compared with normocapnic frequency, paired students t-test.

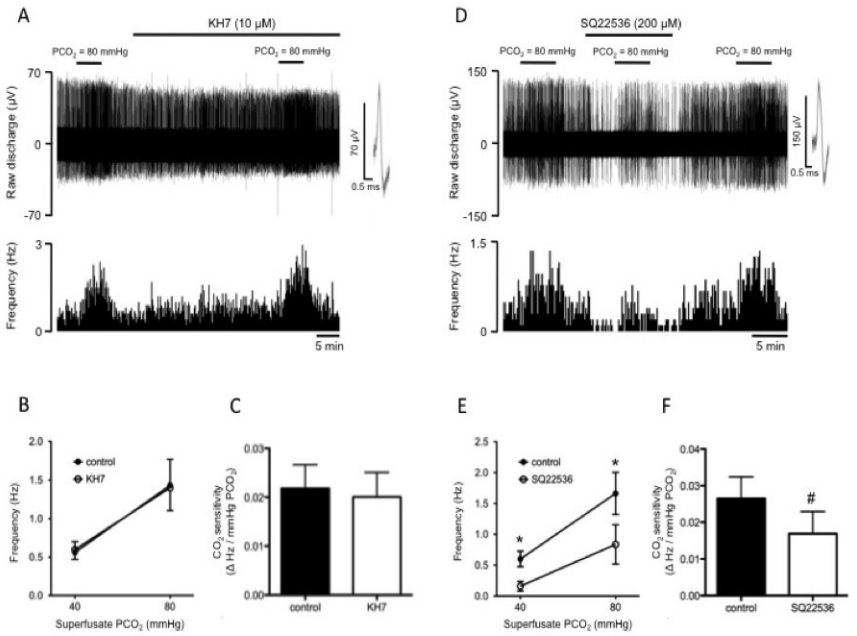

Figure 10- tmAC but not sAC modulates the basal normocapnic carotid body chemoafferent discharge frequency and the response to acidic hypercapnia. A) An example trace showing raw chemoafferent discharge (upper) and frequency interval histograms in 10s groups (lower) in normocapnia and acidic hypercapnia in the presence and absence of sAC inhibitor KH7. B) Grouped absolute frequencies measured in normocapnia and acidic hypercapnia in the presence and absence of KH7. C) Calculated CO_2 sensitivity plots for control and KH7 determined by taking the difference in frequency per mmHg PCO2. D) Example trace showing the raw chemoafferent discharge (upper) and frequency interval histograms in 10s groups (lower) in normocapnia and acidic hypercapnia in the presence or absence of tmAC inhbitor SQ 22536. E) As in B but in the presence and absence of the tmAC inhibitor S!22536. F) As in C) but CO_2 sensitivity was calculated for control and in the presence of SQ 22536. Data presented is from 5 fibers from 4 animals for KH7 and 7 fibers from 4 animals for SQ22536. Error bars indicate mean ±SEM. * denotes $P<0.05$ compared with control frequency, repeated measure ANOVA, Bonferroni pos hoc test, # denotes $P<0.05$ compare with control CO_2 sensitivity.

The CO_2-sensing mechanism in the CB is not fully understood. CO_2, H^+ and HCO_3^- are intimately connected yet the nature of the primary stimuli remains uncertain. Some studies have demonstrated that in the CB this mechanism is mediated via decreasing intracellular pH (pH_i), leading to a membrane depolarization, increasing intracellular calcium levels and neurotransmitter release (Buckler and Vaughan-Jones, 1994). Acidosis can also activate Na^+/H^+ exchange promoting the reversal of Na^{2+}/Ca^{2+} exchange, which results in elevated intracellular calcium concentrations (Rocher *et al.*, 1991). Other studies report that molecular CO_2 (isohydric hypercapnia) is directly involved in the activation of calcium currents leading to an increase of intracellular Ca^{2+} (Summers *et al.*, 2002). Once in the cell, CO_2 is in dynamic equilibrium with HCO_3^-

and pH, through the reaction catalyzed by carbonic anhydrases (Ridderstrale and Hanson, 1984). Thus increases in CO_2 could lead to increases in HCO_3^- that could activate sAC (Chen et al, 2000) and consequently increase cAMP levels.

Our group had previously identified the expression of sAC gene in the CB and suggested a functional role for sAC in this organ since: 1) sAC gene expression levels in the CB were at least 10 times higher than in non-chemoreceptors, except testis, a tissue where high levels of sAC have been observed; 2) sAC mRNA levels in the CB were up-regulated by HCO_3^-/CO_2 and 3) sAC protein was present in the CB (Nunes et al, 2009). Other than the CB, the role of sAC has been described in tissues where changes in HCO_3^-/CO_2 are essential to their function. For instance in the testis, where sAC is highly expressed, sAC mediates sperm maturation and acquisition of motility, in kidneys it regulates recycling of V-ATPse, in airway epithelial cells sAC regulates the ciliary beat frequency, and in corneal endothelium it plays a role in the activation of the cystic fibrosis transmembrane conductance regulator, among others (Chen *et al.*, 2000, Sun *et al.*, 2004, Buck *et al.*, 1999, Hess *et al.*, 2005, Pastor-Soler *et al.*, 2003a, Schmid *et al.*, 2007). The role of sAC in CO_2 sensing has never been studied in the CB chemoreceptors.

cAMP levels can also be synthesized by tmAC. Recently, it was demonstrated tmAC activity is modulated by CO_2 (Townsend *et al.,* 2009). Since it was been suggested that, in the CB, cAMP levels increase in response to acidic and isohydric hypercapnia (Perez-Garcia *et al*., 1990; Summers *et al.*, 2002), it was of interest to understand the role of tmAC and sAC in the CO_2 sensing mechanism of the CB.

We characterized for the first time the nine tmAC isoforms (tmAC1-9) in the CB and PG. Differences in the tissue distribution of the different isoforms were observed with a predominance of tmAC vs sAC in both tissues. The information available in literature is not sufficient to allow a correlation between AC mRNA profiles and specific G-proteins and consequently specific G-protein coupled receptors. Dopamine D2 and muscarinic M2 receptors, which inhibit tmAC have been identified in both PG and CB (Gonzalez *et al.*, 1994, Alcayaga *et al.*, 1999, Bairam *et al.*, 2006). Adenosine A2 receptors and β-receptors, which are positively coupled to tmAC, are described in the CB (Gonzalez *et al.*, 1994, Gauda,

2002). While β-adrenergic and D2 dopamine receptors in heart and striatum are coupled to AC5 (Chern, 2000, Sadana and Dessauer, 2009), in the CB and PG these receptors would have to be coupled to a different tmAC isoform because we here demontrate that AC5 is not expressed in the PG and CB.

Although tmAC and sAC were expressed and functional in the CB, the results presented here suggested that the increases in cAMP levels in response to isohydric hypercapnia described by others (Summers et al, 2002), could not be directly attributed to increases in sAC and tmAC activity mediated by CO_2. sAC and tmAC inhibitors did not alter cAMP levels between normocapnia and isohydric hypercapnia. Also, in the absence of adenylyl cyclase inhibitors, cAMP levels did not increase in response to hypercapnic concentrations either after 5 or 30 min of incubation. PKA activity did not change with isohydric hypercapnia. These results were not dependent on decreases in intracellular pH with CO_2 since we designed our experiments to maintain the extracellular pH constant at 7.4 in all solutions and confirmed that exposure to different concentrations of HCO_3^-/CO_2 did not modify intracellular pH. It is known that when extracellular pH remains constant minimal changes are observed in pH_i of type I cells; when PCO_2 increases, pH_i transiently decreases and then rapidly equilibrates to the extracellular pH (Buckler *et al.*, 1991).

Hornbein and Roos (1963) reported that bicarbonate and CO_2 do not appear to affect pH_i in Type 1 cells (Wilding *et al.*, 1992). Furthermore, pH varying from 7.0 to 8.0 does not alter sAC mRNA expression (Sun *et al.*, 2004). sAC enzyme activity is also *independent* of pH_i (Chen *et al.*, 2000). Perez-Garcia *et al*. (1990) described that increases in cAMP levels mediated by CO_2 were associated with decreases in intracellular pH. In the present work, we also observed that a fall in pHi is essential for CSN discharge to increase in response to elevated CO_2. We observed that tmAC tmAC-derived cAMP may be necessary but not essential to establish normal basal CSN activity and the increase in frequency observed in acidic hypercapnia.

Although sAC and tmAC do not play a role in the detection of isohydric hypercapnia, we demonstrated that these enzymes seem to be important in the adaptation of hypocapnia to normocapnia, with an eventual saturation of the enzyme in normocapnia.

All together we propose that in hypocapnia and normocapnia there is a dependence on cAMP levels derived from

sAC. In normocapnia this cAMP-dependence does not translate into basal chemoafferent discharge. tmAC induce an increase in cAMP accumulation much greater and important in the generation of basal chemodischarge than sAC. For future experiments it will be necessary to acess the role of these enzymes in the response to hypocapnia in chemoafferent discharge. Isohydric hypercapnic causes no change in sAC or tmAC activity, which translates into no change in cAMP, PKA or discharge frequency. For the frequency to increase with CO_2 it needs to be associated with a fall in pH. This increase in discharge is dependent on tmAC-derived cAMP. Thus, acid sensing leads to calcium dependent neurotransmitter release followed by K^+ channel inhibition to cause autocrine activation of GPCR and further activation of tmAC.

The interpretation of our data is limited by several factors that deserve discussion. First, we quantified mRNA levels, pH_i and cAMP amounts in the whole CB, which preserves cell-cell interactions but does not enable determination of the specific contribution of chemo and non-chemosensitive units within the CB. However, the results obtained measuring PKA activity using FRET based reporters in isolated type I cells were consistent with those in the whole CB. Second, high levels of sAC mRNA expression in the CB did not distinguish between the two sAC isoforms, truncated and full length, and thus we are not able to identify whether the increases in sAC gene expression correspond to the truncated active isoform. Third, we used 44mM HCO_3^-/10%CO_2 as a hypercapnic condition, and since this lies outside the physiologically relevant range, we can not exclude the possibility that the HCO_3/CO_2 transport mechanism could be saturated or that the HCO_3/CO_2 sensor may no longer be sensitive to such supra-shysiological conditions. Moreover, the different tmAC inhibitors used in this work allowed us to conclude that MDL-12,330 is not a good pharmacological tool to be used in experiments aimed to distinguish between tmAC and sAC activity. The effects of MDL-12,330A (500μM) on cAMP levels and PKA activity seemed to not be selective for tmAC and 100μM of this inhibitor abolished completely the CSN discharge. Furthermore, KH7, a selective sAC inhibitor does precipitate at concentrations higher than 50μM (Tresguerres et al, 2009), however, our results suggest that concentrations higher than 10 μM may not be selective for sAC in the CB.

While these are limitations to our study design, we believe that our through approach of examining the contribution of sAC and tmAC on PCO2 transduction at multiple levels (mRNA, PKA regulation, cAMP production and integrated chemodischarge) using robust pharmacological and novel (FRET) approaches has contributed to our understanding of this basic signalling pathway in carotid chemoreceptors. Taken together our findings, and based in similar data on O_2 sensing at the CB where highest levels of cAMP were observed in normoxic conditions (physiological conditions, Monteiro *et al.*, 2011), and in this work, where sAC mRNA was up-regulated by tmAC-induced cAMP production, we postulated that sAC and tmAC cooperate to maintain adequate cAMP levels in physiological conditions.

In conclusion, we have shown that sAC and tmAC are active in the CB and postulate that they co-operate to maintain adequate cAMP levels in physiological conditions. In addition, we support the notion that a functional response to CO_2 requires a decrease in pHi, and show, for the first tme, that this transduction mechanism is dependent upon tmAC-derived cAMP.

Acknowledgments

AR Nunes was supported by Science and Technology Foundation Fellowship (FCT, SFRH/BD/ 39473/2007). This work was also financially supported by R01 HL 072748 (EBG) and R01 DK073368 (JZ). The authors would like to thank Dr. Yang K. Xiang for supplying the adenoviruses expressing the AKAR3 for FRET experiments. We would like to thank Kim Insook for her help and time to discuss protocols about dissociation and identification of type I cells.

References

Alcayaga, J, Varas, R, Arroyo, J, Iturriaga, R & Zapata, P (1999). Dopamine modulates carotid nerve responses induced by acetylcholine on the cat petrosal ganglion in vitro. *Brain Res* **831**: 97-103.

Allen, MD, Zhang, J (2006). Subcellular dynamics of protein kinase A activity visualized by FRET-based reporters. *Biochem Biophys Res Commun* **348**: 716-21.

Bairam, A, Joseph, V, Lajeunesse, Y & Kinkead, R (2006). Developmental pattern of M1 and M2 muscarinic gene expression and receptor levels in cat carotid body, petrosal and superior cervical ganglion. *Neuroscience* **139**: 711-21.

Batuca, JR, Monteiro, TC & Monteiro, EC (2003). Contribution of dopamine D2 receptors for the cAMP levels at the carotid body. *Adv Exp Med Biol* **536**: 367-73.

Braun, T, Dods, RF (1975). Development of a Mn-2+-sensitive, "soluble" adenylate cyclase in rat testis. *Proc Natl Acad Sci U S A* **72**: 1097-101.

Buck, J, Sinclair, ML, Schapal, L, Cann, MJ & Levin, LR (1999). Cytosolic adenylyl cyclase defines a unique signaling molecule in mammals. *Proc Natl Acad Sci U S A* **96**: 79-84.

Buckler, KJ, Vaughan-Jones, RD (1994). Effects of hypercapnia on membrane potential and intracellular

calcium in rat carotid body type I cells. *J Physiol* **478 (Pt 1)**: 157-71.

Buckler, KJ, Vaughan-Jones, RD, Peers, C & Nye, PC (1991). Intracellular pH and its regulation in isolated type I carotid body cells of the neonatal rat. *J Physiol* **436**: 107-29.

Carroll JL, Boyle KM, Wasicko MJ, Sterni LM(2005). Dopamine D2 receptor modulation of carotid body type 1 cell intracellular calcium in developing rats. *Am J Physiol Lung Cell Mol Physiol* **288**(5): L910-6.

Chang, LC, Wang, CJ, Lin, YL & Wang, JP (2003). Expression of adenylyl cyclase isoforms in neutrophils. *Biochim Biophys Acta* **1640**: 53-60.

Chen, Y, Cann, MJ, Litvin, TN, Iourgenko, V, Sinclair, ML, Levin, LR*, et al.* (2000). Soluble adenylyl cyclase as an evolutionarily conserved bicarbonate sensor. *Science* **289**: 625-8.

Chern, Y (2000). Regulation of adenylyl cyclase in the central nervous system. *Cell Signal* **12**: 195-204.

Cook ZC, Gray MA and Cann MJ (2012). Elevated carbon dioxide blunts mammalian cAMP signalling dependent on inositol 1,4,5-triphosphate receptor-mediator Ca^{2+} release. *J Biol CHem* 287, 26291-301.

Delpiano, MA, Acker, H (1991). Hypoxia increases the cyclic AMP content of the cat carotid body in vitro. *J Neurochem* **57**: 291-7.

Fitzgerald, RS, Parks, DC (1971). Effect of hypoxia on carotid chemoreceptor response to carbon dioxide in cats. *Respir Physiol* **12**: 218-29.

Forster, HV, Smith, CA (2010). Contributions of central and peripheral chemoreceptors to the ventilatory response to CO2/H+. *J Appl Physiol* **108**: 989-94.

Gauda, EB (2002). Gene expression in peripheral arterial chemoreceptors. *Microsc Res Tech* **59**: 153-67.

Gonzalez, C, Almaraz, L, Obeso, A & Rigual, R (1994). Carotid body chemoreceptors: from natural stimuli to sensory discharges. *Physiol Rev* **74**: 829-98.

Guellaen G, Mahu JL, Mavier P, Berthelot P, Hanoune J (1977). RMI 12330A, an inhibitor of adenylate cyclase in rat liver. *Biochim Biophys Acta*. **484**(2):465-75.

Halls M and Cooper DM (2011). Regulation by Ca 2+ signalling pathways of adenylyl cyclases. *Cold Spring Harb Perspect Bio*l, 3, a004143.

Hess, KC, Jones, BH, Marquez, B, Chen, Y, Ord, TS, Kamenetsky, M*, et al.* (2005). The "soluble" adenylyl cyclase in sperm mediates multiple signaling events required for fertilization. *Dev Cell* **9**: 249-59.

Huckstepp RT, id Bihi R, Eason R, Spyer KM, Dicke N, Willecke K, Marina N, Gourine AV and Dale N (2010). Connexin hemichannel-mediated CO2 – dependent release of ATP in the medulla oblongata contributes to central respiratory chemosensitivity. *J Physio*l 588, 3901-3920.

Iturriaga, R, Rumsey, WL, Lahiri, S, Spergel, D & Wilson, DF (1992). Intracellular pH and oxygen chemoreception in the cat carotid body in vitro. *J Appl Physiol* **72**: 2259-66.

Kamenetsky, M, Middelhaufe, S, Bank, EM, Levin, LR, Buck, J & Steegborn, C (2006). Molecular details of cAMP generation in mammalian cells: a tale of two systems. *J Mol Biol* **362**: 623-39.

Karege F, Lambercy C, Schwald M, Steimer T, Cisse M (2001). Differential changes of cAMP-dependent protein kinase activity and 3H-cAMP binding sites in rat hippocampus during maturation and aging. *Neurosci Lett*. **315**(1-2):89-92.

Kholwadwala, D, Donnelly, DF (1992). Maturation of carotid chemoreceptor sensitivity to hypoxia: in vitro studies in the newborn rat. *J Physiol* **453**: 461-73.

Kim I, Yang DJ, Donnelly DF, Carroll JL (2009). Fluoresceinated peanut agglutinin (PNA) is a marker for live O(2) sensing glomus cells in rat carotid body. *Adv Exp Med Biol*, **648**:185-90

Lahiri, S, Roy, A, Baby, SM, Hoshi, T, Semenza, GL & Prabhakar, NR (2006). Oxygen sensing in the body. *Prog Biophys Mol Biol* **91**: 249-86.

Lugnier, C (2006). Cyclic nucleotide phosphodiesterase (PDE) superfamily: a new target for the development of specific therapeutic agents. *Pharmacol Ther* **109**: 366-98.

Monteiro, TC, Batuca, JR, Obeso, A, Gonzalez, C & Monteiro, EC (2011). Carotid body function in aged rats: responses to hypoxia, ischemia, dopamine, and adenosine. *Age (Dordr)* **33**: 337-50.

Nunes, AR, Monteiro, EC, Johnson, SM & Gauda, EB (2009). Bicarbonate-regulated soluble adenylyl cyclase (sAC) mRNA expression and activity in peripheral chemoreceptors. *Adv Exp Med Biol* **648**: 235-41.

Pastor-Soler, N, Beaulieu, V, Litvin, TN, Da Silva, N, Chen, Y, Brown, D*, et al.* (2003). Bicarbonate-regulated adenylyl cyclase (sAC) is a sensor that

regulates pH-dependent V-ATPase recycling. *J Biol Chem* **278**: 49523-9.

Perez-Garcia, MT, Almaraz, L & Gonzalez, C (1990). Effects of different types of stimulation on cyclic AMP content in the rabbit carotid body: functional significance. *J Neurochem* **55**: 1287-93.

Pepper DR, Landauer RC, Kumar P (1995). Postnatal development of CO2-O2 interaction in the rat carotid body in vitro. *J Physiol* **485**:531-41.

Pfaffl, MW (2001). A new mathematical model for relative quantification in real-time RT-PCR. *Nucleic Acids Res* **29**: e45.

Ramos LS, Zippin JH, Kamenetsky M, Buck J, Levin LR (2008). Glucose and GLP-1 stimulate cAMP production via distinct adenylyl cyclises in INS-1E insulinoma cells. *J Gen Physiol* **132**(3):329-38.

Ridderstrale Y and Hanson MA (1984). Histochemical localization of carbonic anhydrase in the cat carotid body. *Ann N Y Acad Sci*, 429, 398-400.

Rocher, A, Obeso, A, Gonzalez, C & Herreros, B (1991). Ionic mechanisms for the transduction of acidic stimuli in rabbit carotid body glomus cells. *J Physiol* **433**: 533-48.

Rocher, A, Caceres AL, Almaraz L, Gonzalez C (2009). EPAC signalling pathways are involved in low PO2 chemoreception in carotid body chemoreceptor cells. *J Physiol* **587**:4015-27.

Sadana, R, Dessauer, CW (2009). Physiological roles for G protein-regulated adenylyl cyclase isoforms: insights from knockout and overexpression studies. *Neurosignals* **17**: 5-22.

Schmid, A, Sutto, Z, Nlend, MC, Horvath, G, Schmid, N, Buck, J, *et al.* (2007). Soluble adenylyl cyclase is localized to cilia and contributes to ciliary beat frequency regulation via production of cAMP. *J Gen Physiol* **130**: 99-109.

Sinclair, ML, Wang, XY, Mattia, M, Conti, M, Buck, J, Wolgemuth, DJ, *et al.* (2000). Specific expression of soluble adenylyl cyclase in male germ cells. *Mol Reprod Dev* **56**: 6-11, 2-M.

Summers, BA, Overholt, JL & Prabhakar, NR (2002). CO(2) and pH independently modulate L-type Ca(2+) current in rabbit carotid body glomus cells. *J Neurophysiol* **88**: 604-12.

Sun, XC, Cui, M & Bonanno, JA (2004). HCO3-]-regulated expression and activity of soluble adenylyl cyclase in corneal endothelial and Calu-3 cells. *BMC Physiol* **4**: 8.

Thomas JA, Buchsbaum RM, Zimniack A and Racker A (1976). Intracellular pH measurements in Ehrlich ascites tumor cells utilizing spectroscopic probes generated in situ. *Biochemistry* **18**: 2210-18.

Townsend PD, Holliday PM, Fenyk S, Hess KC, Gray MA, Hodgson DR and Cann MJ (2009). Stimulation of mammalian G-protein-responsive adenylyl cyclases by carbon dioxide. *J Biol Chem*, 284, 784-91.

Tresguerres, M, Parks, SK, Salazar, E, Levin, LR, Goss, GG & Buck, J (2010). Bicarbonate-sensing soluble adenylyl cyclase is an essential sensor for acid/base homeostasis. *Proc Natl Acad Sci U S A* **107**: 442-7.

Wang, GP, Xu, CS (2010). Reference gene selection for real-time RT-PCR in eight kinds of rat regenerating hepatic cells. *Mol Biotechnol* **46**: 49-57.

Wang WJ, Cheng GF, Yoshizaki K, Dinger B. and Fidone S (1991). The role of cyclic AMP in chemoreception in the rabbit carotid body. *Brain Research* **540**:96-104.

Wilding, TJ, Cheng, B & Roos, A (1992). pH regulation in adult rat carotid body glomus cells. Importance of extracellular pH, sodium, and potassium. *J Gen Physiol* **100**: 593-608

RESEARCH PAPER

BICARBONATE-SENSITIVE SOLUBLE AND TRANSMEMBRANE ADENYLYL CYCLASES IN CENTRAL CO_2 CHEMORECEPTORS – A COMPARATIVE STUDY WITH THE CAROTID BODY

A R Nunes[1,2], E C Monteiro[2], E B Gauda[1*]

[1]Pediatrics, Johns Hopkins Medical Institutions, Baltimore, MD; [2]CEDOC, Pharmacology, Faculdade de Ciências Médicas, Universidade Nova de Lisboa, Portugal

Background and purpose: Changes in cAMP levels have been associated with the CO_2-sensing chemotransduction mechanism of the mammalian chemoreceptors. Two types of adenylyl cyclase (AC) are responsible for the production of cAMP: a soluble AC (sAC) activated by bicarbonate (HCO_3^-) /CO_2 and a transmembrane AC (tmAC) regulated by neurotransmitters/hormones. In the carotid body (CB), these enzymes are both expressed and functional but do not play a role in response to isohydric hypercapnia (Nunes et al, in submittion). The CB is sensitive to changes in CO_2 but the main CO_2 sensors in the organism are the central chemoreceptors. Thus this work aims to determine if there are differences in the expression and activity of these enzymes between peripheral and central chemoreceptors. **Experimental approach**: We assayed for changes in sAC expression (RT-qPCR) in central chemoreceptors (locus coeruelus, ventrolateral medulla and raphe nucleus) and CB and investigated if changes in HCO_3^-/CO_2 up-regulated sAC gene expression in the central chemoreceptors. We compared the expression of sAC and the 9 isoforms of the tmAC in the locus coeruleus and compared the effect of these enzymes on the cAMP levels (quantified by EIA), in the presence and absence of activators or inhibitors of sAC and tmAC. **Key Results**: sAC is expressed in central chemoreceptos, but in lower levels than in the CB. sAC mRNA and cAMP levels in the locus coeruleus augmented in response to increases in HCO_3^-/CO_2 from 0/0% to normocapnia (24/5%). In this tissue, higher concentrations of HCO_3^-/CO_2 had no additional effect on cAMP levels. While in the CB we had previously observed that tmAC
contribute greater to cAMP accumulation than sAC, in both normocapnic and hypercapnic conditions (Nunes et al in submission), in the locus coeruleus tmAC had little effect in

cAMP accumulation in hypercapnic conditions. However, the expression of the 9 tmAC isoforms, except tmAC5 and 7, were higher than sAC mRNA in LC.

Conclusions and Implications: sAC is ubiquitously expressed and functional in central chemoreceptors, and as demonstrated previously in the CB, it does not seem to play a role in response to hypercapnia conditions.

Keywords: cAMP, cyclic adenosine monophosphate; CB, carotid body; sAC, soluble adenylyl cyclase; tmAC, transmembrane adenylate cyclase; peripheral arterial chemoreceptors; central chemoreceptors; HCO_3^-/CO_2, bicarbonate/ CO_2.

***Correspondence author:** Estelle B. Gauda, M.D., Department of Pediatrics, Division of Neonatology, Johns Hopkins Medical University, 600 N. Wolfe Street, CMSC 6-104, Baltimore, MD 21287-3200 USA**,** egauda@mail.jhmi.edu

Running title: sAC and tmAC in CO_2 chemoreceptors.

Introduction

The central chemoreceptors located in the brainstem are the major CO_2/pH sensors of the mammalian organism. Central chemosensitive cells are dispersed within distinct regions of the brainstem (reviewed by (Nattie, 1999)) including the locus coeruleus (LC), the retrotrapezoid nucleus, the ventrolateral medulla (VLM), and the medullary raphe (RN) (Filosa *et al.*, 2002, Guyenet *et al.*, 2005, Richerson, 1995, Schlaefke *et al.*, 1970, Wang *et al.*, 2002).

There is evidence suggesting that the central sensitivity to CO_2/pH is modulated by peripheral chemoreceptors (for a review see Forster and Smith, 2010).

As cAMP levels have been associated with the chemotransduction mechanism of the CB, we have recently investigated the effect of isohydric hypercapnia in the activity of HCO_3^-/CO_2 responsive-soluble adenylyl cyclase and neurotransmitter responsive-transmembrane adenylyl cyclase (Nunes et al, in submission). A particular role of these enzymes in the response to isohydric hypercapnia in the CB was discarded (Nunes et al, in submittion).

Since central chemoreceptors contribute apparently more to CO_2 sensitivity than CB, we hypothesized that tmAC and sAC could be more relevant in CO_2-sensing in the central chemoreceptors than in the CB.

Thus, this work aims to investigate the relative contribution of sAC and tmAC in response to isohydric

hypercapnia in central chemoreceptors, namely in the locus coeruleus (LC), a central chemoreceptor that is apparently more sensitive to CO_2 than changes in pH (Filosa, 2003).

Materials and Methods

Surgical procedures

The Animal Care and Use Committee at the Johns Hopkins University School of Medicine approved all experimental protocols. CB and central chemoreceptors tissues, were isolated from Sprague-Dawley rats (SD, Charles River Laboratories, Wilmington, MA) of both sexes at postnatal days (P) 16 and 17. Central chemoreceptor tissues used in the present work included: LC, RN and VLM. The non-chemoreceptor tissues included the cortex.

Prior to tissue removal or dissection, the animals were anesthetized briefly with isoflurane and immediately decapitated. The CB was dissected as described in Nunes et al (in submission). Briefly, the carotid bifurcation including the CB, SCG and the NG/PG complex was removed en bloc and tissues were isolated and cleaned of surrounded connective tissue. The brainstem was removed *en bloc* and micro-dissected to obtain midline medullary RN, as previously described (Wang *et al.*, 1998). The micro-dissected region captured the raphé pallidus, raphé magnus, a segment of the raphé obscurus, and tissue immediately adjacent to these nuclei. Similarly, the VLM was micro-dissected using a slightly modified approach, as described by Johnson and co-workers (Johnson *et al.*, 2008, Johnson *et al.*, 2001). The brainstem was sliced manually in ~500 μm increments with a micro-knife to capture a transverse slice containing the VLM. Tissue samples were taken from a slice where the inferior olive, midline raphé, pyramids, and semi-compact division of nucleus ambiguous were visualized and used as identifying landmarks. Finally, LC samples were obtained from pontine slices at the level of the 4th ventricle and the tract of 7th cranial nerve. The LC and adjacent tissue was bilaterally excised from the slice.

sAC and tmAC mRNA gene expression

In one set of experiments, we compared sAC mRNA expression levels present in the central chemo- (VLM, RN and LC) and non-chemoreceptors (cortex) with the levels present in the CB. In another set of experiments we compared mRNA expression levels between sAC and the nine isoforms of tmAC in the LC. For both sets of experiments, the different

tissues were isolated as mentioned in surgical procedure (4 rats per condition; n=3 independent experiments), cleaned from surrounded tissue and quick-frozen on dry ice and stored at -80ºC.

To study the effect of HCO_3^-/CO_2 in the regulation of sAC gene expression, LC, VLM, RN and cortex were isolated and treated as described in Nunes et al (in submission). The tissues were pre-incubated in Krebs modified solution containing (in mM): NaCl 135; KCl 5; $CaCl_2$ 2; $MgCl_2$ 1.1; HEPES 10; glucose 5.5, pH 7.40 (Perez-Garcia *et al.*, 1990) without HCO_3^- and equilibrated with $0\%CO_2/60\%O_2$. After 30 minutes, we replaced the pre-incubation buffer with incubation buffer containing one of the following HCO_3^-/CO_2 concentrations: 1) 0 mM HCO_3^-/0% CO_2/60% O_2, 2) 24 mM HCO_3^-/5% CO_2/60% O_2, and 3) 44 mM HCO_3^-/10% CO_2/60% O_2 for 1 hour at 37ºC, pH 7.4. We modified the incubation buffer by changing CO_2 and HCO_3^- concentrations, adjusting the osmolarity with NaCl. This approach allows the assessment of CO_2 effect, preventing major changes in pH. Tissues were pooled from 4 animals from the same litter and the experiments were repeated 3 or more times using animals from different litters.

In a separate set of experiments, we also investigated the effect of forskolin (FSK), a tmAC activator, in the regulation of sAC gene expression in LC and cortex. The tissues were pre-incubated in Krebs modified solution containing 24 mM $NaHCO_3$ equilibrated with $5\%CO_2/60\%O_2$. After 30 minutes, we replaced the pre-incubation buffer with incubation buffer containing 24 mM $NaHCO_3$ and FSK (100 µM), for 1 hour at 37ºC, pH 7.4.

Tissues were quick-frozen on dry ice and stored at -80ºC until further processing for RT-qPCR, as outlined below.

Quantitative Real time – PCR

Tissues used to study sAC and tmAC mRNA gene expression and regulation levels were processed to obtain total RNA (Micro-to-Midi Total RNA Purification, Invitrogen, Carlsbad, CA) according to the manufacturer's instructions. DNase treatment (PureLink DNase, Invitrogen) was performed to avoid genomic DNA contamination. RNA yield and quality was measured at 260 and 280 nm by conventional UV spectrophotometer (Beckman Du 530). Total RNA (about 1 µg) was used for first-strand cDNA synthesis using an iSCRIPt cDNA synthesis kit (Bio-Rad Laboratories, Hercules, CA).

The respective primer sequences for each adenylate cyclase isoform used

are shown in Table 2, *General methods - RT-qPCR section* (Pastor-Soler *et al.*, 2003b, Chang *et al.*, 2003). Relative expression of AC genes between the tissues and conditions was standardized with levels of glucose-6-phosphate dehydrogenase (G6PDH) expression, the reference gene. We also validate our results using more two reference genes: glyceraldehyde 3-phosphate dehydrogenase (GAPDH) and Beta-actin (β-actin) (Table 2, *General methods, RT-qPCR section,* Wang and Xu, 2010). We evaluated the expression of the three reference genes in all the studied tissues and conditions using a web site that combined 4 different algorithms used to determine the stability of the reference genes: geNorm, Normfinder, Bestkeeper and comparative ΔCt method (http://www.leonxie.com/referencegene.php?type=reference). We found that GAPDH is the most stable gene across our experiments, but AC gene expression levels normalized with this reference gene showed the same trend of results as shown when normalized with G6PDH.

RT-qPCR was performed with a MyiQ iCycler RT-qPCR system (Bio-Rad) with the SYBR Green detection system. Each qPCR reaction consisted of 1 µl of cDNA and 3.5 µl of 300 nM primers diluted in DEPC-H_2O and 10 µl of SYBR Green Supermix (Bio-Rad) for a final volume of 20 µl. We performed triplicates for each sample. qPCR conditions for sAC gene expression and regulation were: denaturing 8 min at 95°C, followed by 40 cycles at 95°C for 1 min, 60°C for 30 sec, 72°C for 45 sec, and a terminal extension period (72°C, 10 min). qPCR conditions for AC (tmAC and sAC) expression and regulation were: denaturing 5 min at 95°C, followed by 40 cycles at 95°C for 20 sec, 62°C for 20 sec, 72°C for 20 sec, and a terminal extension period (72°C, 10 min). We analyzed the specificity of the RT-qPCR product by performing a melting curve with 0.5°C increments in temperature. Product formation during the exponential phase of the reaction was analyzed for semi-quantification of relative expression in the specific tissues using the Pfaffl method (Pfaffl, 2001) or relative quantification to reference gene based on the threshold cycle (CT) for amplification as $2^{(\Delta CT)}$, where $\Delta C_T = C_{T,reference} - C_{T,target}$.

Effects of HCO_3^-/CO_2 on cAMP levels

To study the effect of different concentrations in HCO_3^-/CO_2 in cAMP levels, as an indirect measurement of sAC activity, we pre-incubated chemosensitive (RN, VLM and LC) and non-chemosensitive (cortex) tissues according

with the protocol described in Nunes et al (in submission). The tissues were incubated in Krebs modified solution without HCO_3^-/CO_2 and in the presence of MDL-12,330A (500 µM), a tmAC inhibitor (Delpiano and Acker, 1991). After 30 minutes, we incubated the tissues in fresh Krebs modified solution in the presence of MDL-12,330A (500 µM), and either 0 mM HCO_3^-/0 % CO_2; 12 mM HCO_3^-/2.5% CO_2; 24 mM HCO_3^-/5% CO_2; or 44 mM HCO_3^-/10 % CO_2 for 30 minutes, pH 7.4, 37°C. All the experiments were conducted in the presence of a non-specific inhibitor for phosphodiesterase (PDE) IBMX (500 µM). Tissues were pooled from 2 animals from the same litter and the experiments were repeated using animals from different litters. Tissues were processed for cAMP extraction and the quantification was done as outlined below.

Contribution of sAC and tmAC to cAMP levels in normocapnia and isohydric hypercapnia

To study the contribution of tmAC and sAC on cAMP accumulation under normocapnia and isohydric hypercapnia, we pre-incubated LC tissues with Krebs modified solution containing 24 mM $NaHCO_3$ and perfused with 60%O_2/5%CO_2 in the absence or in the presence of MDL-12,330A (500 µM) or KH7 (100 µM, a selective sAC inhibitor) or both. After 30 min we incubated the tissues in fresh Krebs modified solution containing either 24mM $NaHCO_3$/60%O_2/5%CO_2 or 44mM $NaHCO_3$/60%O_2/10%CO_2, IBMX (500 µM), in the presence of absence of MDL-12,330A (500 µM), KH7 (100 µM), or both, for 30 min at 37°C.

Cyclic nucleotide extraction and quantification

cAMP was measured as previously reported (Batuca *et al.*, 2003) and briefly described here. We immersed tissues in cold 6% (w/v) trichloroacetic acid (TCA; 600 µl) for 10 minutes, homogenized the tissues at 2 - 8ºC, and centrifuged them at 12,000 g for 10 minutes at 4ºC. The supernatants were washed four times in 3 ml of water saturated with diethyl ether solution (50:50) and then lyophilized. The sample was then stored at -20ºC until cAMP quantification by enzyme immunoassay (EIA, RPN 2255, GE Healthcare Bio-Sciences AB, Piscataway, NJ). Protein pellets were stored at -20°C until measured with the standard Bradford Protein Assay (Bio-RAD). cAMP levels are expressed in femtomoles per microgram of protein (fmol/µg protein).

Data analysis and statistical procedures

The data are represented as mean ± SEM and differences between the experimental groups were determined using statistical software from GraphPad Prism (GraphPad Software Inc., version 4, San Diego, CA) or SPSS (SPSS Inc, version 12, Chicago, IL). Statistical significance was set at $P<0.05$.

Results

sAC mRNA gene expression and regulation

We had previously identified sAC mRNA in the CB and related peripheral non-chemosensitive structures (PG, NG, SCG, Nunes *et al*, 2009). In the present work, we first investigated whether higher levels of expression were specific to the CB or to both peripheral and central CO_2-chemosenstive tissues. We observed that sAC mRNA was expressed ubiquitously in central chemo- (LC, VLM, RN) and non-chemosensitive tissues (cortex). As observed in **Fig.1A**, sAC gene expression levels in the CB were at least 10 times higher than in the central chemo and non-chemoreceptors.

We next explored the effect of different concentrations of HCO_3^-/CO_2 (mM/%: 0/0, 24/5, 44/10) in sAC gene expression in central chemo- and non-chemosensitive tissues. We had previously observed that sAC gene expression was up-regulated by HCO_3^-/CO_2 in the CB (Nunes et al, 2009). Here, we observed that increases from 0 mM HCO_3^-/0%CO_2 to 24 mM HCO_3^-/5%CO_2 up-regulated sAC gene expression in the LC; no significant changes on the level of sAC mRNA gene were observed in RN, VLM and cortex (**Fig.1B**). These results suggested that sAC may be functional in some central chemoreceptors.

Bicarbonate-regulated cAMP levels

We previously reported that sAC is functional in the CB, but not in non-chemosensitive tissues, under concentrations up to 24 mM HCO_3/5%CO_2 (Nunes *et al.*, in submission). In this work we investigated if sAC is functional in central chemoreceptors and whether the results obtained in the central chemoreceptors are similar to those obtained previously in the CB. For these experiments, we explored the effects of different concentrations of HCO_3^-/CO_2 (mM/%: 0/0, 12/2.5, 24/5, and 44/10) on cAMP production in central chemo- and non-chemosensitive tissues.

To differentiate between the activity of tmAC and sAC, we incubated the tissues with MDL-12,330A (500μM) and IBMX (500 μM), a non-specific PDE

inhibitor. Although previous results had shown that MDL-12,330A was able to inhibit about 95% of the cAMP production induced by FSK in the CB (Nunes et al, in submittion), we observed that in the LC, it inhibited only 45.6±9.6% (n=6) (**Fig.2A**). Higher concentrations of MDL-12,330A (1000 µM) did not decrease the amount of cAMP produced in LC (51.3±7.9% of inhibition,n=6).

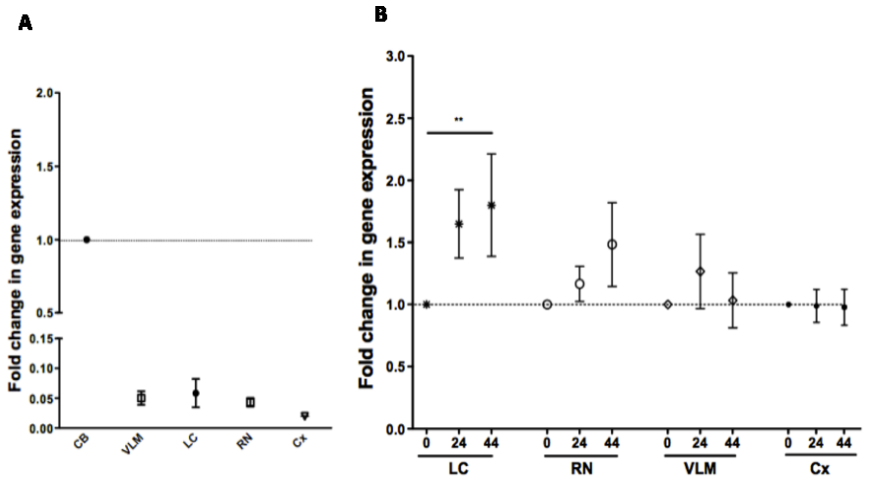

Figure 1- A) sAC mRNA expression in carotid body and central chemoreceptors and non-chemoreceptor tissues. B) Effect of increasing HCO_3^- concentrations on sAC mRNA gene expression in central chemoreceptors and non-chemoreceptor tissues using qRT-PCR. 0, 24, and 44 mM corresponds to 0 mM HCO_3^-/0%CO_2, 24 mM HCO_3^-/5% CO_2, and 44 mM HCO_3^- /10%CO_2, respectively. *CB*, carotid body; *LC*, locus ceruleus; *RN*, raphé nucleus; *VLM*, ventrolateral medulla; *Cx*, cortex. Non Parametric correlation (Spearman) ** p<0.01

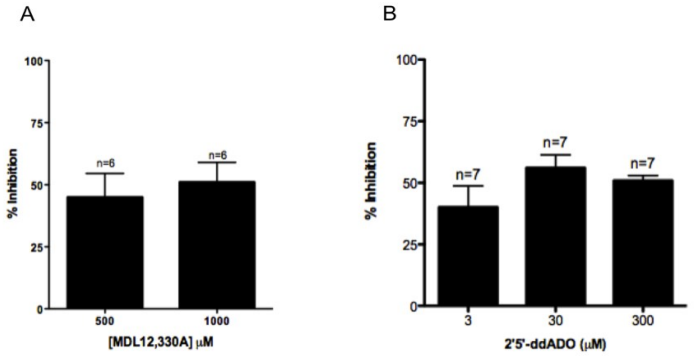

Figure 2- Effect of A) MDL-12,330A (500-1000 µM) and B) 2'5'-ddADO (3-300 µM) on cAMP production induced by forskolin in locus coeruleus (LC).

We also investigated the effect of other specific tmAC inhibitor, 2'5'-ddADO (3-300 μM), on cAMP production in the LC in the presence of FSK (**Fig.2B)**. 2'5'-ddADO (300 μM) was able to inhibit 50.9±2.0% (n=7) of cAMP production induced by FSK in the LC (**Fig.2B**), an effect similar obtained with MDL-12,330A (500 μM). These results either raise concerns about the viability of the LC tissue or suggest a high concentration of α1 and α2-adrenoceptor receptors negatively coupled to tmAC in LC. Considering a viability problem, we would expect a compromised response to different concentrations of HCO_3/CO_2 in this tissue. However, as observed in **Fig.3,** the amount of cAMP was dependent on the concentration of HCO_3^-/CO_2 (0/0,12/2.5,24/5 mM HCO_3^- /%CO_2), not only in the LC, but also in VLM and RN. Higher levels of cAMP were obtained in normocapnia conditions. However, comparing with the results obtained previously in the CB (Nunes et al, in submission), normocapnia induced a lower effect on cAMP levels in the central chemoreceptors (82.0± 14.9 % increase in LC, 69.5± 22.2 % increase in RN and 48.7± 11.6 % increase in VLM, **Fig.3)** than in the CB (158.4 ± 32.7 % increase). Higher concentrations of HCO_3^-/CO_2 (44 mM HCO_3^- /10%CO_2) had no additional effect on cAMP levels in central chemosensitive tissues, an effect also observed previously in the CB (Nunes et al, in submission). In the cortex, higher concentrations of HCO_3^-/CO_2 did not induce changes in cAMP levels (**Fig.3**).

These results suggested to us that when tmAC is blocked, sAC reached a maximal level of activity under physiological conditions, 24 mM HCO_3^- /5%CO_2 (normocapnia conditions) in the CO_2 central chemoreceptors, a result that had been previsouly reported in the CB (Nunes et al, in submission). However, we can not exclude that tmAC may be affecting these responses.

sAC and tmAC (I-IX isoforms) gene expression

We characterized the 9 specific tmAC isoforms in the LC. As observed in **Fig.4**, except for tmAC5 and tmAC7 (PKC-stimulated), the levels of expression for the tmAC isoforms were higher than sAC expression.

Comparing the levels of tmAC isoforms expression in the LC with the ones previously observed for the CB (Nunes et al, in submission), we observed that the levels of expression for tmAC1

(Ca^{2+} and calmodulin stimulated, 0.46±0.09 in CB vs 0.22±0.02 in the LC), tmAC4 (Gβγ stimulated, 0.51±0.09 in CB vs 0.05±0.00 in the LC), and tmAC6 (PKA, PKC and Ca^{2+} inhibited, 0.26±0.06 in CB vs 0.07±0.00 in the LC) were higher in the CB than in the LC, while the levels of tmAC2 (0.03±0.47 in CB vs 0.47±0.07 in the LC, Gβγ and PKC stimulated) were lower. The levels of expression for tmAC3 and tmAC8 (calmodulin- Ca^{2+} stimulated), tmAC5 and tmAC7 (PKC-stimulated), and tmAC9 (Ca^{2+}-inhibited) were not significantly different in the CB and LC. These results suggest that the expression of tmAC isoforms differ between the LC and CB.

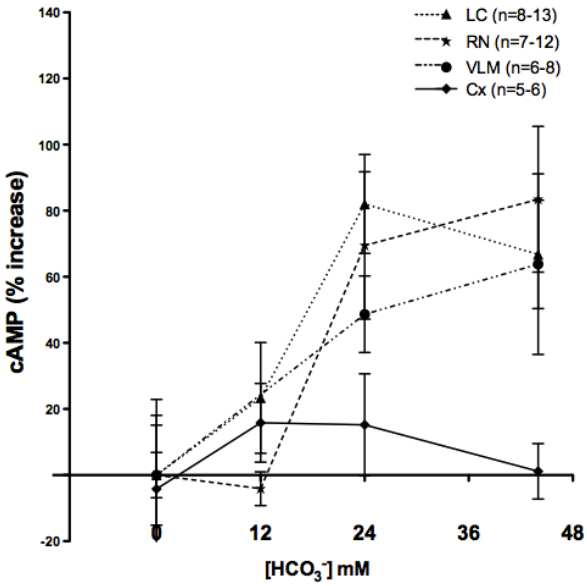

Figure 3- Concentration- response curves of HCO_3^-/%CO_2 for effects on cAMP levels in central chemo- and non-chemosensitive tissues. 0% increase was obtained with 0 mM HCO3/0%CO2: 22.5±3.4 fmol/µg protein (LC, n=13); 18.1±1.2 fmol/µg protein (RN, n=12); 15.1 ±3.9 fmol/µg protein (VLM, n=9); 10.1 ± 2.6 fmol/µg protein (Cx, n=8).

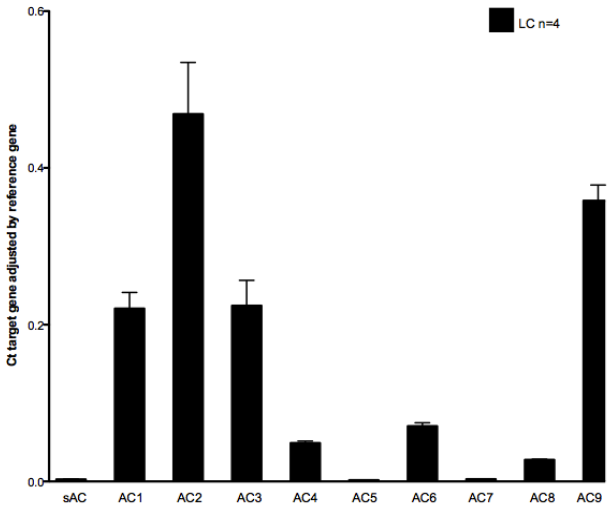

Figure 4 - sAC and tmAC mRNA expression in the carotid body locus coeruleus (LC) using qRT-PCR.

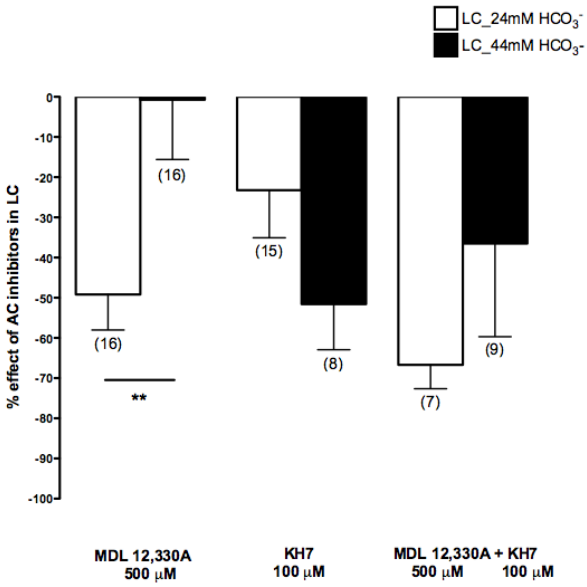

Figure 5- Effect of MDL-12,330A, a tmAC inhibitor and KH7, a sAC inhibitor, on cAMP levels in normocapnia (24mM HCO_3^-/5%CO_2) and hypercapnia (44mM HCO_3^-/10%CO_2) conditions in locus coeruleus (LC). Paired t-test **p<0.01.

Relative contribution of sAC and tmAC to cAMP levels in LC

To compare the levels of cAMP generated by sAC and by tmAC in normocapnia and hypercapnia, we studied the effect of MDL-12,330A (500μM) and/or KH7 (100μM) in cAMP production in LC using an enzyme immunoassay. KH7 (IC_{50}= 3-5 μM) is a specific sAC inhibitor. All the experiments were performed in the presence of IBMX (500μM). We observed that in the LC, the amounts of cAMP induced by hypercapnia decreases significantly from those observed in normocapnia ($p<0.05$, paired t-test, 30.6 ± 1.8 fmol/ug protein, n=16, in normocapnia and 19.9 ±2,5 fmol/ug protein, n=8 in hypercapnia). In normocapnia the ACs were partially blocked by MDL-12,330A and KH7 (66.7 ±5.9%, n=7, **Fig.5**). We have used a higher concentration of MDL (1000μM) but no significant differences on cAMP levels were obtained in the presence of either 500 or 1000μM (p=0.7). In hypercapnia, MDL-12,330A apparently did not affect cAMP production and KH7 inhibited cAMP production in the same magnitude between normocapnia and hypercapnia (p=0.5, paired t test, **Fig.5**). These results suggest that both tmAC and sAC are partially active in the LC in normocapnia but in hypercapnia, tmAC may not be functional.

Effect of tmAC on the regulation of sAC gene expression

We have shown above that changes from 0 mM HCO_3^-/0%CO_2 to 24 mM HCO_3^-/5%CO_2 up regulated sAC in LC. Here, we investigated whether cAMP produced by tmAC contributes to the regulation of sAC gene expression. We had previously observed that FSK up-regulated sAC gene expression by 144% in the CB (Nunes et al, in submission).

In the present work, we observed that in normocapnic conditions, FSK (100 μM) increased sAC gene expression in LC (n=9) by 57 %, respectively, but not in cortex (n=5, **Fig.6**) supporting that sAC expression is dependent on tmAC activity.

Discussion

The present results demonstrate for the first time that soluble AC is expressed in some CO_2 central chemoreceptors and cortex. sAC mRNA was up-regulated with changes in HCO_3/CO_2 from 0mM/0% to 24mM/5% in the LC. In this tissue increases from 0%CO_2 to normocapnic conditions induced an increase in cAMP accumulation but no further increases were observed with isohydric hypercapnia.

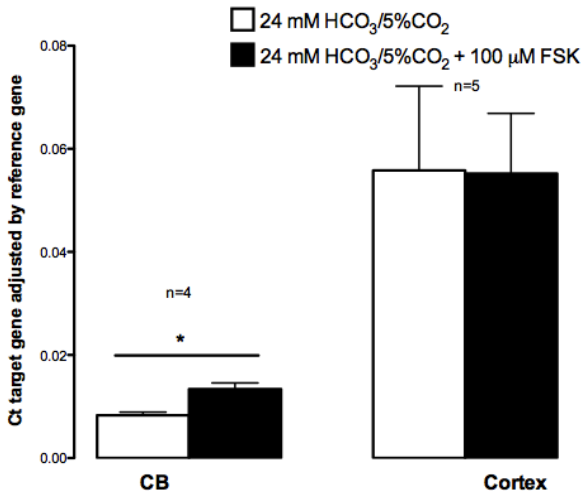

Figure 6 - Effect of foskolin (FSK) on sAC gene expression in locus coeruleus (LC) and cortex. Paired t-test * $p<0.05$.

Our data, together with previous results obtained in the CB (Nunes et al, in submission), suggest that sAC plays a similar role in LC (central) and CB (peripheral chemoreceptors), and thus, it seems not relevant in the response to isohydric hypercapnia.

The central chemoreceptors are found in many regions of the brainstem (VLM, LC, raphe, retrotrapezoid nucleus, PreBotzinger complex, and nucleus tractos solitarius (for a review see (Nattie, 1999)) but their specific location and cellular identity is controversial. Although the present work includes results in LC, VLM and RN regions we deeply explored the LC.

Evidences in literature suggest that VLM and RN could be more sensitive to pH and LC to CO_2, since direct CO_2 activation of central neurons through calcium channels has been shown only for LC (Filosa and Putnam, 2003). The experimental conditions of the present work were aimed to particularly investigate CO_2 sensitivity.

The CO_2 chemosensitivity of these tissues differ with age, which may affect sAC and tmAC function. In our model we used animals at the age of 16-17 days old. LC CO_2 chemosensitivity appears to be well developed at birth but in RN it increases with postnatal development until the second week of life, in parallel with the hypercapnic ventilatory response in vivo (Stunden *et al.*, 2001, Wang and Richerson, 1999). There is no direct link for CO_2 maturation in VLM.

In the CB it has been suggested that CO_2 and O_2 sensitivity increases during the first 2 weeks after birth in the rat (Kholwadwala and Donnelly, 1992, Abu-Shaweesh *et al.*, 1999). Thus, the differences in sAC expression and function observed between the CB and central regions are not likely to be due to differences in chemoreceptor maturation.

Characterization of tmAC isoforms in LC showed differences between LC and the CB. AC1 and AC8 have been demonstrated in the LC (Zachariou *et al.*, 2008), a tissue with predominance of α1 and α2 adrenoreceptors. Although we have identified AC1 and AC8 mRNA in the LC, the most abundant mRNA isoform in the LC was AC2. The information available in literature is not sufficient to allow a correlation between AC mRNA profiles and specific G-proteins and consequently specific G-coupled receptors.

The interpretation of our data is limited by several factors that deserve discussion. First, high levels of sAC mRNA expression in the CB did not distinguish between the two sAC isoforms, truncated and full length, thus we are not able to identify if the increases in sAC gene expression correspond to the truncated active isoform. Second, to distinguish between tmAC and sAC we used MDL-12,330A, a tmAC inhibitor and KH7, a sAC inhibitor. We had recently reported that MDL-12,330A may not be a good pharmacological tool to distinguish between these two enzymes, since cross reactivity was observed in the CB (Nunes et al, in submission). Although we do not exclude cross reactivity, the effect of these inhibitors was additive in normocapnia and hypercapnia. However, more experiments should be performed using more selective inhibitors. Third, we only studied the effects of these inhibitors after 30 min of incubation, excluding acute effects of these enzymes. However, we had previously observed in the CB that the relative contribution of tmAC and sAC is the same at 5 or 30 min of incubation (Nunes et al, in submission).

Moreover, the effects of MDL-12,330A on the cAMP production induced by FSK suggested the presence of adrenoreceptors negatively coupled to tmAC. Future experiments looking at the expression of these receptors should be considered.

In conclusion, we have shown that sAC and tmAC are ubiquitously expressed in central chemoreceptors, and are not relevant to the CO_2 sensing mechanism in isohydric hypercapnia.

Acknowledgments

AR Nunes was supported by Science and Technology Foundation Fellowship (FCT, SFRH/BD/ 39473/2007). This work was also financially supported by R01 HL 072748 (EBG). The authors would like to thank Shree Johnson (Physiology and Biophysics, Howard University College of Medicine, Washington, DC) for teaching dissociation of the central chemoreceptors.

References

Abu-Shaweesh, JM, Dreshaj, IA, Thomas, AJ, Haxhiu, MA, Strohl, KP & Martin, RJ (1999). Changes in respiratory timing induced by hypercapnia in maturing rats. *J Appl Physiol* **87**: 484-90.

Batuca, JR, Monteiro, TC & Monteiro, EC (2003). Contribution of dopamine D2 receptors for the cAMP levels at the carotid body. *Adv Exp Med Biol* **536**: 367-73.

Chang, LC, Wang, CJ, Lin, YL & Wang, JP (2003). Expression of adenylyl cyclase isoforms in neutrophils. *Biochim Biophys Acta* **1640**: 53-60.

Delpiano, MA, Acker, H (1991). Hypoxia increases the cyclic AMP content of the cat carotid body in vitro. *J Neurochem* **57**: 291-7.

Filosa, JA, Dean, JB & Putnam, RW (2002). Role of intracellular and extracellular pH in the chemosensitive response of rat locus coeruleus neurones. *J Physiol* **541**: 493-509.

Filosa, JA, Putnam, RW (2003). Multiple targets of chemosensitive signaling in locus coeruleus neurons: role of K+ and Ca2+ channels. *Am J Physiol Cell Physiol* **284**: C145-55.

Forster, HV, Smith, CA (2010). Contributions of central and peripheral chemoreceptors to the ventilatory response to CO2/H+. *J Appl Physiol* **108**: 989-94.

Gauda, EB (2002). Gene expression in peripheral arterial chemoreceptors. *Microsc Res Tech* **59**: 153-67.

Guyenet, PG, Stornetta, RL, Bayliss, DA & Mulkey, DK (2005). Retrotrapezoid nucleus: a litmus test for the identification of central chemoreceptors. *Exp Physiol* **90**: 247,53; discussion 253-7.

Johnson, SM, Haxhiu, MA & Richerson, GB (2008). GFP-expressing locus ceruleus neurons from Prp57 transgenic mice exhibit CO2/H+ responses in primary cell culture. *J Appl Physiol* **105**: 1301-11.

Johnson, SM, Koshiya, N & Smith, JC (2001). Isolation of the kernel for respiratory rhythm generation in a novel preparation: the pre-Botzinger complex "island". *J Neurophysiol* **85**: 1772-6.

Kholwadwala, D, Donnelly, DF (1992). Maturation of carotid chemoreceptor sensitivity to hypoxia: in vitro studies in the newborn rat. *J Physiol* **453**: 461-73.

Nattie, E (1999). CO2, brainstem chemoreceptors and breathing. *Prog Neurobiol* **59**: 299-331.

Nunes, AR, Monteiro, EC, Johnson, SM & Gauda, EB (2009). Bicarbonate-regulated soluble adenylyl cyclase (sAC) mRNA expression and activity in peripheral chemoreceptors. *Adv Exp Med Biol* **648**: 235-41.

Pastor-Soler, N, Beaulieu, V, Litvin, TN, Da Silva, N, Chen, Y, Brown, D, *et al.* (2003). Bicarbonate-regulated adenylyl cyclase (sAC) is a sensor that regulates pH-dependent V-ATPase recycling. *J Biol Chem* **278**: 49523-9.

Pfaffl, MW (2001). A new mathematical model for relative quantification in real-time RT-PCR. *Nucleic Acids Res* **29**: e45.

Richerson, GB (1995). Response to CO2 of neurons in the rostral ventral medulla in vitro. *J Neurophysiol* **73**: 933-44.

Schlaefke, ME, See, WR & Loeschcke, HH (1970). Ventilatory response to alterations of H+ ion concentration in small areas of the ventral medullary surface. *Respir Physiol* **10**: 198-212.

Stunden, CE, Filosa, JA, Garcia, AJ, Dean, JB & Putnam, RW (2001). Development of in vivo ventilatory and single chemosensitive neuron responses to hypercapnia in rats. *Respir Physiol* **127**: 135-55.

Wang, GP, Xu, CS (2010). Reference gene selection for real-time RT-PCR in eight kinds of rat regenerating hepatic cells. *Mol Biotechnol* **46**: 49-57.

Wang, W, Bradley, SR & Richerson, GB (2002). Quantification of the response of rat medullary raphe neurones to independent changes in pH(o) and P(CO2). *J Physiol* **540**: 951-70.

Wang, W, Pizzonia, JH & Richerson, GB (1998). Chemosensitivity of rat medullary raphe neurones in primary tissue culture. *J Physiol* **511 (Pt 2)**: 433-50.

Wang, W, Richerson, GB (1999). Development of chemosensitivity of rat medullary raphe neurons. *Neuroscience* **90**: 1001-11.

Zachariou, V, Liu, R, LaPlant, Q, Xiao, G, Renthal, W, Chan, GC*, et al.* (2008). Distinct roles of adenylyl cyclases 1 and 8 in opiate dependence: behavioral, electrophysiological, and molecular studies. *Biol Psychiatry* **63**: 1013-2.

DISCUSSION

Summary of findings

The work presented in this dissertation was aimed to establish how specific is cAMP-signaling pathways in the CB mainly in different CO_2 conditions and how O_2 concentrations alter/drives the manipulation of cAMP signaling in the CB. The experimental studies included in this thesis sought to investigate the role of cAMP in the rat CB chemotransduction mechanisms and to determine whether the enzymes that participate in cAMP signal transduction in the CB are regulated by O_2/CO_2. We characterized the enzymes involved in the cAMP-signaling pathway in the CB (sAC, tmAC, PDE) under different O_2/CO_2 conditions. Our results demonstrated that many of these enzymes are involved in CO_2/O_2 sensing and while they may be useful in treating conditions with alterations in CO_2/O_2 sensing, they will not be specific to chemoreception within the CB: 1) PDE4 is ubiquitously expressed in CB and non-chemoreceptor related tissues and their affinity to inhibitors change with O_2 tensions in both CB and carotid arteries, and 2) sAC and tmAC are expressed in peripheral and central chemo- and non-chemoreceptor tissues and their effect on cAMP levels do not change between normocapnic and isohydric hypercapnic conditions. Our results provide evidence against a specific role of cAMP as a mediator for O_2 and CO_2 chemotransduction in the rat CB and emphasized the role of pH in CO_2 sensitivity of the CB. Furthermore, our results demonstrate that cAMP levels are maintained higher under physiological conditions, supporting recent finding from our lab, which all together suggests that cAMP has a homeostatic function in this organ.

First of all, using a pharmacological approach, we characterized PDE4 in the CB and non-chemoreceptor related tissues (chapter 1 and 2). PDEs are important in the regulation of cAMP levels and have been considered good therapeutic targets. According to the basic pharmacological principle, the regulation of degradation of a second messenger can often make a faster and larger

percentage change in concentration than comparable rates of synthesis (Bender and Beavo, 2006). Also, the PDE inhibitors compete effectively with the low concentration of cAMP in the cells (in microMolar range) and up to 50 different PDE isoforms with different regulation and inhibition properties (Bender and Beavor, 2006) are available. The results obtained demonstrate that, although PDE4 is apparently a good therapeutic target in the CB, its activity is non-specific for this tissue and hypoxia changed the affinity of the inhibitors to this enzyme. Specifically hypoxia potentiated the effects of PDE inhibitors on cAMP levels in the CB and carotid arteries and decreased in superior cervical ganglia. These findings should be considered when these inhibitors are used clinically and suggest that the effects of PDE inhibitors should be more intense in situations of acute hypoxia. Also, because of the lack of tissue-specificity, the vasodilation caused by PDE4 inhibitors can decrease the CB activity and compensate for the CB-mediated hyperventilatory response induced by the release of neurotransmitters in response to increases in cAMP. Moreover, the lack of tissue-specificity suggests that PDE regulation/affinity by O_2 tension is not apparently a specific characteristic of chemoreceptor tissues.

We also observed a differential pattern of PDE regulation within the cell bodies of superior cervical ganglion neurons. This finding suggests that each of these different subpopulations of superior cervical ganglion (or SCG) neurons may innervate different targets. For instance, the subpopulation with high PDE3 activity (high PKA activity induced by PDE3 inhibitors) could project to the heart, since PDE3 is the isoform more highly expressed in this organ (Lakics *et al.*, 2010). SCG is a sympathetic organ that pos-synaptically modulates type I cell activity. Thus our findings may also suggest that a specific supopulation of SCG neurons may synapse with type I cells that have a similar PDE profile.

Next, we characterized the cAMP synthesis pathway in the CB (chapter 3), specifically focusing on soluble adenylyl cyclase, a novel adenylyl cyclase that is activated by HCO_3^-/CO_2. Since CB is also sensitive to changes in CO_2, we proposed that sAC could be a CO_2 sensor in this organ, via a mechanism

dependent on HCO_3^- and thus, cAMP could mediate hypercapnia transduction. Furthermore, we also characterize the 9 tmAC isoforms and compared the relative contribution of both sAC and tmAC to the cAMP accumulation at different concentrations of CO_2. We observed that sAC and tmAC expression and function were not specific to the CB but these enzymes were also expressed in central chemoreceptors and non-chemoreceptors and high CO_2 levels (isohydric hypercapnic conditions) did not change the cAMP levels produced by these enzymes. These results suggested that these enzymes are not good/specific therapeutic targets under isohydric hypercapnia, however they may be important in hypocapnic conditions (respiratory alkalosis; hypocapnia is common in several diseases: early asthma, high altitute pulmonary edema, lung injury, for a review Curley et al 2010).

We determined the role of CO_2 chemosensing in the carotid body at a constant pH. Although we are aware that changes in PCO_2 are routinely accompanied by changes in pH in vivo, this approach allowed us to delineate the role of PCO_2 from pH in carotid body sensitivity; our data supports that the CB is not directly sensitive to CO_2 but is to changes in pH.

How our results integrate with what has previously been published

One of the goals of this work was to investigate the role of cAMP as a specific mediator of chemotransduction in the rat CB. As mentioned in the *Introduction*, changes in pH are important for CB chemosensitivity, through a mechanism that involves inhibition of K^+ channels with consequent cell depolarization, activation of Ca^{2+} channels, and increase of intracellular Ca^{2+} and release of neurotransmitters. It has also been demonstrated that molecular CO_2, independent of its effects on pH, activates L-type Ca^{2+} channels through PKA activation (Summers et al. 2002). As a consequence of increases in CO_2/pH, cAMP levels in the CB increase (Perez-Garcia et al., 1990, Summers et al., 2002). One of our questions was to

understand the mechanism by which cAMP increases. Both pH and molecular CO_2 induce increases in intracellular Ca^{2+} and release of neurotransmitters that bind to GPCR coupled- tmACs, modifying cAMP levels in the CB. Furthermore, molecular CO_2 can also be converted into intracellular HCO_3^- through the activity of carbonic anhydrase, activating sAC, an enzyme that has never been characterized in the CB. Here, we characterized for the first time the expression of sAC and the nine tmAC isoforms in peripheral and central chemo- and non-chemoreceptors. These enzymes were ubiquitously expressed in all the tissues studied, however, their levels of expression varied between each tissue. In contrast to the findings of others who observed that changes in cAMP levels were induced by increases in CO_2 (Summers *et al*., 2002, Perez-Garcia *et al.*, 1990), we observed that increases in HCO_3^-/CO_2 from 24mM HCO_3/5%CO_2 (normocapnia) to 44mM HCO_3/10%CO_2 (isohydric hypercapnia) did not change cAMP levels nor PKA activity, in the presence or absence of tmAC and sAC inhbitors. Besides species-related differences, the dissimilarities between these works and ours suggest that increases in cAMP levels, in hypercapnia, only occur in the presence of an acidic stimulus. We confirmed this supposition by showing that CSN discharge increases in response to hypercapnia acidosis, but not to isohydric hypercapnia, through a mechanism mediated by cAMP. In agreement with our findings, Buckler's et al (Buckler et al, 1991) showed that changes in PCO_2 at constant extracellular pH caused rapid transient changes in intracellular pH in the CB that was not correlated with sustained activation of the glomus cell. However, acidosis (changing PCO_2 at constant HCO_3^-) caused a sustained increase in CB activity (Buckler et al, 1991).

Taken together, we propose that the mechanism for hypercapnia sensing in the CB depends on the enzymatic conversion of CO_2 into H^+, thereby inhibiting the K^+ channels which leads to depolarization, increase in calcium entry and consequent release of neurotransmitters that bind to GPCR and modulate cAMP levels. Since tmAC inhibitors seem to cause a greater reduction in cAMP levels than sAC inhibitors in the presence of hypo, normo and isohydric hypercapnia, that

suggests that tmAC contributes more to cAMP levels than sAC. Also, we can not exclude the hypothesis that molecular CO_2 can regulate tmAC. In fact, it has been recently described that in mammalian recombinant G-protein-activated adenylyl cyclase and in the related Rv1625c adenylyl cyclase of *Mycobacterium tuberculosis*, CO_2 increases the affinity of the enzyme for the metal co-factors, suggesting that while sAC is responsive to HCO_3^-, and consequently CO_2, G-protein-regulated tmAC are responsive to CO_2 (Townsend *et al*., 2009). Furthermore, molecular CO_2 increases steady state cytoplasmatic Ca^{2+} concentrations via IP3 receptor signaling leading to low cAMP levels (Cook *et a*l., 2012). It is unclear how CO_2 causes Ca^{2+} release through IP3 receptor signaling and how elevated intracellular Ca^{2+} levels reduce cAMP levels. Either CO_2 direclty interacts with adenylyl cyclase or there is an alternative signaling pathway which impacts on cAMP levels. The identification of such CO_2 target could be relevant for the chemotrasduction mechanism of the carotid body.

Mammals have multiple CO_2 sensory systems including the peripheral and central chemoreceptors. Understanding molecular mechanisms for CO_2 chemoreception in the different cells increases fundamental knowledge of a process that is essential in health and disease. For example, Chandrashekar *et al.* (2009) identified carbonic anhydrase 4 (CAH4) as a CO_2 receptor in the taste cells. CAH4 is anchored at the surface of gustatory cells in the mammalian tongue, where it produces protons that may acidify the immediate extracellular environment. The amygdala has been considered as a chemosensor that detects CO_2 and acidosis to elicit fear behavior throught the acid-sensing ion channel (ASIC) 1a (Ziemann *et al*., 2009). Also, TRPA1, by sensing intracellular acidification, constitutes an important component of the nociceptive response to CO_2 (Wang *et al*., 2010). Futhermore, increases in CO_2 suppress genes involved in the regulation of innate immunity and inflammation, through decrease of NF-kB family of transcriptors factors activity (for a review Taylor and Cummins, 2011). The signaling cascade proposed for CO_2 detection by the olfactory system

involves soluble CAH II activation with production of HCO_3^- that activates guanylyl cyclases. The consequent increases in cGMP lead to CNG channel opening and causing cell depolarization (Luo et al., 2009). The mechanisms by which CO_2 is detected in other systems may contribute for the to our understanding of CO_2 chemotransduction mechanism in the CB.

We also observed that sAC and tmAC had a particularly compensatory role to return cAMP levels to the "homeostatic set point": tmAC and sAC inhibitors were more efficient under 12-24 mM HCO_3^-/2.5-5% CO_2 in the presence of a PDE inhibitor. Situations of low CO_2 (hypocapnia) may activate Na^+- Cl^+/HCO_3^- exchanger and Na^+-HCO_3^- co-transport resulting in the increase of intracellular HCO_3^- that directly activates sAC. In rat hippocampal slices, HCO_3^- is needed for the recovery of synaptic transmission from anoxia, an effect independent of the effects of HCO_3^- on pHi or pHo (Roberts *et al*., 2000). HCO_3^- levels can be modified by glutamate uptake transporter in astrocytes (Judd *et al*., 1996), a mechanism that seems to be dependent in the ability of HCO_3^- to reduce free radical production by promoting the binding of iron to transferrin (Katsura *et al*., 1994). HCO_3^- levels can be also modified by the activation of $GABA_A$ receptors, resulting in an efflux of HCO_3^- (selectivity for HCO_3^-/Cl^- of 1:5) (Kaila et al., 1993). Our results also suggest that sAC may regulate tmAC activity until cAMP reaches a maximal level, which corresponds to levels measured under physiological conditions (normocapnia conditions).

Higher levels of cAMP can occure during normoxia as reported by Monteiro et al. (2011). Monteiro and co-workers (Monteiro *et al*., 2011) report that in the rat CB, the highest levels of cAMP occur during normoxia when compared to hyperoxia 95-100%O_2. We found that cAMP levels obtained from whole CB from rat during hypoxia are in agreement with the ones obtained by Monteiro et al (2011). In both works, absolute cAMP values obtained in the presence of IBMX, did not change significantly between hypoxic and normoxic conditions, with a trend toward an increase in cAMP levels during normoxia reported by Monteiro et

al. (2011). We attribute this slight difference to the way the cAMP levels were normalized: we normalized the levels of cAMP per weight of each CB, while in Monteiro *et al.* (Monteiro et al., 2011), all the levels of cAMP were normalized per the same mean value of CB weight.

The effect of different oxygen tension on cAMP levels in the rat CB differs from what has been reported for the rabbit and cat CB, where the highest levels of cAMP were observed in hypoxia (0-10%O_2) (Wang *et al.*, 1989, Perez-Garcia *et al.*, 1990, Chen *et al.*, 1997, Delpiano and Acker, 1991, Cachero *et al.*, 1996, Delpiano and Acker, 1984, see also table 5 and table 1 in attachement). These data imply that differences may be species-related. The release of catecholamines during hypoxia is greater in rat than in rabbit CB (Vicario et al., 2000, Fidone et al., 1982). Since dopamine binds to D2 receptors, which are negatively coupled to adenylyl cyclase, cAMP levels are then expected to be lower in rat CB.

The higher levels of cAMP in physiological (normoxic) conditions in the CB support a homeostatic and adaptator role for this second messenger in this organ. In fact, in the CB, cAMP induces a variety of cellular and molecular effects involved in the adaptation of the CB to chronic exposures to hypoxia (Table 1).

Table 1 - Effects of cAMP in the carotid body

Effects of cAMP	Preparation	Technique	Agents that increase cAMP	Reference
Short and long term regulation of rat CB gap junctions: -modulation of junctional conductance, increased electrical coupling and enhanced gap junction formation	Rat type I cells	Dual voltage clamping	db-cAMP (1mM) 8-br-cAMP, 3hrs (1mM)	Abudara and Eyzaguerre, 1998
Regulation of TH gene expression	Whole CB from adult rats	RT-PCR	FSK (10uM), 3 hrs, in hypoxia (10%O2 vs control 100%O2)	Chen et al, 1995
Do not inhibit K^+ currents and Ca^{2+} currents were not altered	Type I cells from rat pups	Whole cell patch clamp recording	8-bromo-cAMP (2mM) dibutyryl-cAMP (5mM) Sp-cAMP (50uM) Sp-8-bromo-cAMPs (50uM), all in the presence of IBMX	Hatton and Peers, 1996
Activates Cl^- currents	Type I cells P10, rat	Whole cell recording	cAMP (200uM) 8-br-cAMP (2mM)	Carpenter and Peers, 1997
Long term modulation/regulation of currents- increase in Na+ and Ca^{2+} inward currents and capacitance	Type I cells from P5-12 rats	Whole cell recording	Dibutyryl- cAMP (0.2-1 mM) and FSK (10uM), 9-14 days	Steal et al, 1995
Induce Na^+ channels and causes hypertrophy of type I cells	Type I cells of rat CB (DOL 5-12)	Whole cell recording	Bt_2cAMP (1mM) In 20%O2/5%CO2 (14 days)	Stea et al, 1992
Inactivate K^+ channels Do not modify Ca^{2+} currents	Type I cells from adult rabbit	Whole cell recording	dBcAMP (2-3mM) FSK (10-20uM)	Lopez-Lopez 1993
Potentiates (30%O_2 in N2)-evoked CA release and CSN discharge (versus no effect of FSK on CSN under 100%O_2)	Whole CB and CSN from rabbits	Recording of CSN activity and tritiated CA release	FSK (10uM) 10 min	Wang et al, 1991
Increases hypoxia (5%O_2/95%N_2)-evoked release of DA (control 100%O_2)	Whole adult rabbit CB f	Tritiated CA release	FSK (10uM) dBcAMP (2mM) ISO (10-50uM) 20 min?	Perez-Garcia, 1990, 1991, 1993
cAMP mimick the effect of acidic hypercapnia (20%O_2/10%CO_2) on Ca^{2+} currents	Type I cells of adult rabitt CB	Whole cell recording	8-Br-cAMP (500uM) for 10 min	Summers et al, 2002
Increases GAP-43 expression, stimulated neurofilament expression and neurite outgrowth	Type I cells from rat (DOL 5-7)	Double immunofluore scence	dbcAMP (1mM) FSK (10uM) Chronic effect (2 weeks)	Jackson and Nurse, 1995

As observed from the table 1: 1) cAMP is potentially involved, but it is not essential in the transduction mechanism to acute hypoxia (Wang *et al.*, 1991, Perez-Garcia *et al.*, 1991); 2) cAMP is involved in long-term adaptative changes to chronic hypoxia (Jackson and Nurse, 1995, Abudara and Eyzaguirre, 1998); 3) the role of cAMP in the transduction mechanism may be different between the rat and rabbit CB: in rabbit, the administration of agents that increase cAMP levels potentiated or mimicked the effects mediated by acute hypoxia, as an example, inihibition of K^+ channels (Lopez-Lopez *et al.*, 1993) while in rat, cAMP levels did not inhibit K^+ currents (Hatton and Peers, 1996).

The role of cAMP in the homeostasis/basal activity of the CB may be involved in the mantainance of a basal activity of the CB (translated in basal release of neurotransmitters or basal CSN electrival activity), which is important to mantain resting ventilation since CB resection or CSN denervation affects leading to hypoventilation (Bisgard et al. 1976, Bisgard and Vogel 1871, Eugenin et al. 1989).

In conclusion, our work is the first to characterize: 1) the expression and function of sAC in the CB and central chemoreceptors; 2) 9 tmAC isoforms in the CB, and 3) PDE4 in the CB. Thus, our work provides new insights concerning the role of cAMP signaling pathway in the CB, how adenylyl cyclases and phosphodiesterases are regulated by O_2/CO_2. Current therapeutics are known to modify cAMP levels via modification of these two enzyme systems; our novel findings provides a better understanding of how these agents could potentially change carotid body function depending on the level of PaO_2/CO_2. Furthermore, new therapeutic agents may be developed targeting ,these enzymes that could potentially be used to treat disorders of respiratory control .

Limitations and future experiments

The conclusions of this work are limited by several factors that deserve discussion and open up new doors for future research to better understand the transduction mechanism of the carotid body.

In this work we used pharmacological, molecular biological and physiology tools to study the effect of changes in O_2/CO_2 in the activity of the enzymes involved in the cAMP-signaling pathway: the adenylyl cyclases and phosphodiesterases. The characterization of these enzymes was performed through gene expression and the pharmacological effect of specific inhibitors and activators of these enzymes on cAMP accumulation. One of the limitations of this work was the lack of a biochemistry approach to study whether changes in O_2 and CO_2 could directly affect the activity and affinity of PDE and AC.

We characterize for the first time the mRNA expression of the nine tmAC isoforms, however we were not able to determine if gene expression correlated with protein since we were limited by the lack of specific pharmacological tools for each isoform. However, since the CB releases a variety of different neurotransmitters, which can bind to pre-synaptic receptors in type I cells, it would be clinically relevant to further investigate which AC isoforms are related with the specific metabotropic receptors identified in the CB. It has been shown for instance, that in mouse airway smooth muscle cells, beta adrenergic receptors couple with AC5/6 in lipid rafts/caveolae, while prostanglandine E2 receptors couple with AC2 in non-raft membranes (Bogard et al, 2012). As far as we are aware of, there is no data in literature that relates GPCR and AC couple in the carotid body, but with the development of more specific AC pharmacological tools (activators and inhibitors), and use of the available KO for the specific tmAC isoforms (for a review (Pierre *et al.*, 2009)), it will be possible to better manipulate cAMP signaling in a clinical perspective. For example, AC5, AC6 and AC9 have been characterized in human airway smooth muscle cells and their activation has been proposed as potential drug targets for asthma treatment (Billington *et al.*, 1999).

In this work, levels of cAMP were quantified in the whole CB through EIA assays. These assays require tissue homogenization and the cAMP levels determined represented an avarege of cAMP change over large number of cells, whithout distinction

between type I cells (the sensor) and other constituintes of the CB. It is known that whithin the cell, cAMP levels change in microdomains regulated by specific cAMP-effectors, and those changes are not measurable when looked at the intact organ. Assays like EIA are static and terminal, limiting the ability to perform time series experiments. Also to detect cAMP levels with these assays it is necessary to bring cAMP changes whithin the assay detection level, which is done using PDE inhibitors. However, there is a clear dynamic role of PDEs controling cAMP levels, and inhibition of these enzymes may provide an inaccurate depiction of the *in vivo* conditions. FRET techniques allow overcoming some of these limitations: it studies cellular location and temporal organization of cAMP signaling. Since it is possible to add a cellular targeting sequence to the FRET sensor, this technique allows studying the signaling pathway in specific compartiments such as nucleus, mitocondrias, and reticulo. In this work we used this novel approach to confirm that the effect observed by HCO_3^-/CO_2 in whole CB was specific of type I cells, However, this technique opens up new doors of research in this organ.

In our experiments we considered the activity of PKA in the cAMP-signaling of the CB. However, we can not discard the contribution of other effectors for the cAMP-signaling, such as EPAC. Although a cAMP-EPAC pathway has been more associated with the O_2 sensing pathway in the CB (Rocher et al, 2009), it would be interesting to explore if the transduction of O_2 and CO_2 are mediated by the same enzymes or if PKA is more specific for a CO_2 transduction mechanism.

Concerning CO_2 sensing, it would also be interesting to study the effect of HCO_3^-/CO_2 in carbonic anhydrases, gap junctions and type II cells (and glial cells).

Intracellular calcium is a second messenger that highly influences cAMP signaling pathway. Evidence shows a role of $[Ca^{2+}]_i$ in the chemotransduction of both hypoxic and hyperoxic stimuli in type I cells (Biscoe and Duchen, 1990; Rigual et al, 1991). It is also known that $[Ca^{2+}]_i$ and intracellular pH interact in these cells (Buckler et al, 1991). Activation of ionotropic receptors induce a rapid increase of $[Ca^{2+}]_i$. Of particular interest, increase of ATP release from the CB induces increases of $[Ca^{2+}]_i$ in the PG neurons (Nunes et al, 2012), which can induce the activation of NTS neurons. I hypothesize that intracellular calcium could be the second messenger that mediates the O_2/CO_2 sensing, while cAMP would be more relevant as an adaptor for chronic conditions in the CB. Thus,

it would be interesting to better investigate the regulation of these two second messengers.

It is unknown if the different patterns of PDE expression/regulation that were observed in the SCG, also occur in the CB. It also remains to be explored if the different patterns of PDEs could be responsible for functional synapses between specific subpopulations of type I cells of the CB with nTS and petrosal ganglia.

Lastely, our results provide new insights to explain the efficacy of PDE inhibitors (PDE related drugs) in certain hypoxia related conditions such as pulmonary hypertension and to develop more PDE efficient inhibitors.

VI

ATTACHMENTS

Resumo Alargado

O corpo carotídeo (CB) é um pequeno órgão sensível a variações na PaO_2, $PaCO_2$ e pH. As células tipo I (células glómicas) do corpo carotídeo, as unidades sensoriais deste órgão, libertam neurotransmissores em resposta às variações dos gases arteriais. Estes neurotransmissores atuam quer em recetores pré-sinápticos, localizados nas células tipo I, quer em recetores pós-sinápticos, localizados nas terminações do nervo do seio carotídeo, ou em ambos. A activação dos recetores pré-sinápticos modula a atividade do corpo carotídeo, enquanto que, a activação dos recetores pós-sinápticos, de carater excitatório, desencadeia um aumento da frequência de descarga das fibras do CSN, com subsequente despolarização dos neurónios do gânglio petroso, e posterior despolarização de um grupo específico de neurónios do centro respiratório central, desencadeando, como resposta final, hiperventilação. Estes recetores pré- e pós-sinápticos podem ser classificados em ionotrópicos ou metabotrópicos, estando os últimos acoplados a adenilatos ciclases transmembranares (tmAC). O mecanismo exato pelo qual as variações dos gases arteriais são detetadas pelo CB não se encontra ainda completamente elucidado, mas tem sido sugerido que alterações nos níveis de cAMP estejam associadas ao mecanismo de deteção de variações de O_2 e CO_2. Os níveis de cAMP podem ser regulados através da sua via de síntese, mediada por dois tipos de adenilatos ciclases: tmAC sensível aos neurotransmissores e adenilato ciclase solúvel (sAC) sensível a variações de HCO_3/CO_2, e pela sua via de degradação mediada por fosfodiesterases. A via de degradação do cAMP pode ser manipulada farmacologicamente, funcionando enquanto alvo terapêutico para o tratamento de patologias do foro respiratório (e.g. asma, hipertensão pulmonar, doença pulmonar obstructiva crónica e apneia do sono), que induzem um aumento da actividade do CB.

O trabalho descrito nesta dissertação partiu da hipótese de que a actividade do CB é manipulada por fármacos, que interferem com a via de sinalização do cAMP, tendo sido nosso objectivo geral, investigar o papel do cAMP na quimiotransdução do CB de rato, e determinar se a actividade dos enzimas responsáveis pela via de sinalização do cAMP é ou não regulada por variações de O_2/CO_2. Assim, a relevância deste trabalho é a de estudar e identificar possíveis alvos moleculares (sAC, isoformas de tmAC e PDE) com potencial para serem usados no tratamento de patologias relacionadas com o controlo respiratório.

A primeira parte do presente trabalho, centrou-se na caracterização farmacológica da PDE4 no CB e em tecidos não quimiorecetores (e.g. gânglio cervical superior e artérias carótidas), e na observação do efeito de hipóxia aguda na acumulação dos níveis de cAMP, induzidos pelos inibidores de PDE, nestes tecidos. A quantificação de cAMP foi efectuada por técnica imunoenzimática (EIA), tendo sido elaboradas curvas de dose-resposta para os efeitos de inibidores, não específicos (IBMX) e específicos para a PDE2 e PDE4 (EHNA, Rolipram e Ro 20-1724), nos níveis de cAMP acumulados, em situações de normóxia ($20\%O_2/5\%CO_2$) e hipóxia ($5\%O_2/5\%CO_2$). A caracterização das PDE no gânglio cervical superior foi aprofundada, utilizando-se a técnica de transferência de energia de ressonância por fluorescência (FRET) em culturas primárias de neurónios, na presença de inibidores não específicos (IBMX) e específicos para a PDE3 e PDE4 (milrinone e rolipram, respetivamente). Foram igualmente estudadas, através de RT-qPCR, as alterações na expressão de PDE3A-B e PDE4A-D, no gânglio cervical superior, em resposta a diferentes percentagens de oxigénio.

Na segunda parte do trabalho investigou-se a via de síntese do cAMP no CB em resposta a variações na concentração de HCO_3/CO_2. Em concreto, o protocolo experimental centrou-se na caracterização da sAC, dado que a sua actividade é regulada por variações de HCO_3/CO_2. A caracterização da expressão e regulação da sAC, em resposta a variações de HCO_3/CO_2 ,foi efectuada no CB

e em tecidos não quimioreceptores periféricos (e.g. gânglio cervical superior, petroso e nodoso) por qRT-PCR. A actividade deste enzima foi caracterizada indirectamente através da quantificação dos níveis de cAMP (quantificação por EIA), induzidos por diferentes concentrações de HCO_3/CO_2, na presença de MDL-12,33-A, um inibidore da tmAC. A expressão das isoformas da tmAC no CB e gânglio petroso foi determinada por RT-qPCR. Adicionalmente, estudámos a contribuição relativa da tmAC e sAC no mecanismo de sensibilidade ao CO_2 no CB. Para o efeito foram estudadas as alterações: 1) nos níveis de cAMP (quantificado por EIA) na presença de diferentes concentrações de HCO_3/CO_2 e ao longo do tempo (5-30 min); 2) na ativação da proteína cinase A (PKA, FRET baseado em sensores) em células tipo I do CB; e 3) na frequência de descarga do CSN (registos) na presença e ausência de ativadores e inibidores da sAC, tmAC e PKA. Por último, foi caracterizada a expressão e actividade da sAC nos quimioreceptors centrais (locus ceruleus, rafe e medula ventro-lateral) através de técnicas de RT-qPCR e EIA. A expressão das isoformas da tmAC foi aprofundada no locus coeruleus através de RT-qPCR. Por fim, comparámos a contribuição da tmAC e sAC nos níveis de cAMP no locus coeruleus em condições de normocapnia e hipercapnia.

O nosso trabalho teve os seguintes resultados principais: 1) PDE4 está funcional no corpo carotídeo, artérias carótidas e gânglio cervical superior de rato, embora a PDE2 só se encontre funcional neste último; 2) Os efeitos dos inibidores de PDE nos níveis de acumulação de cAMP foram exacerbados em situações de hipóxia aguda no CB e artérias carótidas, mas foram atenuados no gânglio cervical superior; 3) No gânglio cervical superior, diferentes tipos de células apresentaram uma caracterização específica de PDEs, sugerindo uma subpopulação de células neste gânglio com funções fisiológicas distintas; 4) Embora todas as isoformas de PDE4 e PDE3 estivessem presentes no gânglio, a PDE3a, PDE4b e a PDE4d foram as isoformas mais expressas. Por outro lado, incubações de gânglio cervical superior, em diferentes percentagens de oxigénio,

não alteraram (não regularam) significativamente a expressão das diferentes isoformas de PDE neste órgão; 5) a sAC encontra-se expressa e funcional no CB e nos quimiorecetores centrais estudados (locus coeruleus, rafe e medula ventrolateral). A sAC apresenta maior expressão no CB comparativamente aos restantes orgãos estudados, exceptuando os testículos, orgão controlo. Variações de HCO_3/CO_2 de 0/0 para 24/5 aumentaram os níveis de cAMP no CB e quimiorecetores centrais, tendo sido o aumento mais significativo observado no CB. Concentrações acima dos 24mM $HCO_3/5\%CO_2$ não induziram alterações nos níveis de cAMP, sugerindo que a actividade da sAC se encontra saturada em condições fisiológicas (normocapnia) e que este enzima não desempenha qualquer papel na deteção de situações de hipercapnia; 6) No CB, a expressão das isoformas tmAC1, tmAC4, tmAC6 e tmAC9 é mais elevada comparativamente à expressão da sAC; 7) Utilizamos diferentes inibidores da tmAC (MDL 12-330A, 500μM, 2'5'-ddADO, 30-300μM, SQ 22536, 200μM) e da sAC (KH7, 10-100μM) para estudar a contribuição relativa destes enzimas na acumulação do cAMP no CB. Tanto a tmAC como a sAC contribuem para a acumulação dos níveis de cAMP em condições de hipercapnia. Contudo, existe um maior efeito destes inibidores nas condições de 12 mM $HCO_3/2.5\%CO_2$ do que em condições de normocapnia e hipercapnia, sugerindo um papel relevante destes enzimas na atividade do CB em situações de hipocapnia; 8) Não se observaram variações nos níveis de cAMP em resposta a diferentes concentrações de HCO_3/CO_2 ao longo do tempo (5-30 min). O efeito inibitório induzido por ddADO e KH7 foi sobreponível após 5 ou 30 minutos de incubação em todas as concentrações de HCO_3/CO_2 estudadas; 9) Por último, verificou-se um aumento na frequência da descarga do nervo do seio carotídeo entre as condições de normocapnia e hipercapnia acídica. Ao contrário do KH7 (10μM), o 2'5'-ddADO reduziu significativamente a frequência de descarga do nervo, quer em condições de normocapnia quer de hipercapnia acídica. Contudo, não se verificou aumento na frequência de descarga do nervo entre normocapnia e hipercapnia isohídrica, sugerindo que a sensibilidade à hipercapnia no CB é

mediada por variações de pH.

Em conclusão, os resultados decorrentes deste trabalho permitiram demonstrar que, embora os enzimas que medeiam a via de sinalização do cAMP possam ser bons alvos terapêuticos em condições particulares, a sua actividade não é específica para o CB. Os resultados sugerem ainda que o cAMP não é um mediador específico da transdução à hipercapnia neste orgão. Contudo, os nossos resultados demonstraram que os níveis de cAMP são mais elevados em condições fisiológicas, o que sugere que o cAMP possa ter uma função homeostática neste orgão. Por último, o presente trabalho demonstrou que os aumentos de cAMP descritos por outros em condições de hipercapnia, não são observáveis quando o pH se encontra controlado.

Table 1- cAMP

Species	Prep	Anest.	Methods/ PO_2	Results	Ref.
Cat (12 months)	Whole CB, n vivo and in vitro	Sodium pentobarbital 45 mg/Kg i.p.	**In vivo**: one CB removed in room air and the other under 5%O_2 inspired gas (3, 10, 20 min) **In vitro:** 30%O_2/3%CO_2 (normoxia) for 1-2 hrs and then submitted either to: 97%N_2/3%CO_2 (hypoxia) for 2 min or IBMX (0.8mM) for 2, 5 or 60 mi, in Locke's solution. cAMP detected by radioimmunoassay (NEN)	Variability during the year in control situations: -[cAMP] $_{in\ vivo}$ 0.5-1.5 pmol/CB -[cAMP] $_{in\ vitro}$ 0.1-1.1 pmol/CB **In vivo**: $[cAMP]_{hyp;3\ min}$=1.0-2.0 pmol/CB vs [cAMP]normo=0.8-1.0 pmol/CB) $[cAMP]_{hyp;10\ min}$=0.5 pmol/CB vs [cAMP]normo=0.2 pmol/CB) $[cAMP]_{hyp;20\ min}$=1.0-1.5 pmol/CB vs [cAMP]normo=0.6-0.8 pmol/CB **In vitro:** no changes (in the presence of IBMX during 60 min): $[cAMP]_{normo}$ = 4 pmol/CB and $[cAMP]_{hyp}$ = 5 pmol/CB	Delpiano et al, 1984
SD male rats (120-170g)	Whole CB, n vivo and in vitro	Urethane	**In vivo**: rats ventilated with normoxia room air, or 5%O_2 (hypoxia) **In vitro**: -1st incubation: Krebs Ringer bicarbonate medium, 30 min in 95%O_2/5%CO_2; -2nd incubation: Krebs Ringer bicarbonate medium, with IBMX 1mM, and isoprenaline 10uM, 37C. cAMP detected by protein-binding saturation method (Brown et al,1971)	In vivo: hypoxia did not increase cAMP levels in vivo In vitro: - [cAMP] 95%O2 = 0.59 pmol/CB - [cAMP]95%O2, isoprenaline, IBMX = 5.2 pmol/CB	Mir et al, 1983
Cat, 12 months	Whole CB, in vitro	Sodium pentobarbital 45 mg/Kg i.p.	-1st incubation: 3 hrs in Locke's modified solution, equilibrated with PO_2 230 torr, PCO_2 24 torr, pH 7.4 - 2nd incubation: Control CB fixed. Experimental CB incubated with Locke's medium equilibrated with PO_2 20 torr, PCO_2 24 torr in the presence and absence of IBMX (0.8mM), propranolol (34uM), haloperidol (27uM), MDL 12330A, during different incubation times: 2, 5 and 60 min cAMP measured by radioimmunoassay	-[cAMP]control= 0.41- 1.51 pmol/CB (seasonal variation: 1.31±0.24 pmol/CB during spring and 0.31 ± 0.08pmol/CB during autumn). - [cAMP] control= 0.79±0.1 pmol/CB vs [cAMP]2 min hypoxia= 1.13 ±0.14pmol/CB - Propranolol and haloperidol did not affect cAMP levels but depressed sinus nerve discharge -[cAMP]control, no IBMX= 0.31±0.09 , [cAMP]control, IBMX, 2 min= 1.46±0.29, [cAMP]control, IBMX, 5 min= 2.43±0.04 and [cAMP]control, IBMX, 60min= 6.97±1.38; [cAMP]hypoxia, no IBMX= 0.62±0.08; [cAMP]hypoxia, IBMX, 2min= 2.18±0.15; [cAMP]hypoxia, 5min= 3.84±0.39; [cAMP]hypoxia, 60 min= 5.56±1.75 pmol/CB 1mM MDL12330A reduced cAMP levels by 94%.	Delpiano and Acker, 1991
Rabbit	Whole CB, in vitro	Sodium pentobarbital	1st incubation: 30 min in tyrode solution at 100%O2/5%CO2 2nd incubation:10 min in either 100%O2 or 5%O2/N2 or 10%O2/N2 or FSK cAMP detected by RIA	cAMP control = 5.57 ±0.32 pmol/mg tissue -[cAMP] 10%O2= 12.4± 1.5pmol'mg tissue -[cAMP] 5%O2= 19.6± 3.9pmol'mg tissue - -[cAMP] 100%O2, FSK= 260± 87 pmol'mg tissue -[cAMP] 10%O2, FSK= 288± 75pmol'mg tissue	Wang et al, 1990

Table 1- cAMP

Species	Prep	Anest.	Methods/ PO_2	Results	Ref.
Rabbit	Whole CB, in vitro	Pentobarbital	- 1st incubation: 30 min incubation in Tyrode's solution equilibrated with 100%O_2, 37C. - 2nd incubation: 10 min incubation in tyrode solution equilibrated with 100%O_2 (control), 5%O_2 (hypoxia), FSK (10uM) or SNP (1 mM) cAMP measured by RIA (New England Nuclear)	-[cAMP]control= 5.4 ±0.36 pmol/mg tissue -[cAMP]hypoxia= 19.6 ± 3.9 pmol/mg tissue -[cAMP]100%O2, FSK 10uM= 260 ±87 pmol/CB	Wang et al, 1989
Rabbit	Whole CB.wh.p.e. NG	Pentobarbital anesthesia	In some animals the CSN was resected bilaterally; in others the SCG were bilaterally removed. The CB and NG were removed from both groups of animals and the following experiments in vitro were done: - 1st incubation: 30 min in 100%O2-Tyrode's solution, 37C - 2nd incubation: 10 min in tyrode's solution perfused with 100%O2 (control), or 5%O2 or 10%O2, or containing FSK 10uM and 100%O2 or FSK 10uM and 10%O2. cAMP measured by RIA (New England Nuclear)	-[cAMP]control= 5.57 pmol/mg of CB and ~ 12 pmol/mg of NG -[cAMP]10%O2= 12.4 pmol/mg of CB and ~ 11 pmol/mg of NG -[cAMP]5%O2= 19.6 pmol/mg of CB and ~ 15 pmol/mg og NG -[cAMP]100%O2,FSK10uM=260pmol/mg of CB and ~120pmol/mg of NG -[cAMP]10%O2, FSK10uM= 288 pmol/mg tissue - Basal cAMP levels were 3.92 fold higher after CSN deervation and 2.91 fold higher after sympathectomy but the ratio of cAMP contente in 10%O2/100%O2was similar between them. - Removal of calcium from 100%O2 equilibrated medium elevates cAMP levels by 2.91 fold and potentiates hypoxic stimulus by 5 fold	Wang et al, 1991
Adult rabbit	Whole CB	Sodium pentobarbital	In vitro: -1st incubation: tyrode modified solution equilibrated with 100%O2 or medium equilibrated with 95%O2 (24mM NaCl replaced by NaHCO3), 30 min, 37C. -2nd incubation: tyrode modified solution equilibrated with 100%O2 or 95%O2 (control) or 0%O2,5%O2,7%O2 or 10%O2 (10 min) in the presence or absence of IBMX 500uM (10-30 min), FSK 0-10uM (30 min), KCL 30 and 60 mM (10 min). 5%O2- 33 mm during 10 min stimuli. Medium contained IBMX cAMP was assayed using a commercial kit (Amersham)	In vitro: -[cAMP]control= 1 pmol/mg tissue -[cAMP]control, calcium free media= 1.1 pmol/mg tissue -[cAMP]control, IBMX 500uM, 10 min= 13.7pmol/mg tissue -[cAMP]control, IBMX500uM, 30 min= 4 pmol/mg tissue -[cAMP] control, FSK 10uM= 30 pmol/mg tissue -from 0-10%O2, the maximal cAMP levels were obtained with 7%O2 (7 x the control levels) -[cAMP] 95%O2/5%CO2= 0.8pmol/mg tissue vs [cAMP]80%O2/20%CO2 (pH 6.6)=3.2 pmol/mg tissue (no changes between these two in calcium free medium). -[cAMP] 100%O2, IBMX= 11.9 pmol/mg tissue; [cAMP] 100%O2, 30 mM KCl= 20.3 pmol/mg tissue and [cAMP] 100%O2, 60mM KCl= 30.52pmol/mg - both NE and DA (10uM) increased cAMP levels	Perez Garcia, 1990
Adult rabbit	Whole CB		In vitro: 1st incubation: 20 min, bicarbonate medium 2nd incubation: 5 min, bicarbonate medium equilibrated with normocapnia (normo) (20%O2/5%CO2) or hypercapnia (hyper, 21%O2/ 10%CO2) other series of experiments: CB incubated in Hepes medium with pH 6.8 or 7.4 cAMP measurment by EIA (Cayman Chemical)	[cAMP] normo = 1.98 pmol/ µg protein. [cAMP] hyper = 9.0 pmol/µg protein. [cAMP] normo, FSK = 38 pmol/ µg protein [cAMP] 100%O2, pH 7.4, Hepes= 3.58 pmol/µg protein [cAMP] 100%O2, pH 6.8, Hepes= 5.0 pmol/µg protein	Summers et al, 2002

Table 1- cAMP

Species	Prep	Anest.	Methods/ PO_2	Results	Ref.
Adult rabbit	Whole CB	Sodium pentobarbitoll	In vitro: 1st incubation- 30 min, 37C, bicarbonate-buffered tyrode solution, 20%O2, 5%CO2 (normoxia). 2nd incubation- 20 min in incubation buffer in 20%O2 plus 10 min with IBMX or 10 min with IBMX in the presence of 7%O2/5%CO2 (hypoxia). For both, in the presence or absence of Ca^{2+}. cAMP levels: radioassay kit (Amersham)	-[cAMP]control= 14.2 pmol cAMP/mg tissue = 300 pmol cAMP/mg protein - [cAMP]hyp= 36.0 pmol cAMP/mg tissue = 550 pmol cAMP/ mg protein -[cAMP] control, $0Ca^{2+}$= 9 pmol cAMP/ mg tissue 100 pmol cAMP/ mg protein - [cAMP] hyp, $0Ca^{2+}$= 21.9 pmol cAMP/mg tissue 300 pmol cAMP/mg protein	Cachero et al, 1996
Adult rabbit	Whole CB	Sodium pentobarbitoll	In vitro: - 1st incubation: 30 min in tyrode medium with 100%O2 - 2nd incubation: 10 min in tyrode medium with100%O2 or 5%O2, in the presence or absence of slective drugs cAMP measured by RIA (Dupont, NEN)	-[cAMP]$_{100\%O2}$=1pmol/mgtissue and [cAMP]$_{100\%O2, Ado\ 1mM}$=2.5pmol/mgtissue -[cAMP]$_{100\%O2}$=3pmol/mg tissue and [cAMP]$_{100\%O2, Ado\ 1mM}$=7pmol/mg tissue and [cAMP]$_{100\%O2, Ado\ 1mM, DPSPX\ 10uM}$=4pmol/mg tissue. -[cAMP]$_{100\%O2}$=2.5pmol/mg tissue and [cAMP]$_{100\%O2, CGS-2168\ 100nM}$=4 pmol/mg tissue and [cAMP]$_{100\%O2, CGS-2168\ 100nM, DMPX\ 50uM}$=3 pmol/mg tissue -[cAMP]$_{100\%O2}$ =2 pmol/mg tissue and [cAMP]$_{100\%O2, dipyridamole\ 100nM}$ =4pmol/mg tissue and [cAMP]$_{5\%O2, dipyridamole}$=6pmol/mg tissue; -[cAMP]$_{100\%O2}$ =4pmol/mg tissue, [cAMP]$_{5\%O2}$ =2.5 pmol/mg tissue and [cAMP]$_{100\%O2, DPSPX\ 10uM}$ =2pmol/mg tissue and [cAMP]$_{5\%O2, DPSPX\ 10uM}$=4.5pmol/mg tissue, [cAMP]$_{5\%O2, DPSPX\ 10uM}$=3.5pmol/mg tissue. -[cAMP]$_{100\%O2}$ =2.5 pmol/mg tissue and [cAMP]$_{100\%O2, DMPX\ 50uM}$ =2pmol/mg tissue and [cAMP]$_{5\%O2}$=5pmol/mg tissue, [cAMP]$_{5\%O2, DMPX\ 50uM}$=3pmol/mg tissue. -[cAMP]$_{100\%O2}$ =2 pmol/mg tissue and [cAMP]$_{100\%O2, aminophylline\ 20uM}$ =2pmol/mg tissue and [cAMP]$_{5\%O2}$=5pmol/mg tissue, [cAMP]$_{5\%O2, aminophylline\ 50uM}$=2pmol/mg tissue.	Chen et al, 1997
rabbits	Whole CB		In vitro: 1st incubation: tyrode solution equilibrated with 100%O2 - 2ndincubation: tyrode solution equilibrated with 10%O2 for 10 min AMP RIA Kits DuPOnt	[cAMP] 100%O2 = 2 pmol/ mg tissue [cAMP]10%O2 = 5 pmol/mg tissue	Chen et al, 2000
Adult rabbits	Whole CB, in vitro	Sodium pentobarbital 30-40 mg/Kg	1st: 30 min, 37C, 100%O2, modified Tyrode medium. 2nd medium: tyrode modified medium in the presence of IBMX 500mM during 10 min or 30 min in the presence of FSK 5uM, or KCL (30 mM), equilibrated in 100%O2 or hypoxia (5%O2/95%N2-37mM Hg) cAMP measured by RIA (Amersham)	-[cAMP]control=1.0±0.08 pmol/mg tissue [cAMP]control, IBMX= 14 pmol/mg tissue, 10 min [cAMP]control, FSK.5uM, 100%O2= 40.4 ± 3.13 pmol/mg tissue, for 30 min [cAMP]hyp, IBMX= 43 ±3.9 pmol/mg tissue, 10 min	Perez-Garcia et al, 1990
Adult rabbits	Whole CB	Sodium pentobarbital	Acording to Perez-Garcia (1990), all with IBMX 500uM cAMP measured by RIA (Amersham).	-[cAMP] control, IBMX= 13.1 ±1.6 pmol/mg tissue -[cAMP] IBMX, DA 1uM= 24.4± 2.85pmol/mg tissue -[cAMP]IBMX, SKF38393 1uM= 23.9 ± 2.3pmol/mg tissue -[cAMP]IBMX, DA 10uM= 40.6±3.29 pmol/mg tissue and SCH23390 (D1 antagonist) completely abolished the action of DA.	Perez-Garcia et al, 1991

Table 2- Characteristics of the specific AC isoforms

Isoform	Activators	Inhibitors	Tissue distribution	KO	Putative function
AC1	Gsα, FSK, Ca^{2+}/CaM, PKC(weak)	Giα, Gβγ, CaM Kinase IV, P-site analogs	Brain (hippocampus, dentate gyrus, cerebellum, córtex, thalamus), retina, adrenal medulla, spinal cord	+	Learning, memory, LTP, synaptic plasticity
AC2	Gsα, FSK, Gβγ, PKC	P-site analogs	Brain, olphactory bulb, lung, heart, muscle	-	Neurodegenerative diseases, alzeimer
AC3	Gsα, FSK, Ca^{2+}/CaM, PKC(weak)	CaM Kinase II, P-site analogs	Olfactory neurons, brain, heart, lung, testes, brown tissue	+	Olfaction
AC4	Gsα, FSK, Gβγ, PKC	P-site analogs	Kidney, brain, liver, heart, lung, brown tissue,	+	
AC5	Gsα, FSK, PKCα/ζ	Giα, PKA,Gβγ (β1γ2),Ca^{2+} +(<1 μM), P-site analogs	Brain (striatum, brainstem, prefrontral córtex), heart, spinal cord, heart, lung, testes, brown tissue, kidney, liver, adrenal gland	+	human motor dysfunctions, acute or chronic heart failure pressure overload
AC6	Gsα, FSK	Giα, PKA, PKC, Ca^{2+}(<1 μM), P-site analogs	Heart, brain,kidney,testis, liver, spinal cord, lung, testes, brown tissue, muscle, adrenal gland	+	Acute or chronic heart failure and pressure overload
AC7	Gsα, FSK, Gβγ, PKC	P-site analogs	Lung, heart, sleen, kidney, brain, testes, liver, muscle,	+	Drug depency
AC8	Gsα, FSK, Ca^{2+}/CaM	Giα(Ca^{2+} rises),P-site analogs	Brain (hippocampus, cerebellum, thalamus, hypothalamus), spinal cord, heart, lungs,testes, brown tissue, muscle, adrenal gland	+	Learning, memory, LTP, synaptic plasticity
AC9	Gsα, FSK (weak)	Ca^{2+}/calcine urin, Giα	Scheletal muscle, brain, lung, liver, spinal cord,heart, kidney, adrenal gland	+	
sAC	Ca^{2+}, HCO_3^-	___	Testis, brain, heart, kidney, muscle, liver	+	Sperm capacitation

AC, adenylate cyclase; **FSK**, forskolin; **CaM**, calmoduline; **PKC**, protein kinase C; Gsα, ; Giα, Gβγ; **Ca^{2+}**, calcium ion; **HCO_3^-**, bicarbonate ion; KO, knockout
Based on (Hanoune and Defer, 2001; Pierre et al, 2009)

Table 3- PDE families

PDE	Isoform	Inhibitors/ (K_i or IC_{50}) (uM)	Substract	Regulators	Expression
PDE I	PDE1A	Vinpocetine (14)	cGMP> cAMP	(+)Ca^{2+}/CaM (-) PKA, CamKII	Thyroid, testis, brain
	PDE1B	Zaprinast (6)	cGMP> cAMP		Brain, lymphocytes
	PDE1C	Sildnafil (0.35)	cGMP = cAMP		Blood vessels, testis
PDE II	PDE2A	BAY 60-7550 (0.047) EHNA (1)	cAMP	(+)cGMP, PKC (=/-)N-terminal targeting domain	Brain, heart, platelets, liver, thymocytes
PDE III	PDE3A	Cilostamide (0.020)	cAMP>cGMP	(+)-PKA, PKB (-)cGMP (+/-) N-terminal – targeting domain	Heart, blood vessels
	PDE3B	Milrinone (0.150) Zardaverine (0.5-2)			Adipocytes, hepatocytes, lymphocytes
PDE IV	PDE4A	Rolipram/ 9.0 Ro 20-1724/ 6.5	cAMP	(+)PKA, ERK, phosphatidic acid (-) ERK, caspases (+/-) N-terminal targeting domains.	Lung, immune cells, brain, blood vessels
	PDE4B	Rolipram/ 9.0 Ro 20-1724/ 6.4			
	PDE4C	Rolipram/ 6.5 Ro 20-1724/5.4			
	PDE4D	Rolipram/ 7.2 Ro 20-1724/6.2			
PDE V	PDE5A	Sildenafil (0.1) Zaprinast (0.130)	cGMP	(+)PKA, PKG, cGMP (-) caspases	Smooth muscle, platelets, Purkinje cells, gastro intestinal epithelium, pulmonary endothelium
PDEV I	PDE6A	Sildenafil (0.050), zaprinast (0.4), Dipyridamole (0.125), Tadalafil (2)	cGMP	(-)cGMP	Retinal photoreceptors
	PDE6B				
	PDE6C				
	PDE6D				
	PDE6G				
	PDE6H				
PDE VII	PDE7A	BRL50481/ 6.7	cAMP	(+/-) PKA	Brain, lymphocytes, kidney
	PDE7B	Dipyridamole (0.6)			
PDE VIII	PDE8A	Dipyridamole (9)	cAMP	Pas domain	Thyroid
	PDE8B				
PDE IX	PDE9A	Zaprinast (35)	cGMP	unknown	kidney
PDE X	PDE10A	Zaprinast (22)	cAMP, cGMP	cGMP	
PDE XI	PDE11A	Dipyridamole (0.4), zaprinast (12)	cAMP and cGMP	unknown	Skeletal muscle, prostate, testis, corpus cavernosum, heart

I-sobutyl-1methylxantine (IBMX) is a non-specific PDE inhibitor, but it is ineffective for inhibition of PDE8 and PDE9. (+)- positive regulation, (-) negative regulation. (adapted from Francis et al, 2011, and Makhlouf et al, 2006).

Table 4- Pharmacological tools

Name	Abbrev.	Company	Function
Forskolin	FSK	Sigma (St Louis, Mo, USA)	Transmembrane adenylate cyclase activator
1-methyl-3-(2-methylpropyl)-7H-purine-2,6-dione	IBMX	Sigma (St Louis, Mo, USA)	PDE non-selective inhibitor
(±)-2-(1*H*-benzimidazol-2-ylthio)prop anoic acid 2-[(5-bromo-2-hydroxyphenyl)methylene]hydrazide	KH7	Sigma (St Louis, Mo, USA)	Soluble adenylate cyclase inhibitor
cis-N-(2-Phenylcyclopentyl)azacyclotridec-1-en-2-amine	MDL-12,330A	Sigma (St Louis, Mo, USA)	Transmenbrane adenylate cyclase inhibitor
4-[3-(Cyclopentyloxy)-4-methoxyphenyl]-2-pyrrolidinone	Rolipram (ROL)	Sigma (St Louis, Mo, USA)	PDE 4 selective inhibitor
4-(3-Butoxy-4-methoxybenzyl)imidazolidin-2-one	Ro-201724	Sigma (St Louis, Mo, USA)	PDE 4 selective inhibitor
Erythro-9(2-hydroxy-3-nonyl) adenine	EHNA	Sigma (St Louis, Mo, USA)	PDE2 selective inhibitor and ADA inhibitor
Dipyridamole	Dipyridamole	Sigma (St Louis, Mo, USA)	Selective inhibitor of phosphodiesterase V (PDE 5); potent coronary vasodilator drug; adenosine transport inhibitor; inhibitor of platelet aggregation.
N-[2-(p-Bromocinnamylamino)ethyl]-5-isoquinolinesulfonamide dihydrochloride	H89	Sigma (St Louis, Mo, USA)	Protein kinase A inhibitor
1,6-Dihydro-2-methyl-6-oxo-(3,4′-bipyridine)-5-carbonitrile	Milrinone (MIL)	Sigma (St Louis, Mo, USA)	PDE 3 selective inhibitor
9-(Tetrahydro-2-furanyl)-9H-purin-6-amine	SQ 22,536	Sigma (St Louis, Mo, USA)	Transmenbrane adenylate cyclase inhibitor
2′,5′-Dideoxyadenosine	2'5'-ddADO	Sigma (St Louis, Mo, USA)	Transmenbrane adenylate cyclase inhibitor

VII

REFERENCES

References

Abudara, V, Eyzaguirre, C (1998). Modulation of junctional conductance between rat carotid body glomus cells by hypoxia, cAMP and acidity. *Brain Res* **792**: 114-25.

Abudara, V, Eyzaguirre, C (1996). Effects of calcium on the electric coupling of carotid body glomus cells. *Brain Res* **725**: 125-31.

Abudara, V, Eyzaguirre, C & Saez, JC (2000). Short- and long-term regulation of rat carotid body gap junctions by cAMP. Identification of connexin43, a gap junction subunit. *Adv Exp Med Biol* **475**: 359-6, 10.1007/0-306-46825-5_33.

Ahonen, M (1991). Neurofilament immunoreactivity and acetylcholinesterase activity in the developing sympathetic tissues of the rat. *Histochemistry* **96**: 467-78.

Almaraz, L, Perez-Garcia, MT & Gonzalez, C (1991). Presence of D1 receptors in the rabbit carotid body. *Neurosci Lett* **132**: 259-62.

Aubry, L, Firtel, R (1999). Integration of signaling networks that regulate Dictyostelium differentiation. *Annu Rev Cell Dev Biol* **15**: 469-517, 10.1146/annurev.cellbio.15.1.469.

Bairam A, Joseph V, Lajeunesse Y, Kinkead R (2007). Developmental profile of cholinergic and purinergic traits and receptors in peripheral chemoreflex pathway in cats. *Neuroscience* **146(4)**:1841-53.

Bairam A, Joseph V, Lajeunesse Y, Kinkead R (2006). Developmental pattern of M1 and M2 muscarinic gene expression and receptor levels in cat carotid body, petrosal and superior cervical ganglion. *Neuroscience* **139(2)**:711-21. Epub 2006 Feb 2.

Bairam, A, Carroll, JL (2005). Neurotransmitters in carotid body development. *Respir Physiol Neurobiol* **149**: 217-32, 10.1016/j.resp.2005.04.017.

Bairam A, Frenette J, Dauphin C, Carroll JL, Khandjian EW (1998). Expression of dopamine D1-receptor mRNA in the carotid body of adult rabbits, cats and rats. *Neurosci Res*. **31(2)**:147-54.

Bairam A, Khandjian EW (1997). Expression of dopamine D2 receptor mRNA isoforms in the carotid body of rat, cat and rabbit. *Brain Res.* **760(1-2)**:287-9.

Bankir, L, Ahloulay, M, Devreotes, PN & Parent, CA (2002). Extracellular cAMP inhibits proximal reabsorption: are plasma membrane cAMP receptors involved? *Am J Physiol Renal Physiol* **282**: F376-92, 10.1152/ajprenal.00202.2001.

Batuca, JR, Monteiro, TC & Monteiro, EC (2003). Contribution of dopamine D2 receptors for the cAMP levels at the carotid body. *Adv Exp Med Biol* **536**: 367- 73.

Bauer, K, Dietersdorfer, F, Sertl, K, Kaik, B & Kaik, G (1993). Pharmacodynamic effects of inhaled dry powder formulations of fenoterol and colforsin in asthma. *Clin Pharmacol Ther* **53**: 76-83.

Beene, DL, Scott, JD (2007). A-kinase anchoring proteins take shape. *Curr Opin Cell Biol* **19**: 192-8, 10.1016/j.ceb.2007.02.011.

Bender, AT, Beavo, JA (2006). Cyclic nucleotide phosphodiesterases: molecular regulation to clinical use. *Pharmacol Rev* **58**: 488-520, 10.1124/pr.58.3.5.

Bennett, MV, Barrio, LC, Bargiello, TA, Spray, DC, Hertzberg, E & Saez, JC (1991). Gap junctions: new tools, new answers, new questions. *Neuron* **6**: 305-20.

Benvenuti LA, Reis MM, de Lourdes Higuchi M (1996). Immunohistochemical detection of atrial natriuretic peptide (ANP) in the chief cells of human carotid bodies. *Acta Histochem* **98(1)**:89-92.

Bevans, CG, Kordel, M, Rhee, SK & Harris, AL (1998). Isoform composition of connexin channels determines selectivity among second messengers and uncharged molecules. *J Biol Chem* **273**: 2808-16.

Billington, CK, Hall, IP, Mundell, SJ, Parent, JL, Panettieri, RA,Jr, Benovic, JL*, et al.* (1999). Inflammatory and contractile agents sensitize specific adenylyl cyclase isoforms in human airway smooth muscle. *Am J Respir Cell Mol Biol* **21**: 597-606.

Biscoe, TJ, Duchen MR (1990). Responses of type I cells dissociated from the rabbit carotid body to hypoxia. *J Physiol* **428**:39-59.

Böck P (1980). Histochemical demonstration of adenine nucleotides in carotid body type I cells. *Adv Biochem Psychopharmacol* **25**:235-9.

Bos, JL (2003). Epac: a new cAMP target and new avenues in cAMP research. *Nat Rev Mol Cell Biol* **4**: 733-8, 10.1038/nrm1197.

Braun, T (1991). Purification of soluble form of adenylyl cyclase from testes. *Methods Enzymol* **195**: 130-6.

Buckler, KJ, Williams, BA & Honore, E (2000). An oxygen-, acid- and anaesthetic-sensitive TASK-like background potassium channel in rat arterial chemoreceptor cells. *J Physiol* **525 Pt 1**: 135-42.

Buckler, KJ, Vaughan-Jones, RD (1994b). Effects of hypercapnia on membrane potential and intracellular calcium in rat carotid body type I cells. *J Physiol* **478 (Pt 1)**: 157-71.

Buckler, KJ, Vaughan-Jones, RD (1994a). Effects of hypoxia on membrane potential and intracellular calcium in rat neonatal carotid body type I cells. *J Physiol* **476**: 423-8.

Buckler, KJ, Vaughan-Jones, RD, Peers, C & Nye, PC (1991a). Intracellular pH and its regulation in isolated type I carotid body cells of the neonatal rat. *J Physiol* **436**: 107-29.

Buckler, KJ, Vaughan-Jones, RD, Peers, C, Lagadic-Gossmann, D & Nye, PC (1991b). Effects of extracellular pH, PCO2 and HCO3- on intracellular pH in isolated type I cells of the neonatal rat carotid body. *J Physiol* **444**: 703-721.

Cachero, TG, Rigual, R, Rocher, A & Gonzalez, C (1996). Cholera and pertussis toxins reveal multiple regulation of cAMP levels in the rabbit carotid body. *Eur J Neurosci* **8**: 2320-7.

Campanucci VA, Dookhoo L, Vollmer C, Nurse CA (2012). Modulation of the carotid body sensory discharge by NO: An up-dated hypothesis. *Respir Physiol Neurobiol* [Epub ahead of print]

Cann MJ, Hammer A, Zhou J, Kanacher T(2003). A defined subset of adenylyl cyclasses is regulated by bicarbonate ion. *J Biol Chem* 278:35033-8.

Carnegie, GK, Means, CK & Scott, JD (2009). A-kinase anchoring proteins: from protein complexes to physiology and disease. *IUBMB Life* **61**: 394-406, 10.1002/iub.168.

Carpenter E, Peers C (1997). Swelling- and cAMP-activated Cl- currents in isolated rat carotid body type I cells. *J Physiol* **503** (Pt 3):497-511.

Carroll, JL, Boyle, KM, Wasicko, MJ & Sterni, LM (2005). Dopamine D2 receptor modulation of carotid body type 1 cell intracellular calcium in developing rats. *Am J Physiol Lung Cell Mol Physiol* **288**: L910-6, 10.1152/ajplung.00414.2003.

Caterina, MJ, Devreotes, PN, Borleis, J & Hereld, D (1995). Agonist-induced loss of ligand binding is correlated with phosphorylation of cAR1, a G protein-coupled chemoattractant receptor from Dictyostelium. *J Biol Chem* **270**: 8667-72.

Chang, LC, Wang, CJ, Lin, YL & Wang, JP (2003). Expression of adenylyl cyclase isoforms in neutrophils. *Biochim Biophys Acta* **1640**: 53-60.

Chandrashekar J, Yarmolinsky D, von Buchholtz L, Oka Y, Sly W, Ryba NJ, Zuker CS (2009). The taste of carbonation. *Science*. **326**(5951):443-5.

Chen J, He L, Dinger B, Fidone S (2000). Cellular mechanisms involved in rabbit carotid body excitation elicited by endothelin peptides. *Respir Physiol* **121(1)**:13-23.

Chen, J, Dinger, B & Fidone, SJ (1997). cAMP production in rabbit carotid body: role of adenosine. *J Appl Physiol* **82**: 1771-5.

Chen J, Dinger B, Fidone SJ (1995). Second messenger regulation of tyrosine hydroxylase gene expression in rat carotid body. *Biol Signals* **4(5)**:277-85.

Chen Y, Tipoe GL, Liong E, Leung S, Lam SY, Iwase R, Tjong YW, Fung ML (2001). Chronic hypoxia enhances endothelin-1-induced intracellular calcium elevation in rat carotid body chemoreceptors and up-regulates ETA receptor expression. *Pflugers Arch*. **443(4)**:565-73.

Chen, Y, Cann, MJ, Litvin, TN, Iourgenko, V, Sinclair, ML, Levin, LR*, et al.* (2000). Soluble adenylyl cyclase as an evolutionarily conserved bicarbonate sensor. *Science* **289**: 625-8.

Conde, SV, Monteiro, EC, Rigual, R, Obeso, A & Gonzalez, C (2012). Hypoxic intensity: a determinant for the contribution of ATP and adenosine to the genesis of carotid body chemosensory activity. *J Appl Physiol* **112**: 2002-10, 10.1152/japplphysiol.01617.2011.

Conde, SV, Monteiro, EC, Obeso, A & Gonzalez, C (2009). Adenosine in peripheral chemoreception: new insights into a historically overlooked molecule--invited article. *Adv Exp Med Biol* **648**: 145-59, 10.1007/978-90-481-2259-2_17.

Conde, SV, Monteiro, EC (2006a). Activation of nicotinic ACh receptors with alpha4 subunits induces adenosine release at the rat carotid body. *Br J Pharmacol* **147**: 783-9, 10.1038/sj.bjp.0706676.

Conde, SV, Obeso, A, Vicario, I, Rigual, R, Rocher, A & Gonzalez, C (2006b). Caffeine inhibition of rat carotid body chemoreceptors is mediated by A2A and A2B adenosine receptors. *J Neurochem* **98**: 616-28, 10.1111/j.1471-4159.2006.03912.x.

Conde SV, & Monteiro EC (2004). Hypoxia induces adenosine release from the rat carotid body. *J Neurochem* 89: 1148-56

Cook ZC, Gray MA and Cann MJ (2012). Elevated carbon dioxide blunts mammalian cAMP signaling dependent on inositol 1,4,5-triphosphate receptor mediated Ca2+ release. *J Biol Chem* **287**, 26291-301.

Christie DS, Hansen JT (1983). Cytochemical evidence for the existence of norepinephrine-containing glomus cells in the rat carotid body. *J Neurocytol* **12(6)**:1041-53.

Curley G, Laffey JG, Kavanagh BP (2010). Bench-to-bedside review: carbon dioxide. *Crit Care* **14(2)**:220.

Czyzyk-Krzeska MF, Lawson EE, Millhorn DE (1992). Expression of D2 dopamine receptor mRNA in the arterial chemoreceptor afferent pathway. *J Auton Nerv Syst*. **41(1-2)**:31-9.

de Rooij, J, Zwartkruis, FJ, Verheijen, MH, Cool, RH, Nijman, SM, Wittinghofer, A*, et al.*

(1998). Epac is a Rap1 guanine-nucleotide-exchange factor directly activated by cyclic AMP. *Nature* **396**: 474-7, 10.1038/24884.

Delpiano, M, Acker, H (1980). Relationship between tissue po2 and chemoreceptor activity of the carotid body in vitro. *Brain Res* **195**: 85-93.

Delpiano, MA, Acker, H (1991). Hypoxia increases the cyclic AMP content of the cat carotid body in vitro. *J Neurochem* **57**: 291-7.

Delpiano, MA, Acker, H (1984). O2 chemoreception of the cat carotid body in vitro. *Adv Exp Med Biol* **169**: 705-17.

Del Rio R, Moya EA, Koenig CS, Fujiwara K, Alcayaga J, Iturriaga R (2008). Modulatory effects of histamine on cat carotid body chemoreception. *Respir Physiol Neurobiol*. **164(3)**:401-10.

Dessauer, CW (2009). Adenylyl cyclase--A-kinase anchoring protein complexes: the next dimension in cAMP signaling. *Mol Pharmacol* **76**: 935-41, 10.1124/mol.109.059345.

Dias, MB, Li, A & Nattie, E (2008). Focal CO2 dialysis in raphe obscurus does not stimulate ventilation but enhances the response to focal CO2 dialysis in the retrotrapezoid nucleus. *J Appl Physiol* **105**: 83-90, 10.1152/japplphysiol.00120.2008.

Donnelly, DF (2009). Nicotinic acetylcholine receptors do not mediate excitatory transmission in young rat carotid body. *J Appl Physiol* **107**: 1806-1, 10.1152/japplphysiol.00135.2009.

Donnelly, DF (2005). Development of carotid body/petrosal ganglion response to hypoxia. *Respir Physiol Neurobiol* **149**: 191-9, 10.1016/j.resp.2005.02.006.

Donnelly, DF (1996). Chemoreceptor nerve excitation may not be proportional to catecholamine secretion. *J Appl Physiol* **81**: 657-64.

Erlichman, JS, Leiter, JC (2010). Glia modulation of the extracellular milieu as a factor in central CO2 chemosensitivity and respiratory control. *J Appl Physiol* **108**: 1803-11, 10.1152/japplphysiol.01321.2009.

EYZAGUIRRE, C, LEWIN, J (1961). Chemoreceptor activity of the carotid body of the cat. *J Physiol* **159**: 222-37.

Fagerlund MJ, Kåhlin J, Ebberyd A, Schulte G, Mkrtchian S, Eriksson LI (2010). The human carotid body: expression of oxygen sensing and signaling genes of relevance for anesthesia. *Anesthesiology*. **113(6)**:1270-9.

Fearon IM, Zhang M, Vollmer C, Nurse CA (2003). GABA mediates autoreceptor feedback inhibition in the rat carotid body via presynaptic GABAB receptors and TASK-1. *J Physiol*

553(Pt 1):83-94.

Fedoroff and Richardson(2001). Protocols for Neural Cell Culture. Third Edition. *Humana Press*

Fernández R, Nardocci G, Simon F, Martin A, Becerra A, Rodríguez-Tirado C, Maisey KR, Acuña-Castillo C, Cortes PP (2010). Lipopolysaccharide signaling in the carotid chemoreceptor pathway of rats with sepsis syndrome. *Respir Physiol Neurobiol* **175(3)**:336-48.

Fidone SJ, Weintraub ST, Stavinoha WB (1976). Acetylcholine content of normal and denervated cat carotid bodies measured by pyrolysis gas chromatography/mass fragmentometry. *J Neurochem* **26(5)**:1047-9.

Fidone, S, Gonzalez, C & Yoshizaki, K (1982). Effects of low oxygen on the release of dopamine from the rabbit carotid body in vitro. *J Physiol* **333**: 93-110.

Filosa, JA, Putnam, RW (2003). Multiple targets of chemosensitive signaling in locus coeruleus neurons: role of K+ and Ca2+ channels. *Am J Physiol Cell Physiol* **284**: C145-55, 10.1152/ajpcell.00346.2002.

Forster, HV, Martino, P, Hodges, M, Krause, K, Bonis, J, Davis, S*, et al.* (2008). The carotid chemoreceptors are a major determinant of ventilatory CO2 sensitivity and of PaCO2 during eupneic breathing. *Adv Exp Med Biol* **605**: 322-6, 10.1007/978-0-387-73693-8_56.

Fortuna, MG, Stornetta, RL, West, GH & Guyenet, PG (2009). Activation of the retrotrapezoid nucleus by posterior hypothalamic stimulation. *J Physiol* **587**: 5121-38, 10.1113/jphysiol.2009.176875.

Francis SH, Blount MA, Corbin JD (2011). Mammalian cyclic nucleotide phosphodiesterases: molecular mechanisms and physiological functions. *Physiol Rev* **91(2)**: 651-90

Francis, SH, Turko, IV & Corbin, JD (2001). Cyclic nucleotide phosphodiesterases: relating structure and function. *Prog Nucleic Acid Res Mol Biol* **65**: 1-52.

Fung ML, Lam SY, Chen Y, Dong X, Leung PS (2001). Functional expression of angiotensin II receptors in type-I cells of the rat carotid body. *Pflugers Arch* **441(4)**:474-80.

Gauda EB (2002). Gene expression in peripheral arterial chemoreceptors. *Microsc Res Tech*. **59(3)**:153-67.

Gauda, EB, Lawson, EE (2000). Developmental influences on carotid body responses to hypoxia. *Respir Physiol* **121**: 199-208.

Gloerich, M, Bos, JL (2010). Epac: defining a new mechanism for cAMP action. *Annu Rev Pharmacol Toxicol* **50**: 355-7, 10.1146/annurev.pharmtox.010909.105714.

Golanov, EV, Ruggiero, DA & Reis, DJ (2000). A brainstem area mediating cerebrovascular and EEG responses to hypoxic excitation of rostral ventrolateral medulla in rat. *J Physiol* **529 Pt 2**: 413-29.

Gonzalez, C, Agapito, MT, Rocher, A, Gomez-Nino, A, Rigual, R, Castaneda, J*, et al.* (2010). A revisit to O2 sensing and transduction in the carotid body chemoreceptors in the context of reactive oxygen species biology. *Respir Physiol Neurobiol* **174**: 317-30, 10.1016/j.resp.2010.09.002.

Gonzalez, C, Vaquero, LM, Lopez-Lopez, JR & Perez-Garcia, MT (2009). Oxygen-sensitive potassium channels in chemoreceptor cell physiology: making a virtue of necessity. *Ann N Y Acad Sci* **1177**: 82-8, 10.1111/j.1749-6632.2009.05037.x.

Gonzalez, C, Almaraz, L, Obeso, A & Rigual, R (1994). Carotid body chemoreceptors: from natural stimuli to sensory discharges. *Physiol Rev* **74**: 829-98.

Gonzalez, C, Almaraz, L, Obeso, A & Rigual, R (1992). Oxygen and acid chemoreception in the carotid body chemoreceptors. *Trends Neurosci* **15**: 146-53.

Grönblad M, Liesi P, Rechardt L (1983). Serotonin-like immunoreactivity in rat carotid body. *Brain Res.* **276(2)**:348-50.

Guellaen, G, Mahu, JL, Mavier, P, Berthelot, P & Hanoune, J (1977). RMI 12330 A, an inhibitor of adenylate cyclase in rat liver. *Biochim Biophys Acta* **484**: 465-7.

Guyenet, PG, Stornetta, RL & Bayliss, DA (2008). Retrotrapezoid nucleus and central chemoreception. *J Physiol* **586**: 2043-8, 10.1113/jphysiol.2008.150870.

Guyenet, PG, Mulkey, DK, Stornetta, RL & Bayliss, DA (2005). Regulation of ventral surface chemoreceptors by the central respiratory pattern generator. *J Neurosci* **25**: 8938-47, 10.1523/JNEUROSCI.2415-05.2005.

Hacker, BM, Tomlinson, JE, Wayman, GA, Sultana, R, Chan, G, Villacres, E*, et al.* (1998). Cloning, chromosomal mapping, and regulatory properties of the human type 9 adenylyl cyclase (ADCY9). *Genomics* **50**: 97-104, 10.1006/geno.1998.5293.

Halls M and Copper DM. (2011). Regulation by Ca2+-signaling pathways of adenylyl cyclases. *Cold spring Harb Perspect Biol* 3, a004143.

Hanbauer, I, Lovenberg, W (1977). Presence of a calcium2+-dependent activator of cyclic-nucleotide phosphodiesterase in rat carotid body: effects of hypoxia. *Neuroscience* **2**: 603-7.

Hanoune J, Defer N (2001). Regulation and role of adenylyl cyclase isoforms. *Annu Rev Pharmacol Toxicol.* **41**:145-74.

Hatton, CJ, Peers, C (1996). Hypoxic inhibition of K+ currents in isolated rat type I carotid body cells: evidence against the involvement of cyclic nucleotides. *Pflugers Arch* **433**: 129-35.

Hayashi, M, Matsushima, K, Ohashi, H, Tsunoda, H, Murase, S, Kawarada, Y*, et al.* (1998). Molecular cloning and characterization of human PDE8B, a novel thyroid-specific isozyme of 3',5'-cyclic nucleotide phosphodiesterase. *Biochem Biophys Res Commun* **250**: 751-6, 10.1006/bbrc.1998.9379.

Heym C, Kummer W (1989). Immunohistochemical distribution and colocalization of regulatory peptides in the carotid body. *J Electron Microsc Tech* 12:331-42.

Hempleman, SC, Pilarski, JQ (2011). Prenatal development of respiratory chemoreceptors in endothermic vertebrates. *Respir Physiol Neurobiol* **178**: 156-62, 10.1016/j.resp.2011.04.027.

Hess, KC, Jones, BH, Marquez, B, Chen, Y, Ord, TS, Kamenetsky, M*, et al.* (2005). The "soluble" adenylyl cyclase in sperm mediates multiple signaling events required for fertilization. *Dev Cell* **9**: 249-5, 10.1016/j.devcel.2005.06.007.

Hetman, JM, Robas, N, Baxendale, R, Fidock, M, Phillips, SC, Soderling, SH*, et al.* (2000). Cloning and characterization of two splice variants of human phosphodiesterase 11A. *Proc Natl Acad Sci U S A* **97**: 12891-5, 10.1073/pnas.200355397.

Hodges, MR, Opansky, C, Qian, B, Davis, S, Bonis, JM, Krause, K*, et al.* (2005). Carotid body denervation alters ventilatory responses to ibotenic acid injections or focal acidosis in the medullary raphe. *J Appl Physiol* **98**: 1234-42, 10.1152/japplphysiol.01011.2004.

Holz, GG, Kang, G, Harbeck, M, Roe, MW & Chepurny, OG (2006). Cell physiology of cAMP sensor Epac. *J Physiol* **577**: 5-15, 10.1113/jphysiol.2006.119644.

Houslay, MD, Schafer, P & Zhang, KY (2005). Keynote review: phosphodiesterase-4 as a therapeutic target. *Drug Discov Today* **10**: 1503-19, 10.1016/S1359-6446(05)03622-6.

Houslay, MD, Adams, DR (2003). PDE4 cAMP phosphodiesterases: modular enzymes that orchestrate signalling cross-talk, desensitization and compartmentalization. *Biochem J* **370**: 1-18, 10.1042/BJ20021698.

Huckstepp, RT, Dale, N (2011). Redefining the components of central CO2 chemosensitivity - towards a better understanding of mechanism. *J Physiol* **589**: 5561-79, 10.1113/jphysiol.2011.214759.

Huckstepp RT, id Bihi R, Eason R, Spyer KM, Dicke N, Willecke K, Marina N, Gourine AV & Dale N (2010). Connexin hemichannel-mediated CO2-dependent release of ATP in the medulla oblongata contributes to central respiratory chemosensitivity. *J Physiol* **588**, 3901–3920.

Ichikawa, H (2002). Innervation of the carotid body: Immunohistochemical, denervation, and retrograde tracing studies. *Microsc Res Tech* **59**: 188-95, 10.1002/jemt.10193.

Igarashi A, Zadzilka N, Shirahata M. (2009). Benzodiazepines and GABA-GABAA receptor system in the cat carotid body. *Adv Exp Med Biol* **648**:169-75.

Iturriaga, R, Alcayaga, J & Gonzalez, C (2009). Neurotransmitters in carotid body function: the case of dopamine--invited article. *Adv Exp Med Biol* **648**: 137-43, 10.1007/978-90-481-2259-2_16.

Iturriaga, R, Rumsey, WL, Lahiri, S, Spergel, D & Wilson, DF (1992). Intracellular pH and oxygen chemoreception in the cat carotid body in vitro. *J Appl Physiol* **72**: 2259-66.

Iturriaga, R, Lahiri, S & Mokashi, A (1991). Carbonic anhydrase and chemoreception in the cat carotid body. *Am J Physiol* **261**: C565-73.

Jackson, A, Nurse, C (1995). Plasticity in cultured carotid body chemoreceptors: environmental modulation of GAP-43 and neurofilament. *J Neurobiol* **26**: 485-96, 10.1002/neu.480260403.

Jaiswal, BS, Conti, M (2003). Calcium regulation of the soluble adenylyl cyclase expressed in mammalian spermatozoa. *Proc Natl Acad Sci U S A* **100**: 10676-81, 10.1073/pnas.1831008100.

Johnson, SM, Haxhiu, MA & Richerson, GB (2008). GFP-expressing locus ceruleus neurons from Prp57 transgenic mice exhibit CO2/H+ responses in primary cell culture. *J Appl Physiol* **105**: 1301-1, 10.1152/japplphysiol.90414.2008.

Johnson, SM, Koshiya, N & Smith, JC (2001). Isolation of the kernel for respiratory rhythm generation in a novel preparation: the pre-Botzinger complex "island". *J Neurophysiol* **85**: 1772-6.

Jones, KH, Senft, JA (1985). An improved method to determine cell viability by simultaneous staining with fluorescein diacetate-propidium iodide. *J Histochem Cytochem* **33**: 77-9.

Judd MG, Nagaraja TN, Brookes N (1996). Potassium-induced stimulation of glutamate uptake in mouse cerebral astrocytes: the role of intracellular pH. J Neurochem. **66(1)**:169-76.

Kåhlin J, Eriksson LI, Ebberyd A, Fagerlund MJ (2010). Presence of nicotinic, purinergic and dopaminergic receptors and the TASK-1 K+-channel in the mouse carotid body. *Respir Physiol Neurobiol* **172(3)**:122-8.

Kameda Y (1990). Distribution of serotonin-immunoreactive cells around arteries arising from the common carotid artery in the chicken. *Anat Rec* **227(1)**:87-96.

Kamenetsky, M, Middelhaufe, S, Bank, EM, Levin, LR, Buck, J & Steegborn, C (2006). Molecular details of cAMP generation in mammalian cells: a tale of two systems. *J Mol Biol* **362**: 623-39, 10.1016/j.jmb.2006.07.045.

Katsura K, Kristián T, Nair R, Siesjö BK (1994). Regulation of intra- and extracellular pH in the rat brain in acute hypercapnia: a re-appraisal. *Brain Res.* **651**(1-2):47-56.

Kaila K, Voipio J, Paalasmaa P, Pasternack M, Deisz RA (1993). The role of bicarbonate in GABAA receptor-mediated IPSPs of rat neocortical neurones. *J Physiol.* 464:273-89.

Kim, I, Yang, DJ, Donnelly, DF & Carroll, JL (2009). Fluoresceinated peanut agglutinin (PNA) is a marker for live O(2) sensing glomus cells in rat carotid body. *Adv Exp Med Biol* **648**: 185-90, 10.1007/978-90-481-2259-2_21.

Kiyashchenko, LI, Mileykovskiy, BY, Lai, YY & Siegel, JM (2001). Increased and decreased muscle tone with orexin (hypocretin) microinjections in the locus coeruleus and pontine inhibitory area. *J Neurophysiol* **85**: 2008-16.

Kobayashi S, Conforti L, Millhorn DE (2000). Gene expression and function of adenosine A(2A) receptor in the rat carotid body. *Am J Physiol Lung Cell Mol Physiol*. **279(2)**:L273-82.

Kruh, GD, Belinsky, MG (2003). The MRP family of drug efflux pumps. *Oncogene* **22**: 7537-52, 10.1038/sj.onc.1206953.

Krupinski, J, Coussen, F, Bakalyar, HA, Tang, WJ, Feinstein, PG, Orth, K*, et al.* (1989). Adenylyl cyclase amino acid sequence: possible channel- or transporter-like structure. *Science* **244**: 1558-64.

Kumar, P (2009). Systemic effects resulting from carotid body stimulation-invited article. *Adv Exp Med Biol* **648**: 223-3, 10.1007/978-90-481-2259-2_26.

Kumar P, Conway AF, Vandier C, Marshall NJ, Bruynseels J, Matthews GM(2000). Effect of adenosine on CO2 chemosensitivity. Functional, cellular, and molecular studies. *Adv Exp Med Biol*. **475**:405-10.

Lahiri, S, Forster, RE,2nd (2003). CO2/H(+) sensing: peripheral and central chemoreception. *Int J Biochem Cell Biol* **35**: 1413-35.

Lakics, V, Karran, EH & Boess, FG (2010). Quantitative comparison of phosphodiesterase mRNA distribution in human brain and peripheral tissues. *Neuropharmacology* **59**: 367-74, 10.1016/j.neuropharm.2010.05.004.

Lam SY, Tipoe GL, Fung ML (2009). Upregulation of erythropoietin and its receptor expression in the rat carotid body during chronic and intermittent hypoxia. *Adv Exp Med Biol.* **648**:207-14.

Lam SY, Leung PS (2002). A locally generated angiotensin system in rat carotid body. *Regul Pept* **107(1-3)**:97-103.

Lamontagne, S, Meadows, E, Luk, P, Normandin, D, Muise, E, Boulet, L*, et al.* (2001). Localization of phosphodiesterase-4 isoforms in the medulla and nodose ganglion of the squirrel monkey. *Brain Res* **920**: 84-96.

Lazarov NE, Reindl S, Fischer F, Gratzl M (2009). Histaminergic and dopaminergic traits in the human carotid body. *Respir Physiol Neurobiol*. **165(2-3)**:131-6.

Litvin, TN, Kamenetsky, M, Zarifyan, A, Buck, J & Levin, LR (2003). Kinetic properties of "soluble" adenylyl cyclase. Synergism between calcium and bicarbonate. *J Biol Chem* **278**: 15922-6, 10.1074/jbc.M212475200.

Lopez-Barneo, J, Lopez-Lopez, JR, Urena, J & Gonzalez, C (1988). Chemotransduction in the carotid body: K+ current modulated by PO2 in type I chemoreceptor cells. *Science* **241**: 580-2.

Lopez-Lopez, JR, De Luis, DA & Gonzalez, C (1993). Properties of a transient K+ current in chemoreceptor cells of rabbit carotid body. *J Physiol* **460**: 15-32.

Luo M, Sun L, Hu J (2009). Neural detection of gases--carbon dioxide, oxygen--in vertebrates and invertebrates. *Curr Opin Neurobiol.* 19(4):354-61.

Makhlouf A, Kshirsagar A and Niederberger C (2006). Phosphodiesterase 11: a brief review of structure, expression and function. *International Journal of Impotence Research* **18**, 501–509.

Martínez A, Saldise L, Ramírez MJ, Belzunegui S, Zudaire E, Luquin MR, Cuttitta F (2003). Adrenomedullin expression and function in the rat carotid body. *J Endocrinol* **176(1)**: 95-102.

Marzouk, SA, Ufer, S, Buck, RP, Johnson, TA, Dunlap, LA & Cascio, WE (1998). Electrodeposited iridium oxide pH electrode for measurement of extracellular myocardial acidosis during acute ischemia. *Anal Chem* **70**: 5054-61.

McDonald, DM (1980). Regulation of chemoreceptor sensitivity in the carotid body: the role of presynaptic sensory nerves. *Fed Proc* **39**: 2627-35.

Menniti, FS, Faraci, WS & Schmidt, CJ (2006). Phosphodiesterases in the CNS: targets for drug development. *Nat Rev Drug Discov* **5**: 660-7, 10.1038/nrd2058.

Milne, JL, Caterina, MJ & Devreotes, PN (1997). Random mutagenesis of the cAMP chemoattractant receptor, cAR1, of Dictyostelium. Evidence for multiple states of activation. *J Biol Chem* **272**: 2069-76.

Mir, AK, McQueen, DS, Pallot, DJ & Nahorski, SR (1984). Direct biochemical and neuropharmacological identification of dopamine D2-receptors in the rabbit carotid body. *Brain Res* **291**: 273-8.

Mir, AK, Pallot, DJ & Nahorski, SR (1983). Biogenic amine-stimulated cyclic adenosine-3',5'-monophosphate formation in the rat carotid body. *J Neurochem* **41**: 663-9.

Monteiro, EC, Vera-Cruz, P, Monteiro, TC & Silva e Sousa, MA (1996). Adenosine increases the cAMP content of the rat carotid body in vitro. *Adv Exp Med Biol* **410**: 299-303.

Monteiro, TC, Batuca, JR, Obeso, A, Gonzalez, C & Monteiro, EC (2011). Carotid body function in aged rats: responses to hypoxia, ischemia, dopamine, and adenosine. *Age (Dordr)* **33**: 337-50, 10.1007/s11357-010-9187-z.

Nattie E, and Li A(2012). Central chemoreceptors: locations and functions. *Compr. Physiol*. 2:221-254

Nattie, E (1999). CO2, brainstem chemoreceptors and breathing. *Prog Neurobiol* **59**: 299-331.

Neubauer, JA, Sunderram, J (2004). Oxygen-sensing neurons in the central nervous system. *J Appl Physiol* **96**: 367-74, 10.1152/japplphysiol.00831.2003.

Niane, LM, Joseph, V & Bairam, A (2012). Systemic blockade of nicotinic- and purinergic-receptors inhibits ventilation and increases apnea frequency in newborn rats. *Exp Physiol*, 10.1113/expphysiol.2012.065011.

Nichols NL, Hartzler LK, Conrad SC, Dean JB, Putnam RW(2008). Intrinsic chemosensitivity of individual nucleus tractus solitarius (NTS) and locus coeruleus (LC) neurons from neonatal rats. *Adv. Exp. Med Biol.* 605:348-52

Nunes, AR, Batuca, JR & Monteiro, EC (2010). Acute hypoxia modifies cAMP levels induced by inhibitors of phosphodiesterase-4 in rat carotid bodies, carotid arteries and superior cervical ganglia. *Br J Pharmacol* **159**: 353-61, 10.1111/j.1476-5381.2009.00534.x.

Oomori Y, Murabayashi H, Ishikawa K, Miyakawa K, Nakaya K, Tanaka H (2002). Neuropeptide Y- and catecholamine-synthesizing enzymes: immunoreactivities in the rat

carotid body during postnatal development. *Anat Embryol (Berl)* 206(1-2):37-47.

Oomori Y, Nakaya K, Tanaka H, Iuchi H, Ishikawa K, Satoh Y, Ono K (1994). Immunohistochemical and histochemical evidence for the presence of noradrenaline, serotonin and gamma-aminobutyric acid in chief cells of the mouse carotid body. *Cell Tissue Res* **278(2)**: 249-54.

Oomori Y, Ishikawa K, Satoh Y, Matsuda M, Ono K (1991). Neuropeptide-Y-immunoreactive chief cells in the carotid body of young rats. *Acta Anat (Basel)* **140(2)**:120-3.

Pardal, R, Ortega-Saenz, P, Duran, R & Lopez-Barneo, J (2007). Glia-like stem cells sustain physiologic neurogenesis in the adult mammalian carotid body. *Cell* **131**: 364-77, 10.1016/j.cell.2007.07.043.

Pastor-Soler, N, Beaulieu, V, Litvin, TN, Da Silva, N, Chen, Y, Brown, D*, et al.* (2003). Bicarbonate-regulated adenylyl cyclase (sAC) is a sensor that regulates pH-dependent V-ATPase recycling. *J Biol Chem* **278**: 49523-9, 10.1074/jbc.M309543200.

Peers, C (1990). Hypoxic suppression of K+ currents in type I carotid body cells: selective effect on the Ca2(+)-activated K+ current. *Neurosci Lett* **119**: 253-6.

Pepper, DR, Landauer, RC & Kumar, P (1995). Postnatal development of CO2-O2 interaction in the rat carotid body in vitro. *J Physiol* **485 (Pt 2)**: 531-4.

Pérez-García MT, Gómez-Niño A, Almaraz L, González C (1993). Neurotransmitters and second messenger systems in the carotid body. *Adv Exp Med Biol* **337**:279-87.

Perez-Garcia, MT, Almaraz, L & Gonzalez, C (1991). Cyclic AMP modulates differentially the release of dopamine induced by hypoxia and other stimuli and increases dopamine synthesis in the rabbit carotid body. *J Neurochem* **57**: 1992-2000.

Perez-Garcia, MT, Almaraz, L & Gonzalez, C (1990). Effects of different types of stimulation on cyclic AMP content in the rabbit carotid body: functional significance. *J Neurochem* **55**: 1287-93.

Perrin DG, Chan W, Cutz E, Madapallimattam A, Sole MJ (1986). Serotonin in the human infant carotid body. *Experientia* **42(5)**:562-4.

Pfaffl, MW (2001). A new mathematical model for relative quantification in real-time RT-PCR. *Nucleic Acids Res* **29**: e45.

Pierre, S, Eschenhagen, T, Geisslinger, G & Scholich, K (2009). Capturing adenylyl cyclases as potential drug targets. *Nat Rev Drug Discov* **8**: 321-35, 10.1038/nrd2827.

Porzionato A, Fenu G, Rucinski M, Macchi V, Montella A, Malendowicz LK, De Caro R. (2011) KISS1 and KISS1R expression in the human and rat carotid body and superior cervical ganglion. *Eur J Histochem* **55(2)**:e14. doi: 10.4081/ejh.2011.e14.

Porzionato A, Macchi V, Parenti A, De Caro R (2008). Trophic factors in the carotid body. *Int Rev Cell Mol Biol* **269**:1-58.

Porzionato A, Macchi V, Sandra Belloni A, Parenti A, De Caro R (2006). Adrenomedullin immunoreactivity in the human carotid body. *Peptides* **27(1)**:69-73.

Prabhakar NR, Dinerman JL, Agani FH, Snyder SH (1995). Carbon monoxide: a role in carotid body chemoreception. *Proc Natl Acad Sci U S A*. **92**(6):1994-7.

Prabhakar NR, Landis SC, Kumar GK, Mullikin-Kilpatrick D, Cherniack NS, Leeman S (1989). Substance P and neurokinin A in the cat carotid body:localization, exogenous effects and changes in content in response to arterial pO2. *Brain Res* **481**:205-14.

Prasad M, Fearon IM, Zhang M, Laing M, Vollmer C, Nurse CA (2001). Expression of P2X2 and P2X3 receptor subunits in rat carotid body afferent neurones: role in chemosensory signalling. *J Physiol* **537(Pt 3)**:667-77.

Putnam, RW, Filosa, JA & Ritucci, NA (2004). Cellular mechanisms involved in CO(2) and acid signaling in chemosensitive neurons. *Am J Physiol Cell Physiol* **287**: C1493-526, 10.1152/ajpcell.00282.2004.

Reyes, EP, Fernandez, R, Larrain, C & Zapata, P (2007). Carotid body chemosensory activity and ventilatory chemoreflexes in cats persist after combined cholinergic-purinergic block. *Respir Physiol Neurobiol* **156**: 23-32, 10.1016/j.resp.2006.07.006.

Ridderstråle Y & Hanson MA (1984). Histochemical localization of carbonic anhydrase 3 in the cat carotid body. *Ann N Y Acad Sci* **429**, 398-400.

Rigual R, López-López JR, Gonzalez C (1991). Release of dopamine and chemoreceptor discharge induced by low pH and high PCO2 stimulation of the cat carotid body. *J Physiol* **433**:519-31.

Rigual R, Gonzalez E, Fidone S, Gonzalez C (1984). Effects of low pH on synthesis and release of catecholamines in the cat carotid body in vitro. Brain Res. **309**(1):178-81.

Rindler, MJ, Bashor, MM, Spitzer, N & Saier, MH,Jr (1978). Regulation of adenosine 3':5'-monophosphate efflux from animal cells. *J Biol Chem* **253**: 5431-6.

Roberts EL Jr, He J, Chih CP (2000). Rat hippocampal slices need bicarbonate for the recovery of synaptic transmission after anoxia. *Brain Res.*;875(1-2):171-4.

Rocher, A, Caceres, AI, Almaraz, L & Gonzalez, C (2009). EPAC signalling pathways are involved in low PO2 chemoreception in carotid body chemoreceptor cells. *J Physiol* **587**: 4015-27, 10.1113/jphysiol.2009.172072.

Rocher A, Gonzalez C, Almaraz L (1999). Adenosine inhibits L-type Ca2+ current and catecholamine release in the rabbit carotid body chemoreceptor cells. *Eur J Neurosci*. **11(2)**:673-81.

Rocher, A, Obeso, A, Gonzalez, C & Herreros, B (1991). Ionic mechanisms for the transduction of acidic stimuli in rabbit carotid body glomus cells. *J Physiol* **433**: 533-48.

Rong W, Gourine AV, Cockayne DA, Xiang Z, Ford AP, Spyer KM, Burnstock G (2003). Pivotal role of nucleotide P2X2 receptor subunit of the ATP-gated ion channel mediating ventilatory responses to hypoxia. *J Neurosci* **23(36)**:11315-21.

Sekine, T, Watanabe, N, Hosoyamada, M, Kanai, Y & Endou, H (1997). Expression cloning and characterization of a novel multispecific organic anion transporter. *J Biol Chem* **272**: 18526-9.

Shirahata, M, Balbir, A, Otsubo, T & Fitzgerald, RS (2007). Role of acetylcholine in neurotransmission of the carotid body. *Respir Physiol Neurobiol* **157**: 93-105, 10.1016/j.resp.2006.12.010.

Smith, CA, Forster, HV, Blain, GM & Dempsey, JA (2010). An interdependent model of central/peripheral chemoreception: evidence and implications for ventilatory control. *Respir Physiol Neurobiol* **173**: 288-97, 10.1016/j.resp.2010.02.015.

Smith, JC, Abdala, AP, Rybak, IA & Paton, JF (2009). Structural and functional architecture of respiratory networks in the mammalian brainstem. *Philos Trans R Soc Lond B Biol Sci* **364**: 2577-8, 10.1098/rstb.2009.0081.

Smith, CA, Rodman, JR, Chenuel, BJ, Henderson, KS & Dempsey, JA (2006). Response time and sensitivity of the ventilatory response to CO2 in unanesthetized intact dogs: central vs. peripheral chemoreceptors. *J Appl Physiol* **100**: 13-9, 10.1152/japplphysiol.00926.2005.

Smith P, Gosney J, Heath D, Burnett H (1990). The occurrence and distribution of certain polypeptides within the human carotid body. *Cell Tissue Res* **261(3)**: 565-71.

Smith, JC, Morrison, DE, Ellenberger, HH, Otto, MR & Feldman, JL (1989). Brainstem projections to the major respiratory neuron populations in the medulla of the cat. *J Comp Neurol* **281**: 69-96, 10.1002/cne.902810107.

Stea, A, Jackson, A, Macintyre, L & Nurse, CA (1995). Long-term modulation of inward currents in O2 chemoreceptors by chronic hypoxia and cyclic AMP in vitro. *J Neurosci* **15**: 2192-20.

Stea A, Jackson A, Nurse CA (1992). Hypoxia and N6,O2'-dibutyryladenosine 3',5'-cyclic monophosphate, but not nerve growth factor, induce Na+ channels and hypertrophy in chromaffin-like arterial chemoreceptors. *Proc Natl Acad Sci U S A*. **89(20)**:9469-73.

Steegborn, C, Litvin, TN, Hess, KC, Capper, AB, Taussig, R, Buck, J*, et al.* (2005a). A novel mechanism for adenylyl cyclase inhibition from the crystal structure of its complex with catechol estrogen. *J Biol Chem* **280**: 31754-9, 10.1074/jbc.M507144200.

Steegborn, C, Litvin, TN, Levin, LR, Buck, J & Wu, H (2005b). Bicarbonate activation of adenylyl cyclase via promotion of catalytic active site closure and metal recruitment. *Nat Struct Mol Biol* **12**: 32-7, 10.1038/nsmb880.

Summers, BA, Overholt, JL & Prabhakar, NR (2002). CO(2) and pH independently modulate L-type Ca(2+) current in rabbit carotid body glomus cells. *J Neurophysiol* **88**: 604-12.

Supuran, CT (2008). Carbonic anhydrases--an overview. *Curr Pharm Des* **14**: 603-14.

SUTHERLAND, EW, RALL, TW (1958). Fractionation and characterization of a cyclic adenine ribonucleotide formed by tissue particles. *J Biol Chem* **232**: 1077-91.

Takakura, AC, Moreira, TS, Colombari, E, West, GH, Stornetta, RL & Guyenet, PG (2006). Peripheral chemoreceptor inputs to retrotrapezoid nucleus (RTN) CO2-sensitive neurons in rats. *J Physiol* **572**: 503-2, 10.1113/jphysiol.2005.103788.

Taylor CT, Cummins EP (2011). Regulation of gene expression by carbon dioxide. *J Physiol.* 589(Pt 4):797-803.

Tesmer, JJ, Dessauer, CW, Sunahara, RK, Murray, LD, Johnson, RA, Gilman, AG*, et al.* (2000). Molecular basis for P-site inhibition of adenylyl cyclase. *Biochemistry* **39**: 14464-71.

Tesmer, JJ, Sunahara, RK, Gilman, AG & Sprang, SR (1997). Crystal structure of the catalytic domains of adenylyl cyclase in a complex with Gsalpha.GTPgammaS. *Science* **278**: 1907-16.

Thomas, JA, Buchsbaum, RN, Zimniak, A & Racker, E (1979). Intracellular pH measurements in Ehrlich ascites tumor cells utilizing spectroscopic probes generated in situ. *Biochemistry* **18**: 2210-8.

Thompson, WJ (1991). Cyclic nucleotide phosphodiesterases: pharmacology, biochemistry and function. *Pharmacol Ther* **51**: 13-3.

Topal H, Fulcher NB, Bitterman J, Salazar E, Buck J, Levin LR, Cann MJ, Wolfgang MC, Steegborn C (2011). Crystal structure and regulation mechanisms of the CyaB adenylyl cyclase from the human pathogen Pseudomonas aeruginosa. *J Mol Biol.* **416(**2):271-86.

Townsend PD, Holliday PM, Fenyk S, Hess KC, Gray MA, Hodgson DR and Cann MJ (2009). Stimulation of mammalian G-protein – responsive adenylyl cyclases by carbon dioxide. *J biol chem*. **284**, 784-91.

van Aubel, RA, Smeets, PH, Peters, JG, Bindels, RJ & Russel, FG (2002). The MRP4/ABCC4 gene encodes a novel apical organic anion transporter in human kidney proximal tubules: putative efflux pump for urinary cAMP and cGMP. *J Am Soc Nephrol* **13**: 595-603.

Vardhan, A, Kachroo, A & Sapru, HN (1993). Excitatory amino acid receptors in commissural nucleus of the NTS mediate carotid chemoreceptor responses. *Am J Physiol* **264**: R41-50.

Vicario, I, Rigual, R, Obeso, A & Gonzalez, C (2000). Characterization of the synthesis and release of catecholamine in the rat carotid body in vitro. *Am J Physiol Cell Physiol* **278**: C490-9.

Wang, GP, Xu, CS (2010). Reference gene selection for real-time RT-PCR in eight kinds of rat regenerating hepatic cells. *Mol Biotechnol* **46**: 49-57, 10.1007/s12033-010-9274-5.

Wang, WJ, Cheng, GF, Yoshizaki, K, Dinger, B & Fidone, S (1991). The role of cyclic AMP in chemoreception in the rabbit carotid body. *Brain Res* **540**: 96-104.

Wang, WJ, Cheng, GF, Dinger, BG & Fidone, SJ (1989). Effects of hypoxia on cyclic nucleotide formation in rabbit carotid body in vitro. *Neurosci Lett* **105**: 164-8.

Wang W, Richerson GB(1989). Development of chemosensitivity of rat medullary raphe neurons. *Neuroscience* 90:1001-1011

Wang, W, Pizzonia, JH & Richerson, GB (1998). Chemosensitivity of rat medullary raphe neurones in primary tissue culture. *J Physiol* **511 (Pt 2)**: 433-50.

Wang YY, Chang RB, Liman ER (2010). TRPA1 is a component of the nociceptive response to CO2. *J Neurosci.* **30(**39):12958-63.

Wang ZY, Keith IM, Olson EB Jr, Vidruk EH, Bisgard GE (2002). Expression of 5-HT3 receptors in primary sensory neurons of the petrosal ganglion of adult rats. *Auton Neurosci.* **95**(1-2):121-4.

Wang ZY, Keith IM, Beckman MJ, Brownfield MS, Vidruk EH, Bisgard GE (2000). 5-HT5a receptors in the carotid body chemoreception pathway of rat. *Neurosci Lett.* **278**(1-2):9-12.

Wang, ZZ, He, L, Chen, J, Dinger, B, Stensaas, L & Fidone, S (1999). Protein phosphorylation signaling mechanisms in carotid body chemoreception. *Biol Signals Recept* **8**: 366-74.

Wang ZZ, He L, Stensaas LJ, Dinger BG, Fidone SJ (1991). Localization and in vitro actions of atrial natriuretic peptide in the cat carotid body. *J Appl Physiol* **70(2)**: 942-6.

Wang ZZ, Stensaas LJ, Dinger B, Fidone SJ (1989). Immunocytochemical localization of choline acetyltransferase in the carotid body of the cat and rabbit. *Brain Res* **498(1)**:131-4.

Wickstrom R, Hokfelt T, Lagercrantz H(2002). Development of CO(2)-response in the early newborn period in rat. *Respir Physiol Neurobiol.* 132(2):145-58

Xu, F, Tse, FW & Tse, A (2007). Pituitary adenylate cyclase-activating polypeptide (PACAP) stimulates the oxygen sensing type I (glomus) cells of rat carotid bodies via reduction of a background TASK-like K+ current. *J Neurochem* **101**: 1284-93, 10.1111/j.1471-4159.2007.04468.x.

Xu, F, Xu, J, Tse, FW & Tse, A (2006). Adenosine stimulates depolarization and rise in cytoplasmic [Ca2+] in type I cells of rat carotid bodies. *Am J Physiol Cell Physiol* **290**: C1592-8, 10.1152/ajpcell.00546.2005.

Xu J, Xu F, Tse FW, Tse A (2005). ATP inhibits the hypoxia response in type I cells of rat carotid bodies. *J Neurochem*. **92(6)**:1419-30.

Xu J, Tse FW, Tse A (2003). ATP triggers intracellular Ca2+ release in type II cells of the rat carotid body. *J Physiol* **549(Pt 3)**:739-47.

Yamamoto, Y, Fujimura, M, Nishita, T, Nishijima, K, Atoji, Y & Suzuki, Y (2003). Immunohistochemical localization of carbonic anhydrase isozymes in the rat carotid body. *J Anat* **202**: 573-7.

Zhang, J, Ma, Y, Taylor, SS & Tsien, RY (2001). Genetically encoded reporters of protein kinase A activity reveal impact of substrate tethering. *Proc Natl Acad Sci U S A* **98**: 14997-5002, 10.1073/pnas.211566798.

Zhang, KY, Card, GL, Suzuki, Y, Artis, DR, Fong, D, Gillette, S*, et al.* (2004). A glutamine switch mechanism for nucleotide selectivity by phosphodiesterases. *Mol Cell* **15**: 279-86, 10.1016/j.molcel.2004.07.005.

Zhang M, Piskuric NA, Vollmer C, Nurse CA (2012). P2Y2 receptor activation opens pannexin-1 channels in rat carotid body type II cells: Potential role in amplifying the neurotransmitter ATP. *J Physiol*. [Epub ahead of print]

Zhang M, Clarke K, Zhong H, Vollmer C, Nurse CA (2009). Postsynaptic action of GABA in modulating sensory transmission in co-cultures of rat carotid body via GABA(A) receptors. *J Physiol.* **587(Pt 2):**329-44.

Zhang M, Nurse CA (2004).CO2/pH chemosensory signaling in co-cultures of rat carotid body receptors and petrosal neurons: role of ATP and ACh. *J Neurophysiol.* **92**(6):3433-45.

Zhang M, Fearon IM, Zhong H, Nurse CA (2003). Presynaptic modulation of rat arterial chemoreceptor function by 5-HT: role of K+ channel inhibition via protein kinase C. *J Physiol.* **551(Pt 3)**:825-42.

Zhang, M, Zhong, H, Vollmer, C & Nurse, CA (2000). Co-release of ATP and ACh mediates hypoxic signalling at rat carotid body chemoreceptors. *J Physiol* **525 Pt 1**: 143-58.

Ziemann AE, Allen JE, Dahdaleh NS, Drebot II, Coryell MW, Wunsch AM, Lynch CM, Faraci FM, Howard MA 3rd, Welsh MJ, Wemmie JA (2009). The amygdala is a chemosensor that detects carbon dioxide and acidosis to elicit fear behavior. *Cell* **139**:1012–1021.

Zippin, JH, Chen, Y, Nahirney, P, Kamenetsky, M, Wuttke, MS, Fischman, DA*, et al.* (2003). Compartmentalization of bicarbonate-sensitive adenylyl cyclase in distinct signaling microdomains. *FASEB J* **17**: 82-4, 10.1096/fj.02-0598fje.

Faculdade de Ciências Médicas | Universidade Nova de Lisboa